Influence of Prosthetic Ankle-Foot Mechanics on Intact-Limb Biomechanical Demand during Ambulatory Functional Tasks

Satria Ardianuari

A dissertation

submitted in partial fulfillment of the

requirements for the degree of

Doctor of Philosophy

University of Washington

2026

Reading Committee:

Glenn K. Klute, Chair

Katherine M. Steele

Jenny Robinson

Stefania Fatone

Program Authorized to Offer Degree:

Mechanical Engineering

University of Washington

Abstract

Influence of Prosthetic Ankle-Foot Mechanics on Intact-Limb Biomechanical Demand during Ambulatory Functional Tasks

Satria Ardianuari

Chair of the Supervisory Committee:

Glenn K. Klute
Department of Mechanical Engineering

Individuals with single (unilateral), below-knee (transtibial) amputation (TTA) often exhibit altered gait biomechanics that increase mechanical demand on the non-amputated (intact) limb, contributing to an elevated risk of secondary osteoarthritis, particularly in the medial compartment of the knee. Because prosthetic ankle-foot devices play a central role in restoring mobility, their mechanics may influence how individuals with TTA adapt to various walking activities. This dissertation describes multiple studies investigating how prosthetic ankle-foot mechanical metrics influence lower-limb biomechanical demand during functional tasks, with particular emphasis on intact-limb medial knee loading during load carriage and other ambulatory activities. Across the studies, there are three overarching objectives: 1) influence of prosthetic ankle-foot type on measures of biomechanical demand, including gait kinetics, mechanical energy (i.e., joint work), and motor control during load carriage; 2) influence of prosthetic ankle-foot type

on medial knee loading during load carriage; 3) influence of prosthetic ankle-foot stiffness on medial knee loading across ambulatory activities.

The first study examined the effects of side load carriage on gait kinetics during steady-state walking. Twelve individuals with TTA carried a moderate load while walking with a clinically prescribed, passive prosthetic ankle-foot. Prosthetic-side load carriage reduced intact-limb propulsive force, whereas intact-side load carriage was associated with smaller intact-limb hip flexor and knee flexor moments. Hip and knee abductor moments increased when the load was carried on the opposite limb, and hip extensor power increased when the load was carried on the same limb. These mixed findings suggest that the preferred side for carrying a load depends on the desired biomechanical effect, particularly on the intact limb, to inform targeted gait rehabilitation strategies.

Using the same protocol, we investigated how various load carriage positions and prosthetic ankle-foot types affect intact-limb medial knee loading associated with osteoarthritis risk. Five load-carriage conditions were tested: unloaded, front (anterior), back (posterior), intact side, and prosthetic side. In addition to the clinically prescribed, passive prosthetic ankle-foot, four other commercially available types were compared, including the same type but one category stiffer, the same type with a heel-stiffening wedge, a dual-keel type, and a powered type. Intact-side load carriage resulted in the smallest first peak knee adduction moment and impulse (surrogate measures of medial knee loading), whereas prosthetic-side load carriage produced the highest values, increasing these measures by approximately 30%. Prosthetic ankle-foot type did not significantly affect these outcomes, and only a weak trend was observed between prosthetic push-off work and first peak knee adduction moment. These findings indicate that load carriage strategy plays a greater role than prosthetic ankle-foot selection in modulating intact-limb medial knee loading during load carriage.

Given the more significant influence of load carriage than prosthetic ankle-foot type on intact-limb medial knee loading during load carriage, we further investigated how prosthetic ankle-foot selection influences lower-limb joint total energy (mechanical joint work). Across unloaded, anterior, posterior, intact-side, and prosthetic-side load conditions, most differences were observed in the prosthetic limb. Ankle joint work differed significantly between prosthetic ankle-foot types within each load condition, with the powered type producing the greatest net positive ankle work in late stance and the clinically prescribed and heel-wedge types producing the greatest net negative ankle work in early stance of the gait cycle. By contrast, knee and hip joint work did not differ substantially across types, suggesting that prosthetic ankle-foot primarily modulates prosthetic ankle mechanics without markedly altering proximal joint work under moderate load carriage.

To determine whether these biomechanical changes translate to altered motor control, we investigated the effect of changes in prosthetic ankle-foot selection on muscle activation patterns and coordinated muscle groupings (motor modules) during load carriage. Prosthetic ankle-foot type influenced activation of several intact-limb muscles, with powered and stiffer types often associated with greater plantarflexor and knee extensor activity, compared with the clinically prescribed type. Differences in muscle co-contraction were limited and occurred primarily during unloaded walking. Despite these muscle-level changes, motor module complexity, composition, and activation timing remained largely conserved across prosthetic ankle-foot types and load carriage conditions. These results indicate that individuals with TTA accommodate altered prosthetic ankle-foot mechanics and added load primarily through modulation of muscle activation rather than through reorganization of motor control strategies.

Subsequently, we focused on stiffness, an important mechanical property of prosthetic ankle-feet. We evaluated the influence of commercial prosthetic ankle-foot stiffness (variation in ±2 categories from the clinically prescribed stiffness category) on medial knee contact force, another surrogate measure of medial knee loading, across a range of ambulatory activities. Prosthetic ankle-foot stiffness affected peak medial knee contact force in an activity-dependent manner. Intact limb results found that stiffer prosthetic ankle-feet were generally associated with reduced peak medial knee contact force during level, faster, and loaded walking, whereas different patterns emerged during downhill walking and turning. Residual limb findings were inconsistent. Although several differences were statistically significant, they remained below the minimal detectable change threshold, indicating that prosthetic ankle-foot stiffness alone may contribute only moderately to changes in medial knee loading across ambulatory activities.

We extended this work by examining how stiffness-related prosthetic ankle-foot biomechanical metrics, including forward push (push-off), dynamic mean ankle moment arm, and roll-over radius, are associated with intact-limb medial knee contact force. Surprisingly, greater prosthetic push-off was not consistently associated with reduced intact-limb peak medial knee contact force across ambulatory activities. Instead, roll-over radius demonstrated the most consistent inverse associations with intact-limb peak medial knee contact force, particularly during more demanding walking activities such as upslope walking, faster walking, and load carriage. These findings suggest that effective forefoot lever arm behavior may be more important than push-off alone for reducing intact-limb medial knee loading.

Collectively, this dissertation demonstrates that lower-limb biomechanical demand, particularly on the intact limb of individuals with unilateral TTA, is influenced by both activity demands and prosthetic ankle-foot mechanics. Load carriage strategy is consistently associated with changes in intact-limb medial knee loading, while prosthetic ankle-foot stiffness and other mechanical metrics like push-off exhibit more complex, activity-dependent effects. Overall, this dissertation advances understanding of how prosthetic ankle-foot mechanics interact with users during various ambulatory activities and highlights the importance of activity-adaptive prosthetic ankle-foot systems, as well as specific local biomechanical metrics, for reducing increases in medial knee loading, potentially preventing elevated OA risks in the intact limb and ultimately improving mobility in individuals with unilateral TTA.

ACKNOWLEDGEMENTS

This dissertation marks the culmination of a journey shaped not only by academic curiosity, but by the unwavering support, mentorship, and generosity of many individuals and communities. My path, from training in rehabilitation science and technology to pursuing a Ph.D. in mechanical engineering, has been guided by a deep fascination with biomechanics and a desire to contribute to improving amputee mobility, as well as advancing prosthetic technology. This work would not have been possible without the people who believed in me along the way.

First and foremost, I am grateful to my supervisor, Dr. Glenn Klute. His mentorship has been both empowering and grounding, offering me the freedom to explore my ideas while providing steady guidance and support. Through him, I learned not only how to think critically as a scientist, but also how to write, collaborate, and secure funding. His guidance enabled me to receive competitive pre-doctoral fellowships. I would also like to specially thank my dissertation committee for their support: Drs. Katherine Steele, Jenny Robinson, Stefania Fatone, and Christopher Neils.

I am equally thankful for the past and present members of what I fondly call "KLUTEAM" at the VA Puget Sound Center for Limb Loss and MoBility (CLiMB). To Christina Carranza, whose clinical expertise as a research prosthetist has been invaluable; to Jocelyn Berge, Krista Cyr, and other CLiMBers, thank you for your support throughout this journey. I am also grateful to our other research prosthetist, Charles King, for his collaboration and shared dedication to advancing prosthetics research.

I would like to extend my sincere appreciation to Dr. Richard Neptune at The University of Texas at Austin Walker Department of Mechanical Engineering. Working alongside Drs. Klute and Neptune on research and publications has been one of the most formative aspects of my

doctoral training. Through these collaborations, I gained invaluable insight into scientific writing, interdisciplinary thinking, and the rigor required to push our field forward.

My journey to this point began long before my doctoral studies. I am honored to have been a Fulbright Scholar, which first brought me to the United States for graduate education. That experience laid the foundation for everything that followed, and I remain grateful for the doors of opportunity it opened.

To my friends and colleagues in the University of Washington Department of Mechanical Engineering (including our most beloved graduate advisor, Wanwisa Kisalang), and to my close friends in Indonesia, thank you for your support and encouragement. Your presence has made this journey less solitary and far more meaningful.

Finally, I dedicate this work to my family. To my beloved late mother, whose love and sacrifices continue to guide me; to my father and my sisters back home, whose unwavering support has sustained me across distance and time, this achievement is as much yours as it is mine. I also hope this work inspires my nephews and nieces to pursue science and use their knowledge to serve their communities in the future.

At its core, this dissertation is more than an academic milestone - it is a commitment to advancing science in service of others, particularly those who rely on prosthetic devices to move through the world. It is my hope that this work contributes, even in a small way, to improving their mobility, independence, and quality of life.

PREFACE

Chapters 2-7 were prepared as separate manuscripts for publication; therefore, some material is repeated across chapters. Chapters 2-5 are based on analyses from the same full dataset, resulting in some overlap in content and methods. Chapters 6-7 are based on analyses from a subset of a separate dataset and similarly contain overlapping material. Chapters 2-4 have been published, Chapters 5-6 are currently under review, and Chapter 7 is in preparation for submission.

TABLE OF CONTENTS

LIST OF FIGURES

LIST OF TABLES

CHAPTER 1

INTRODUCTION

Mobility is central to independence, participation, and quality of life. For individuals with single (unilateral), below-knee (transtibial) amputation (TTA), prosthetic ankle-foot devices are essential for restoring walking ability and supporting activities of daily living. However, even with more advanced prosthetic technology, individuals with TTA often experience suboptimal biomechanical outcomes during various activities compared to individuals without amputation, including asymmetrical ground reaction forces, altered lower-limb joint moments and powers, and increased mechanical demand on the non-amputated (intact) limb (Bateni and Olney, 2002; Grumillier et al., 2008; Madou et al., 2022; Nolan et al., 2003; Silverman et al., 2008; Teater et al., 2023). Over time, the greater reliance on the intact limb may contribute to secondary musculoskeletal conditions, including low back pain (including increased spinal loads), chronic limb pain, knee pain and osteoarthritis (OA) (Butowicz et al., 2024; Gailey et al., 2008; Highsmith et al., 2019; Morgenroth et al., 2012; Norvell et al., 2005; Struyf et al., 2009).

1.1 Background

1.1.1 Clinical Relevance

Among secondary musculoskeletal complications, OA of the intact knee is of particular clinical concern. Individuals with lower-limb amputation exhibit elevated prevalence of knee OA compared to the general population, with mechanical loading believed to contribute substantially to this increased risk (Gailey et al., 2008; Morgenroth et al., 2012; Norvell et al., 2005; Parr et al., 2024; Struyf et al., 2009). Individuals with TTA have been shown to experience increased intact-limb knee joint contact forces compared to non-amputees (Silverman and Neptune, 2014). This elevated loading on the intact limb may develop over time among established prosthesis users and those with joint disorder onset (Fey and Neptune, 2012). Because medial knee OA is about 5-10 times more prevalent than lateral knee OA, measures related to medial compartment loading are frequently used to evaluate OA risk (Jiang et al., 2025; Jones et al., 2013).

External knee adduction moment (KAM) is among the most commonly used non-invasive surrogates of medial knee loading and has been associated with the development and progression of medial knee OA (Andrag et al., 2024; Andriacchi et al., 2004; Miyazaki et al., 2002; Morgenroth et al., 2014). KAM impulse has also been used to capture cumulative loading exposure over stance phase of the gait cycle. Although KAM does not directly measure joint contact force, it is often interpreted as reflecting the frontal-plane distribution of tibiofemoral load. In parallel, medial knee contact force (MCF) provides a complementary surrogate more directly related to medial knee loading. Additionally, inclusion of external knee flexion moment (KFM) may further improve estimation of medial joint loading beyond KAM alone (Manal et al., 2015; Miller et al., 2017).

Such measures can be used to quantify elevated mechanical loading on the intact limb, a clinically significant issue among individuals with TTA that has motivated efforts to identify behavioral and prosthetic strategies to mitigate long-term knee OA risk.

1.1.2 Functional Tasks: Load Carriage and Ambulatory Activities

Many activities of daily living beyond steady-state walking may impose mechanical demands. Load carriage is common in everyday life and is part of personal, occupational, and leisure activities. During these activities, people also change speeds instantaneously, navigate through slopes, and turn. Therefore, both load carriage and activities beyond level-ground, steady-state walking are especially relevant because the added mass and demand can alter gait biomechanics and may further increase lower-limb loading, particularly in the intact limb.

In individuals without amputation, front and back load carriage can increase metabolic cost, increase lower-limb muscle activity, alter hip and knee kinematics, and change stride parameters (Attwells et al., 2006; Birrell and Haslam, 2009; Silder et al., 2013). However, comparable research in load carriage for individuals with lower-limb amputation remains relatively limited. In individuals with TTA, back load carriage has been shown to alter joint kinetics and trunk/pelvic motion and increase metabolic demand compared to individuals without lower-limb amputation (Doyle et al., 2015, 2014; Schnall et al., 2014, 2012). Front load carriage has been shown to alter ankle joint work symmetry in this population (Molitor et al., 2026). However, less is known about how different load positions, including side load carriage, and prosthetic ankle-foot types influence intact-limb medial knee loading and broader measures of lower-limb biomechanical demand.

Beyond load carriage, daily ambulatory activities such as faster walking, downhill walking, and turning may impose distinct biomechanical demands. Activities beyond level-ground walking, such as sloped walking, significantly increase knee compressive forces in individuals without amputation (Alexander and Schwameder, 2016; Haggerty et al., 2014). Yet for those with TTA, prosthetic ankle-foot prescriptions are typically optimized under level-ground, unloaded walking, raising the possibility that mechanical behavior may be suboptimal under functional task demands. Understanding how this potentially increased demand on the intact limb may be modified by adaptable prosthetic ankle-foot mechanical behavior to varying ambulatory walking conditions is important to help mitigate knee OA risk.

1.1.3 Prosthetic Ankle-Foot Mechanics

Prosthetic ankle-foot devices play an essential role in how individuals with TTA walk and adapt to different environments. The major function of the biological ankle-foot complex contributes to body support, forward propulsion, swing initiation, and balance control during walking (Anderson and Pandy, 2003; Liu et al., 2006; Neptune et al., 2004, 2001; Neptune and McGowan, 2016, 2011). In contrast, most clinically prescribed prosthetic feet are passive devices with fixed mechanical properties (metrics), such as stiffness, that are typically selected based on user body mass and anticipated activity level. Individuals without amputation can modulate ankle-foot behavior in response to changing task demands (Kern et al., 2019), but individuals with TTA must rely on prosthetic ankle-foot components that may not adapt to changing speeds or different surface conditions. This limitation may become especially important during functional activities that differ from level-ground, steady-state walking.

A central hypothesis in prosthetic biomechanics is that prosthetic ankle-foot mechanical metrics influence intact-limb loading by affecting whole-body center-of-mass (COM) dynamics during walking.

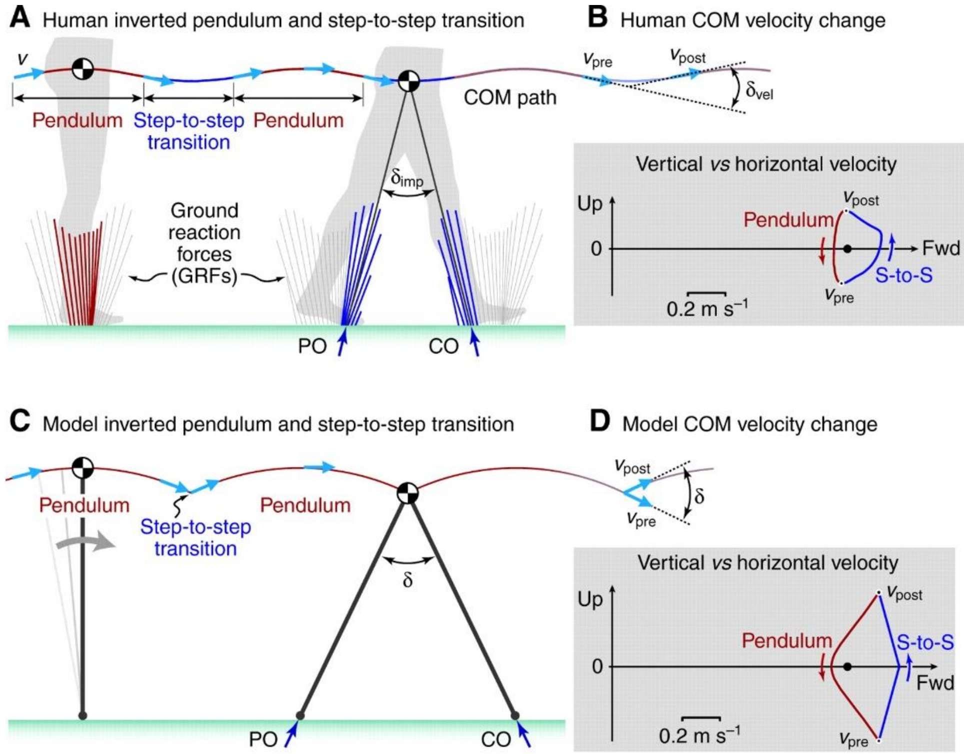

Fig 1.1 A) The human COM motions; B) The COM velocity during the step-to-step transition; C) The COM velocity as a simple pendulum with an impulsive step-to-step transition; D) The angular differences in the model's impulses. This figure is adapted from (Adamczyk and Kuo, 2009) with permission.

During human walking, the COM follows a roughly sinusoidal trajectory that can be conceptually divided into an inverted-pendulum phase during single support and a step-to-step transition during double support (Adamczyk and Kuo, 2009; Donelan et al., 2002a; Kuo et al., 2005). During this transition, the trailing limb generates a push-off impulse while the leading limb undergoes a collision impulse (Fig.1.1A). Together, these impulses redirect COM velocity from a forward-and-downward direction before transition to a forward-and-upward direction after transition (Fig.1.1A and C). This redirection can be described in terms of the angular separation between impulses and corresponding changes in COM velocity (Fig. 1.1B and D).

Dynamic walking models suggest that greater trailing-limb push-off reduces leading-limb collision losses and lowers the demand placed on the leading limb during the transition (Adamczyk and Kuo, 2009; Kuo, 2007; Kuo et al., 2005). Experimental studies in non-amputees support this concept, showing that augmenting push-off can reduce collision and lower leading-limb loading (Adamczyk and Kuo, 2009; Donelan et al., 2002a).

One proposed explanation for elevated intact-limb medial knee loading in individuals with TTA is reduced prosthetic ankle-foot push-off power produced by conventional passive prosthetic ankle-foot devices. If the trailing prosthetic limb generates insufficient push-off, the leading intact limb may be required to perform a greater share of COM velocity redirection, increasing collision impulse and potentially increasing intact-limb medial knee loading during early stance (Morgenroth et al., 2011). A prosthetic ankle-foot that improves push-off could, therefore, potentially reduce intact-limb medial knee loading.

Stiffness may also influence intact-limb medial knee loading with partially distinct mechanisms through modulation of energy storage and return, forefoot deformation and lever-arm behavior during late stance. Increased prosthetic ankle-foot stiffness has been hypothesized to reduce mechanical loading transferred to the intact limb, although findings have been mixed due to reduced push-off. For example, some studies demonstrated associations between increased stiffness and decreased knee contact forces (Fey et al., 2012) and decreased KAM (Slater et al., 2024). However, other studies found no significant stiffness effects on KAM (Tacca et al., 2026) or instead, associated increased stiffness with increased peak ground reaction forces (Fey et al., 2011) and loading rates (Adamczyk et al., 2017).

While push-off is more commonly studied in relation to prosthetic ankle-foot function, they may not fully capture the comprehensive influence of prosthetic ankle-foot stiffness on intact-limb medial knee loading. Other relevant biomechanical metrics may further explain this association. Dynamic mean ankle moment arm (DMAMA) measures the cumulative prosthetic ankle-foot loading dynamics and is related to ankle angle and stiffness interaction (Adamczyk, 2020; Leestma et al., 2021), potentially playing a significant role in modulating intact-limb medial knee loading (Fig. 1.2E). Another functional biomechanical metric is roll-over radius (ROR), representing the effective rocker shape and prosthetic ankle-foot mechanics during walking (Fig. 1.2B) (Adamczyk et al., 2006; Curtze et al., 2009; Hansen et al., 2004a; Hansen and Childress, 2010). A larger or more effective roll-over radius may reduce abrupt loading transfer to the intact limb and thus reduce the collisional loading on the intact-limb knee.

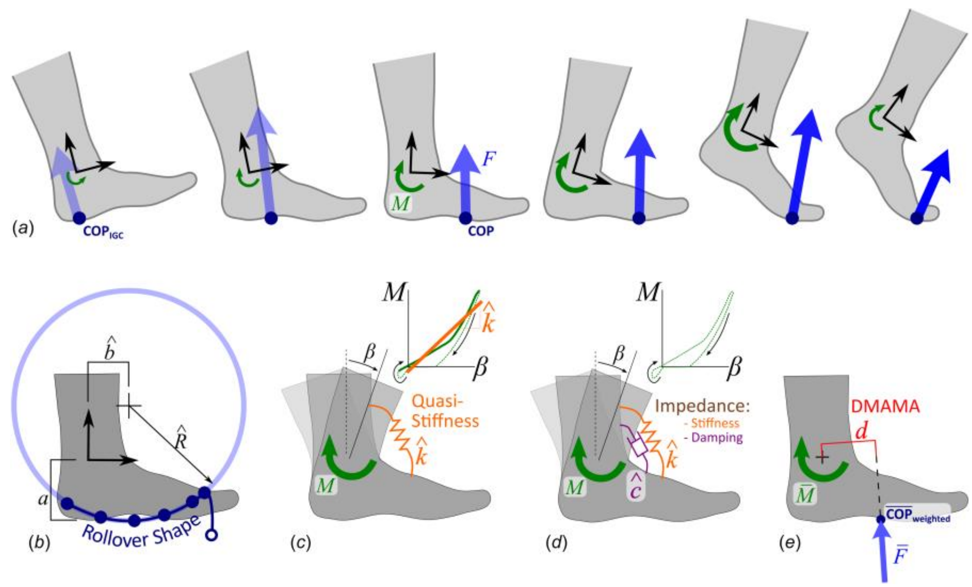

Fig 1.2 A) Sagittal ankle mechanics involves joint angle and moment, dynamically balancing the applied ground reaction force; B) roll-over radius, relating COP to shank angle; C) ankle quasi-stiffness (≈ spring $\hat{k}$), relating ankle moment to ankle angle; D) ankle impedance (≈ spring $\hat{k}$ and damper $\hat{c}$, and sometimes inertia), describing angular joint dynamics. A, B, and C models capture local control fluctuations, but only apply during specific portions of stance and do not summarize the ankle's net effect; E) dynamic mean ankle moment arm, summarizing ankle control during the whole stance phase. This figure is adapted from (Adamczyk, 2020) with permission.

These metrics may provide complementary information as push-off primarily captures propulsive energy generation in late stance, DMAMA captures cumulative moment-arm behavior over stance, and ROR captures effective forefoot lever-arm in late stance. Together, they may better explain variations in intact-limb medial knee loading than push-off alone, particularly across functional tasks where mechanical demands vary.

Because walking on slopes, walking at different speeds, load carriage, and turning may exacerbate the elevated intact-limb medial knee loading in individuals with TTA, stiffness effects may be more significant under such demanding activities. Together, stiffness, push-off and several other metrics relevant to prosthetic ankle-foot mechanical behavior may influence intact-limb medial knee loading through effects on forward propulsion and lever-arm mechanics.

1.2 Focus of the Dissertation

The overall focus of this dissertation is to understand how functional task demands and prosthetic ankle-foot mechanics influence measures of intact-limb biomechanical demand in individuals with unilateral TTA. Specifically, this dissertation has three related objectives or themes: 1) how load carriage strategy and prosthetic ankle-foot type influence measures of biomechanical demand, including gait kinetic responses, mechanical joint work, and neuromuscular control; 2) how load carriage strategy and prosthetic ankle-foot type influence medial knee loading; and 3) how prosthetic ankle-foot stiffness and stiffness-related metrics, local to ankle-foot system, influence medial knee loading across common ambulatory activities.

The first part of this dissertation focuses on load carriage. We began by examining how carrying a moderate side load on either the intact-limb or prosthetic-limb side affects gait kinetics during steady-state walking with a clinically prescribed, passive-elastic prosthetic ankle-foot with a single fixed stiffness. Side load carriage is common in daily life, such as carrying an object over one shoulder or on one hip, but its biomechanical effects in individuals with TTA had not been well characterized.

We then extended this work by evaluating how load carriage position and prosthetic ankle-foot type influence intact-limb medial knee loading associated with OA risk. Participants walked under unloaded, anterior load, posterior load, intact-side load, and prosthetic-side load conditions while using several commercially available prosthetic ankle-foot types purported for load carriage. These study feet varied by stiffness and push-off capabilities, and included the clinically prescribed foot, a one-category stiffer foot, the same prescribed foot with heel-stiffening wedge, a dual-keel foot, and an active powered ankle-foot.

We further examined lower-limb joint mechanical work to better understand how different prosthetic ankle-feet influence device-user interaction during load carriage. We also investigated whether these biomechanical changes were accompanied by changes in neuromuscular control. We used electromyography data to examine the influence of prosthetic ankle-foot type on activation and co-contraction of intact-limb muscles. Motor module analysis was performed to examine prosthetic ankle-foot effects on motor module complexity and composition.

The second part of this dissertation focuses on prosthetic ankle-foot stiffness across a broader range of ambulatory activities. We evaluated how commercial prosthetic ankle-foot stiffness, varied by two categories above and below the clinically prescribed stiffness, affects peak MCF during ambulatory activities relative to surface (level, uphill, downhill), speed (15% faster, 15% slower), load carriage, and direction (turning with the prosthesis inside and outside).

Finally, we examined whether commonly used prosthetic ankle-foot biomechanical metrics explain changes in intact-limb peak MCF across the ambulatory activities. Specifically, we evaluated prosthetic peak push-off and work, DMAMA, and ROR.

1.3 Significance of the Dissertation

The work in this dissertation contributes to clinical prosthetics, gait biomechanics, and biomechanical engineering by clarifying how prosthetic ankle-foot mechanics interact with functional task demands. The primary contributions are:

Identifying load carriage strategies that may reduce intact-limb knee loading

Individuals with TTA commonly experience increased intact-limb loading, which may contribute to knee pain and OA risk (Gailey et al., 2008; Morgenroth et al., 2012; Norvell et al., 2005; Parr et al., 2024; Struyf et al., 2009). This dissertation shows that load carriage position strongly influences intact-limb medial knee loading. This work provides clinically relevant evidence that load carriage strategy may be a modifiable behavioral factor for reducing intact-limb medial knee loading during daily activities.

Clarifying the role of prosthetic foot type during load carriage

Commercial prosthetic feet are often designed or marketed to improve function under demanding tasks, such as load carriage. This dissertation demonstrates that prosthetic ankle-foot type has limited effects on intact-limb medial knee loading and primarily modulates prosthetic ankle mechanics during moderate load carriage. This distinction is important because improvements in prosthetic ankle-foot behavior do not necessarily translate directly to reduced intact-limb medial knee loading. Prosthetic engineering may therefore prioritize user-specific cost functions, while clinical prosthetic prescription may need to consider the user's task-specific goals, such as push-off for forward propulsion, energy absorption for stability, or intact-limb medial knee offloading.

Linking prosthetic mechanics, muscle activation, and motor control

Biomechanical adaptations to prosthetic foot mechanics are not limited to joint moments and powers. This dissertation shows that changing prosthetic foot mechanics can alter intact-limb muscle activation, yet motor module complexity and timing remain largely conserved. These findings suggest that individuals with TTA may preserve overall motor control organization while adjusting muscle-level recruitment to accommodate changes in prosthetic mechanics and task demand. This contributes to a more complete understanding of device-user interaction during functional walking.

Showing that prosthetic stiffness effects on medial knee loading are activity-dependent

Prosthetic stiffness is a central mechanical metric in passive prosthetic ankle-foot devices, yet its influence on intact-limb medial knee loading is not uniform across activities. This dissertation shows that stiffer feet may reduce intact-limb peak MCF during certain activities, including level, faster, and loaded walking, but not consistently across downhill walking or turning. These findings suggest that no single stiffness category may be optimal across all functional tasks. Instead, activity-appropriate or activity-adaptive stiffness may be needed to better support long-term joint health.

Reframing the role of prosthetic push-off in reducing intact-limb knee loading

Prior work has suggested that increased prosthetic push-off may or may not reduce intact-limb knee loading during unloaded walking (Davidson et al., 2021; Golyski et al., 2026; Grabowski and D'Andrea, 2013; Morgenroth et al., 2011). This dissertation shows that greater push-off was not consistently associated with reduced intact-limb MCF across functional ambulatory activities beyond level-ground walking. Instead, ROR showed more consistent inverse associations with peak MCF in several demanding walking activities. This suggests that prosthetic design features related to effective forefoot lever behavior may be as important as, or more important than, push-off magnitude alone when attempting to reduce intact-limb medial knee loading.

1.4 Overview of the Dissertation

This dissertation includes six experimental studies. Collectively, this dissertation demonstrates that intact-limb biomechanical demand in individuals with TTA is influenced by both activity demands and prosthetic ankle-foot mechanics. The findings highlight the need for activity-specific prescription guidance and support the future development of prosthetic ankle-foot designs with activity-adaptive stiffness capabilities to preserve long-term joint health and improve mobility in individuals with TTA.

Chapter 2 examines whether individuals with unilateral TTA should carry a side load on the intact or prosthetic side. This study evaluates ground reaction forces, loading rates, loading symmetry, and lower-limb joint kinetics during unloaded, intact-side load, and prosthetic-side load walking.

Chapter 3 investigates how load carriage position and prosthetic foot type influence intact-limb knee loading estimates associated with OA risk. This chapter focuses on KAM, KAM impulse, KFM, and prosthetic push-off across five load conditions and five prosthetic foot conditions.

Chapter 4 evaluates how prosthetic foot selection influences lower-limb mechanical work during load carriage. This chapter examines positive and negative joint work at the ankle, knee, and hip to determine whether different prosthetic feet alter intact-limb compensation or primarily affect prosthetic-limb mechanics.

Chapter 5 examines muscle activation and motor module organization during loaded walking with stiffer and powered prosthetic feet. This chapter determines whether changes in prosthetic foot mechanics alter neuromuscular control during load carriage.

Chapter 6 investigates the influence of prosthetic foot stiffness on medial knee contact force across common ambulatory activities, including level walking, slopes, speed changes, load carriage, uneven terrain, and turning.

Chapter 7 extends the stiffness analysis by evaluating whether prosthetic ankle-foot peak push-off power, push-off work, dynamic mean ankle moment arm, and roll-over radius are associated with intact-limb peak MCF across activities.

The final chapter summarizes the major findings, clinical implications, limitations, and future directions.

Throughout this dissertation, the pronoun *we* is used to reflect the collaborative nature of the research conducted by a multidisciplinary team. Contributors to each study are identified at the beginning and in the acknowledgments of the corresponding chapters.

CHAPTER 2

SHOULD INDIVIDUALS WITH UNILATERAL TRANSTIBIAL AMPUTATION CARRY A LOAD ON THEIR INTACT OR PROSTHETIC SIDE?

Published in *Journal of Biomechanics*

DOI: https://doi.org/10.1016/j.jbiomech.2024.112385

Satria Ardianuari

Krista M. Cyr

Richard R. Neptune

Glenn K. Klute

2.1 ABSTRACT

Carrying side loads often occurs during activities of daily living. As walking is most unstable mediolaterally, side load carriage may further compromise gait biomechanics, especially for transtibial amputees (TTAs). This study investigated the effects of side load carriage on gait kinetics during steady-state walking to determine which side, intact or prosthetic, TTAs should carry a load. Twelve unilateral TTAs wore a passive-elastic foot and carried a side load of 13.6 kg while walking at their self-selected speed. Kinetic metrics, including ground reaction force peaks and impulses, loading and unloading rates, and joint moments and powers, were analyzed. TTAs had smaller propulsive forces on their intact limb during the prosthetic side load condition. During the intact side load condition, they exhibited smaller hip flexor moment in late stance and smaller knee flexor moment at the end of swing on their intact limb. They had higher hip and knee abductor moments on their intact limb and prosthetic limb in early and late stance during the contralateral side load condition. TTAs generated higher hip extensor power at weight acceptance during the ipsilateral side load. Significant interactions were observed in hip extensor power and abductor moment, suggesting strong associations between hip extensor power generation and the ipsilateral side load and between hip abductor moment and the contralateral side load. These mixed results demonstrate some kinetic changes due to side load carriage and suggest that the side TTAs should carry a load depends on the desired effects, primarily on their intact limb.

2.2 INTRODUCTION

Carrying loads is essential for activities of daily life, from mundane tasks to specialized occupations and recreational pursuits. There are several different ways to carry loads, and each method may have a different effect on an individual's gait biomechanics. Front and back load carriage methods have been shown to induce higher metabolic costs and increase lower limb muscle activity in early stance for healthy individuals (Silder et al., 2013). Front load carriage has also been shown to elevate the risk of falling (Yang et al., 2022) Others have shown that back load carriage can increase hip and knee flexion (Attwells et al., 2006; Harman et al., 1992), alter hip adduction/abduction, hip rotation, and pelvic tilt (Birrell and Haslam, 2009), and reduce stride length and increase cadence (Birrell and Haslam, 2009). Loads may also be carried laterally for convenience over short distances or for intermittent periods, such as carrying a bag over one shoulder or holding a baby or child on one hip while walking. Despite the frequency of side load carriage, there have been little to no biomechanical analyses of gait with this load carriage method, particularly for individuals who exhibit higher fall risk, such as those with a lower-limb amputation.

Individuals without a lower-limb amputation can modulate power generated by the biological ankle to accommodate added loads during walking. Ankle dorsiflexors provide body support in early stance (Anderson and Pandy, 2003). In addition to support, ankle plantarflexors provide essential functions for forward propulsion (Liu et al., 2006; Neptune et al., 2004, 2001), initiation of swing (Neptune et al., 2001), as well as dynamic balance control (Neptune and McGowan, 2016, 2011). Absence of ankle plantarflexors in the residual limb of transtibial amputees (TTAs) may aggravate asymmetrical gait biomechanics and require additional compensatory mechanisms in response to carrying a side load.

TTAs have been shown to experience altered biomechanics, even during unloaded walking. These changes include higher peak ground reaction force (GRF) in their intact limb (Nolan et al., 2003), which can lead to knee osteoarthritis (Gailey et al., 2008; Norvell et al., 2005; Struyf et al., 2009), chronic low back pain (Highsmith et al., 2019), and chronic lower limb pain (Burke et al., 1978). Further, TTAs have been observed to have increased prosthetic limb hip extensor moment, power, and positive work in early stance (Bateni and Olney, 2002; Gitter et al., 1991; Grumillier et al., 2008; Silverman et al., 2008), and a greater prosthetic limb hip flexor moment in pre-swing (Sadeghi et al., 2001). With added loads, these effects may be magnified. TTAs with passive-elastic feet respond to back load conditions with smaller ankle dorsiflexor moment in the intact limb, smaller hip extensor power in early stance in both limbs, and smaller ankle plantarflexor and knee flexor moment in the prosthetic limb (Doyle et al., 2014). Further, carrying a back load has been shown to affect gait kinematics in TTAs, such as smaller trunk and pelvic range of motion (Doyle et al., 2015, 2014; Schnall et al., 2014) and higher metabolic demand compared to individuals without an amputation (Schnall et al., 2012). Using modeling and simulation, an individual TTA demonstrated a higher dependence on their intact limb to compensate for the higher demands of added front and back loads (Templin et al., 2021).

Effects of load carriage have primarily been studied for front and back load conditions, and thus an understanding of gait biomechanics in TTAs when carrying a side load is still poorly understood. Further, it has been demonstrated that walking is most unstable in the mediolateral direction (Dean et al., 2007; McAndrew et al., 2011). Thus, it remains an open question whether side load carriage would exacerbate the already altered gait kinetics in TTAs. Therefore, the objective of this study was to determine which side, intact or prosthetic, TTAs should carry a load by exploring the effects on gait kinetics. We hypothesized that TTAs would exhibit significant differences in GRF peaks and impulses, loading and unloading rates, loading symmetry, and lower limb kinetics (i.e., moments and powers) while carrying a side load compared to unloaded walking. We also hypothesized that the association between these metrics and loading condition would vary depending on which limb side, intact or prosthetic, the load was carried.

2.3 METHODS

2.3.1 Human Subjects

Twelve unilateral TTAs (Table 2.1) provided informed consent to participate in a larger protocol approved by the governing institutional review boards. Prior to testing, all subjects were screened to ensure they were moderately active, had used their prosthesis daily for at least six months, and had no self-reported musculoskeletal (including knee pain) or gait disorders.

Table 2.1 Subject demographic characteristics, in which body mass includes prosthetic components. For other information including prosthetic components, please refer to Tables 3.1 and 4.1.

TTA subject	Age (years)	Sex	Body mass (kg)	Height (m)	Amputation etiology	Amputated limb	Residual limb length (mm)	Time since amputation (years)	Study foot stiffness category	Self-selected walking speed (m/s)
1	59	M	83.5	1.67	Trauma	L	130	15	6	1.16
2	40	M	102.3	1.81	Trauma	L	145	10	7	1.67
3	60	M	111.9	1.80	Trauma	R	150	3	7	1.30
4	58	F	96.6	1.69	Congenital	R	190	5	6	1.12
5	39	M	105.7	1.71	Trauma	R	150	12	7	1.43
6	25	F	52.6	1.56	Congenital	R	155	24	2	1.37
7	43	M	107.0	1.82	Infection	L	220	1	7	1.32
8	31	M	98.5	1.83	Trauma	R	[a]	11	7	1.26
9	36	M	110.4	1.86	Trauma	R	200	15	7	1.20
10	29	M	83.9	1.64	Trauma	L	130	3	6	1.16
11	53	M	106.6	1.86	Dysvascular	L	170	7	7	0.92
12	75	M	93.6	1.83	Trauma	L	165	55	7	1.17
Mean (SD)	46 (15)	-	96.1 (16.6)	1.76 (0.10)	-	-	164 (29)	13 (15)	-	1.26 (0.19)

[a] Not measured.

2.3.2 Instrumentation

All subjects wore a study-provided passive-elastic prosthetic foot (Sierra; Freedom Innovations, Irvine, CA). To add a side load, subjects donned a padded carrier (Ergobaby, Torrance, CA) to carry a cylindrical pack filled with sand for a total added mass of 13.6 kg (30 lbs.). This mass was chosen because it exceeded a 10 kg range, for which an immediate stiffness category change to the study prosthetic foot would be recommended if the additional mass was permanent. Additionally, it simulated a common load carried over one shoulder or hip during walking, such as objects carried in a non-sedentary occupation (> 5 kg) (National Bureau of Economic Research, 2016), a toddler (ages 1-2 years) (National Center for Health Statistics, 2021), grocery items, or a sling bag.

Five embedded force plates (AMTI, Watertown, MA) were used to capture three-dimensional GRFs. A 16-camera motion capture system (Vicon Motion Systems, Oxford, UK) recorded marker trajectories at 120 Hz and force plate data at 1,200 Hz. All subjects were provided with tight-fitting clothing to wear during data collection. The same researcher placed 14 mm reflective tracking markers on each subject using Vicon's standard Plug-in-Gait marker configuration, with additional markers placed bilaterally on the medial elbow, medial knee epicondyle, medial malleolus, tibial tuberosity, fibular head, and first and fifth metatarsal heads. Clusters of four markers were also placed bilaterally on the upper arms and thighs. The markers on the prosthetic limb mirrored the intact limb. Lastly, three markers were placed to define the load segment (two on top, one on bottom). During loaded conditions, any physical markers obstructed by the load carrier were removed, and virtual markers were reconstructed using a digitizing procedure during post-processing.

2.3.3 Experimental Protocol

The first study visit was for acclimation and prosthesis fitting. During this study visit, self-selected walking speed was measured over four repeated trials along a 14m straight hallway while subjects wore their own as-prescribed prosthesis. Subject height, body mass, and anthropometrics were also measured. The study prosthetic foot was then fit and aligned by a certified prosthetist using standard clinical procedures. Subjects walked for up to 15 minutes to acclimate to each load condition: no load (NL), intact-side load carriage (IL), and prosthetic-side load carriage (PL) (Fig. 2.1).

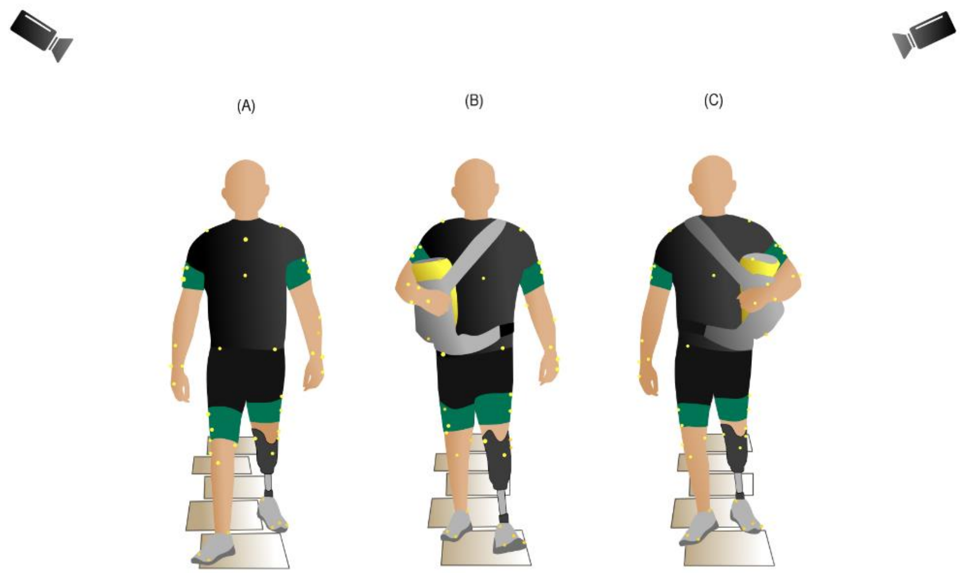

Fig 2.1 An illustration of a TTA subject walking overground across five embedded force plates during (A) no load (NL) (B) intact-side load (IL) (C) prosthetic-side load (PL) conditions.

For the second study visit, the load conditions were randomized for each subject. Subjects were fit with the study prosthesis, and then reflective markers were placed. Subjects walked at their self-selected speed across the five embedded force plates for a minimum of two repeated trials per condition. Subjects were allowed adequate rest as needed.

2.3.4 Data Analysis

Raw marker trajectory data were filtered in Vicon Nexus software (Vicon Motion Systems, Oxford, UK) using a Woltring filter with a mean-square-error value of 10 mm^2, based on a fifth-order spline-interpolating function (Woltring, 1986). GRF and lower-limb joint kinetic data were processed and calculated in Visual 3D software (C-Motion, Germantown, USA) with a 15-segment whole-body model (i.e., head, torso, Visual 3D Composite pelvis, and bilateral upper arm, forearm, hand, thigh, shank, and foot; plus, a load segment when applicable). Each segment's mass was estimated as a percentage of whole-body (Dempster, 1995), and the inertial properties and center of mass positions were based on geometric approximations calculated in Visual 3D. The prosthetic shank mass was reduced to 35% of the intact shank, and the prosthetic center of mass location was moved 35% closer to the knee joint (Smith et al., 2014). All metrics were calculated for both the intact and prosthetic limbs. Heel strike and toe off events were automatically detected based on a force plate loading threshold of 25 N. These events were also inspected visually, confirming them with kinematic patterns. GRF data included Fx (mediolateral component), Fy (anteroposterior component), and Fz (vertical component). Anterior positive and posterior negative GRF represent propulsive and braking forces, respectively. GRF data were filtered using a digital, fourth order, low-pass Butterworth filter with a cut-off frequency of 25 Hz and normalized by the subject's body mass (kg) for all NL, IL, and PL, including the added side load for IL and PL. Each GRF impulse was determined by time integrating the corresponding GRF component. Loading and unloading rates (Fig. 2.2) were calculated from vertical GRF (vGRF) curves using a similar method used in other studies (Crowell et al., 2010; Ueda et al., 2016). This method was chosen as it uses the most linear portions of vGRF curves during stance phase. Joint kinetics including hip and knee moments and powers were calculated using inverse dynamics techniques. The joint kinetic profiles were labeled for specific bursts of energy absorption and generation (for powers) and peaks (for moments) (Winter and Sienko, 1988). Ankle power was calculated using the unified deformable segment method (Takahashi et al., 2012). Further data analysis was performed using MATLAB software (The MathWorks Inc., Natick, MA, USA).

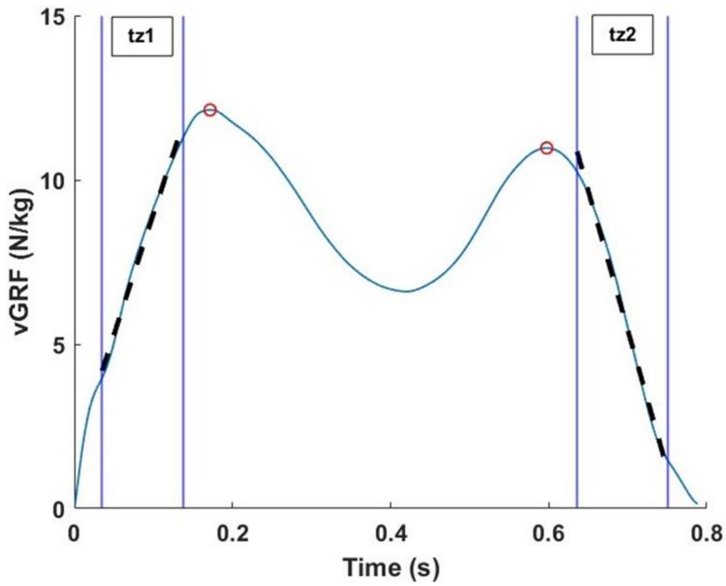

Fig 2.2 A representative vertical GRF (vGRF) curve from which loading and unloading rates were calculated. In the figure, tz1: loading period that occurs from heel strike to the first peak vGRF (first red dot), and tz2: unloading period that occurs from the second peak vGRF (second red dot) to toe-off. Loading and unloading rates were estimated as the slope of $vGRF_{max}$ (first black dashed line) over 20-80% time window of tz1 (first blue vertical lines), and as the slope of $vGRF_{max}$ (second black dashed line) over 20-80% time window of tz2 (second blue vertical lines), respectively.

$$\text{Loading rates} = \frac{\Delta vGRF1_{max}}{\Delta t(20\% < tz1 < 80\%)} \quad \text{(eq.1)}$$

$$\text{Unloading rates} = \frac{\Delta vGRF2_{max}}{\Delta t(20\% < tz2 < 80\%)} \quad \text{(eq.2)}$$

Loading symmetry was calculated by estimating the bilateral symmetry index (Cutti et al., 2018), where a value of 1 represents perfect symmetry.

$$\text{vGRF Impulse Symmetry Index} = \frac{\text{vGRF Impulse (intact)}}{\text{vGRF Impulse (prosthetic)}} \quad \text{(eq.3)}$$

$$\text{First Peak Symmetry Index} = \frac{\text{first peak vGRF (intact)}}{\text{first peak vGRF (prosthetic)}} \quad \text{(eq.4)}$$

Similarly, stance time symmetry (the period in which loading occurred) was also calculated.

2.3.5 Statistical Methods

Linear mixed-effects regression was used to test for an association between metric (the dependent variable) and load conditions (NL, IL, or PL) for each limb (intact vs. prosthetic), by modeling a load by limb interaction. The load by limb interaction terms allowed estimation of pairwise differences between NL vs. IL, NL vs. PL, and IL vs. PL for each limb. A random intercept for each subject was included to account for overall variability in outcomes across subjects. Random effects were also modeled to allow differences across loads to vary by limb within subject if these estimates could be obtained, otherwise, simpler random effects were modeled. Variance heterogeneity was assessed using plots of residuals against the fitted values, with variance stabilizing transformations of the dependent variable (e.g., logs) considered if necessary. Hypothesis testing was carried out using F-tests for the association between metric and load for each limb, as well as the difference in the association between metric and load by limb by testing for the significance of the load by limb interaction term. The significance of pairwise comparisons between load conditions was assessed using t-tests. The Benjamini-Hochberg correction for multiple testing (Benjamini and Hochberg, 1995) was applied to hypothesis tests for differences in kinetic metrics by limb for each load condition separately, and to interaction effects, to restrict the false discovery rate of the rejected hypotheses to 0.05. A statistical significance level was set at an $\alpha < 0.05$. Pairwise mean differences between load conditions were reported to represent corresponding effect sizes, and 95% confidence intervals for pairwise comparisons were presented. All statistical analyses were carried out using R 4.3.0 software (R Foundation for Statistical Computing, Vienna, Austria, 2023) and packages tidyverse, lme4 and emmeans.

2.4 RESULTS

2.4.1 GRF-related Metrics

Within limb comparisons showed that the intact limb had a smaller peak propulsive force in PL compared to NL (pairwise mean difference, p-value [confidence interval]) (0.21 N/kg, $p < 0.01$ [0.06, 0.33]). No strong evidence of associations between load and GRF-related metrics or interaction effects were observed (Table 2.2 and Fig. 2.3). Additionally, pairwise comparisons for bilateral loading symmetry showed no significant differences between load conditions (Fig. .2.4).

No change was observed in subjects' self-selected walking speed across load conditions.

Table 2.2 Mean (Standard Error) GRF-related metrics and within limb comparisons for intact and prosthetic limbs. Data are presented and compared according to leading intact and prosthetic limbs. **Bolded** p-values with an asterisk (*) indicate statistical significance (shading for clarity). Pairwise p-values indicate statistical significance for pairwise comparisons between load conditions (NL vs. IL, NL vs. PL, and IL vs. PL). Abbreviations: (NL) no load condition, (IL) intact-side load condition, (PL) prosthetic-side load condition, (GRF) ground reaction force.

Metrics	**Units**	**Mean (Standard Error)**								**Pairwise p-value [95% confidence interval]**						**p-value**
		Intact Limb				**Prosthetic Limb**				**Intact Limb**			**Prosthetic Limb**			**Interaction (Load*Limb)**
		NL	**IL**	**PL**	**p-value**	**NL**	**IL**	**PL**	**p-value**	**NL vs. IL**	**NL vs. PL**	**IL vs. PL**	**NL vs. IL**	**NL vs. PL**	**IL vs. PL**	
First peak vertical GRF	N/kg	11.74 (0.27)	11.72 (0.30)	11.36 (0.30)	0.21	10.61 (0.27)	10.13 (0.30)	10.74 (0.31)	0.09	0.99 [-0.43, 0.48]	0.09 [-0.05, 0.81]	0.26 [-0.19, 0.90)	**0.03*** [**0.04, 0.91**]	0.76 [-0.60, 0.34]	**0.03*** [-**1.17, -0.04**]	0.13
Peak propulsive force		2.05 (0.15)	1.85 (0.12)	1.84 (0.14)	**0.04***	1.53 (0.15)	1.41 (0.12)	1.39 (0.14)	0.18	0.07 [-0.001, 0.041]	**<0.01*** [**0.06, 0.33**]	0.99 [-0.14,0.13]	0.31 [-0.08,0.33]	0.06 [-0.01,0.27]	0.97 [-0.12,0.14]	0.79
Peak braking force		-1.88 (0.12)	-1.76 (0.13)	-1.94 (0.13)	0.61	-1.22 (0.12)	-1.12 (0.13)	-1.27 (0.14)	0.71	0.69 [-0.47,0.23]	0.91 [-0.28,0.39]	0.47 [-0.19,0.54]	0.75 [-0.45,0.24]	0.94 [-0.32,0.41]	0.59 [-0.23, 0.53]	0.99
Loading rates	N/kg/s	8.03 (0.71)	8.07 (0.73)	7.94 (0.72)	0.97	6.91 (0.72)	6.18 (0.72)	7.52 (0.75)	0.18	1.00 [-1.30, 1.22]	0.98 [-1.13, 1.31]	0.97 [-1.16, 1.42]	0.33 [-0.50, 1.95]	0.50 [-1.93, 0.71]	**0.05*** [-**2.65, -0.01**]	0.43
Unloading rates		-9.00 (0.69)	-8.13 (0.70)	-7.77 (0.69)	0.21	-7.96 (0.69)	-7.80 (0.69)	-7.82 (0.72)	0.97	0.30 [-2.26, 0.53]	0.08 [-2.59, 0.13]	0.81 [-1.76, 1.04]	0.96 [-1.52, 1.20]	0.97 [-1.58, 1.31]	1.00 [-1.43, 1.47]	0.64
Vertical impulse	Ns/kg	5.81 (0.17)	5.80 (0.17)	5.74 (0.16)	0.93	5.26 (0.17)	5.26 (0.17)	5.32 (0.17)	0.90	0.99 [-0.24, 0.27]	0.95 [-0.30, 0.23]	0.88 [-0.27, 0.19]	1.00 [-0.25, 0.25]	0.87 [-0.34, 0.22]	0.82 [-0.30, 0.18]	0.99
Propulsive impulse		0.36 (0.02)	0.34 (0.02)	0.35 (0.02)	0.08	0.24 (0.02)	0.23 (0.02)	0.22 (0.02)	0.34	**0.02*** [**0.00, 0.04**]	0.12 [0.00, 0.03]	0.49 [-0.03, 0.01]	0.53 [-0.01, 0.03]	0.19 [0.00, 0.03]	0.84 [-0.02,0.02]	0.64
Braking impulse		-0.33 (0.02)	-0.33 (0.02)	-0.34 (0.02)	0.93	-0.25 (0.02)	-0.23 (0.02)	-0.25 (0.02)	0.74	0.93 [-0.04, 0.05]	0.87 [-0.03, 0.05]	0.99 [-0.04, 0.05]	0.65 [-0.06, 0.03]	0.99 [-0.05, 0.05]	0.76 [-0.03, 0.06]	0.79
Mediolateral impulse		0.24 (0.04)	0.29 (0.04)	0.24 (0.04)	0.31	0.13 (0.04)	0.19 (0.04)	0.19 (0.04)	0.43	0.49 [-0.16, 0.06]	0.99 [-0.08, 0.09]	0.18 [-0.02, 0.13]	0.42 [-0.16, 0.05]	0.26 [-0.15,0.03]	0.99 [-0.08, 0.07]	0.44

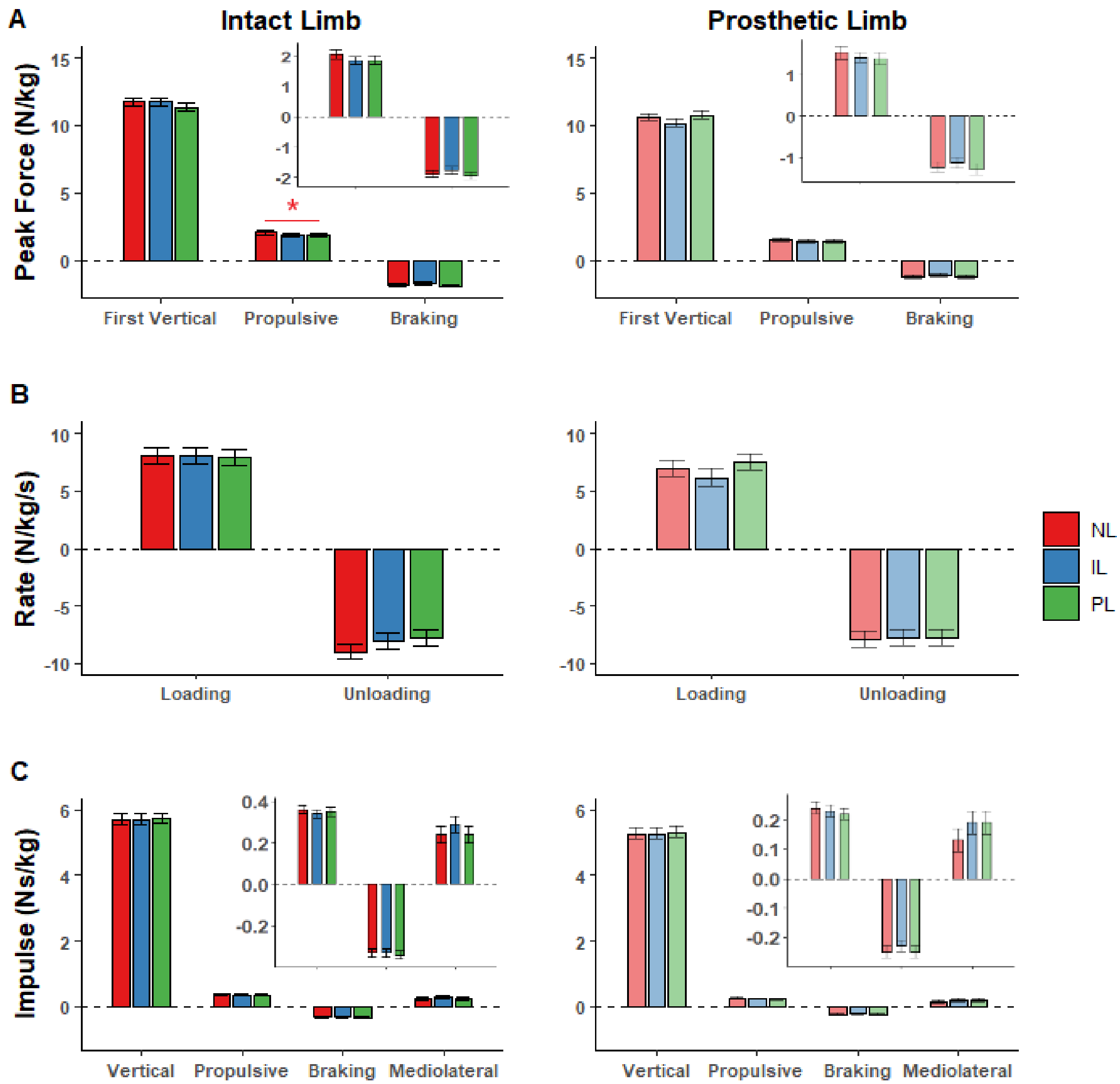

Fig 2.3 Within limb comparisons of GRF-related metrics between load conditions for intact limb and prosthetic limb for (A) First peak vGRF, Peak propulsive force, and peak braking force (B) Loading and unloading rates, and (C) Vertical, propulsive, braking, and mediolateral impulses. Asterisk signs represent significant differences between load conditions: (*) indicates $p < 0.05$. NL: no load condition, IL: intact-side load condition, PL: prosthetic-side load condition.

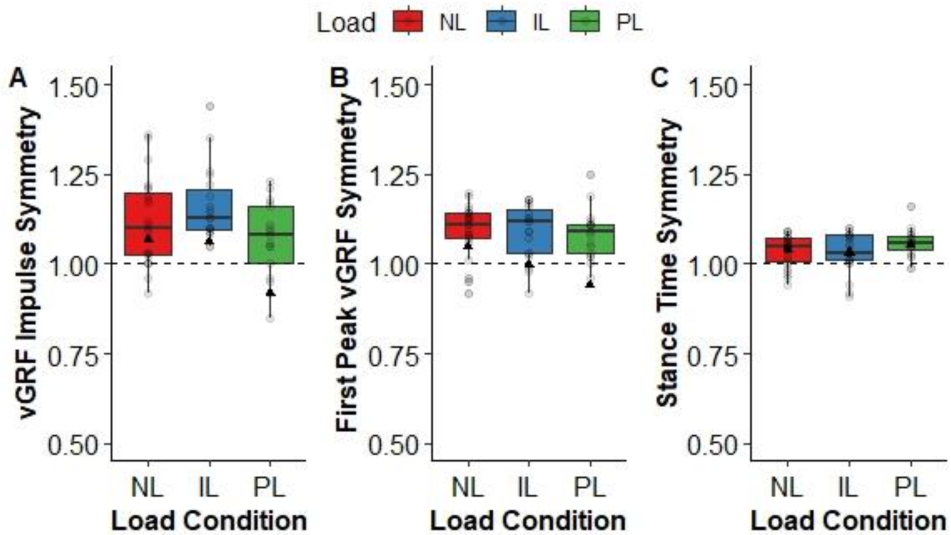

Fig 2.4 Pairwise comparisons between load conditions for loading symmetry index of (A) Vertical impulse and (B) First peak vGRF, and for temporal symmetry index of (C) Stance time. Black triangles represent mean values and dash lines at y-axis = 1 represent perfect bilateral symmetry. Asterisk signs represent significant differences between load conditions: (*) indicates $p < 0.05$. NL: no load condition, IL: intact-side load condition, PL: prosthetic-side load condition.

2.4.2 Joint Kinetic Metrics

For joint power, within limb comparisons revealed a higher intact limb hip extensor power at weight acceptance (HP1) in IL compared to NL (0.32 W/kg, $p < 0.01$ [-0.51, -0.13]). The intact limb also had marginally smaller hip flexor power at push-off (HP3) in PL by 0.18 W/kg compared to NL ($p < 0.01$ [0.1, 0.3]) (Table 2.3 and Fig. 2.5). The prosthetic limb had a higher hip extensor power at weight acceptance (HP1) in PL compared to NL (0.39 W/kg, $p < 0.01$ [-0.54, -0.23]). The prosthetic limb also exhibited smaller hip flexor power (HP2) in PL compared to NL (0.19 W/kg, $p < 0.01$ [-0.32, -0.06]). Additionally, the prosthetic limb exhibited smaller hip flexor power at push-off (HP3) in IL by 0.25 W/kg compared to NL ($p < 0.01$ [0.1, 0.4]) (Table 2.3 and Fig. 2.5).

Within limb comparisons for sagittal-plane joint moments showed a smaller intact limb hip flexor moment in the stance-swing transition (HM2) in IL (0.18 Nm/kg, $p < 0.01$ [-0.3, -0.06]) and PL (0.16 Nm/kg, $p < 0.01$ [-0.23, -0.08]) compared to NL. The intact limb also had marginally smaller knee flexor moment at the end of swing (KM2) in IL compared to NL (0.07 Nm/kg, $p = 0.01$ [-0.12, -0.01]). The prosthetic limb had smaller hip flexor moment in the stance-swing transition (HM2) in PL by 0.15 Nm/kg compared to NL ($p < 0.01$ [-0.23, -0.07]). (Table 2.3 and Fig. 2.6). Interestingly, within limb comparisons showed differences in most frontal-plane joint moments. The intact limb had higher hip abductor moment in early (HMf1) (0.27 Nm/kg, $p = 0.01$ [-0.45, -0.08]) and late (HMf2) (0.22 Nm/kg, $p < 0.01$ [-0.34, -0.11]) stance in PL compared to NL. Knee abductor moment in early (KMf1) and late (KMf2) stance was also higher by 0.1 Nm/kg ($p = 0.01$ [-0.16, -0.02]) and 0.06 Nm/kg ($p = 0.05$ [-0.12, -0.00]), respectively, in PL compared to NL. Similarly, the prosthetic limb had 0.14 Nm/kg higher hip abductor moment in early stance (HMf1) ($p = 0.02$ [-0.26, -0.02]) and 0.14 Nm/kg higher hip abductor moment in late stance (HMf2) ($p < 0.01$ [-0.23, -0.05]) in IL compared to NL. Additionally, knee abductor moment in early (KMf1) and late (KMf2) stance were higher in IL compared to NL (0.08 Nm/kg, $p = 0.03$ [-

0.15, -0.01] and $p < 0.01$ [-0.14, -0.03], respectively) (Table 2.3 and Fig. 2.6). All other joint kinetic metrics were not different across load conditions, and no strong evidence of associations between load and these other metrics were observed (Table 2.3).

A significant interaction effect ($p < 0.01$) was observed for hip extensor power at weight acceptance (HP1) due to the higher hip power generation associated with the limb that carried the load. Significant interactions were also observed for hip abductor moment in early (HMf1) and late (HMf2) stance, and knee abductor moment in early (KMf1) and late (KMf2) stance due to the higher abductor moment on the contralateral limb with respect to the load side (Table 2.3).

To supplement our findings for kinetic metrics, a figure showing the intact and prosthetic hip and knee angles during NL, IL, and PL conditions is provided in the Supplementary Material. Consistent with the kinetic results, the intact and prosthetic hip and knee kinematics during no load and loaded conditions demonstrate less variability in the sagittal plane than the frontal plane (see Fig. 2.6 A2).

Table 2.3 Mean (Standard Error) sagittal peak joint power, sagittal and frontal peak joint moment metrics and within limb comparisons for intact and prosthetic limbs. Data are presented and compared according to leading intact and prosthetic limbs. **Bolded** p-values with an asterisk (*) indicate statistical significance (shading for clarity). Pairwise p-values indicate statistical significance for pairwise comparisons between load conditions (NL vs. IL, NL vs. PL, and IL vs. PL). Abbreviations: (NL) no load condition, (IL) intact-side load condition, (PL) prosthetic-side load condition, (HP) hip power, (KP) knee power, (AP) ankle power, (HM) hip moment, (KM) knee moment.

Metrics	Units	Mean (Standard Error)								Pairwise p-value [95% confidence interval]						p-value
		Intact Limb				Prosthetic Limb				Intact Limb			Prosthetic Limb			Interaction (Load*Limb)
		NL	IL	PL	p-value	NL	IL	PL	p-value	NL vs. IL	NL vs. PL	IL vs. PL	NL vs. IL	NL vs. PL	IL vs. PL	
Sagittal Power																
HP1 (generation)		0.35 (0.1)	0.68 (0.1)	0.36 (0.1)	**0.01***	0.67 (0.1)	0.51 (0.1)	1.06 (0.1)	**<0.01***	**<0.01* [-0.51, -0.13]**	1 [-0.14, 0.14]	**0.02* [0.1, 0.6]**	0.08 [-0.02, 0.34]	**<0.01* [-0.54, -0.23]**	**<0.01* [-0.8, -0.3]**	**<0.01***
HP2 (absorption)		-0.39 (0.08)	-0.27 (0.06)	-0.31 (0.05)	0.3	-0.5 (0.08)	-0.36 (0.06)	-0.31 (0.06)	**0.04***	0.17 [-0.29, 0.04]	0.26 [-0.21, 0.04]	0.7 [-0.1, 0.2]	0.11 [-0.29, 0.02]	**<0.01* [-0.32, -0.06]**	0.54 [-0.2, 0.1]	0.48
HP3 (generation)		0.83 (0.1)	0.83 (0.1)	0.65 (0.1)	**0.05***	0.88 (0.1)	0.64 (0.1)	0.83 (0.1)	**0.01***	1 [-0.2, 0.2]	**<0.01* [0.1, 0.3]**	0.08 [-0.02, 0.39]	**<0.01* [0.1, 0.4]**	0.68 [-0.1, 0.2]	0.05 [-0.4, 0.0]	0.11
KP1 (absorption)		-1.1 (0.15)	-1.09 (0.16)	-0.89 (0.15)	0.18	-0.35 (0.15)	-0.29 (0.15)	-0.45 (0.16)	0.43	-0.99 [-0.26, 0.23]	0.08 [-0.44, 0.02]	0.14 [-0.4, 0.1]	0.82 [-0.28, 0.17]	0.59 [-0.15, 0.34]	0.27 [-0.1, 0.4]	0.19
KP2 (generation)	W/kg	0.75 (0.08)	0.59 (0.09)	0.58 (0.08)	0.22	0.24 (0.08)	0.09 (0.08)	0.16 (0.09)	0.34	0.18 [-0.05, 0.37]	0.11 [-0.03, 0.38]	0.98 [-0.2, 0.2]	0.17 [-0.05, 0.35]	0.61 [-0.13, 0.29]	0.71 [-0.3, 0.1]	0.82
KP3 (absorption)		-0.97 (0.16)	-1.05 (0.19)	-1.07 (0.14)	0.43	-1.06 (0.16)	-1.17 (0.19)	-1.05 (0.14)	0.56	0.73 [-0.2, 0.4]	0.31 [-0.1, 0.3]	0.99 [-0.3, 0.3]	0.48 [-0.1, 0.4]	0.97 [-0.2, 0.2]	0.46 [-0.4, 0.1]	0.68
KP4 (absorption)		-1.26 (0.09)	-1.16 (0.09)	-1.29 (0.09)	0.25	-0.94 (0.09)	-0.88 (0.09)	-0.83 (0.09)	0.34	0.26 [-0.26, 0.05]	0.87 [-0.12, 0.18]	0.11 [-0.02, 0.29]	0.54 [-0.21, 0.08]	0.18 [-0.27, 0.04]	0.7 [-0.2, 0.1]	0.36
AP1 (absorption)		-0.99 (0.09)	-1.03 (0.1)	-1.05 (0.09)	0.81	-1.21 (0.09)	-1.14 (0.09)	-1.31 (0.1)	0.34	0.93 [-0.2, 0.3]	0.8 [-0.2, 0.3]	0.97 [-0.2, 0.25]	0.69 [-0.3, 0.1]	0.49 [-0.1, 0.3]	0.14 [-0.1, 0.4]	0.68
AP2 (generation)		2.61 (0.23)	2.57 (0.24)	2.41 (0.23)	0.25	1.64 (0.23)	1.62 (0.23)	1.61 (0.24)	0.99	0.92 [-0.2, 0.3]	0.13 [-0.1, 0.5]	0.31 [-0.1, 0.4]	0.99 [-0.2, 0.3]	0.97 [-0.2, 0.3]	0.99 [-0.2, 0.3]	0.68
Sagittal Moment																
HM1 (extension)	Nm/kg	0.45 (0.06)	0.49 (0.06)	0.47 (0.09)	0.61	0.49 (0.06)	0.5 (0.06)	0.56 (0.09)	0.56	0.47 [-0.11, 0.04]	0.93 [-0.14, 0.11]	0.93 [-0.1, 0.2]	0.97 [-0.08, 0.07]	0.42 [-0.2, 0.07]	0.52 [-0.2, 0.1]	0.72
HM2 (flexion)		-0.7 (0.07)	-0.52 (0.06)	-0.55 (0.07)	**<0.01***	-0.7 (0.07)	-0.6 (0.06)	-0.55 (0.07)	**<0.01***	**<0.01* [-0.3, -0.06]**	**<0.01* [-0.23, -0.08]**	0.75 [-0.1, 0.1]	0.11 [-0.21, 0.02]	**<0.01* [-0.23, -0.07]**	0.29 [-0.13, 0.03]	0.56

HM3 (extension)		0.4 (0.04)	0.36 (0.04)	0.4 (0.04)	0.43	0.38 (0.04)	0.33 (0.04)	0.3 (0.04)	0.08	0.31 [-0.03, 0.12]	0.99 [-0.07, 0.08]	0.39 [-0.12, 0.03]	0.17 [-0.02, 0.12]	**0.02* [0.01, 0.16]**	0.47 [-0.03, 0.1]	0.36
KM1 (extension)		0.89 (0.06)	0.81 (0.07)	0.77 (0.06)	0.12	0.43 (0.06)	0.36 (0.06)	0.43 (0.07)	0.34	0.2 [-0.03, 0.2]	**0.03* [0.01, 0.23]**	0.74 [-0.08, 0.15]	0.25 [-0.04, 0.18]	1 [-0.11, 0.12]	0.31 [-0.18, 0.04]	0.48
KM2 (flexion)		-0.31 (0.02)	-0.24 (0.02)	-0.3 (0.02)	**0.05***	-0.27 (0.02)	-0.23 (0.02)	-0.22 (0.02)	0.18	**0.01* [-0.12, -0.01]**	0.85 [-0.06, 0.04]	**0.04* [0.00, 0.11]**	0.15 [-0.09, 0.01]	0.08 [-0.1, 0.01]	0.9 [-0.06, 0.04]	0.36
Frontal Moment																
HMf1 (abduction)	Nm/kg	0.91 (0.07)	0.60 (0.06)	1.18 (0.05)	**<0.01***	0.74 (0.07)	0.88 (0.06)	0.39 (0.05)	**<0.01***	**<0.01* [0.18, 0.44]**	**0.01* [-0.45, -0.08]**	**<0.01* [-0.72, -0.43]**	**0.02* [-0.26, -0.02]**	**<0.01* [0.16, 0.54]**	**<0.01* [0.35, 0.64]**	**<0.01***
HMf2 (abduction)		0.72 (0.06)	0.47 (0.05)	0.94 (0.04)	**<0.01***	0.67 (0.06)	0.81 (0.05)	0.39 (0.05)	**<0.01***	**<0.01* [0.15, 0.35]**	**<0.01* [-0.34, -0.11]**	**<0.01* [-0.58, -0.37]**	**<0.01* [-0.23, -0.05]**	**<0.01* [0.17, 0.42]**	**<0.01* [0.33, 0.54]**	**<0.01***
KMf1 (abduction)		0.36 (0.03)	0.25 (0.04)	0.46 (0.03)	**<0.01***	0.23 (0.03)	0.31 (0.03)	0.14 (0.04)	**<0.01***	**<0.01* [0.04, 0.19]**	**0.01* [-0.16, -0.02]**	**<0.01* [-0.28, -0.13]**	**0.03* [-0.15, -0.01]**	**0.01* [0.02, 0.17]**	**<0.01* [0.10, 0.25]**	**<0.01***
KMf2 (abduction)		0.31 (0.03)	0.24 (0.03)	0.37 (0.03)	**<0.01***	0.12 (0.03)	0.20 (0.03)	0.09 (0.03)	**<0.01***	**0.01* [0.02, 0.12]**	**0.05* [-0.12, -0.00]**	**<0.01 [-0.18, -0.08]**	**<0.01* [-0.14, -0.03]**	0.57 [-0.04, 0.09]	**<0.01* [0.05, 0.17]**	**<0.01***

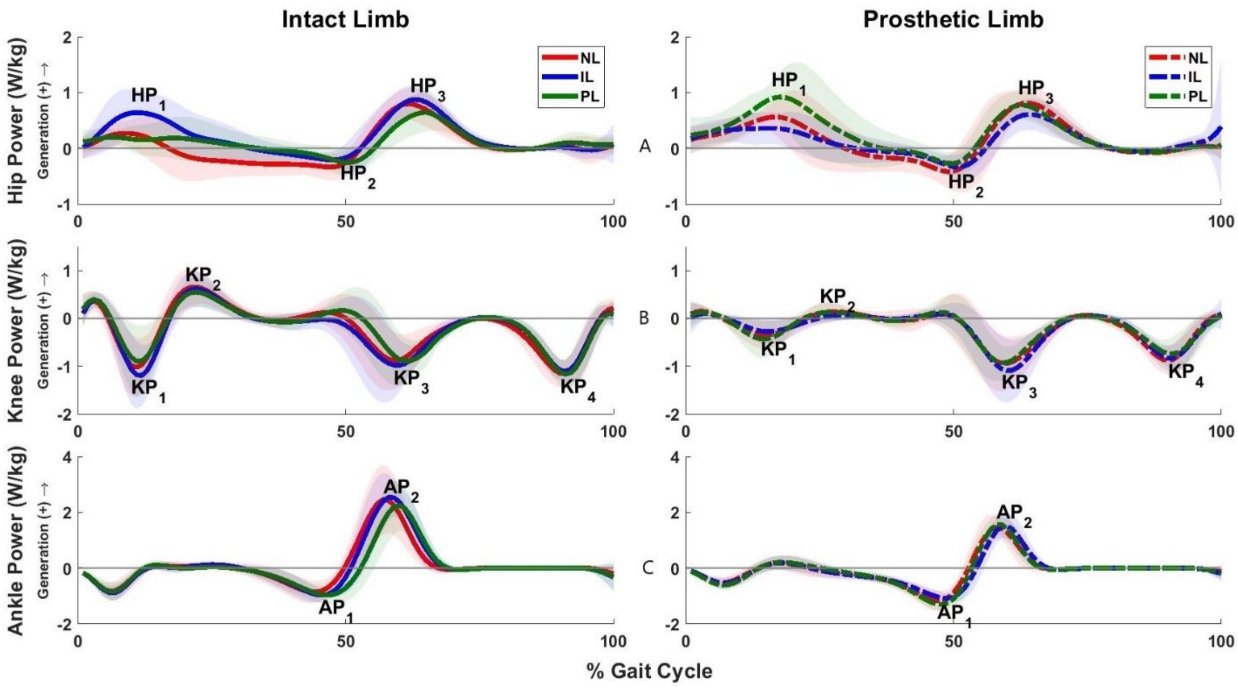

Fig 2.5 Mean sagittal joint power profiles at the (A) hip, (B) knee, and (C) ankle for the intact (solid lines) and prosthetic (dashed lines) limbs in NL, IL, and PL. Power generation indicating concentric muscle contraction is positive. NL: no load condition, IL: intact-side load condition, PL: prosthetic-side load condition.

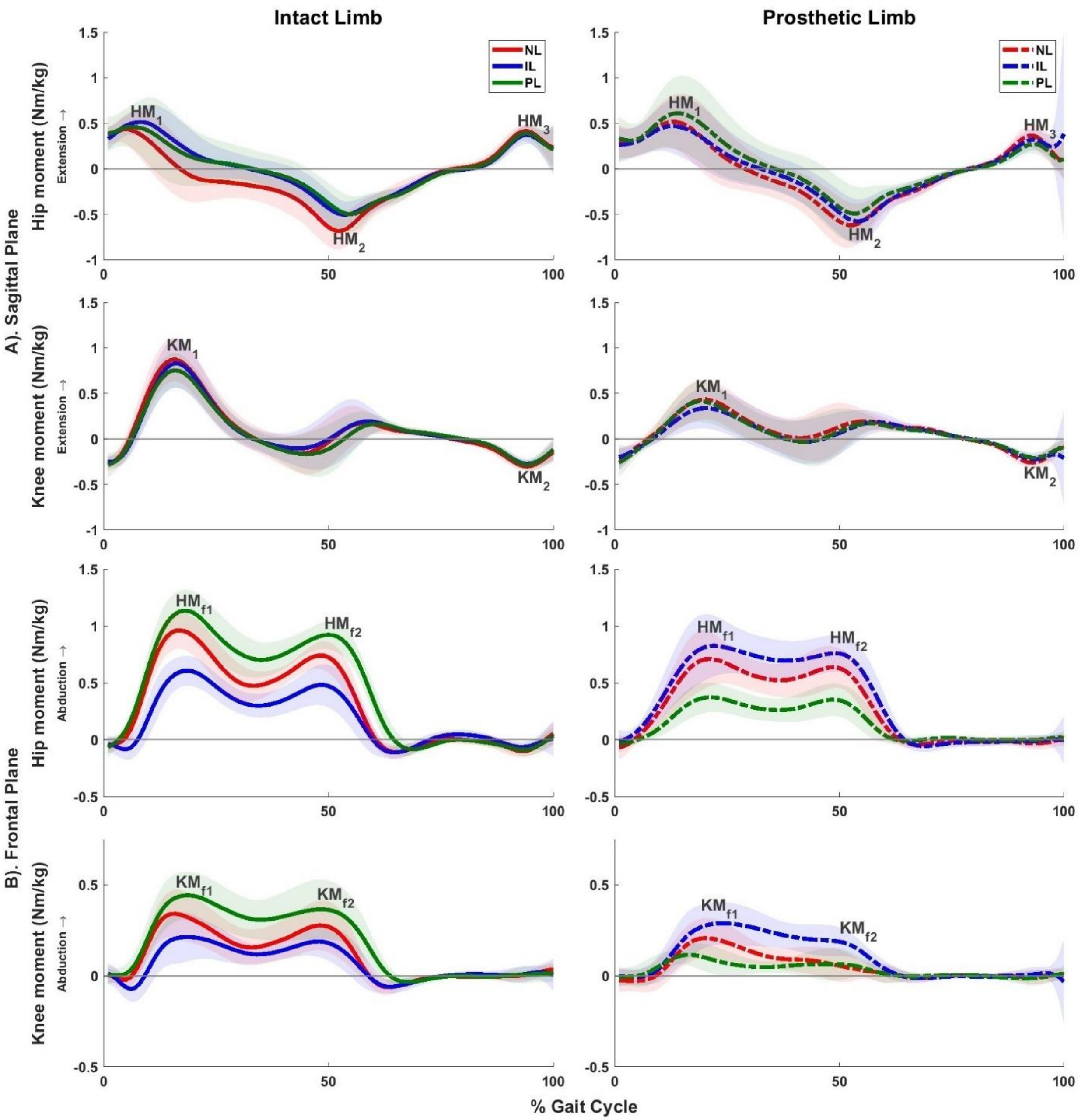

Fig 2.6 A). Mean sagittal internal joint moments and B). Mean frontal internal joint moments at the hip and knee for the intact (solid lines) and prosthetic (dashed lines) limbs in NL, IL, and PL. Extensor and abductor moments are positive. NL: no load condition, IL: intact-side load condition, PL: prosthetic-side load condition.

2.5 DISCUSSION

The objective of this study was to determine which side, intact or prosthetic, TTAs should carry a load by exploring loading effects on their gait kinetics. TTAs were found to have a smaller peak propulsive force on their intact limb while carrying a load on their prosthetic side, compared to unloaded walking. The activity of ankle plantarflexors (i.e., gastrocnemius and soleus) may explain this effect. Previous research has shown that these muscles act to rotate the body towards the contralateral side and provide frontal plane balance control in late stance (Neptune and McGowan, 2016). With the added contralateral load, the ankle plantarflexor activity would need to decrease rotating the body towards the swinging (prosthetic) limb that is further assisted by gravity, leading to smaller propulsion.

Findings from joint powers showed that TTAs had a higher hip extensor power generation at weight acceptance on the limb carrying the load, compared to unloaded walking. They also had a smaller power generated by hip flexors at push-off in the opposite-side load condition. When the load was carried on the prosthetic side, TTA subjects had a smaller power absorbed by hip flexors on the prosthetic limb compared to unloaded walking. These results suggest that higher hip extensor power generation and smaller hip flexor power absorption are observed on the loaded limb. A significant interaction effect for powers indicates that the higher extensor power generation at weight acceptance was associated with the ipsilateral side load. The hip muscles are known to be important contributors to the dynamic balance of the head-arms-trunk segment. For example, adductor magnus and hamstring muscles act similar to plantarflexors in controlling frontal plane balance (Neptune and McGowan, 2016). During early stance, the activity of the biarticular hamstrings would rotate the body toward the contralateral limb, generating higher hip extensor power on the ipsilateral limb with the added load. By contrast, other studies demonstrate smaller hip extensor power generation at weight acceptance on both limbs when TTAs walk with a back load (Doyle et al., 2014), suggesting that kinetic response at the hip may vary depending on the location of the added load.

TTAs had a smaller hip flexor moment in the stance-swing transition on their intact limb during side loaded conditions compared to unloaded condition. Further, they had 23% smaller knee flexor moment on their intact limb at the end of swing during the intact-side load condition compared to the prosthetic-side loaded and unloaded conditions. This phenomenon may be explained by prolonged activity in the ipsilateral vastus lateralis throughout swing phase, observed in non-amputee individuals carrying hand-held and back loads (20-50% body mass) (Ghori and Luckwill, 1985). Significant prolongation of the knee extensors activity to increase body support for the extra load may contribute to the decrease in knee flexor moment. A similar trend was also observed in TTA walking with a back load as they reduced knee flexor moment by 20% on their prosthetic limb compared to no load condition (Doyle et al., 2014). A surprising result was the absence of a knee extensor response with the added loads. Prior research has shown that the knee extensors act to rotate the body towards the swing leg (Neptune and McGowan, 2016). However, with the added load comes an increased demand for body support, provided by the knee extensors. Thus, it appears the intact hip abductor moment was sufficient to offset the rotation caused by the intact side load.

A significant interaction for moments showed that hip abductor moments on the intact limb and prosthetic limb increased the most in early and late stance during the prosthetic side and intact side load conditions, respectively. These findings are consistent with previous work suggesting that a contralateral load requires higher hip abductor activity on the contralateral side due to higher internal torque demand (Neumann et al., 1992; Neumann and Hase, 1994), and that hip abductor (gluteus medius) is a primary contributor to body support and a regulator of frontal plane balance control that acts to rotate the body towards the ipsilateral limb (Neptune and McGowan, 2016) to counteract the added side load.

2.5.1 Limitations

Certain limitations should be acknowledged while interpreting these results. First, these data are from a relatively small sample of mostly male, traumatic TTAs. While statistical significance was found for some outcome metrics, more subjects would be needed to generalize these results to a larger TTA population, including those with diabetic/dysvascular etiology (for whom load carriage may induce fatigue). These results may not generalize to transfemoral amputees who adopt different gait compensatory strategies (Varrecchia et al., 2019) due to greater musculoskeletal loss. For instance, those with osseointegrated prostheses have improved static balance (Gaffney et al., 2023) but maintain loading asymmetry (Thomsen et al., 2024). Second, we used an added load that exceeded the 10 kg range for which an immediate change to a stiffer prosthetic foot would be recommended, and to simulate a typical side load carried by individuals with and without TTA in daily activities. However, this load was not as heavy as those reported by other studies in individuals without amputation (Wang et al., 2012) and TTAs (Doyle et al., 2015, 2014). Higher loads (e.g., >20% body mass) that are typically required for military activities may yield more significant differences in GRF parameters. Next, we only included a passive elastic prosthetic foot in the analysis of this current study. This foot was selected to reflect the standard-of-care feet. This is a realistic scenario in which most TTAs do not have adapting feet, and this is what they would experience in their daily lives. Further, we selected this foot to avoid potential confounds due to differing prosthetic systems and foot designs that may influence GRF (Snyder et al., 1995). However, we acknowledge that the constant stiffness characteristics of the study prosthetic foot represent a substantial limitation in functionality. There could be potential benefits of a more versatile prosthetic foot design for load carriage applications that were not explored here. Additionally, while we discussed the kinetic changes in this study in light of the biomechanical activity of relevant muscles, we did not collect EMG data to support our arguments and confirm these results. Future work should include EMG observations to confirm these discussions.

This study provides insight into certain gait kinetics for TTAs walking overground during side load carriage conditions. While the results may provide some evidence to support our hypotheses, our study demonstrated mixed findings to determine which side TTAs should carry a load, suggesting that it depends on the desired kinetic effects, particularly on their intact limb. For example, the intact limb propulsive force would be smaller if the load were carried on the prosthetic side, suggesting two clinical implications. First, it may reduce the demand on ankle plantarflexors, which can benefit individuals, including TTAs, who have muscle weakness by reducing mechanical strain during loaded walking. Second, the decreased intact limb propulsion may potentially lead to inefficient gait and compensatory patterns over time. To address this, rehabilitation strategies associated with prosthetic-side load carriage could focus on physical therapy to strengthen key muscle contributors to forward propulsion (e.g., intact-side gastrocnemius and soleus) (Liu et al., 2006; Neptune et al., 2004, 2001) and balance control (e.g., vasti, gluteus medius) (Neptune and McGowan, 2016). In contrast to prosthetic-side load condition, the intact hip flexor moment in late stance and knee flexor moment in late swing would be slightly smaller if TTAs carried their load on the intact side. This finding may compromise balance control by increasing the risk of insufficient foot clearance on their intact limb. The decrease in hip and knee flexor moments can lead to a higher likelihood of tripping, which may be mitigated with rehabilitation strategies such as muscle strengthening (e.g., for intact-side iliopsoas, hamstrings, and gastrocnemius) and balance training. Further, targeted prosthetic gait training could improve load distribution across both limbs and enhance walking coordination during load carriage activities. However, further study is warranted to investigate if these effects are substantial when carrying a side load over time. Additionally, future work may increase the mass of side load to reflect more heavy-duty activities, for which a stiffer prosthetic foot or one purported for sudden increased loading (e.g., powered foot, foot with heel-stiffening wedge or dual keel) is recommended. If the effects are indeed clinically significant, prosthetic designs, as well as gait rehabilitation for TTAs who routinely carry a side load, should take these results into consideration.

Acknowledgments

Christina Carranza, L/CPO (licensed/certified prosthetist) fit and aligned the study prosthesis for all TTA subjects, and Jane Shofer, MS (biostatistician) provided consulting for the statistical analyses.

This work was supported in part by Merit Review Award Number I01 RX00318 and by Career Development/Capacity Building Award Number IK6 RX002974 from the United States Department of Veterans Affairs Rehabilitation Research and Development Service, and through the 2022 Fellowship funds from the Orthotic and Prosthetic Education and Research Foundation, Inc.

CHAPTER 3

LOAD CARRIAGE INFLUENCES INTACT LIMB KNEE LOADING ESTIMATE ASSOCIATED WITH OSTEOARTHRITIS IN INDIVIDUALS WITH TRANSTIBIAL AMPUTATION

Published in *Clinical Biomechanics*

DOI: https://doi.org/10.1016/j.clinbiomech.2025.106486

Satria Ardianuari

David C. Morgenroth

Richard R. Neptune

Glenn K. Klute

3.1 ABSTRACT

Background: Load carriage can exacerbate the elevated intact limb knee loading in individuals with transtibial amputation, potentially contributing to osteoarthritis. Prosthetic foot mechanical properties like push-off power have the potential to reduce this elevated knee loading. This study investigated how load carriage position and prosthetic foot type affect intact limb knee loading measures for these individuals.

Methods: Twelve participants with unilateral transtibial amputation were recruited. Intact limb external knee adduction and flexion moments were analyzed, with prosthetic push-off power and work quantified for effects on first peak knee adduction moment. A linear mixed-effects regression evaluated the effects of load position and prosthetic foot on these metrics.

Findings: Participants exhibited the smallest first peak knee adduction moment and impulse with the intact-side load condition, followed by the back load and front load conditions, with the prosthetic-side load condition having the highest magnitude (20-35% increase). However, we found no significant differences in these metrics by prosthetic foot. Additionally, load position and prosthetic foot did not significantly affect peak knee flexion moment. Only a negative trend toward correlation (P=0.089) was observed between first peak knee adduction moment and prosthetic push-off work in the back load condition.

Interpretation: Intact-side load carriage may be more clinically beneficial for mitigating the risk of increased intact limb knee loading. Further, load carriage strategy affects intact limb knee loading more than specific prosthetic foot type. These biomechanical findings can help guide rehabilitative load carriage strategies to minimize the elevated risk of knee osteoarthritis in individuals with transtibial amputation.

3.2 INTRODUCTION

Lower limb amputation can increase the risk of secondary musculoskeletal impairments, such as intact limb knee osteoarthritis (OA), resulting in detrimental additive disability (Morgenroth et al., 2012; Norvell et al., 2005; Struyf et al., 2009). The prevalence of knee OA in individuals with lower limb amputation is 17 times higher than in the general population (Struyf et al., 2009), with corresponding increased knee joint degenerative changes demonstrated through imaging studies (Melzer et al., 2001). Individuals with transtibial amputation (TTA) are more prone to knee pain in their intact limb than in their residual limb (Norvell et al., 2005), likely due to increased loading of their intact limb (Gailey et al., 2008). This finding suggests a substantial contribution from mechanical factors to knee pain and the increased prevalence of intact limb knee OA. Walking while carrying loads external to the body may also contribute to these mechanical factors affecting the risk of intact limb knee OA.

Many occupations and daily tasks often involve walking while carrying loads. For example, industrial activities such as construction, warehousing and transportation require load carriage (Soangra et al., 2018). Adults, including individuals with TTA, may also often encounter load carriage in various positions (e.g., carrying a backpack or a child on one hip) during daily activities. Despite the frequency of load carriage in daily living, there is limited evidence on how load carriage affects gait biomechanics of individuals with TTA. There is some evidence that load position impacts gait mechanics for those with TTA using a passive prosthetic foot. For example, a load worn on the back (back load) alters kinetics and kinematics, including smaller ankle dorsiflexor moment and hip power in the intact limb, smaller plantarflexor and knee flexor moments in the residual limb (Doyle et al., 2014), and smaller trunk/pelvis range of motion (Doyle et al., 2015; Schnall et al., 2014). In a modeling study of an individual with TTA there was decreased metabolic energy but increased intact limb knee joint impulse with a back load compared to a front load (Templin et al., 2021), suggesting increased intact limb knee loading as a compensatory strategy. Despite existing research on gait mechanics, no human-subjects studies have yet explored the effect of load carriage on intact limb knee loading related to osteoarthritis for individuals with TTA.

The added mass from load carriage increases the mechanical loads through the lower limbs during walking, which may exacerbate the increased loading commonly observed on the intact limb knee in individuals with lower limb amputation. Evidence suggests that the mechanical properties of prosthetic feet, such as stiffness and push-off power, can influence intact limb knee loading. For example, increased prosthetic foot stiffness (Slater et al., 2024) and increased prosthetic push-off work (Morgenroth et al., 2011) have been found to significantly decrease intact limb knee loading during unloaded walking. Powered prostheses with additional active push-off have therefore been demonstrated to decrease intact limb external knee adduction moment (KAM) when walking without loads (Grabowski and D'Andrea, 2013). Apart from powered prosthetic feet, there are a few other commercially available designs purported to facilitate load carriage for daily activities. In addition to a stiffer category foot, lower-cost options also include the prescription of a dual-keel prosthetic foot or adding a heel wedge to stiffen the heel. For example, the dual-keel type incorporating a full-length primary keel and a truncated secondary keel becomes stiffer when additional loads are applied (i.e., the primary keel engages the secondary keel). The stiffer design mimics the biological foot to minimize deformation under load and has been demonstrated to reduce intact limb peak ground reaction force (GRF) (Schnall et al., 2020). However, the effect of different prosthetic foot designs and properties on intact limb knee loading associated with OA is not sufficiently understood and warrants further investigation.

Although GRF outcomes are frequently studied, they are not specific to intact limb knee loading associated with OA risk. A targeted and specific metric associated with knee OA is KAM (Morgenroth et al., 2014). KAM is a reliable and commonly studied predictor of the development and progression of knee OA in amputees (Andrag et al., 2024). While KAM is the primary and most widely used metric for predicting knee loading, including peak external knee flexion moment (KFM) can provide more accuracy in estimating medial joint loading than using KAM alone (Manal et al., 2015; Miller et al., 2017).

The objective of this study was therefore to investigate the influence of load carriage position and prosthetic foot type on the measure of intact limb knee loading, i.e., intact KAM and corresponding intact KFM. Specifically, we sought to identify which load carrying position would minimize intact KAM and KFM for individuals with TTA, and which prosthetic foot would minimize intact KAM and KFM during load carrying conditions. Secondarily, we sought to explore the relationship between prosthetic foot push-off and intact KAM and KFM during load carriage. We hypothesized that: 1) each prosthetic foot has a load condition that minimizes intact limb knee loading estimate (i.e., intact KAM and KFM), 2) each load condition has a prosthetic foot that minimizes intact KAM and KFM, and 3) greater prosthetic push-off reduces the first peak KAM during double limb support in each load condition.

3.3 METHODS

3.3.1 Participants

Individuals with unilateral TTA provided informed consent prior to participating in this Institutional Review Board-approved study. Participants were screened to meet the following inclusion criteria: age ≥ 18 years, daily prosthesis use for at least six months, self-report as moderately active community ambulators and free from neurological/musculoskeletal disorders affecting gait (including knee pain associated with possible OA).

3.3.2 Instrumentation

Each participant walked with no load (NL), back load (BL), front load (FL), intact-side load (IL), and prosthetic-side load (PL) (Fig. 3.1A). For the loaded conditions, participants carried a 13.6 kg (30 lbs) weighted pack which exceeds the approximately 10 kg range for which a prosthetic foot stiffness category change is recommended. This estimate is applicable to an average manufacturer-recommended body mass and above, or a lower-limit body mass and above for a particular prosthetic foot in moderate and high impact levels, such as one that we used in the present study (i.e., Sierra foot) (Steeper, 2024). The added mass was also selected to reflect common loads carried in the daily tasks of individuals with TTA, for example, objects in a non-sedentary occupation (> 5 kg) (National Bureau of Economic Research, 2016), toddlers aged 1-2 years (during parenting activities) (National Center for Health Statistics, 2021), and backpack/sling bags. The five prosthetic feet tested (Fig. 3.1B) included a commonly prescribed energy storage and return foot with prescribed stiffness category (PR) selected by a clinician to optimize function for each individual participant. For each participant, all study feet were of the same stiffness category based on the participant's body mass as would be considered clinically (except for the one category stiffer). Additionally, all other prosthetic feet than the one category stiffer varied in design (see Fig. 3.1B for visualization).

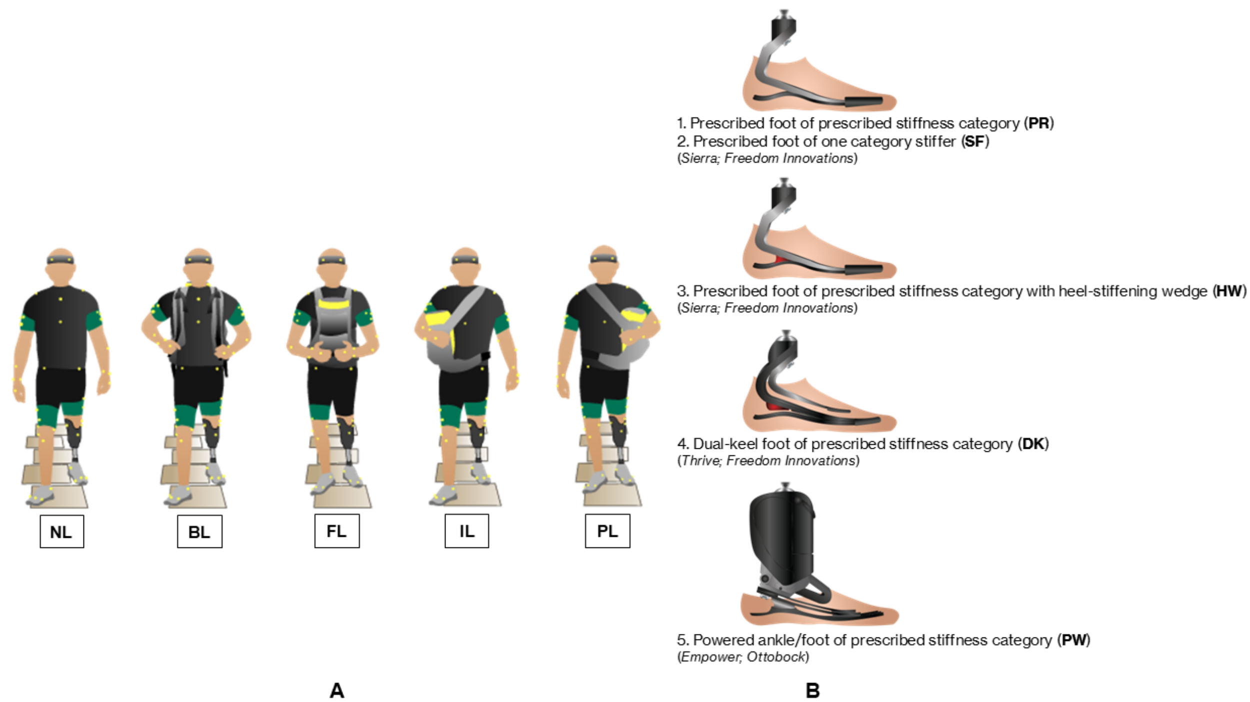

Fig 3.1 Schematic illustrations of A) Load conditions (showing participant outfitted with reflective markers walking overground across force plates with and without a weighted pack) and B) Prosthetic foot types used in this study. Abbreviations: load conditions (NL: no load, BL: back load, FL: front load, IL: intact load, PL: prosthetic load).

A 16-camera motion capture system (Vicon Motion Systems, Oxford, UK) and five overground force plates (AMTI, Watertown, MA, USA) recorded marker trajectories at 120 Hz and collected GRF data at 1,200 Hz, respectively. Participants wore tight-fitting clothing during data collection. Sixty-two 14-mm reflective tracking markers were placed on each participant at locations consistent with the Vicon Plug-in-Gait full-body model. Additional markers and marker clusters were placed bilaterally (illustrated in Fig. 3.1A). The markers on the prosthetic limb mirrored those on the intact limb. Lastly, three markers were placed on the pack (two on top, one on bottom) to track translation of the added load relative to the trunk. During loaded conditions, any physical markers obstructed by the load carrier were removed, and virtual markers were reconstructed using a digitizing procedure during post-processing.

3.3.3 Experimental Protocol

The protocol consisted of two visits to the laboratory. At the first visit, participants walked at their self-selected "comfortable" speed along a 14-m straight hallway wearing their prescribed prosthesis. Their self-selected walking speed was measured from an average of four walking trials. Information on height, body mass, and anthropometrics was collected. The prosthetic feet were then fit in random order and aligned by the same certified prosthetist using standard clinical procedures. Each participant practiced walking with and without all five of the different added load positions for at least 15 minutes or until they felt comfortable with each prosthetic foot, with additional acclimation time for the PW foot due to its distinct function (i.e., propulsive power output) compared to the other prosthetic feet.

At the second visit, the five load conditions were randomized for each participant, as was the order of the prosthetic feet used with each load condition. Kinematic and kinetic data were collected while participants walked overground in a straight line along a 10-m walkway with embedded force plates. Participants were instructed to adjust their walking speed to stay within 10% of their self-selected walking speed. Each participant completed a minimum of two trials per load condition and prosthetic foot, resulting in ~50 total trials per participant. Rest breaks were provided as needed to avoid fatigue. Only trials within ±10% of self-selected walking speed were included in the analysis. Additionally, only trials with a single, complete foot contact on the force plates were analyzed.

3.3.4 Data Processing and Analysis

Kinematic and kinetic data were filtered using Vicon's Woltring quintic spline-interpolating algorithm (Woltring, 1986) with a mean-square-error of 10 mm^2. A 15-segment inverse dynamics model was created for each participant in Visual 3D (C-Motion, Boyds, MD, USA) to compute kinematics and kinetics, including lower-limb joint moments and powers. Subsequently, data were low-pass filtered with a fourth-order double-pass Butterworth filter (cutoff frequency of 25 Hz) using custom MATLAB scripts (The MathWorks Inc., Natick, MA, USA). Intact KAM metrics were calculated using inverse dynamics, including the first peak, loading rate (i.e., rate of rise), and impulse. KAM loading rate was calculated as the slope between 20 and 80% of the period from initial contact to first peak. This method is more consistent compared to the maximum instantaneous rate occurring at variable points along the individual KAM rise curve. Prosthetic ankle power was calculated using the unified deformable segment model (Takahashi et al., 2012), and positive ankle work was quantified to test for associations with intact KAM during double-limb support.

Most studies normalize the KAM by body mass (Byrnes et al., 2022) to reduce its confounding effects and enable consistent between-participant comparisons. However, non-body mass normalized KAM has been reported to have higher sensitivity to severity levels of knee OA (Robbins et al., 2009), and KAM is positively associated with body fat in midstance (Mahaffey et al., 2018). Therefore, this study analyzed both body mass- and non-body mass normalized KAM. Other metrics were normalized by body mass (body mass + 13.6 kg) for conditions without (with) added load. Additionally, the first peak KFM at weight acceptance was analyzed to aid our interpretation for more accuracy in estimating medial joint loading (Manal et al., 2015). Data analysis was performed using custom MATLAB scripts.

3.3.5 Statistical Analysis

We performed linear mixed-effects regression to assess the effect of load condition and prosthetic foot (independent variables) on intact KAM and peak KFM metrics (dependent variables). The model was specified with fixed effects for load, foot and their interaction, the latter terms to allow for mean outcomes by load to vary across foot, and vice versa. Random effects included random intercepts for participant and load nested within participant. Residuals were plotted against fitted values to assess variance heterogeneity. Hypothesis testing for differences in outcomes by load or foot was conducted using conditional F-tests. Results were summarized with estimated marginal means (± standard errors) for each load and foot combination, and pairwise mean differences among loads (i.e., relative to NL and between loaded conditions) and feet representing corresponding effect sizes. Linear mixed effects regression was also used to test for the association between intact first peak KAM (dependent variable) and prosthetic ankle push-off work (independent fixed effect) with covariates load and load by ankle push-off work interaction to allow separate estimates of association for each load. Results were summarized as slopes of change in intact first peak KAM per increase in prosthetic ankle push-off work. Hypothesis testing was carried out as above. Statistical significance was set *a priori* and concluded at P-value < 0.05. The Benjamini-Hochberg correction (Benjamini and Hochberg, 1995) was applied for each outcome across load or foot to maintain a false discovery rate of 5% (type-I errors). All statistical analyses were performed in R software v4.4.0 (R Foundation for Statistical Computing, Vienna, Austria) using packages tidyverse, ggplot2, lme4, and emmeans.

3.4 RESULTS

Twelve participants (n = 12) with TTA completed the study protocol. Table 3.1 lists the demographic information and participant characteristics. Only 7/12 participants were tested with the PW foot due to inadequate pylon length for its high build height.

Table 3.1 Participant demographic characteristics. For other information including residual limb length and prosthetic components, please refer to Tables 2.1 and 4.1. Amputation-adjusted BMI was calculated with an online calculator widget (amputee-coalition.org), according to Wong et al.(Wong and Wong, 2017). The adjusted BMI excluded prosthetic components, and a value ≥ 30.0 indicates obesity. Abbreviations: BMI: body mass index; SSWS: self-selected walking speed; PTB: patellar tendon bearing; TSB: total surface bearing.

Subject	Age (yrs)	Sex	Amputation etiology	Mass with prosthesis (kg)	Height (m)	Adjusted BMI ($kg.m^{-2}$)	SSWS ($m.s^{-1}$)	Prescribed prosthesis		
								Foot stiffness category (1-9)	Socket	Suspension
01	59	M	Trauma	83.5	1.67	30.0	1.16	6	hybrid PTB	pin lock
02	40	M	Trauma	102.3	1.81	31.2	1.67	7	hybrid PTB	sleeve
03	60	M	Trauma	111.9	1.80	34.7	1.30	7	TSB	pin lock
04	58	F	Congenital	96.6	1.69	34.0	1.12	6	hybrid PTB	sleeve+suction
05	39	M	Trauma	105.7	1.71	36.4	1.43	7	hybrid PTB	pin lock+BOA
06	25	F	Congenital	52.6	1.56	21.2	1.37	2	TSB	sleeve
07	43	M	Infection	107.0	1.82	32.4	1.32	7	hybrid PTB	pin lock
08	31	M	Trauma	98.5	1.83	29.6	1.26	7	TSB	pin lock+BOA
09	36	M	Trauma	110.4	1.86	31.9	1.20	7	TSB	suction
10	29	M	Trauma	83.9	1.64	31.1	1.16	6	TSB	pin lock+suction
11	53	M	Dysvascular	106.6	1.86	31.0	0.92	7	PTB	pin lock
12	75	M	Trauma	93.6	1.83	28.1	1.17	7	hybrid PTB	sleeve+seal in
Mean ± SD	**46 ± 15**			**96.1 ± 16.6**	**1.76 ± 0.10**	**31.0 ± 3.8**	**1.26 ± 0.19**			

3.4.1 Comparison of knee loading across load carrying conditions

Strong evidence of associations between loading position and intact limb knee load was observed for first peak KAM and KAM impulse, with non-significant associations for KAM loading rate and peak KFM (Fig. 3.2).

Comparison between no load and loaded conditions

Significant differences in first peak KAM between the NL condition and loaded conditions were observed with the HW foot, but not with the other feet (Table 3.2 and Fig. 3.2). Participants demonstrated smaller first peak KAM during the IL condition (mean difference: 0.11 $Nm·kg^{-1}$ [percent mean difference: 29%]). There was no difference in KAM loading rate between NL and loaded conditions for all prosthetic feet. Relative to the NL condition, KAM impulse increased in the PL condition with all prosthetic feet. The increases were as follows: 0.07 $Nms·kg^{-1}$ [35%] with the PW foot, 0.07 $Nms·kg^{-1}$ [32%] with the DK and PR feet, 0.06 $Nms·kg^{-1}$ [28%] with the HW foot, and 0.04 $Nms·kg^{-1}$ [23%] with the SF foot.

Comparison between loaded conditions

When comparing between load position conditions (Table 3.2 and Fig. 3.2), participants consistently showed smaller first peak KAM in the IL condition than in the other load positions across all prosthetic foot types. For example, smaller first peak KAM was observed in the IL condition than in the other loaded conditions with the HW foot (i.e., 0.11 $Nm \cdot kg^{-1}$ [29%] smaller than the FL condition, 0.13 $Nm \cdot kg^{-1}$ [34%] smaller than the BL condition, and 0.13 $Nm \cdot kg^{-1}$ [33%] smaller than the PL condition). Using the SF foot, the first peak KAM was also smaller in the IL condition (by 0.13 $Nm \cdot kg^{-1}$ [28%]), FL condition (by 0.12 $Nm \cdot kg^{-1}$ [27%]), and BL condition (by 0.10 $Nm \cdot kg^{-1}$ [23%]) compared to the PL condition. With the DK foot, smaller first peak KAM found in the IL condition than in the FL (0.12 $Nm \cdot kg^{-1}$ [26%]) and PL conditions (0.12 $Nm \cdot kg^{-1}$ [27%]). With the PW foot, smaller first peak KAM was also observed in the IL and BL conditions compared to the PL conditions (0.20 $Nm \cdot kg^{-1}$ [47%] and 0.13 $Nm \cdot kg^{-1}$ [31%] lower, respectively). KAM profiles depicting peak trends can be seen in Fig. 3.3A.

Participants demonstrated significant differences in KAM impulse between loaded conditions (Table 3.2 and Fig. 3.2). Across all prosthetic feet, KAM impulse was smaller in all other loaded conditions compared to the PL condition. For example, reductions in KAM impulse were seen with the HW foot in the IL and BL conditions compared to the PL condition (0.05 $Nms \cdot kg^{-1}$ [33%] and 0.05 $Nms \cdot kg^{-1}$ [31%] smaller, respectively). Additionally, smaller KAM impulse was demonstrated in the IL condition compared to the BL and FL conditions (40%-46% reductions) with the SF and DK feet.

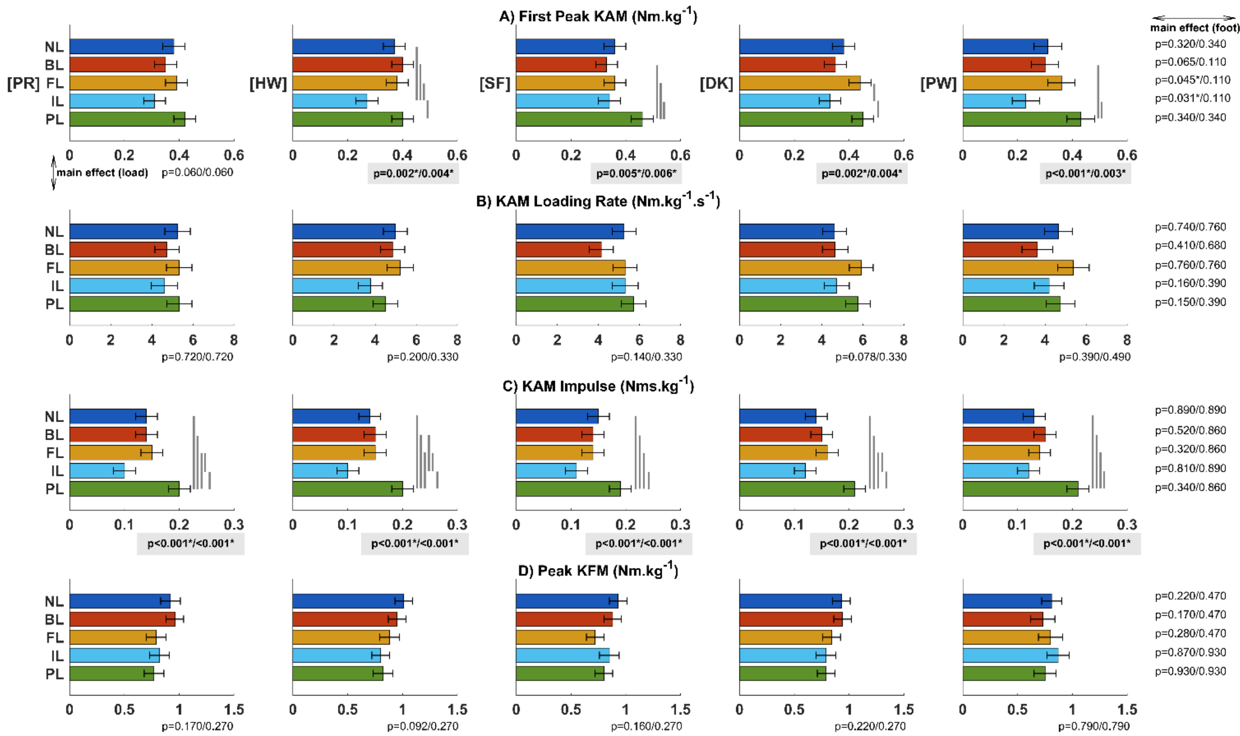

Fig 3.2 Mean (standard error) outcome metrics: intact first peak external knee adduction moment (KAM), KAM loading rate, KAM impulse and peak knee flexion moment (KFM) by load and foot from the fitted linear mixed-effect models. Bars and error bars represent means and standard errors, respectively. Vertical lines represent significant within-foot pairwise differences between loads (corresponding pairwise P-values are reported in Table 3.2). Values are normalized to body mass for NL and body mass + 13.6 kg for loaded conditions. Statistical significance is annotated by bold P-value with an asterisk (*). ↕ P-values below plots = main effect of load, and ↔ P-values right of plots = main effect of foot. P-values: unadjusted/adjusted. Abbreviations: load conditions (NL: no load, BL: back load, FL: front load, IL: intact load, PL: prosthetic load) and prosthetic foot types (PR: prescribed, HW: heel wedge, SF: one category stiffer, SK: dual-keel, PW: powered). Refer to Fig.3.1 for details.

Table 3.2 Within-foot pairwise comparisons between loads showing significance for intact first peak external knee adduction moment (KAM) and KAM impulse. Values are normalized to body mass for NL and body mass + 13.6 kg for loaded conditions. Statistical significance is annotated by **bold** P-value with an asterisk (*) (shaded for clarity). Abbreviations: load conditions (NL: no load, BL: back load, FL: front load, IL: intact load, PL: prosthetic load) and prosthetic foot types (PR: prescribed, HW: heel wedge, SF: one category stiffer, SK: dual-keel, PW: powered). Refer to Fig.3.1 for details.

Mean difference [95% confidence interval] | Pairwise *P*-value										
First Peak KAM (Nm.kg^{-1})										
	PR		**HW**		**SF**		**DK**		**PW**	
NL vs **BL**	0.03 [-0.08, 0.14]	0.932	-0.03 [-0.13, 0.07]	0.934	0.03 [-0.07, 0.13]	0.905	0.03 [-0.07, 0.13]	0.909	0.01 [-0.12, 0.14]	0.999
NL vs **FL**	-0.01 [-0.12, 0.09]	0.996	-0.01 [-0.11, 0.10]	1.000	0.01 [-0.09, 0.11]	0.999	-0.06 [-0.16, 0.03]	0.364	-0.05 [-0.18, 0.09]	0.875
NL vs **IL**	0.07 [-0.05, 0.18]	0.469	**0.11 [0.01, 0.21]**	**0.034***	0.03 [-0.08, 0.13]	0.955	0.05 [-0.05, 0.15]	0.636	0.08 [-0.05, 0.21]	0.428
NL vs **PL**	-0.04 [-0.15, 0.06]	0.787	-0.02 [-0.13, 0.08]	0.963	-0.10 [-0.20, 0.00]	0.066	-0.07 [-0.17, 0.03]	0.310	-0.12 [-0.25, 0.00]	0.056
BL vs **FL**	-0.05 [-0.15, 0.06]	0.759	0.02 [-0.08, 0.13]	0.976	-0.02 [-0.13, 0.08]	0.966	-0.10 [-0.20, 0.01]	0.072	-0.06 [-0.20, 0.08]	0.794

BL vs **IL**	0.04 [-0.07, 0.14]	0.884	**0.13 [0.03, 0.24]**	**0.003***	0.00 [-0.11, 0.10]	1.000	0.02 [-0.09, 0.12]	0.987	0.07 [-0.07, 0.20]	0.651
BL vs **PL**	-0.07 [-0.18, 0.03]	0.278	0.00 [-0.10, 0.11]	1.000	**-0.13 [-0.23, -0.03]**	**0.006***	-0.10 [-0.20, 0.00]	0.056	**-0.13 [-0.27, 0.00]**	**0.050***
FL vs **IL**	0.08 [-0.03, 0.19]	0.260	**0.11 [0.01, 0.22]**	**0.032***	0.02 [-0.09, 0.12]	0.988	**0.12 [0.01, 0.22]**	**0.017***	0.13 [-0.01, 0.26]	0.094
FL vs **PL**	-0.03 [-0.14,0.08]	0.945	-0.02 [-0.12, 0.09]	0.989	**-0.10 [-0.21, -0.00]**	**0.039***	0.00 [-0.10, 0.10]	1.000	-0.07 [-0.21, 0.06]	0.550
IL vs **PL**	-0.11 [-0.22, 0.00]	0.046	**-0.13 [-0.23, -0.03]**	**0.006***	**-0.12 [-0.23, -0.02]**	**0.015***	**-0.12 [-0.22, -0.02]**	**0.013***	**-0.20 [-0.33, -0.07]**	**<.001***
KAM Impulse (Nms.kg^{-1})										
NL vs **BL**	0.00 [-0.03, 0.04]	1.000	-0.01 [-0.05, 0.02]	0.762	0.00 [-0.03, 0.04]	0.998	0.00 [-0.04, 0.03]	0.999	-0.01 [-0.06, 0.03]	0.946
NL vs **FL**	-0.01 [-0.05, 0.03]	0.975	-0.01 [-0.05, 0.02]	0.910	0.00 [-0.03, 0.04]	1.000	-0.02 [-0.05, 0.01]	0.406	-0.01 [-0.06, 0.04]	0.975
NL vs **IL**	0.03 [0.00, 0.07]	0.101	0.03 [0.00, 0.07]	0.064	0.03 [-0.01, 0.07]	0.114	0.03 [-0.01, 0.06]	0.178	0.02 [-0.03, 0.06]	0.806
NL vs **PL**	**-0.06 [-0.10, -0.03]**	**<.001***	**-0.06 [-0.09, -0.02]**	**<.001***	**-0.04 [-0.08, -0.01]**	**0.008***	**-0.07 [-0.10, -0.03]**	**<.001***	**-0.07 [-0.12, -0.03]**	**<.001***
BL vs **FL**	-0.01 [-0.05, 0.03]	0.915	0.00 [-0.03, 0.04]	0.999	0.00 [-0.04, 0.03]	1.000	-0.02 [-0.05, 0.02]	0.609	0.00 [-0.05, 0.05]	1.000
BL vs **IL**	0.03 [-0.01, 0.07]	0.127	**0.05 [0.01, 0.09]**	**0.002***	0.03 [-0.01, 0.07]	0.209	0.03 [-0.01, 0.07]	0.135	0.03 [-0.02, 0.08]	0.418
BL vs **PL**	**-0.07 [-0.10, -0.03]**	**<.001***	**-0.04 [-0.08, -0.01]**	**0.015***	**-0.05 [-0.08, -0.01]**	**0.003***	**-0.06 [-0.10, -0.03]**	**<.001***	**-0.06 [-0.11, -0.02]**	**0.002***
FL vs **IL**	**0.04 [0.01, 0.08]**	**0.019***	**0.05 [0.01, 0.08]**	**0.009***	0.03 [-0.01, 0.07]	0.145	**0.05 [0.01, 0.08]**	**0.002***	0.03 [-0.02, 0.08]	0.511
FL vs **PL**	**-0.06 [-0.09, -0.02]**	**0.001***	**-0.05 [-0.08, -0.01]**	**0.009***	**-0.04 [-0.08, -0.01]**	**0.005***	**-0.05 [-0.08, -0.01]**	**0.002***	**-0.06 [-0.11, -0.02]**	**0.002***
IL vs **PL**	**-0.10 [-0.14, -0.06]**	**<.001***	**-0.09 [-0.13, -0.05]**	**<.001***	**-0.08 [-0.11, -0.04]**	**<.001***	**-0.09 [-0.13, -0.06]**	**<.001***	**-0.09 [-0.14, -0.05]**	**<.001***

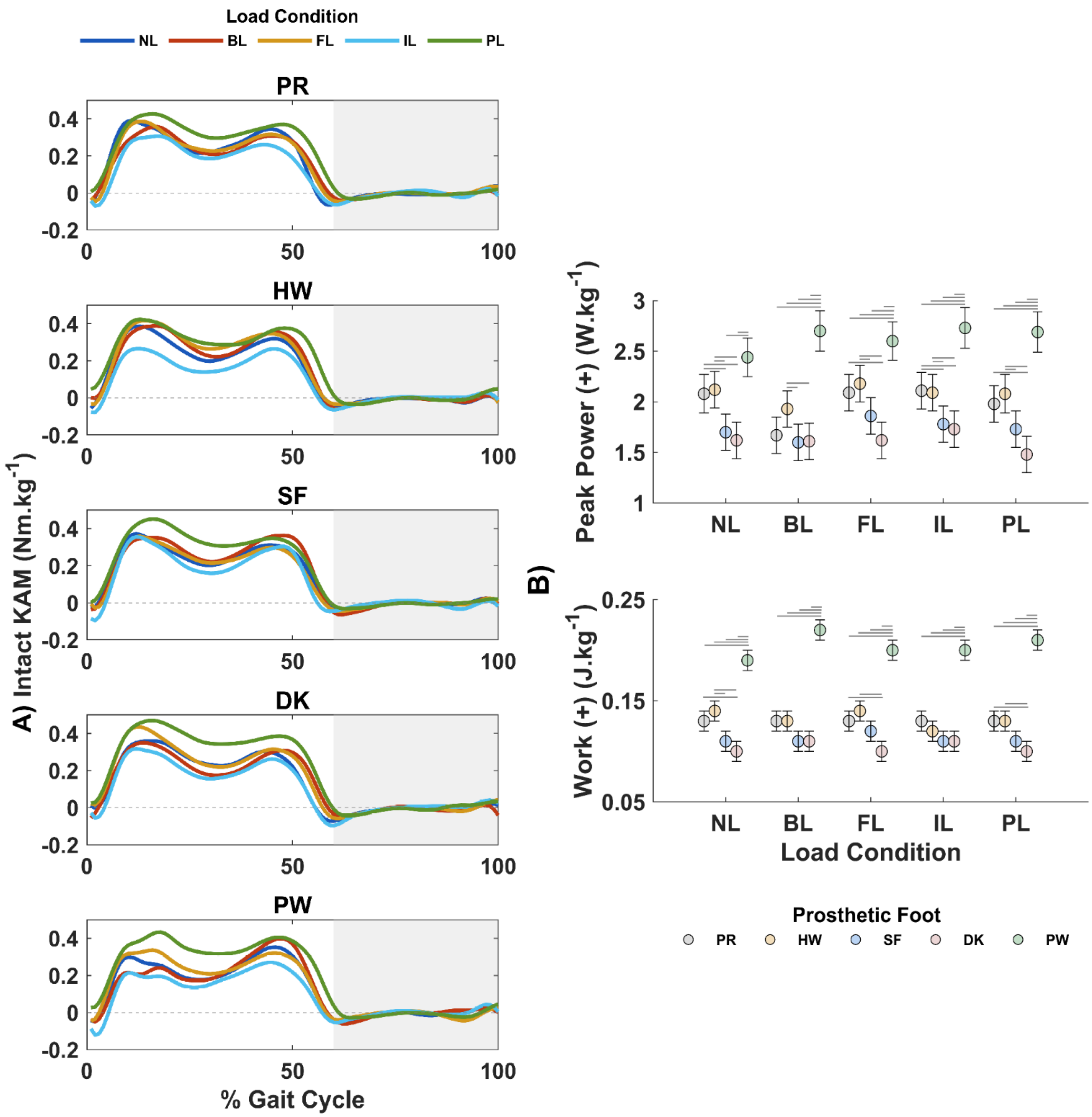

Fig 3.3 A) Ensemble means of intact external knee adduction moment (KAM) by load in each foot. Unshaded (shaded) area represents average stance (swing) phase of % gait cycle. B): Mean prosthetic ankle peak power and work. Vertical lines represent standard errors, and horizontal lines represent significant within-load pairwise differences between feet ($P < 0.05$) (See Appendix 2 for pairwise significance). Values are normalized to body mass for NL and body mass + 13.6 kg for loaded conditions. Abbreviations: load conditions (NL: no load, BL: back load, FL: front load, IL: intact load, PL: prosthetic load) and prosthetic foot types (PR: prescribed, HW: heel wedge, SF: one category stiffer, SK: dual-keel, PW: powered). Refer to Fig.3.1 for details.

3.4.2 Comparison of knee loading between prosthetic foot types

No significant differences were found in intact KAM and peak KFM by prosthetic foot type (Fig. 3.2). We only observed a few borderline significant comparisons in which participants walking with the PW foot tended to have smaller first peak KAM than with the other feet for most of the load conditions (i.e., $P = 0.045$ in FL condition and $P = 0.031$ in IL condition). However, these differences were no longer significant after correction for multiple testing ($P = 0.11$) (Fig. 3.2).

3.4.3 Association between prosthetic push-off and intact limb knee loading

As anticipated, we found that the PW foot consistently produced the highest positive ankle peak push-off power and work compared to the other feet in all load conditions (Fig. 3.3B). Significance for pairwise comparisons in prosthetic ankle peak power and work between prosthetic feet can be found in Appendix (Table A3).

Prosthetic ankle work was strongly correlated with peak ankle power ($r = 0.81$); thus, the analysis of the association between intact first peak KAM focused only on prosthetic ankle work. No significant associations between prosthetic ankle work and intact first peak KAM were found in any of the load conditions across feet. The only trend toward a correlation was observed in the BL condition, although it did not achieve statistical significance ($P = 0.089$) (Fig. 3.4).

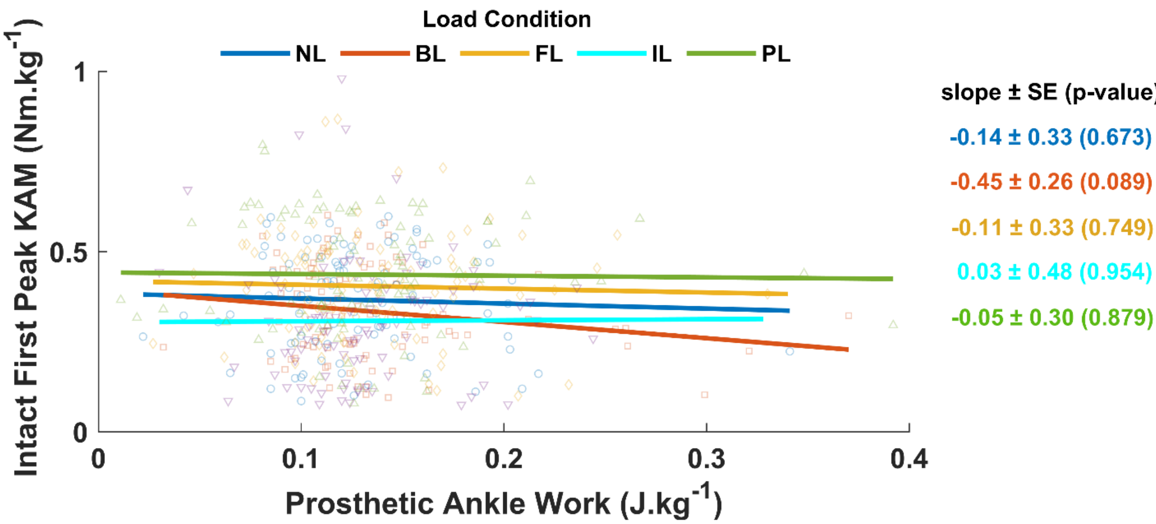

Fig 3.4 Association between (trailing) prosthetic push-off and (leading) external knee adduction moment during double-limb support phase in each load condition across feet. Values are normalized to body mass for NL and body mass + 13.6 kg loaded conditions. Abbreviations: load conditions (NL: no load, BL: back load, FL: front load, IL: intact load, PL: prosthetic load).

The associations between mass-normalized outcomes and load or foot were similar to those for non-mass-normalized outcomes (Fig. 3.2 vs. Appendix Fig. A3). Thus, only associations for mass-normalized outcomes are discussed. Additionally, participants' self-selected walking speed did not significantly change across load conditions ($P > 0.05$).

3.5 DISCUSSION

This study investigated the influence of load carriage position and prosthetic foot type on intact limb knee loading among individuals with TTA. The results supported the hypothesis that load condition (i.e., load carriage positions with the same amount of added mass) affects intact KAM across prosthetic foot types. However, we found that prosthetic foot type did not significantly affect intact KAM for loaded conditions, nor did we observe a statistically significant relationship between prosthetic push-off and intact KAM for each load condition.

Participants demonstrated a >30% increase in first peak KAM in certain load position conditions when carrying a 13.6-kg added load, particularly in the prosthetic-side and back load positions relative to the intact-side load position with PW and HW feet. This increase exceeds the change seen in patients with radiographically confirmed OA compared to healthy controls (Foroughi et al., 2009; Wilson et al., 2008). These results suggest that walking with body-borne loads may exacerbate knee loading associated with OA development in people with TTA. However, it should be noted that the observed increases in first peak KAM with load carriage were not universal (e.g., the no load condition did not lead to significantly reduced first peak KAM).

Compared to unloaded walking, the intact-side load condition resulted in smaller peak KAM in early stance (Fig. 3.2 and Fig. 3.3A). In contrast, the prosthetic-side load condition demonstrated a higher KAM impulse throughout stance compared to unloaded condition (Fig. 3.2). Among loaded conditions, the intact-side load condition produced the smallest peak KAM in early stance (Fig. 3.2 and Fig. 3.3A) and KAM impulse throughout stance, followed by the back load and front load conditions, with the prosthetic-side load condition having the highest magnitude (Fig. 3.2). One potential explanation could be that prosthetic-side load increases hip abductor activity due to higher internal torque demand produced by the muscle force (Neumann et al., 1992; Neumann and

Hase, 1994) to counteract the increased gravitational moment of the load (MacKinnon and Winter, 1993). The gluteus medius regulates frontal plane balance by rotating the trunk toward the intact limb (Neptune and McGowan, 2016). To counteract the added load on the prosthetic side, the activity of the gluteus medius on the intact side must increase to shift the body's center of mass toward the (stance) intact limb. The prosthetic-side added load increases the magnitude of the GRF vector acting through the intact limb, thereby increasing KAM.

Previous work on non-amputee individuals walking with sagittal load carriage reported that front load increased peak KAM (Drew et al., 2021). The front load condition was found to increase muscle contributions to body support compared to the back load condition (Lefranc et al., 2024). The activity of hamstrings is likely a mechanism to increase backward angular momentum during the front load condition while reducing it during the back load condition (Neptune and McGowan, 2011). Additionally, medial hamstrings have been shown to influence knee stability (Toor et al., 2019). Thus, increased hamstrings activity during the front load condition may also potentially increase KAM.

In contrast to the KAM findings described above, there were no statistically significant changes in KFM with added loads. This is consistent with previous research reporting borderline significance (before mass normalization) and no significant differences (after mass normalization) in maximum KFM at weight acceptance between the back load condition and no load condition in individuals with TTA (Doyle et al., 2014). This phenomenon may be attributable to gait strategies adopted by the participants in response to load carriage. Individuals with TTA demonstrate higher sagittal hip power at weight acceptance on the limb that carries a side load (Ardianuari et al., 2024) (Chapter 2). Because the participants in our study did not exhibit significant changes in peak KFM at weight acceptance on their intact limb, other compensatory changes might have occurred (e.g., at the hip) to accommodate the added loads.

Despite using prosthetic feet with substantially different properties for load carriage applications, there were no statistically significant differences in intact KAM across prosthetic foot types. The non-significant associations between (trailing) prosthetic ankle work and (leading) intact first peak KAM could have contributed to this finding, suggesting that the amount of prosthetic push-off (Fig. 3.3B) does not have a strong influence on intact KAM during loaded walking. This contrasts with studies that found a negative correlation between prosthetic push-off work and intact KAM at a similar self-selected walking speed (Morgenroth et al., 2011) and higher walking speeds (Grabowski and D'Andrea, 2013) during unloaded walking. One potential reason for this discrepancy could be the limited acclimation time in our study. These prior studies provided at least 2 hours to 2 days of acclimation before data collection. Longer acclimation times may result in better use of increased push-off (e.g., more optimal timing of peak ankle push-off (Malcolm et al., 2015)) that may be associated with reduced intact limb loading for individuals with lower limb amputation.

Our study found that carrying a load on the intact limb side reduced intact limb KAM more than other load positions, suggesting it may help mitigate the elevated risk of knee OA. Individuals with TTA who routinely carry loads may be encouraged to utilize this load carriage method whenever possible during their daily vocational and/or avocational activities. Rehabilitation strategies could incorporate this load carriage method into gait balance training and include physical therapy to help reduce the risk of potentially increased knee loading by strengthening key muscle contributors to frontal-plane balance control (i.e., hip abductors) (Neptune and McGowan, 2016), as we discussed earlier. However, given the multifaceted nature of knee joint loading and OA risk, further research is needed to fully understand the long-term implications of different load carriage strategies. Further investigation is also warranted to assess other more immediate considerations associated with intact-side load carriage (e.g., patient preference, comfort, stability and other performance-based metrics).

3.5.1 Limitations

There are several potential limitations to this study. First, challenges due to the COVID-19 pandemic and the extensive experimental protocol resulted in n = 12, a relatively small sample. However, this sample size is consistent with many human motion capture/biomechanics studies involving individuals with lower limb amputations. Next, only 7/12 participants were tested with the PW foot due to inadequate pylon length for its high build height, which limited our ability to detect more modest effect sizes for the differences between the PW foot and other feet within each load condition. Therefore, the results of our study may not generalize to the population with TTA with different residual limb morphology because of the exclusion of individuals with longer residual limbs walking with the PW foot. Third, the alignment of each prosthetic foot for each participant was individually optimized by the prosthetist. While methodological control such as holding alignment constant across feet might have reduced variability, such a procedure would not have reflected clinical practice (thus our choice to optimize alignment in this study to maintain clinical relevance). Fourth, participants maintained a constant walking speed in this study. Although the evidence for other biomechanical outcomes is mixed and inconclusive, powered prostheses have been shown to reduce first peak KAM by 10-20% at faster speeds (i.e., ≥1.5 m/s) (Grabowski and D'Andrea, 2013). Higher speeds during loaded walking in individuals with TTA may provide further insights into the effect of prosthetic push-off on changes in intact KAM.

Additionally, there are important considerations when interpreting our results. Our study analyzed external knee moments (i.e., KAM and KFM) to estimate knee joint loading and provide insights into knee OA risk. Despite being frequently reported in the literature, these surrogate measures are incomplete due to the lack of consideration of potentially increased internal joint loads from muscle forces. Further studies may utilize other methods, such as musculoskeletal modeling and simulation, to estimate medial contact forces, providing further insights into changes in intact limb knee loading. While the intact-side load condition showed reduced peak KAM/KAM impulse, it is still possible that participants were exerting greater muscular demand to compensate for the added load. It may be argued that carrying the load on the intact side takes physiological advantage of participants' habitually stronger limb, and that the increased load is accommodated elsewhere e.g., at the expense of increased loads on the intact limb hip, as we alluded earlier. This strategy may increase the risk of more proximal joint wear, particularly through increased compressive joint loads. This finding relative to side load conditions may in turn exacerbate loading asymmetry. Additional data/research is needed to understand the adjacent joint compensations. Finally, although we discussed some changes in intact limb knee loading in relation to muscle activity, we did not collect EMG data to support these arguments. Future research should measure EMG to confirm these results.

3.5.2 Conclusion

Individuals with lower limb amputation, including those with TTA, have a high prevalence of knee OA in their intact limb. This is likely a consequence of the increased intact limb loading that may be exacerbated while walking with load carriage. This study demonstrated that load carriage position affects intact KAM in individuals with TTA. Front loads resulted in a higher measure of intact limb knee loading than back loads, and the highest magnitude was observed with prosthetic-side loads. In contrast, intact-side load carriage reduced intact limb knee loading compared with other load carry positions. Therefore, intact-side load carriage may be more clinically advantageous than prosthetic-side and other load carriage positions for mitigating the risk of increased intact limb knee loading. This study also highlights that load carriage strategy has a more substantial effect on intact limb knee loading than the specific prosthetic foot type used. Understanding these biomechanical principles can guide rehabilitative interventions to minimize intact limb knee joint loading associated with the elevated risk of OA and improve mobility in individuals with TTA.

Acknowledgments

This work was supported by grants from the US Department of Veterans Affairs Rehabilitation Research and Development Service [Merit Review Award Number I01 RX003138 and Career Development/Capacity Building Award Number IK6 RX002974]. The contents of this work are those of the authors and do not represent the views of the U.S. Department of Veterans Affairs or the United States Government. We thank the following individuals for their significant contributions to this current study: Krista Cyr, MS for collecting the experimental data; Christina Carranza, L/CPO for fitting the study prostheses; and Jane Shofer, MS for providing consulting for the statistical analyses.

CHAPTER 4

INFLUENCE OF PROSTHETIC FOOT SELECTION FOR LOAD CARRIAGE ON LOWER LIMB MECHANICAL WORK

Published in *Gait & Posture*

DOI: https://doi.org/10.1016/j.gaitpost.2026.110195

Published version: Influence of prosthetic foot selection for load carriage on prosthetic limb mechanical work

Satria Ardianuari

Krista M. Cyr

Richard R. Neptune

Glenn K. Klute

4.1 ABSTRACT

Background: Prosthetic foot selection may influence gait biomechanics in individuals with transtibial amputation, particularly during load carriage. While prior work often emphasizes intact limb compensation, this study also examined prosthetic limb mechanics to directly assess device-user interaction. We compared five commercially available feet: a clinically prescribed foot, a stiffer category of the same foot, the same foot with a heel-stiffening wedge, a dual-keel foot, and a powered ankle-foot, across five load conditions: unloaded, anterior, posterior, intact side, and prosthetic side.

Methods: Twelve participants performed overground walking trials at self-selected speed with each foot-load combination. Lower-limb net positive and negative joint work at the ankles, knees, and hips was calculated over the gait cycle and specific gait subphases via inverse dynamics. Linear mixed-effects models evaluated foot effects within load conditions.

Results: Most differences were observed in the prosthetic limb. Ankle joint work differed significantly between feet within all load conditions. The powered ankle-foot generated the highest net positive ankle work in late stance, suggesting enhanced propulsion. The clinically prescribed and heel-wedge feet produced the highest negative ankle work in early stance, indicating increased energy absorption. The stiffer and dual-keel feet reduced both positive and negative ankle work. Knee and hip joint work did not differ significantly across feet within load conditions.

Conclusions: Prosthetic foot type primarily modulates prosthetic ankle mechanics without altering proximal joint work under moderate load carriage. The powered ankle-foot may benefit users seeking propulsion, while non-powered designs may support energy absorption and stability. Prosthetic prescription should align with user mobility goals and expected load demands.

4.2 INTRODUCTION

Individuals with lower limb amputations rely on their prosthetic feet to help restore mobility for activities of daily living. A primary objective of prosthetic feet is to facilitate a more natural gait by attempting to emulate the biomechanical functions of the biological ankle-foot complex. Despite this fundamental goal, the majority of individuals with transtibial amputations (TTA) are clinically prescribed passive prosthetic feet, which have fixed mechanical properties (i.e., stiffness) typically tuned to specific body weight and activity level. Unlike individuals with an intact ankle-foot complex who can automatically modulate stiffness to accommodate varying loads (Kern et al., 2019), individuals with TTA lack this neuromuscular adaptability. Consequently, when carrying external loads as a part of occupational or recreational activities, their prosthetic foot stiffness may no longer be optimal for their new combined weight.

Load carriage is a common and essential task in daily life which may impose additional biomechanical demands that necessitate compensatory strategies, particularly in individuals with TTA. Previous research on load carriage has primarily focused on posterior loads, reporting altered spatiotemporal, kinematic, and kinetic outcomes in individuals with TTA while walking with passive prosthetic feet (Doyle et al., 2015, 2014; Schnall et al., 2014; Sinitski et al., 2016). These changes may result from an increase in prosthetic foot deflection (Doyle et al., 2014), suggesting a substantial limitation with standard passive prosthesis during loaded walking (Koehler-McNicholas et al., 2018). However, external loads are not exclusively carried on the back and may be positioned anteriorly or laterally on either side, creating additional variability in gait demands for individuals with TTA.

Foot stiffness could play a key role in loaded walking adaptations. A stiffer prosthetic foot may be beneficial during loaded walking, but this can become ineffective during unloaded walking due to a decrease in energy storage and release function (Klodd et al., 2010). Additionally, a stiffer foot has been shown to decrease ankle push-off peak power and work during walking with no load (Halsne et al., 2020; Slater et al., 2024), suggesting a stiffer foot may adversely affect propulsion. The impact of prosthetic foot stiffness on mechanical demand during loaded walking remains largely unexplored, and understanding these effects is crucial for optimizing the design of prosthetic feet.

Mechanical work around the center of mass accounts for approximately 50% of the metabolic cost of walking (Grabowski, 2010), but this estimate is considered an underrepresentation of total muscle work (Sasaki et al., 2009). An alternative approach to assess adaptations in mechanical work is through individual joint power and work contributions derived from inverse dynamics (Umberger and Martin, 2007), which provides insight into energy generation and absorption throughout the lower limbs during walking. Previous research suggests that joint work patterns differ between prosthetic and intact limbs, as well as compared to able-bodied controls. For example, without an added load, individuals with TTA exhibit greater concentric (positive) work at the hip and knee of the intact limb relative to both their prosthetic limb and those of individuals without amputation (Prinsen et al., 2011). Further, unloaded walking with a less stiff prosthetic foot leads to a decrease in positive sagittal hip work and an increase in both eccentric (negative) sagittal knee work and positive sagittal ankle work (Shell et al., 2017). When carrying a back load with a prescribed stiffness foot, individuals with TTA demonstrate smaller hip extensor power in early stance in both the intact and prosthetic limbs (Doyle et al., 2014). These patterns reflect the reliance on prosthetic feet to provide the necessary mechanical work, a demand that standard passive prostheses may not fully meet.

To address this limitation, powered lower-limb prostheses have been studied with adaptive stiffness capabilities in response to an added load to reduce metabolic cost (Brandt et al., 2017). However, these devices remain experimental and have mechanical characteristics that may not reflect commercially available prosthetic feet. There is a limited range of commercially available feet that can be prescribed to try to facilitate load carrying activities. These options include the prescription of lower-cost feet such as a stiffer category foot, a foot with additional heel-stiffening wedge, or a dual-keel prosthetic foot (e.g., Thrive, Freedom Innovations). The dual-keel prosthetic foot is suitable for load carriage applications because it responds to an added load as the primary keel engages the secondary keel such that the prosthetic foot becomes stiffer. A more costly prescription option purported to adapt to changing loads is a powered ankle-foot prosthesis (e.g., Empower, Ottobock). While it has been shown to reduce metabolic cost due to increased propulsive ankle power output (Herr and Grabowski, 2012; Montgomery and Grabowski, 2018), others report mixed and inconsistent effects, including decreased intact limb knee loading measures (Russell Esposito and Wilken, 2014), increased compensatory demands at the ipsilateral hip and knee (Ferris et al., 2012), and no clear advantages in walking speed or perceived mobility over non-powered, passive prostheses (Kim et al., 2021b). Specific gait and rehabilitation training may be necessary to fully utilize the potential benefits of a powered ankle-foot (Kannenberg et al., 2022). However, the response of a powered ankle-foot to load carriage still remains an open question.

The objective of this research was to inform prosthesis prescription guidance by identifying which commercially available feet optimize lower-limb joint work during walking under five conditions: unloaded and four loaded (anterior, posterior, intact-side, prosthetic-side). Our primary aim was to investigate the effects of load carriage and foot type on intact-limb mechanical work.

Our secondary aim was to isolate these effects on the prosthetic limb, independent of the contralateral limb contributions. While intact-limb work is often examined for compensatory strategies, we also focused on the prosthetic side to directly evaluate device-user interaction at the limb most mechanically constrained by the intervention. We hypothesized that, for each load condition, a prosthetic foot exists that maximizes positive and negative ankle work, while minimizing negative knee work and positive hip work (i.e., to optimize ankle work while minimizing compensatory work at the knee and hip and allow for more efficient locomotion).

4.3 METHODS

4.3.1 Participants

Eligible participants had unilateral TTA, were moderately active community ambulators (i.e., Medicare Functional Classification K-Levels 3 or 4 by self-report and prosthetist assessment), had used a prosthesis for ≥ six months, and had no other conditions affecting gait. All provided informed consent approved by the governing Institutional Review Board.

4.3.2 Instrumentation

To simulate carriage of children, backpacks, or other loads during daily or occupational tasks (Fryar et al., 2021; Gittleman et al., 2016), participants carried a 13.6 kg (30 lb) padded load (Ergobaby, Los Angeles, CA, USA). This mass was not standardized relative to percent body mass, but rather, was selected to represent a load that exceeded the approximately 10-kg threshold often used by manufacturers to justify a change in prosthetic foot stiffness category (e.g., the clinically prescribed (CP) Sierra foot, (Steeper, 2024)). The CP foot was selected to represent a standard-of-care foot matching the participant's specific size and category but was different from their own prescribed foot. Participants completed four load conditions with five different commercially available prosthetic feet (illustrated in Fig.4.1). All study prostheses were purchased through commercial channels.

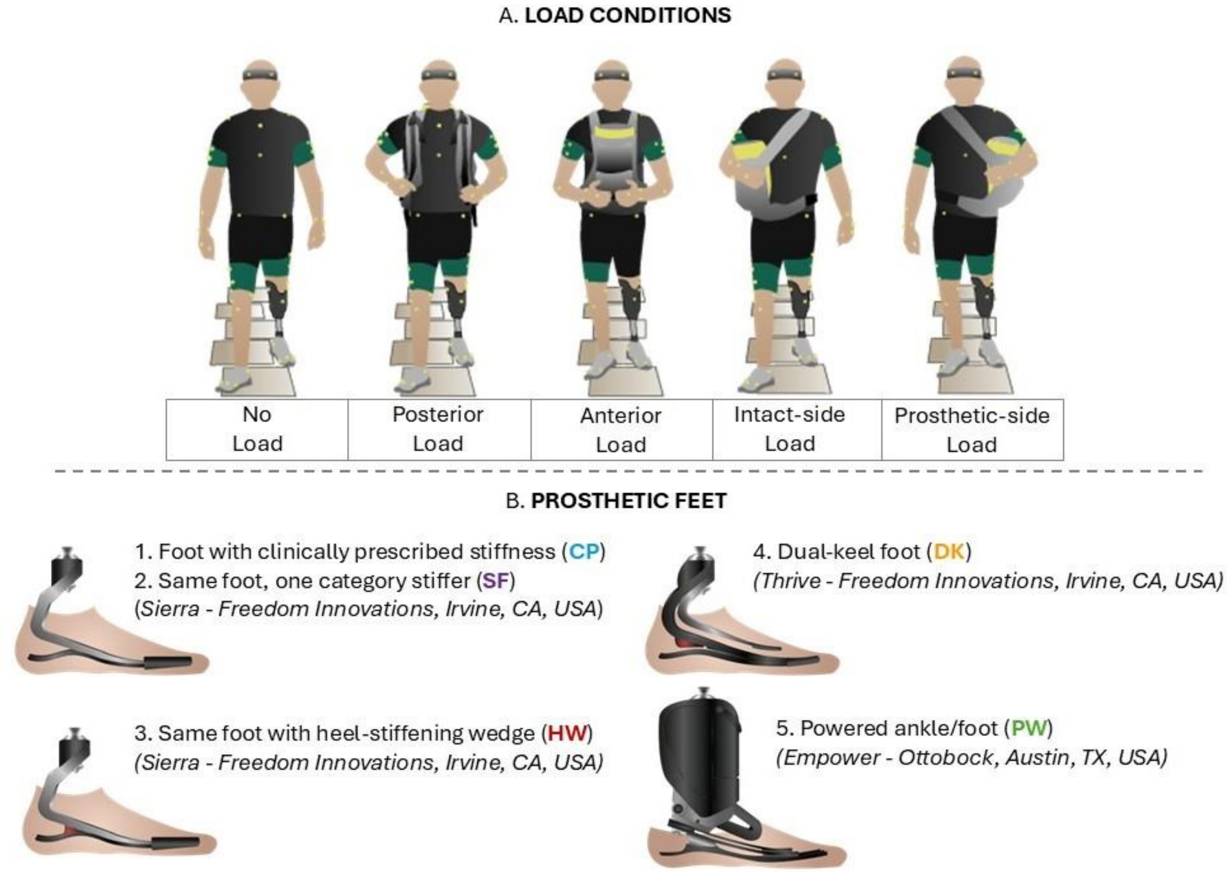

Fig 4.1 A: load conditions, B: study prosthetic feet (commercially available models). Note that for each participant, all study feet were of the same clinically prescribed stiffness category, except for the one category stiffer foot (SF).

During data collection, participants wore study-provided spandex clothing. The same researcher placed 14-mm reflective markers following Vicon's Plug-in-Gait marker set. For accurate joint center locations and segment tracking, additional markers were placed bilaterally on the medial malleolus, medial knee epicondyle, medial elbow, tibial tuberosity, fibular head, first and fifth metatarsal heads, as well as clusters of markers placed on the upper arms and thighs. The markers on the prosthetic limb mirrored their intact limb. Three markers were placed to track and define the load segment (two on top, one on bottom). During loaded conditions, any physical markers obstructed by the load carrier were removed, and virtual markers were reconstructed using a digitizing procedure during post-processing. Marker trajectories were recorded at 120 Hz using a 16-camera motion capture system (Vantage V8, Vicon Motion Systems, Oxford, UK). Overground kinetic data were also captured from five embedded force plates (AMTI, Watertown, MA, USA) at 1200 Hz, time synced with marker trajectory data.

4.3.3 Protocol

At the first study visit, participants were fitted with and acclimated to all study feet and load conditions (randomized), and had self-selected walking speed (SSWS), anthropometrics, and amputation details recorded. At the second study visit, participants completed walking trials across randomized load and foot conditions while wearing their prescribed socket and suspension. Each trial involved overground walking at SSWS across the five force plates, with ≥ 2 repetitions per foot-load combination. Rest was allowed as needed.

4.3.4 Data Analysis

Raw marker trajectory data were filtered using Woltring quintic spline-interpolation with a mean-square-error of 10 mm^2, and ground reaction force data was low-pass filtered using a 4^{th}-order Butterworth filter with a cutoff frequency of 25 Hz. A 15-segment whole body model was created using Visual 3D software (HAS-Motion, Kingston, Ontario, Canada), and was used to calculate net ankle, knee, and hip joint power of the lower limbs. See (Ardianuari et al., 2024; Cyr et al., 2025) (Chapter 2) for details.

Net ankle power was calculated using the unified deformable segment method, accounting for power contributions from the deforming structures of the prosthesis (Takahashi et al., 2015; Zelik and Honert, 2018). Knee and hip joint powers were calculated using standard inverse dynamics techniques (Winter, 1991). Work contributions from all three anatomical planes were summed together for each joint to calculate net joint work (i.e., summation of sagittal, frontal, transverse joint works). All joint powers were normalized by participant body mass (kg), including the mass of the added load when applicable. The time-integral of the net joint power curves above zero (net positive work) and below zero (net negative work) were calculated for the ankle, hip, and knee joints. The resulting work was first calculated over each gait cycle (heel strike to heel strike) and then calculated within subphases: early stance (heel strike to foot adjacent), late stance (foot adjacent to toe-off), and swing (toe-off to heel strike) to provide further insights into work contributions over the entire gait cycle.

4.3.5 Statistical Analysis

Linear mixed-effects regression assessed differences in lower-limb joint work over the entire gait cycle across prosthetic feet within each load condition. All loads were modeled together with a foot-by-load interaction, assuming a common variance and thus similar standard errors (SE) across loads and feet. Participant and foot-within-participant were included as random effects, with multiple random effects structures compared via likelihood ratio tests to select the best-fitting model. The dependent variable was transformed if residual heteroscedasticity was detected. Hypothesis testing for the overall associations between foot and outcome variables were performed using conditional F-tests for each load, with Benjamini-Hochberg correction applied across the loads to control the false discovery rate at 5%. Hypothesis testing for pairwise differences across feet was performed using Tukey method to account for the inflation of the Type-1 error due to multiple testing (10 comparisons per load). All analyses were conducted in R v4.2.3 (R Foundation for Statistical Computing, Vienna, Austria) using the following packages: *tidyverse*, *lme4*, *emmeans*, and *lmerTest*.

4.4 RESULTS

4.4.1 Participants

Completing the protocol were twelve participants (Table 4.1). Due to residual limb lengths and prosthetic build height restrictions, only seven participants were able to be fit with the PW foot.

Table 4.1 Participant demographic characteristics. For other information including residual limb length, please refer to Tables 2.1 and 3.1. Superscripts correspond to the manufacturers: [a]College Park, [b]Fillauer, [c]Ossur, [d]Blatchford. Abbreviations: Medicare Functional Classification (MFC), self-selected walking speed (SSWS), Patellar Tendon Bearing (PTB), Total Surface Bearing (TSB).

Participant	Age (yrs)	Sex	Amputation etiology	Mass with prosthesis (kg)	Height (m)	MFC K-Level (0-4)	SSWS (m/s)	Prescribed prosthesis: Foot	Foot stiffness category (1-9)	Socket design	Suspension system
01	59	M	Trauma	83.5	1.67	3	1.16	Trustep[a]	6	hybrid PTB	pin lock
02	40	M	Trauma	102.3	1.81	4	1.67	All Pro[b]	7	hybrid PTB	sleeve
03	60	M	Trauma	111.9	1.80	3	1.30	Proflex Pivot[c]	7	TSB	pin lock
04	58	F	Congenital	96.6	1.69	3	1.12	ElanIC[d]	6	hybrid PTB	sleeve + suction
05	39	M	Trauma	105.7	1.71	4	1.43	Proflex Torsion[c]	7	hybrid PTB	pin lock + BOA
06	25	F	Congenital	52.6	1.56	4	1.37	EchelonVAC[d]	2	TSB	sleeve
07	43	M	Infection	107.0	1.82	3	1.32	Proflex XC[c]	7	hybrid PTB	pin lock
08	31	M	Trauma	98.5	1.83	3	1.26	Soleus Tactical[a]	7	TSB	pin lock + BOA
09	36	M	Trauma	110.4	1.86	3	1.20	All Pro[b]	7	TSB	suction
10	29	M	Trauma	83.9	1.64	3	1.16	Proflex XC Torsion[c]	6	TSB	pin lock + suction
11	53	M	Dysvascular	106.6	1.86	3	0.92	Tribute[a]	7	PTB	pin lock
12	75	M	Trauma	93.6	1.83	3	1.17	All Pro[b]	7	hybrid PTB	sleeve + seal in
Mean ± SD	**46 ± 15**			**96.1 ± 16.6**	**1.76 ± 0.10**		**1.26 ± 0.19**				

4.4.2 Intact Limb Work

Significant differences were only observed between feet for positive net knee work during the posterior load condition (Fig. 4.2.B and Table 4.2.B). Participants had significantly less positive knee work with the PW foot compared to the HW (p = 0.001) and DK feet (p = 0.007). During the anterior load condition, positive net ankle work differed between the PW and CP foot (p = 0.035) and between the PW and SF feet (p = 0.028), but these differences did not remain significant after multiple-comparison correction (Fig. 4.2.A and Table 4.2.A).

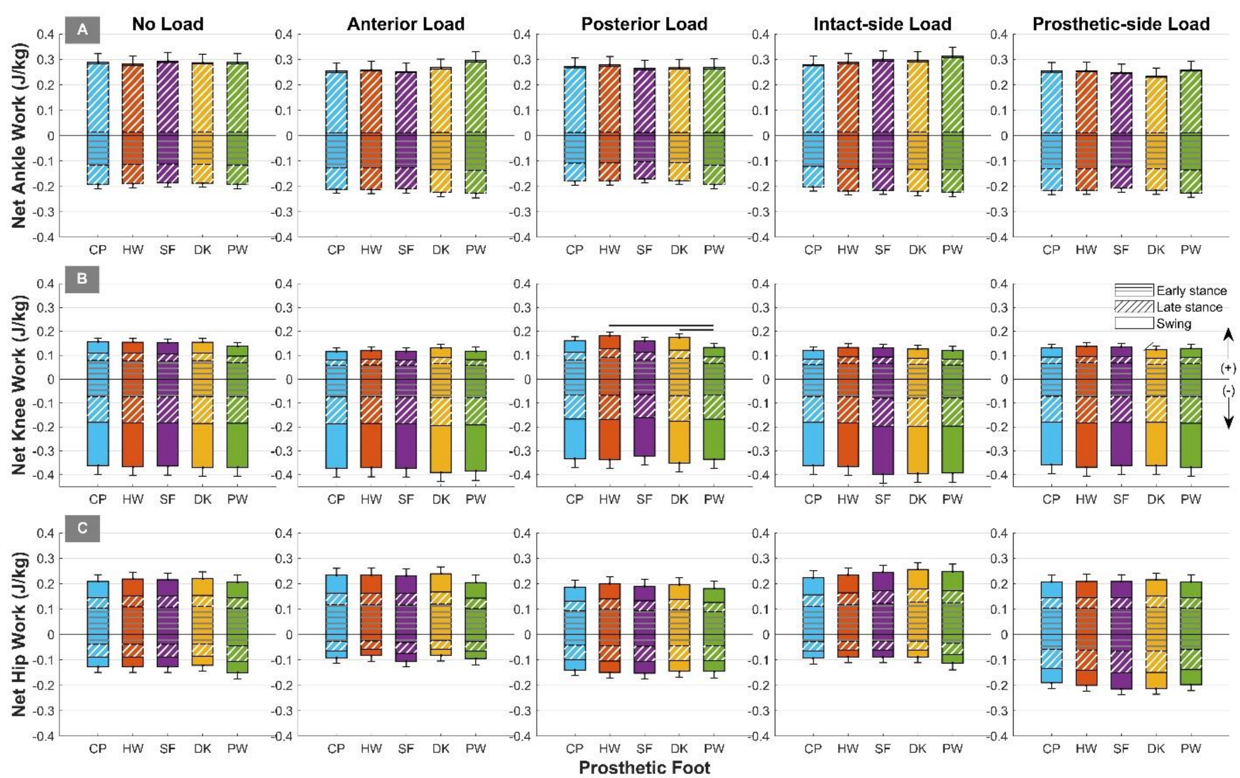

Fig 4.2 Bars represent intact limb mean joint work over the entire gait cycle (heel strike to heel strike), with vertical error bars denoting SE, for each foot within each load condition. Stacked segments indicate the proportional contributions of early stance, late stance, and swing, which together sum to the total mean values. Horizontal lines indicate pairwise significant differences over the intact limb gait cycle. Abbreviations: clinically prescribed prosthetic foot (CP), same foot with a heel-stiffening wedge (HW), same foot but one category stiffer (SF), dual-keel foot (DK), powered ankle-foot (PW).

Table 4.2 Mean ± SE net negative and positive joint mechanical work over the intact limb gait cycle (heel strike to heel strike) for each foot within each load condition. Positive work represents energy generation, and negative work represents energy absorption/dissipation. Asterisk (*) indicates statistical significance. Abbreviations: Benjamini-Hochberg adjustment (BH adj), clinically prescribed prosthetic foot (CP), same foot with a heel-stiffening wedge (HW), same foot but one category stiffer (SF), dual-keel foot (DK), powered ankle-foot (PW).

A. Net Ankle Work

Positive (J/kg)							
	CP	HW	SF	DK	PW	*p*-value	*p* BH adj
No Load	0.276 ± 0.033	0.268 ± 0.033	0.280 ± 0.033	0.274 ± 0.033	0.275 ± 0.034	0.87	0.87
Anterior Load	0.242 ± 0.033	0.247 ± 0.033	0.241 ± 0.033	0.256 ± 0.033	0.282 ± 0.034	**0.03***	0.15
Posterior Load	0.260 ± 0.033	0.266 ± 0.033	0.252 ± 0.033	0.255 ± 0.033	0.256 ± 0.034	0.79	0.87
Intact-side Load	0.267 ± 0.033	0.276 ± 0.033	0.286 ± 0.033	0.283 ± 0.033	0.298 ± 0.035	0.22	0.38
Prosthetic-side Load	0.243 ± 0.033	0.244 ± 0.033	0.237 ± 0.033	0.223 ± 0.033	0.247 ± 0.034	0.23	0.38

Negative (J/kg)							
	CP	HW	SF	DK	PW	*p*-value	*p* BH adj
No Load	-0.192 ± 0.016	-0.189 ± 0.016	-0.186 ± 0.016	-0.187 ± 0.016	-0.189 ± 0.018	0.96	0.96
Anterior Load	-0.211 ± 0.016	-0.212 ± 0.016	-0.210 ± 0.016	-0.224 ± 0.016	-0.227 ± 0.018	0.42	0.78
Posterior Load	-0.179 ± 0.016	-0.178 ± 0.016	-0.170 ± 0.016	-0.177 ± 0.016	-0.193 ± 0.017	0.47	0.78
Intact-side Load	-0.202 ± 0.016	-0.218 ± 0.016	-0.215 ± 0.016	-0.220 ± 0.016	-0.223 ± 0.018	0.38	0.78
Prosthetic-side Load	-0.216 ± 0.016	-0.215 ± 0.016	-0.207 ± 0.016	-0.215 ± 0.016	-0.225 ± 0.017	0.66	0.83

B. Net Knee Work

Positive (J/kg)							
	CP	HW	SF	DK	PW	*p*-value	*p* BH adj
No Load	0.157 ± 0.015	0.155 ± 0.015	0.152 ± 0.015	0.155 ± 0.015	0.138 ± 0.016	0.51	0.71
Anterior Load	0.115 ± 0.015	0.119 ± 0.015	0.116 ± 0.015	0.131 ± 0.015	0.117 ± 0.017	0.48	0.71
Posterior Load	0.162 ± 0.015	0.182 ± 0.015	0.160 ± 0.015	0.174 ± 0.015	0.133 ± 0.016	**0.001***	**0.006***
Intact-side Load	0.121 ± 0.015	0.133 ± 0.015	0.132 ± 0.015	0.126 ± 0.015	0.120 ± 0.017	0.69	0.71
Prosthetic-side Load	0.132 ± 0.015	0.137 ± 0.015	0.135 ± 0.015	0.124 ± 0.015	0.129 ± 0.016	0.71	0.71

Negative (J/kg)							
	CP	HW	SF	DK	PW	*p*-value	*p* BH adj
No Load	-0.361 ± 0.037	-0.367 ± 0.037	-0.364 ± 0.037	-0.370 ± 0.037	-0.369 ± 0.038	0.98	0.98
Anterior Load	-0.374 ± 0.037	-0.370 ± 0.038	-0.373 ± 0.037	-0.390 ± 0.037	-0.384 ± 0.039	0.75	0.98
Posterior Load	-0.333 ± 0.037	-0.337 ± 0.037	-0.323 ± 0.037	-0.351 ± 0.037	-0.335 ± 0.039	0.56	0.98
Intact-side Load	-0.361 ± 0.037	-0.365 ± 0.037	-0.398 ± 0.037	-0.395 ± 0.037	-0.393 ± 0.040	0.07	0.37
Prosthetic-side Load	-0.358 ± 0.037	-0.368 ± 0.037	-0.361 ± 0.037	-0.361 ± 0.037	-0.369 ± 0.038	0.97	0.98

C. Net Hip Work

Positive (J/kg)

	CP	HW	SF	DK	PW	*p*-value	*p* BH adj
No Load	0.209 ± 0.027	0.219 ± 0.027	0.216 ± 0.027	0.220 ± 0.027	0.206 ± 0.029	0.88	0.98
Anterior Load	0.234 ± 0.027	0.234 ± 0.028	0.232 ± 0.027	0.240 ± 0.027	0.205 ± 0.030	0.45	0.98
Posterior Load	0.187 ± 0.027	0.201 ± 0.027	0.190 ± 0.027	0.197 ± 0.027	0.181 ± 0.029	0.77	0.98
Intact-side Load	0.224 ± 0.027	0.235 ± 0.027	0.246 ± 0.027	0.257 ± 0.027	0.248 ± 0.030	0.23	0.98
Prosthetic-side Load	0.208 ± 0.027	0.209 ± 0.028	0.209 ± 0.027	0.216 ± 0.027	0.208 ± 0.028	0.98	0.98

Negative (J/kg)

	CP	HW	SF	DK	PW	*p*-value	*p* BH adj
No Load	-0.127 ± 0.022	-0.127 ± 0.022	-0.127 ± 0.022	-0.121 ± 0.022	-0.150 ± 0.025	0.7	0.97
Anterior Load	-0.092 ± 0.022	-0.083 ± 0.023	-0.105 ± 0.022	-0.082 ± 0.022	-0.094 ± 0.026	0.71	0.97
Posterior Load	-0.140 ± 0.022	-0.149 ± 0.023	-0.152 ± 0.022	-0.145 ± 0.022	-0.145 ± 0.026	0.97	0.97
Intact-side Load	-0.093 ± 0.023	-0.088 ± 0.023	-0.089 ± 0.022	-0.089 ± 0.022	-0.112 ± 0.027	0.88	0.97
Prosthetic-side Load	-0.190 ± 0.023	-0.200 ± 0.023	-0.214 ± 0.022	-0.213 ± 0.022	-0.197 ± 0.024	0.63	0.97

4.4.3 Prosthetic Limb Work

Significant differences were observed between feet for both positive and negative net ankle work within all load conditions (Fig. 4.3.A and Table 4.3.A). For positive ankle work, participants had significantly higher magnitude when they walked with the PW foot compared to when they walked with the SF foot and DK foot within all load conditions (all $p < 0.03$) and compared to when they walked with the CP foot and HW foot within the posterior load and intact-side load conditions only (all $p < 0.03$) (Fig. 4.3.A and Table 4.4). Additionally, with the CP foot and the HW foot, participants had significantly more positive ankle work compared to when they walked with the SF foot and DK foot within all load conditions (all $p < 0.01$).

Overall, the CP and HW feet resulted in the most negative ankle work, while the PW foot resulted in the most positive ankle work, within all load conditions. Specifically, with the CP foot, participants had significantly more negative ankle work compared to when they walked with the SF foot and DK foot within all load conditions (all $p < 0.001$) and compared to when they walked with the PW foot during the anterior load condition ($p = 0.027$) (Fig. 4.3.A and Table 4.4). With the HW foot, participants also had significantly more negative ankle work compared to when they walked with the SF foot and DK foot within all load conditions (all $p < 0.003$) and compared to when they walked with the PW foot within the anterior load condition ($p = 0.025$).

Surprisingly, no significant differences were found between feet for the knee or hip net positive or net negative work within any of the load conditions (Fig. 4.3.B and Table 4.3.B, Fig. 4.3.C and Table 4.3.C). In general, the magnitude of the mean differences was lower and the within participant variability was higher than that of ankle work, leading to larger confidence intervals and higher p-values (see Appendix for details).

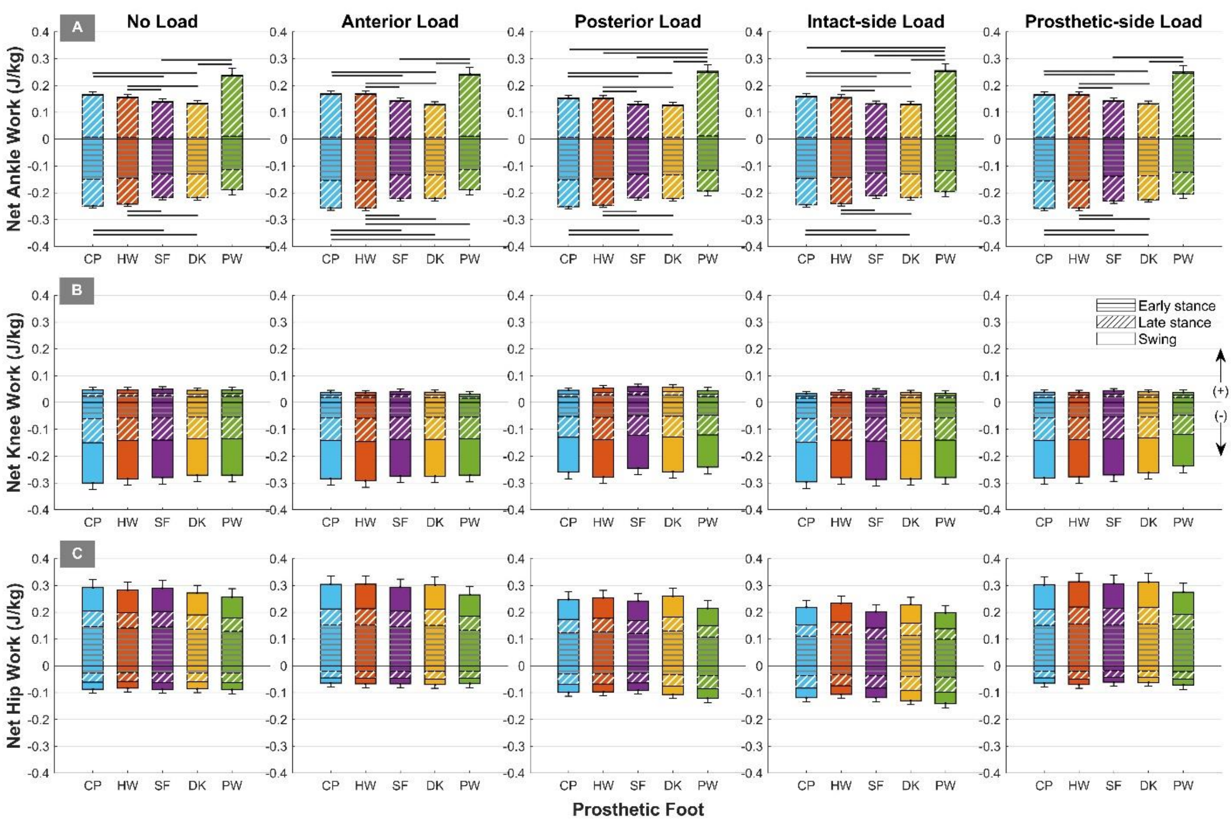

Fig 4.3 Bars represent prosthetic limb mean joint work over the entire gait cycle (heel strike to heel strike), with vertical error bars denoting SE, for each foot within each load condition. Stacked segments indicate the proportional contributions of early stance, late stance, and swing, which together sum to the total mean values. Horizontal lines indicate pairwise significant differences over the prosthetic limb gait cycle. Abbreviations: clinically prescribed prosthetic foot (CP), same foot with a heel-stiffening wedge (HW), same foot but one category stiffer (SF), dual-keel foot (DK), powered ankle-foot (PW).

Table 4.3 Mean ± SE net negative and positive joint mechanical work over the prosthetic limb gait cycle (heel strike to heel strike) for each foot within each load condition. Positive work represents energy generation, and negative work represents energy absorption/dissipation. Asterisk (*) indicates statistical significance. Abbreviations: Benjamini-Hochberg adjustment (BH adj), clinically prescribed prosthetic foot (CP), same foot with a heel-stiffening wedge (HW), same foot but one category stiffer (SF), dual-keel foot (DK), powered ankle-foot (PW).

A. Net Ankle Work

Positive (J/kg)

	CP	HW	SF	DK	PW	*p*-value	*p* BH adj
No Load	0.158 ± 0.010	0.150 ± 0.010	0.133 ± 0.010	0.127 ± 0.010	0.228 ± 0.025	**0.0033***	**0.0033***
Anterior Load	0.161 ± 0.010	0.161 ± 0.010	0.136 ± 0.010	0.123 ± 0.010	0.231 ± 0.025	**9×10^{-04}***	**0.0027***
Posterior Load	0.146 ± 0.010	0.145 ± 0.010	0.124 ± 0.010	0.121 ± 0.010	0.241 ± 0.025	**0.0021***	**0.0027***
Intact-side Load	0.152 ± 0.010	0.148 ± 0.010	0.126 ± 0.010	0.125 ± 0.010	0.244 ± 0.025	**0.0021***	**0.0027***
Prosthetic-side Load	0.158 ± 0.010	0.159 ± 0.010	0.136 ± 0.010	0.126 ± 0.010	0.238 ± 0.025	**0.0016***	**0.0027***

Negative (J/kg)

	CP	HW	SF	DK	PW	*p*-value	*p* BH adj
No Load	-0.249 ± 0.008	-0.242 ± 0.009	-0.217 ± 0.009	-0.218 ± 0.009	-0.189 ± 0.018	**0.0012***	**0.0014***
Anterior Load	-0.257 ± 0.008	-0.257 ± 0.009	-0.222 ± 0.009	-0.221 ± 0.009	-0.189 ± 0.018	**3×10^{-04}***	**0.0014***
Posterior Load	-0.252 ± 0.008	-0.246 ± 0.009	-0.219 ± 0.009	-0.222 ± 0.009	-0.193 ± 0.018	**7×10^{-04}***	**0.0014***
Intact-side Load	-0.245 ± 0.008	-0.24 ± 0.009	-0.211 ± 0.009	-0.218 ± 0.009	-0.196 ± 0.018	**0.0014***	**0.0014***
Prosthetic-side Load	-0.258 ± 0.008	-0.257 ± 0.009	-0.23 ± 0.009	-0.226 ± 0.009	-0.204 ± 0.018	**9×10^{-04}***	**0.0014***

B. Net Knee Work

Positive (J/kg)

	CP	HW	SF	DK	PW	*p*-value	*p* BH adj
No Load	0.048 ± 0.009	0.048 ± 0.009	0.05 ± 0.009	0.046 ± 0.008	0.047 ± 0.011	0.94	0.94
Anterior Load	0.038 ± 0.008	0.037 ± 0.008	0.042 ± 0.008	0.039 ± 0.008	0.032 ± 0.009	0.64	0.83
Posterior Load	0.046 ± 0.008	0.055 ± 0.009	0.059 ± 0.01	0.057 ± 0.009	0.045 ± 0.011	0.1	0.48
Intact-side Load	0.033 ± 0.007	0.039 ± 0.008	0.044 ± 0.008	0.038 ± 0.008	0.035 ± 0.009	0.26	0.64
Prosthetic-side Load	0.039 ± 0.008	0.038 ± 0.008	0.044 ± 0.008	0.04 ± 0.008	0.038 ± 0.01	0.66	0.83

Negative (J/kg)

	CP	HW	SF	DK	PW	*p*-value	*p* BH adj
No Load	-0.300 ± 0.024	-0.285 ± 0.024	-0.280 ± 0.024	-0.271 ± 0.024	-0.271 ± 0.025	0.29	0.48
Anterior Load	-0.284 ± 0.024	-0.292 ± 0.024	-0.274 ± 0.024	-0.275 ± 0.024	-0.271 ± 0.025	0.63	0.77
Posterior Load	-0.260 ± 0.024	-0.278 ± 0.024	-0.245 ± 0.024	-0.258 ± 0.024	-0.241 ± 0.026	0.12	0.31
Intact-side Load	-0.296 ± 0.024	-0.28 ± 0.024	-0.287 ± 0.024	-0.285 ± 0.024	-0.28 ± 0.025	0.77	0.77

Prosthetic-side Load	-0.281 ± 0.024	-0.277 ± 0.024	-0.27 ± 0.024	-0.262 ± 0.024	-0.237 ± 0.026	0.12	0.31

C. Net Hip Work

Positive (J/kg)

	CP	**HW**	**SF**	**DK**	**PW**	***p*-value**	***p* BH adj**
No Load	0.292 ± 0.031	0.283 ± 0.03	0.290 ± 0.03	0.272 ± 0.029	0.257 ± 0.031	0.49	0.58
Anterior Load	0.304 ± 0.031	0.305 ± 0.031	0.294 ± 0.03	0.302 ± 0.031	0.265 ± 0.031	0.42	0.58
Posterior Load	0.248 ± 0.028	0.254 ± 0.028	0.242 ± 0.027	0.26 ± 0.029	0.215 ± 0.029	0.35	0.58
Intact-side Load	0.219 ± 0.026	0.234 ± 0.027	0.202 ± 0.026	0.229 ± 0.027	0.198 ± 0.026	0.2	0.58
Prosthetic-side Load	0.302 ± 0.031	0.314 ± 0.032	0.307 ± 0.031	0.313 ± 0.032	0.275 ± 0.033	0.58	0.58

Negative (J/kg)

	CP	**HW**	**SF**	**DK**	**PW**	***p*-value**	***p* BH adj**
No Load	-0.087 ± 0.015	-0.083 ± 0.014	-0.088 ± 0.014	-0.086 ± 0.014	-0.089 ± 0.016	0.99	0.99
Anterior Load	-0.064 ± 0.014	-0.067 ± 0.015	-0.067 ± 0.014	-0.07 ± 0.014	-0.066 ± 0.016	0.99	0.99
Posterior Load	-0.099 ± 0.014	-0.097 ± 0.014	-0.091 ± 0.014	-0.107 ± 0.014	-0.121 ± 0.017	0.27	0.68
Intact-side Load	-0.119 ± 0.014	-0.106 ± 0.014	-0.119 ± 0.015	-0.130 ± 0.014	-0.140 ± 0.016	0.09	0.46
Prosthetic-side Load	-0.064 ± 0.014	-0.07 ± 0.014	-0.061 ± 0.014	-0.062 ± 0.014	-0.071 ± 0.017	0.89	0.99

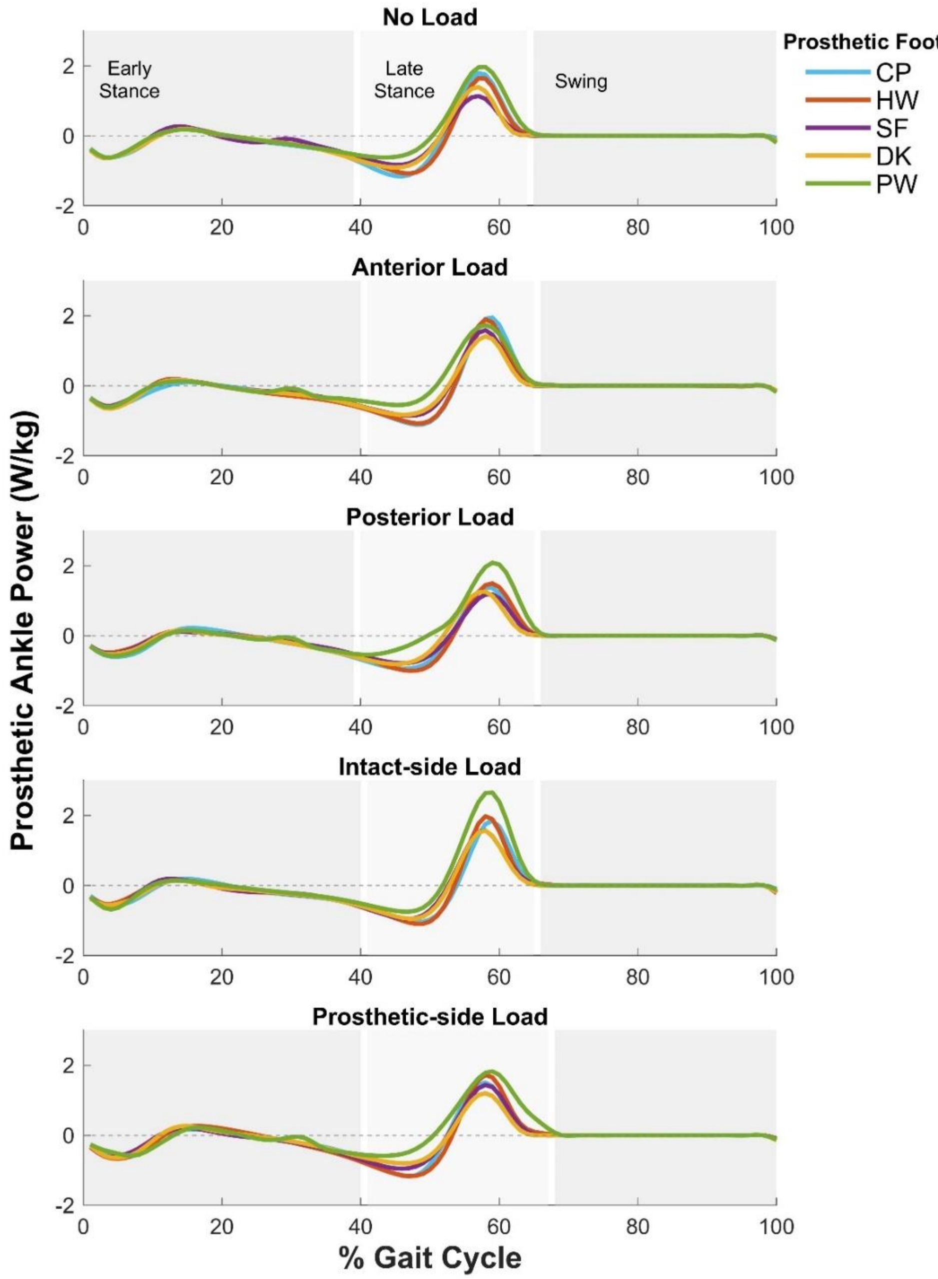

Fig 4.4 Ensemble means of prosthetic-limb ankle (unified deformable) power for each foot across load conditions, with ankle work calculated as the time integral of ankle power. Note that positive ankle power, and therefore positive ankle work, primarily occurs during late stance.

Table 4.4 Mean differences ± SE, [Pairwise 95% confidence intervals], and p-values for net positive and negative ankle work over the prosthetic limb gait cycle (heel strike to heel strike) within each load condition. Bold values with asterisk (*) indicates pairwise significant differences. Note that neither CP – HW nor SF – DK pairwise comparisons had any significant result across load conditions (not shown in the table). Abbreviations: clinically prescribed prosthetic foot (CP), same foot with a heel-stiffening wedge (HW), same foot but one category stiffer (SF), dual-keel foot (DK), powered ankle-foot (PW). Notation (p-values): Xe-yy = x × 10^{-yy}.

Positive (J/kg)

	CP - SF	CP - DK	CP - PW	HW - SF	HW - DK	HW - PW	SF - PW	DK - PW
No Load	**0.024 ± 0.005, [0.010, 0.039], 1e-04** *	**0.031 ± 0.006, [0.013, 0.048], 8e-05** *	-0.070 ± 0.023, [-0.154, 0.014], 0.11	**0.017 ± 0.005, [0.003, 0.031], 0.012** *	**0.023 ± 0.006, [0.006, 0.041], 0.0036** *	-0.077 ± 0.023, [-0.162, 0.007], 0.072	**-0.094 ± 0.023, [-0.179, -0.010], 0.03** *	**-0.100 ± 0.024, [-0.185, -0.016], 0.022** *
Anterior Load	**0.025 ± 0.005, [0.011, 0.040], 3e-05** *	**0.039 ± 0.006, [0.021, 0.056], 3e-07** *	-0.069 ± 0.023, [-0.154, 0.015], 0.11	**0.025 ± 0.005, [0.010, 0.040], 5e-05** *	**0.039 ± 0.006, [0.021, 0.056], 5e-07** *	-0.069 ± 0.023, [-0.154, 0.015], 0.11	**-0.095 ± 0.023, [-0.179, -0.010], 0.03** *	**-0.108 ± 0.024, [-0.192, -0.024], 0.015** *
Posterior Load	**0.023 ± 0.005, [0.008, 0.037], 2e-04** *	**0.025 ± 0.006, [0.007, 0.042], 0.0018** *	**-0.094 ± 0.024, [-0.179, -0.010], 0.03** *	**0.022 ± 0.005, [0.008, 0.036], 4e-04** *	**0.024 ± 0.006, [0.006, 0.041], 0.0026** *	**-0.095 ± 0.024, [-0.179, -0.011], 0.028** *	**-0.117 ± 0.024, [-0.201, -0.033], 0.0099** *	**-0.119 ± 0.024, [-0.203, -0.035], 0.0085** *
Intact-side Load	**0.026 ± 0.005, [0.011, 0.041], 4e-05** *	**0.027 ± 0.006, [0.010, 0.044], 3e-04** *	**-0.092 ± 0.023, [-0.177, -0.008], 0.033** *	**0.021 ± 0.006, [0.006, 0.037], 0.0018** *	**0.023 ± 0.006, [0.005, 0.040], 0.0043** *	**-0.097 ± 0.023, [-0.181, -0.013], 0.027** *	**-0.118 ± 0.023, [-0.203, -0.034], 0.0095** *	**-0.120 ± 0.024, [-0.204, -0.036], 0.0086** *
Prosthetic-side Load	**0.022 ± 0.005, [0.007, 0.037], 7e-04** *	**0.032 ± 0.006, [0.014, 0.049], 4e-05** *	-0.080 ± 0.024, [-0.165, 0.004], 0.061	**0.023 ± 0.005, [0.008, 0.038], 4e-04** *	**0.033 ± 0.006, [0.015, 0.050], 2e-05** *	-0.079 ± 0.024, [-0.164, 0.005], 0.064	**-0.102 ± 0.024, [-0.187, -0.018], 0.02** *	**-0.112 ± 0.024, [-0.196, -0.028], 0.012** *

Negative (J/kg)

	CP - SF	CP - DK	CP - PW	HW - SF	HW - DK	HW - PW	SF - PW	DK - PW
No Load	**-0.031 ± 0.005, [-0.045, -0.017], 2e-07** *	**-0.030 ± 0.005, [-0.046, -0.015], 6e-06** *	-0.059 ± 0.017, [-0.119, 0.000], 0.051	**-0.024 ± 0.005, [-0.039, -0.009], 2e-04** *	**-0.023 ± 0.006, [-0.039, -0.007], 0.0012** *	-0.052 ± 0.017, [-0.112, 0.007], 0.088	-0.028 ± 0.017, [-0.087, 0.032], 0.51	-0.029 ± 0.017, [-0.088, 0.031], 0.48
Anterior Load	**-0.035 ± 0.005, [-0.048, -0.021], 5e-09** *	**-0.036 ± 0.005, [-0.050, -0.021], 8e-08** *	**-0.068 ± 0.017, [-0.127, -0.008], 0.027** *	**-0.035 ± 0.005, [-0.050, -0.020], 8e-08** *	**-0.036 ± 0.006, [-0.052, -0.020], 4e-07** *	**-0.068 ± 0.017, [-0.128, -0.009], 0.025** *	-0.033 ± 0.017, [-0.093, 0.026], 0.36	-0.032 ± 0.017, [-0.092, 0.027], 0.39
Posterior Load	**-0.033 ± 0.005, [-0.047, -0.019], 2e-08** *	**-0.030 ± 0.005, [-0.045, -0.015], 8e-06** *	-0.059 ± 0.017, [-0.118, 0.001], 0.053	**-0.027 ± 0.005, [-0.041, -0.012], 3e-05** *	**-0.024 ± 0.006, [-0.040, -0.008], 0.001** *	-0.053 ± 0.017, [-0.112, 0.007], 0.086	-0.026 ± 0.017, [-0.085, 0.034], 0.58	-0.029 ± 0.017, [-0.088, 0.031], 0.5
Intact-side Load	**-0.033 ± 0.005, [-0.048, -0.019], 4e-08** *	**-0.027 ± 0.005, [-0.041, -0.012], 5e-05** *	-0.049 ± 0.017, [-0.108, 0.011], 0.11	**-0.029 ± 0.006, [-0.045, -0.013], 2e-05** *	**-0.022 ± 0.006, [-0.038, -0.006], 0.0028** *	-0.044 ± 0.017, [-0.104, 0.015], 0.16	-0.015 ± 0.017, [-0.075, 0.044], 0.88	-0.022 ± 0.017, [-0.082, 0.037], 0.69
Prosthetic-side Load	**-0.028 ± 0.005, [-0.042, -0.014], 3e-06** *	**-0.032 ± 0.005, [-0.047, -0.016], 2e-06** *	-0.054 ± 0.017, [-0.114, 0.005], 0.075	**-0.027 ± 0.005, [-0.042, -0.012], 4e-05** *	**-0.031 ± 0.006, [-0.047, -0.015], 2e-05** *	-0.053 ± 0.017, [-0.113, 0.006], 0.081	-0.026 ± 0.017, [-0.085, 0.033], 0.57	-0.022 ± 0.017, [-0.082, 0.037], 0.69

4.5 DISCUSSION

The purpose of this research was to provide evidence to guide prosthesis foot prescription for individuals with TTA who carry loads in daily life. The results partially supported our hypothesis that a prosthetic foot would optimize prosthetic ankle work. We found only a few significant differences in intact limb net ankle work during anterior load condition and net knee work during posterior load condition. Most differences were observed in prosthetic limb net ankle work across feet for each load condition, whereas compensatory knee or hip work was not observed. These findings suggest that prosthetic foot selection primarily influences prosthetic limb distal joint mechanics during load carriage.

4.5.1 Intact Limb

During the anterior load condition, the trend of greater positive net ankle work observed with the PW foot relative to the CP and SF feet likely reflects increased reliance on the intact plantarflexor contributions to accelerate forward propulsion in late stance. This is consistent with prior simulation findings demonstrating higher gastrocnemius contributions with the PW foot during load carriage (Lefranc et al., 2024). The less positive net knee work during the posterior load condition with the PW foot in early stance is also consistent with our EMG findings showing decreased rectus femoris activity (Ardianuari et al., 2026b) (Chapter 5). The PW foot may reduce the need for compensatory energy generation at the intact knee during early stance by mitigating collision losses, resulting in a distal-to-proximal redistribution of mechanical work.

4.5.2 Prosthetic Limb

Ankle Work

<u>No load</u>

Under unloaded conditions, a significant effect of prosthetic foot selection was observed on ankle work. As expected, the PW foot generated the greatest net positive ankle work, indicating superior propulsion capability during late stance (see Fig. 4.3.A and Fig.4.4), potentially enhancing gait efficiency during everyday ambulation. Conversely, the CP and HW feet consistently resulted in greater net negative ankle work compared to the stiffer feet (i.e., SF and DK), suggesting higher energy absorption during early stance from more compliant feet (see Fig. 4.3.A). This effect may benefit users requiring controlled tibial progression (i.e., improved stability) and shock absorption, even in unloaded conditions. Importantly, the CP, HW, and PW feet outperformed the SF and DK feet in promoting either energy absorption or return, which may make them preferable baseline prescriptions when load carriage is not a priority.

<u>Anterior load</u>

The anterior load condition produced more detectable differences between feet. The PW foot generated the highest net positive ankle work of all feet, suggesting that it offers improved propulsion under anteriorly loaded walking. The CP and HW feet produced significantly greater net negative ankle work not only relative to the stiffer feet but also compared to the PW foot. The increased energy absorption has been associated with reduced plantarflexion stiffness which may influence perceived stability during early stance (Boutwell et al., 2017; Voloshina et al., 2025). These results suggest that the PW foot versus both CP and HW feet may offer distinct benefits, depending on user-specific priorities (propulsion vs. stability) when carrying anterior loads.

<u>Posterior load</u>

Ankle work trends during the posterior load condition were most similar to those in the intact-side load condition and were generally similar across all load conditions. The PW foot maintained the highest net positive ankle work and exceeded both CP and HW feet in this condition, suggesting that it may be especially beneficial for users who carry loads on their back. The CP and HW feet again produced greater net negative ankle work compared to the other feet. With the PW foot, users could benefit from enhanced propulsion to counterbalance posterior mass distribution that has been demonstrated to alter spatiotemporal outcomes (Doyle et al., 2014). However, our prior study observed that all feet provided similar forward propulsion relative to ground reaction forces with a posterior load (Cyr et al., 2025).

Intact-side load

When loads were carried on the intact limb, the PW foot generated the greatest net positive ankle work and exceeded CP and HW feet in this condition, implying an advantage in restoring propulsion during lateral load carriage. This could be clinically relevant for individuals who habitually carry items on one side of their body. Additionally, the PW foot has been shown to regulate sagittal whole-body angular momentum more effectively during level-ground walking compared to using a passive-elastic prosthesis (D'Andrea et al., 2014). Our prior work also found that the PW foot improves sagittal balance control but exacerbates frontal balance control compared to other feet across all load conditions (Cyr et al., 2025). The CP and HW feet once again led to greater net negative ankle work compared to the stiffer feet.

Prosthetic-side load

Under prosthetic-side load, ankle work patterns mirrored those seen in other loaded conditions. The PW foot again provided the greatest net positive ankle work but was not significantly different from the CP or HW feet in this condition, indicating that multiple foot designs may be suitable depending on user goals. One plausible explanation is that shifting the load toward the prosthetic limb redistributed mass such that all foot types were required to absorb and return more energy on the prosthetic side, thus diminishing differences between feet. Additionally, the functionality of the PW foot may be dependent on user-specific adaptation (Kannenberg et al., 2022) and optimal timing of ankle push-off assistance (Malcolm et al., 2015), and participants may not have fully exploited the device's powered capabilities when the added mass was carried on the prosthetic side. The CP and HW feet produced greater net negative ankle work than the stiffer feet (i.e., SF and DK), suggesting consistent energy absorption even when mass is shifted toward the prosthetic limb.

Knee and Hip Work

Contrary to our hypothesis, no significant differences in net knee or hip joint work were observed across feet or load conditions. This suggests that prosthetic foot design primarily modulates prosthetic ankle-level mechanics without imposing additional demands on the ipsilateral proximal joints under moderate load carriage. However, sagittal hip power has been demonstrated to increase in response to an ipsilateral load (Ardianuari et al., 2024) (Chapter 2) and decrease in response to a back load relative to no load with the CP foot (Doyle et al., 2014). This discrepancy is likely attributable to methodological differences, as the current study summed joint work across all three planes (i.e., sagittal, frontal and transverse), which may have attenuated changes in sagittal hip power or work. The absence of compensatory hip strategies relative to net mechanical work may reflect sufficient distal modulation by the feet, although a larger cohort of participants is needed to confirm these insignificant trends. However, the absent response from net knee joint work is consistent with prior evidence showing no observable changes in net sagittal knee work with the use of PW foot relative to the CP foot (Molitor et al., 2026). The knee musculature (in particular, rectus femoris and vasti) primarily absorbs energy and facilitates power transfer between the leg and trunk rather than generating work (Neptune et al., 2004). This trend (i.e., negative net knee work across foot types) is observed in this study, and such a biomechanical phenomenon may remain consistent regardless of the type of prosthesis used. Additionally, prolonged adaptation to the study feet may alter proximal joint work in response to long-term load carriage.

4.5.3 Limitations

This study has several limitations. The generalizability of our results to the broader amputee population may be limited due to a relatively small sample. The small sample size may have limited detection of subtle effects at proximal joints of the prosthetic limb, and not all participants were able to complete the protocol with the PW foot. Equal sample sizes across feet and a larger cohort might have confirmed certain trends. Participants were only acutely exposed to each foot, without long-term adaptation. The added load used in this study represented a moderate magnitude. Heavier loads (e.g., 20 up to 45 kg (Orr et al., 2021)), commonly required in military activities, may yield more significant changes in joint work and potentially highlight differences in performance for stiffer feet like SF, HW, or DK more clearly than observed here. Next, our analysis focused on prosthetic limb joint work, excluding metabolic cost, comfort, and functional performance. Future research should examine long-term adaptation, a broader range of load magnitudes, and complementary outcomes such as energy efficiency and user-reported measures. Additionally, the long-term implications of different load carriage strategies remain unclear, particularly given the complex and context-dependent nature of energy expenditure during locomotion. Future work should also evaluate patient-reported outcomes and more immediate, clinically relevant considerations (e.g., user preference, perceived stability, and other performance-based metrics) to better inform amputee rehabilitation and prescription decisions.

4.5.4 Conclusion

The CP and HW feet may enhance stability through increased energy absorption, benefiting users who prioritize control, regardless of the load conditions. In contrast, the PW foot may be advantageous due to less compensatory energy generation at the intact knee, as well as enhanced prosthetic ankle propulsion, particularly with posterior or intact-side loads, but at the cost of frontal balance control. This trade-off, improved propulsion and sagittal balance versus decreased frontal balance, should be weighed carefully in clinical prescription. The CP and HW feet promote shock absorption with less push-off. As the prosthetic limb knee and hip joint work remained unaffected, prescription decisions should focus on optimizing ankle-level mechanics under load carriage. Given their superior ankle work performance, the CP, HW, and PW feet may be preferable to stiffer feet (SF and DK) for users who frequently carry loads. Ultimately, foot selection should balance individual goals for stability versus propulsion, informed by load carriage habits and balance control capabilities.

Acknowledgments

The authors thank Christina Carranza, L/CPO, for fitting and aligning the study prosthetic feet for all participants, and Jane Shofer (Biostatistician) for performing the statistical analyses

CHAPTER 5

AMPUTEE MOTOR CONTROL DURING LOADED WALKING WITH STIFFER AND POWERED FEET

Under Review in *Journal of NeuroEngineering and Rehabilitation*

Satria Ardianuari

Richard R. Neptune

Glenn K. Klute

5.1 ABSTRACT

Background Individuals with transtibial amputation often rely on prosthetic feet with fixed mechanical properties, which may limit distal limb neuromuscular strategies during demanding tasks such as load carriage. Although stiffer and powered prosthetic feet are purported to aid ambulation under load, their influence on motor control during loaded walking remains unclear. This study investigated whether changing prosthetic foot prescription alters muscle activation, and motor module composition and complexity during load carriage.

Methods Twelve individuals with unilateral transtibial amputation walked at their preferred speed while carrying no load and a 13.6-kg load in multiple conditions (front, back, intact-side, and prosthetic-side). Subjects used a clinically prescribed prosthetic foot, the same foot but one category stiffer, and, in a subset (n = 7), a powered ankle-foot prosthesis. Surface electromyography was collected from eight intact-limb muscles. Muscle activation including co-contraction was calculated, and a muscle module analysis was used to quantify motor control using non-negative matrix factorization. Linear mixed-effects models tested differences between feet in muscle activation and module complexity, while module similarity and activation timing were evaluated using cosine similarity and one-dimensional statistical parametric mapping, respectively.

Results Prosthetic foot types influenced activation of several intact-limb muscles across load conditions, with powered and stiffer feet often associated with increased plantarflexor and knee extensor activity. Differences in muscle co-contraction were limited and primarily observed during unloaded walking. Despite these muscle-level changes, motor module complexity was highly conserved across feet and load conditions. Three modules were sufficient to explain over 90% of electromyographic variance, with no systematic differences between feet. A few foot-specific effects on first-module variance were detected in isolated loaded conditions (i.e., back load and intact-side load) but were not consistent. Module composition and activation timing were similar across all feet.

Conclusions Although prosthetic feet with different mechanics alter specific muscle activation patterns during loaded walking, the underlying complexity, composition, and timing of motor modules remain largely unchanged. These findings suggest that individuals with transtibial amputation accommodate changes in prosthetic foot mechanics and added load primarily through adaptation in muscle activation rather than reorganization of motor control strategies.

5.2 BACKGROUND

Lower-limb amputation can lead to neuromuscular changes, especially during demanding daily tasks such as carrying loads. For example, prior studies have demonstrated that carrying front loads increases muscle contributions to body support and forward propulsion (Lefranc et al., 2024), as well as metabolic power (Lefranc et al., 2025). This may pose a challenge for individuals with a transtibial amputation (TTA) who lack active biological ankle musculature. Most of these individuals rely on prosthetic feet with fixed mechanical properties such as stiffness, which cannot modulate distal limb dynamics and may compromise the neuromuscular strategies required to accommodate the added loads. While non-prescribed foot types (e.g., higher-stiffness or powered feet not typically prescribed for everyday walking) designed to aid ambulation during load carriage are increasingly marketed as providing enhanced functionality, little is known about how changing foot prescription influences motor control during load carriage.

Motor control is frequently studied by evaluating low-dimensional structure from electromyography (EMG) (Latash, 2021). The mathematical structures derived from the EMG data are decomposed using common methods such as principal component analysis (with or without rotation and factor extraction), independent component analysis, and non-negative matrix factorization. These reduced-dimensional groupings, often termed “motor modules”, capture sets of muscles that tend to be co-recruited (or co-excited) during functional tasks and have often been interpreted as potential neural control strategies. It should be noted that while correlation-based modules may reflect a combination of mechanical coupling, spinal circuitry, reflex pathways, and task biomechanics, they are not necessarily neural primitives or solutions to the classical problem of motor redundancy (Latash, 2021).

Module-based analyses provide insight into complex human movements (Allen and Neptune, 2012; Neptune et al., 2009), including when mechanical demands from the body are modified (McGowan et al., 2010). Such techniques have been explored to assess motor control in both healthy and clinical populations, including individuals with neurological impairments (e.g., (Hoveizavi et al., 2025; Routson et al., 2014; Seamon et al., 2018)). For individuals with lower-limb amputation, previous work has revealed altered muscle activation and motor control during unloaded level and non-level ground walking. For example, increased co-contraction around the ankle and knee of the residual limb has been observed throughout the gait cycle, likely reflecting a limb-stiffening strategy to enhance stability (Seyedali et al., 2012). Further, they exhibit altered motor module structure and activation profiles. Specifically, differences in module composition and activation timing have been reported between intact and residual limbs across non-amputee and amputee groups (Mehryar et al., 2020, 2017, 2016), and across varying walking speeds (Mehryar et al., 2024). Collectively, these studies show that individuals with lower-limb amputation may reorganize their motor control to compensate for reduced distal limb neuromuscular strategies imposed by fixed mechanical properties of their prosthetic feet.

Despite this growing body of literature, it is an open question about how non-prescribed prosthetic feet for load carriage influence motor control in individuals with TTA. In particular, prior work has almost exclusively focused on unloaded walking and has not examined how changes in prosthetic foot mechanics during load carriage affect muscle activation patterns, module composition (i.e., muscles associated with each module), and module complexity (i.e., overall number of modules). To address these gaps, the objective of this study was to investigate how stiffer and powered prosthetic feet affect motor control across multiple levels, including muscle activation, module composition and module complexity during loaded walking. We hypothesized that muscle activation patterns and module composition would differ between prosthetic feet due to their distinct mechanical behaviors. Further, we hypothesized that motor control, as quantified by module complexity, would systematically change, either increasing as the neuromuscular system adapts to altered distal mechanics or decreasing if stiffer or powered feet reduce the muscular demands required to accommodate the added loads.

By characterizing how prosthetic foot prescription influences muscle activation and module structure, this study provides further insight into motor control and adaptation in individuals with TTA during loaded walking. Additionally, these findings have clinical implications for optimizing and developing adaptive prostheses for load carriage purposes to improve gait rehabilitation of individuals with TTA.

5.3 METHODS

5.3.1 Human Subjects

This study analyzed motion data retrospectively collected from twelve individuals with unilateral TTA (10 males; [mean ± SD] age: 46 ± 15 yrs; mass: 96 ± 16 kg; height: 1.8 ± 0.1 m; and time since amputation: 13 ± 15 yrs; etiology: 8 trauma, 2 congenital, 1 diabetic neuropathy, 1 infection). Subjects were in Medicare Functional Classification K-Levels 3 or 4 by self-report and prosthetist assessment. Please refer to the demographics tables (Tables 2.1, 3.1, and 4.1) in Chapters 2, 3, and 4 for detailed description. All subjects provided their written informed consent prior to participating in this institutionally approved clinical trial (clinicaltrials.gov, NCT07159490).

5.3.2 Experimental Protocol

Marker trajectories were tracked using a 16-camera motion capture system (Vantage V8, Vicon Motion Systems, Oxford, UK) and sampled at 120 Hz. Ground reaction forces (GRF) were collected using five overground force plates (AMTI, Watertown, MA, USA) and sampled at 1,200

Hz. Kinematics and kinetics were collected synchronously. The detailed protocol is reported elsewhere (Ardianuari et al., 2025) (Chapter 3). Briefly, subjects walked at their preferred speed while carrying no load and a 13.6-kg (30-lb) load in four different conditions (i.e., front load, back load, intact-side load, prosthetic-side load) to simulate daily load carriage activities (Fig. 5.1). Within each load condition, all subjects (n = 12) wore their clinically prescribed prosthetic foot (PR) and a one-category stiffer foot (SF). A subset of the subjects (n = 7/12) also wore a powered ankle/foot (PW). Both the SF and PW were commercially available prosthetic foot types purported to aid ambulation during load carriage activities (Fig. 5.1). Due to restrictions related to residual limb length and prosthetic build height, only seven subjects were able to be fit and walk with the PW.

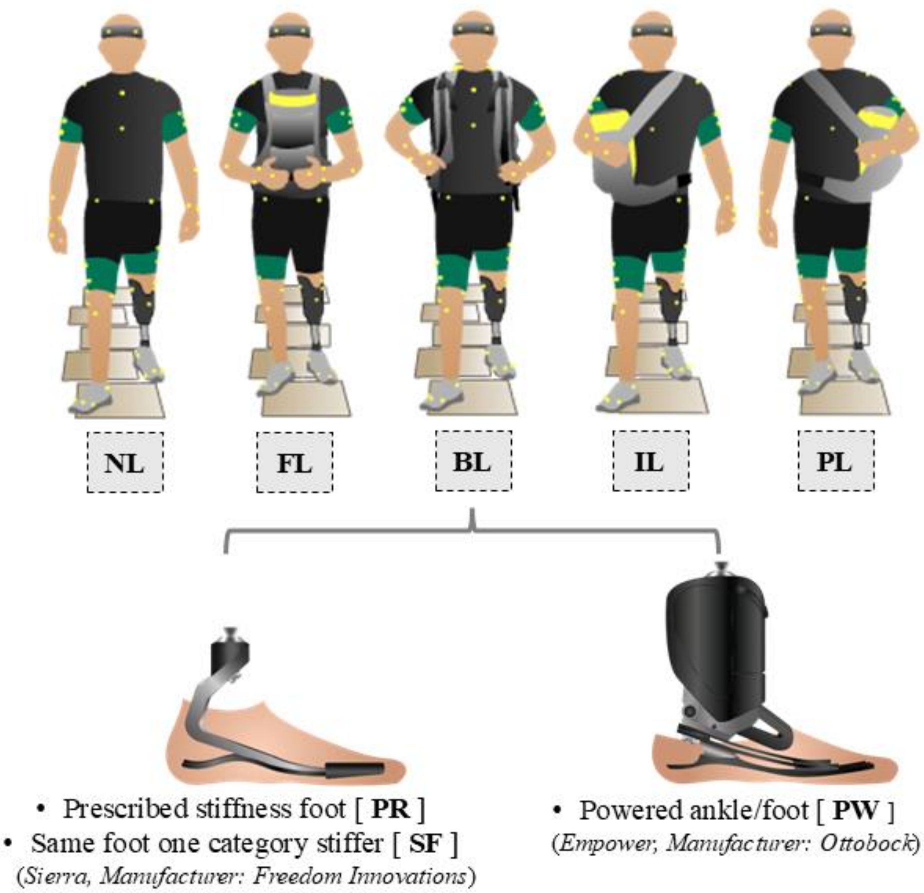

Fig 5.1 An illustration of the different load conditions (NL: no load, FL: front load, BL: back load, IL: intact-side load, PL: prosthetic-side load) and commercially available prosthetic foot models used in the experiment.

5.3.3 EMG Activation and Co-contraction

The preparation and placement of surface EMG electrodes (Delsys, Inc., Boston, MA, USA) followed the Surface Electromyography for the Non-Invasive Assessment of Muscles (SENIAM) guidelines (Hermens et al., 2000). EMG data were collected at either 2,000 Hz (for the first two subjects) or 1,200 Hz from eight intact-limb muscles: gluteus maximus (GMAX), gluteus medius (GMED), biceps femoris-long head (BFLH), rectus femoris (RF), vastus medialis (VASM), peroneus longus (PERL), medial gastrocnemius (MGAS), and tibialis anterior (TA). Residual-limb EMG data were not included in the analysis because distal ankle musculature (PERL, MGAS, TA) was not available, resulting in an incomplete and non-uniform muscle set that would bias module extraction and prevent valid comparisons across conditions. Some trials contained one or more poor or missing EMG channels, and these data were excluded from analysis.

EMG signals were collected as subjects walked across a 14-m walkway with five embedded overground force plates. The first and last two strides were removed to avoid transient accelerations and decelerations near the beginning and end of each trial and maximize data for module analysis (Shuman et al., 2017). The EMG data were exported from Visual 3D (HAS-Motion, Kingston, Ontario, Canada) and processed using custom MATLAB scripts (The MathWorks Inc., Natick, MA, USA). The raw data were bandpass-filtered between 20 and 400 Hz. A linear envelope was calculated for each muscle by high-pass filtering at 20 Hz, rectifying the data, low-pass filtering at 6 Hz, and amplitude-normalizing to the muscle's maximum activation across all trials. The data were then down-sampled to 100 Hz (i.e., 101 data points per gait cycle) to reduce computational demands while preserving temporal resolution for the module analysis (Shuman et al., 2017).

The linear envelopes of the EMG signals were time integrated (iEMG) over the gait cycle to measure changes in muscle activation patterns relative to the baseline prescribed foot (PR) (Δ iEMG). In addition, a co-contraction index (CCI) was used to measure the level of co-contraction between the agonist-antagonist muscle pairs for the knee and ankle joints (Kellis et al., 2003; Kim et al., 2021a) as:

$$CCI = \frac{iEMGmin}{iEMGago + iEMGant} \text{ x } 100\% \qquad \text{(eq.1)}$$

where $iEMG_{min}$ is the lower of the two ($iEMG_{ago}$ or $iEMG_{ant}$) at each sampling point. CCI was calculated for the knee and ankle muscle pairs in specific gait phases (Table 5.1) that have been reported to demonstrate prevalent muscle co-contractions (Seyedali et al., 2012).

Table 5.1 Knee and ankle agonist/antagonist muscle pairs and corresponding gait phases over which co-contractions were calculated.

Agonist muscle	Antagonist muscle	Phase (% gait cycle)	Defined segmentation
TA	MGAS	Early Stance (0-10%)	First 10%
RF	BFLH	Early - Midstance (0-20%)	Heel strike – Foot adjacent
MGAS	TA	Mid - Late Stance (20-60%)	Foot adjacent – Toe off
TA	MGAS	Early Swing (60-80%)	Toe off – Heel strike
BFLH	RF	Late Swing (80-100%)	

TA, tibialis anterior; MGAS, medial gastrocnemius; RF, rectus femoris; BFLH, biceps femoris-long head.

5.3.4 Module Analysis: Complexity

Muscle modules were calculated from the concatenated EMG data using Non-Negative Matrix Factorization (NNMF) using MATLAB Matrix Factorization Toolbox (Li and Ngom, 2013). In NNMF, a muscle activation pattern ($EMG_{m\times t}$) is assumed as a linear combination of a few muscle modules ($W_{m\times n}$), each of which is recruited by a module activation coefficient ($C_{n\times t}$), such that:

$$EMG_{m\times t} = W_{m\times n} \times C_{n\times t} + error \qquad \text{(eq.2)}$$

where m is the number of muscles (m = 8), and n is the number of modules (n = 1–7), and t is the number of time points (t = 101). Module compositions (W) were fixed, and each module was multiplied by a time-varying scalar activation coefficient (C). In the analysis, random initial guesses were generated and then replicated until minimal error was obtained. The NNMF settings used include 50 replicates, 1,000 maximum iterations, a 1×10^{-4} threshold for the relative change in the elements of W and C, and a 1×10^{-6} threshold for the change in the size of the residual (Shuman et al., 2019). The amplitude of each muscle activity vector was scaled to have a unit variance to assure equal weighting before extracting modules (Steele et al., 2013). After module extraction, data were reconstructed by multiplying the W and C vectors ($EMG_{reconstructed} = W \times C$).

The total variance accounted for by n modules (tVAFn) was calculated to evaluate module complexity (Ting and Macpherson, 2005; Torres-Oviedo et al., 2006) as:

$$tVAFn = \left(1 - \frac{[\sum_j^t \sum_i^m (errori,j)^2]}{[\sum_j^t \sum_i^m (EMGi,j)^2]}\right) \times 100\% \qquad \text{(eq.3)}$$

where error is defined as the difference between the reconstructed and measured EMG data: $(W_nC_n)_{i,j} - EMG_{i,j}$

Modules were sorted functionally, based on their structural similarity, muscle composition and module activation profiles (Torres-Oviedo and Ting, 2007). The number of modules is a widely used independent measure to evaluate clinical populations including neurologically impaired and amputee individuals (e.g., (Mehryar et al., 2020; Routson et al., 2013)). tVAF1 provides a strong summary measure of module complexity and has been shown to be related to function and treatment outcomes in neurological impairments (Hoveizavi et al., 2025; Schwartz et al., 2016; Shuman et al., 2018). In addition to tVAFn > 90 %, tVAF4 was evaluated because it has been reported that in 70% of non-amputee individuals, at least four modules were responsible for over 90 % of the variation in the EMG data (Hoveizavi et al., 2025).

To contextualize the magnitude of changes in $tVAF_1$, a relative-Dynamic Motor Control index (relative-DMC_1) was calculated. Dynamic Motor Control Index during Walking (Walk-DMC) formulation (Shuman et al., 2019) was adapted to characterize changes in module complexity. Because normative, non-amputee controls dataset was not available in this study, a *within-subject* relative DMC index was computed. For each subject, tVAF1 values from the PR served as an individualized reference, and DMC values for SF and PW were expressed as z-scores relative to PR. Thus, this metric is interpreted as *relative changes in module complexity across feet*, rather than deviation from normative gait as in Walk-DMC.

$$\text{relative } DMC_{i,cond} = \frac{tVAF1\_i,cond - \mu\_PR,i}{\sigma\_PR,i} \qquad \text{(eq.4)}$$

where μ_PR,i is the mean of $tVAF1_{PR,i}$, and σ_PR,i is the standard deviation of $tVAF1_{PR,i}$. Positive values indicate greater reliance on a dominant first module (reduced module complexity), whereas negative values indicate more distributed muscle coordination (increased module complexity).

Therefore, four measures were used to evaluate module complexity: 1) number of modules required for overall tVAF greater than 90 % (tVAFn > 90%) (N90), 2) tVAFn by one single module (i.e., first module, $tVAF_1$), 3) tVAFn > 90% (including by four modules), and 4) relative DMC_1 to further assess relative changes in module complexity across feet.

5.3.5 Module Analysis: Composition

Module composition was assessed using cosine similarity of module-weight vectors. For each subject, the EMG data were decomposed into four modules using NNMF for every foot and each load condition. Because NNMF solutions are order-indeterminate, modules were aligned across feet within each subject using the Munkres (Hungarian) algorithm (Kuhn, 1955) by maximizing cosine similarity of module weight vectors, with the subject's PR solution serving as the reference template.

CS quantifies how similar each module's muscle weights are between feet. For each module n, similarity between conditions A and B (i.e., PR–SF, PR–PW, SF–PW) was computed (Hoveizavi et al., 2025) as:

$$\text{Cosine Similarity}_n\,(A, B) = \frac{Wn,A \cdot Wn,B}{\|Wn,A\|\,\|Wn,B\|} \qquad \text{(eq.5)}$$

in which the cosine similarity for each module weight (Wn) was calculated as the dot product of the vectors divided by the product of their Euclidean norms, resulting in a scale of 0 (no similarity) to 1 (perfect similarity), with higher values indicating more similar modules.

5.3.6 Statistical Analysis

EMG outcomes, %ΔiEMG (per muscle) and CCI (in five selected gait phases), were analyzed using linear mixed-effects regression (LMER) models with foot as a fixed effect and subject as a random intercept. For each model, three pairwise comparisons (PR–SF, PR–PW, SF–PW) were performed using custom contrast matrices and models were only fitted when ≥ 7 subjects contributed data per condition (i.e., corresponding to the smallest n who completed the protocol with PW). This conservative mixed-effects approach ensured stable variance estimates and valid inference.

For module-related outcomes, differences in % $tVAF_1$ and % $tVAF_n > 90\%$ including $tVAF_3$ and $tVAF_4$ were tested using LMER models per load condition. Similarity in module weights (W) between feet were compared using the cosine similarity for modules 1–4 in each load condition, while time-normalized module activations (C) were compared using 1D statistical parametric mapping (SPM paired or independent two-tailed t-tests, (Pataky, 2012)) with cluster-based inference. Relative-DMC_1 was evaluated per load and pooled across loads as a within-subject z-score inherently referenced to PR and not load-dependent. Where applicable, group results were reported based on the LMER outputs as estimated marginal mean (emmean) ± standard error (SE), and significant pairwise comparisons. Statistical significance was set as $\alpha = 0.05$ and all analyses were performed in MATLAB.

5.4 RESULTS

5.4.1 EMG Activation and Co-contraction

Across load conditions, several muscles exhibited statistically significant differences in activation over the gait cycle between feet (Fig. 5.2). In the NL condition, MGAS activity increased with PW relative to PR (by +29.15%, $p < 0.001$) and relative to SF (by +25.96%, $p < 0.001$), and RF activity increased with PW relative to PR (by +45.73%, p = 0.008). Under the FL condition, RF activity increased with SF relative to PR (by +29.43%, p = 0.009) but decreased with PW relative to SF (by -22.49%, p = 0.023), while GMAX activity decreased with SF relative to PR (by -12.29%, p = 0.019). The BL condition showed increased PERL activity with PW relative to SF (by +15.97%, p = 0.033) and decreased RF activity with PW relative to SF (by -16.38%, p = 0.039). In the IL condition, MGAS activity increased with PW relative to PR (by +25.80%, p = 0.032) and SF (by +22.57%, p = 0.016), while VASM activity increased with SF relative to PR (by +37.24%, p = 0.016). Under the PL condition, TA, PERL, and GMAX activities all increased with PW relative to SF (by +15.27%, p = 0.008; by +17.17%, p = 0.043; by +23.45%, p = 0.048, respectively).

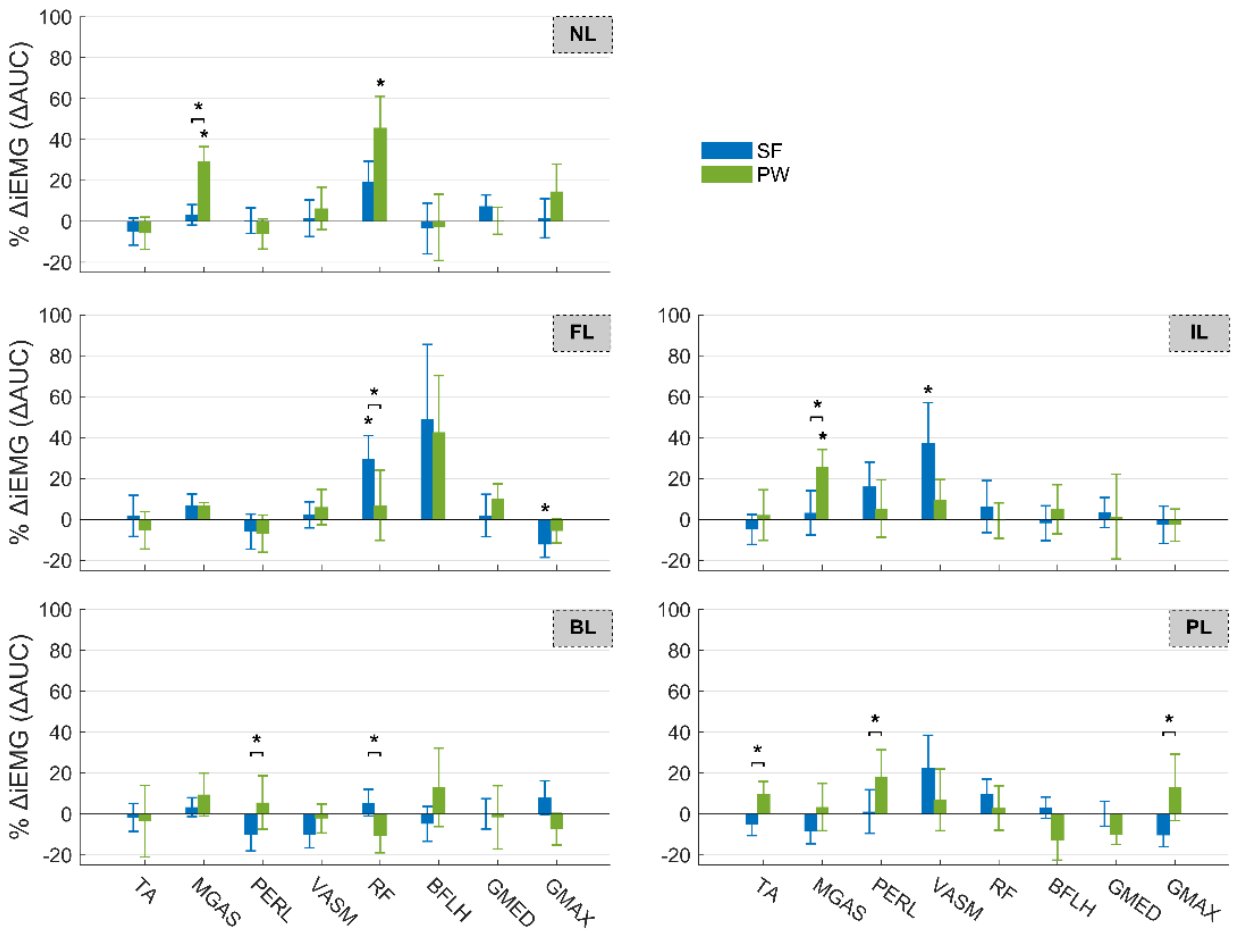

Fig 5.2 Average changes in muscle activation (integrated EMG) (± SE) for SF and PW compared to baseline (PR) as a function of muscles across load conditions. An asterisk (*) indicates muscles with significant pairwise differences

between SF and PR or PW and PR, while an asterisk (*) with a bar represents muscles with significant pairwise differences between SF and PW ($p < 0.05$).

Co-contraction patterns in specific gait phases also varied by foot, but statistically significant differences were observed primarily in the NL condition (Fig. 5.3). During the NL condition, PW showed higher TA/MGAS co-contraction relative to PR in early stance (15.34% ± 5.30 vs. 13.46% ± 2.87, $p = 0.041$), smaller RF/BFLH co-contraction relative to PR in early stance to midstance (24.53% ± 3.44 vs. 31.19% ± 2.16, $p = 0.006$), and higher BFLH/RF co-contraction relative to both PR (33.29% ± 2.82 vs. 26.73% ± 1.86, $p = 0.001$) and SF (33.29% ± 2.82 vs. 28.56% ± 2.03, $p = 0.011$) during late swing. Surprisingly, there were fewer changes in the loaded conditions. In the IL condition, SF demonstrated smaller MGAS/TA co-contraction relative to PR in midstance to late stance (20.84% ± 1.74 vs. 25.17% ± 1.10, $p = 0.013$), while no other pairwise comparisons across other load conditions were found significant.

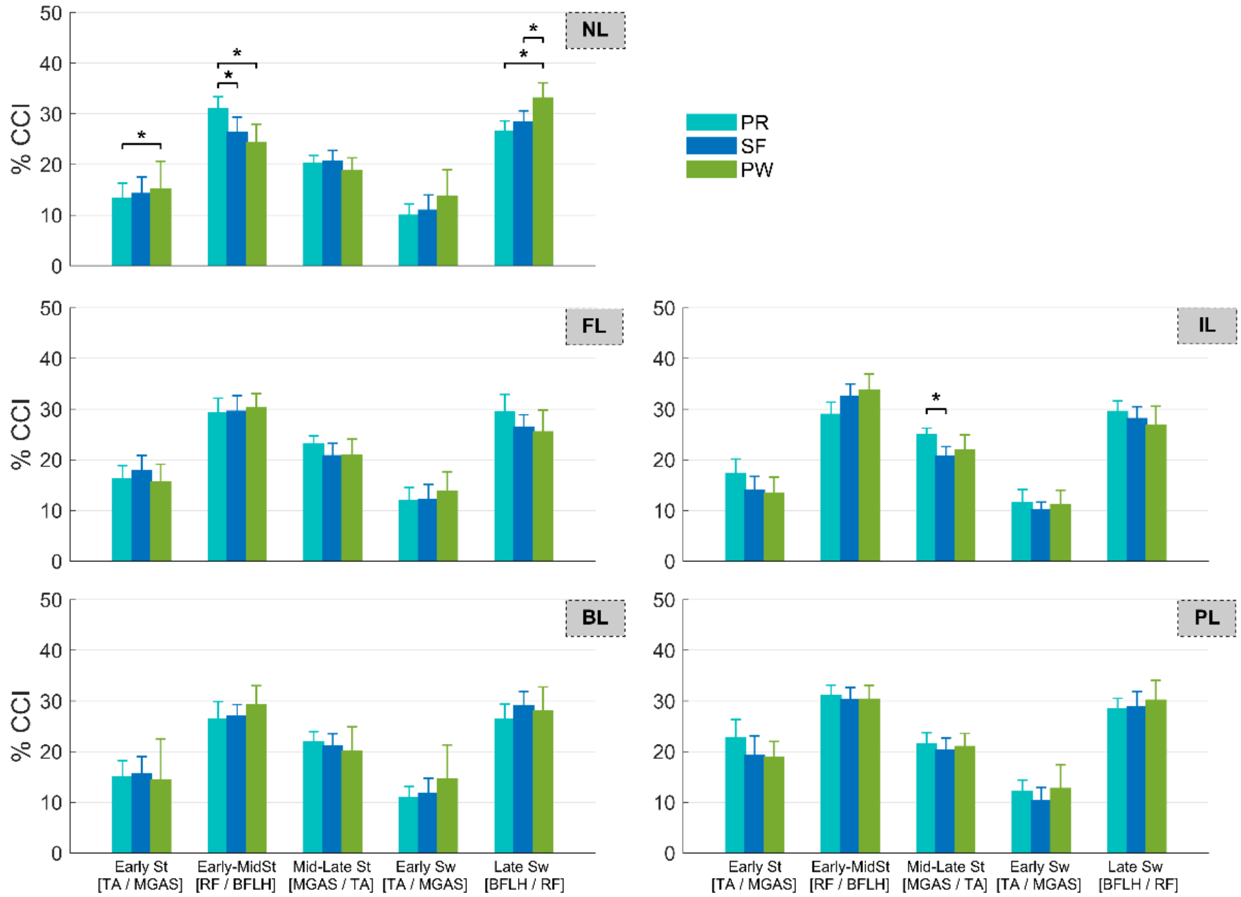

Fig 5.3 Average co-contraction indices (± SE) as a function of knee and ankle [Agonist / Antagonist] muscle pairs in different gait phases across load conditions. An asterisk (*) with a bar indicates co-contraction with significant pairwise differences between feet ($p < 0.05$). Abbreviations: St, stance; Sw, swing.

5.4.2 Module Complexity

Trends of module complexity across feet are shown in Fig. 5.4. Three-module solutions were most common in all load conditions (PR: 70–80%; SF: 56–82%; PW: 60–100%), with two modules found in a small subset of subjects (PR: 18–30%; SF: 10–33%; PW: 0–20%). Four-module solutions were only ≤ 20% across any load condition.

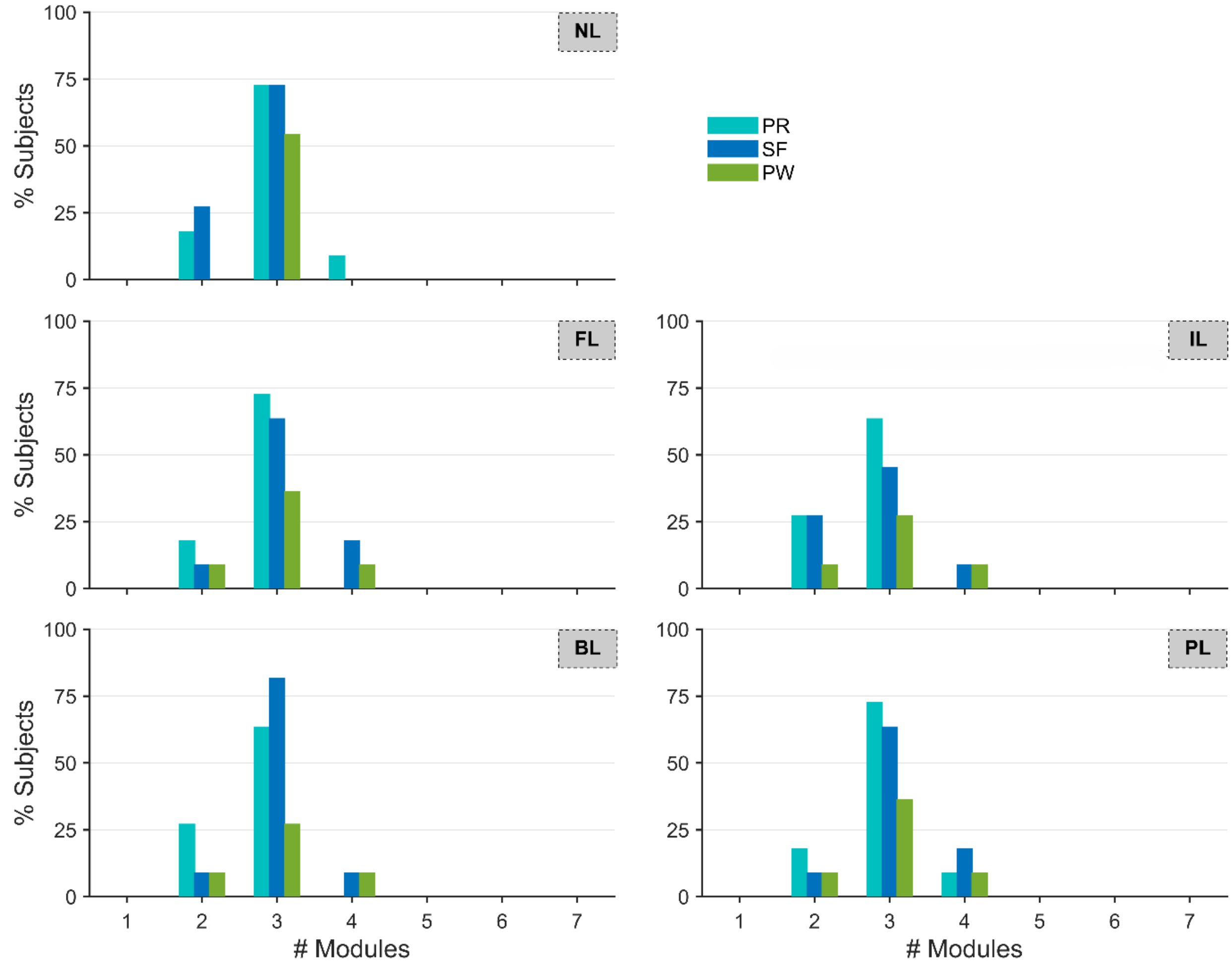

Fig 5.4 Proportion of subjects as a function of the number of modules required for $tVAF_n > 90\%$ (N90).

First-module tVAF was generally consistent across load conditions, although two loaded conditions demonstrated significant foot effects (Fig. 5.5). Under the BL condition, PW resulted in slightly smaller $tVAF_1$ relative to PR (75.13% ± 1.87 vs. 76.95% ± 1.68, $p = 0.015$). In the IL condition, PW resulted in slightly smaller $tVAF_1$ relative to SF (73.83% ± 2.79 vs. 76.68% ± 1.66, $p = 0.047$). No other tVAF1, tVAF3 or tVAF4 pairwise comparisons were found significant.

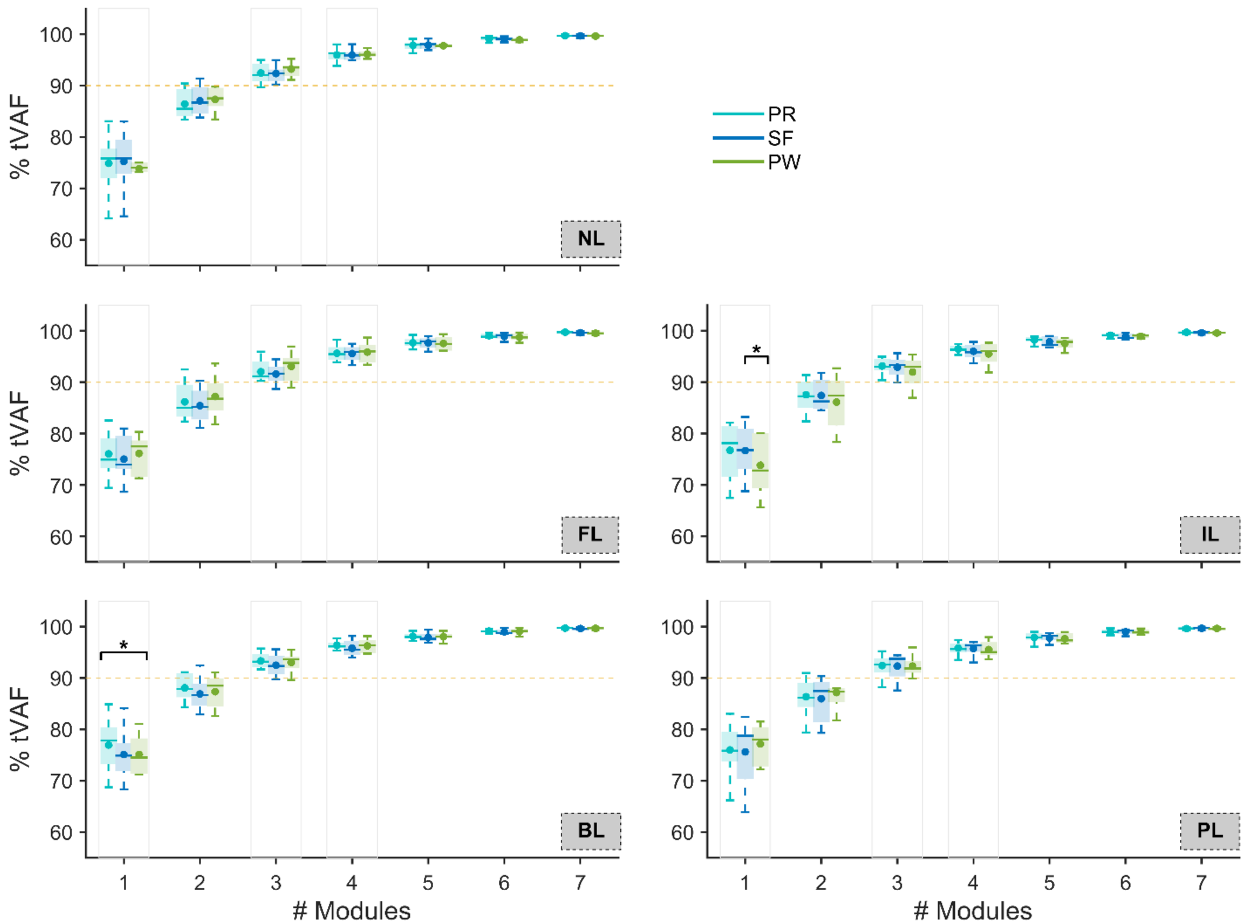

Fig 5.5 Total variance accounted for as a function of n modules, with n ranging from 1 – 7, across load conditions. Box and whisker plots represent the distribution of participant-level % tVAF values for each foot, with solid circles indicating averages. Horizontal dashed lines represent the 90% threshold used to estimate the minimum n-modules required for adequate reconstruction. Shaded modules ($tVAF_1$, $tVAF_3$ and $tVAF_4$) were tested for pairwise significant differences between feet, indicated by an asterisk (*) ($p < 0.05$).

Variability was observed in relative DMC_1 (z-scored $tVAF_1$) across load conditions (Fig. 5.6). There were 3.64- and 2.81-point decreases in relative DMC_1 for PW relative to PR for the BL and IL conditions, respectively, while SF resulted in a 1.67-point decrease in the BL condition. Group-level point differences (pooled across load conditions) between feet were also observed, with mean relative DMC_1 showing smaller shifts (SF: -0.31 and PW: -0.89 point relative to PR) (Fig. 5.6).

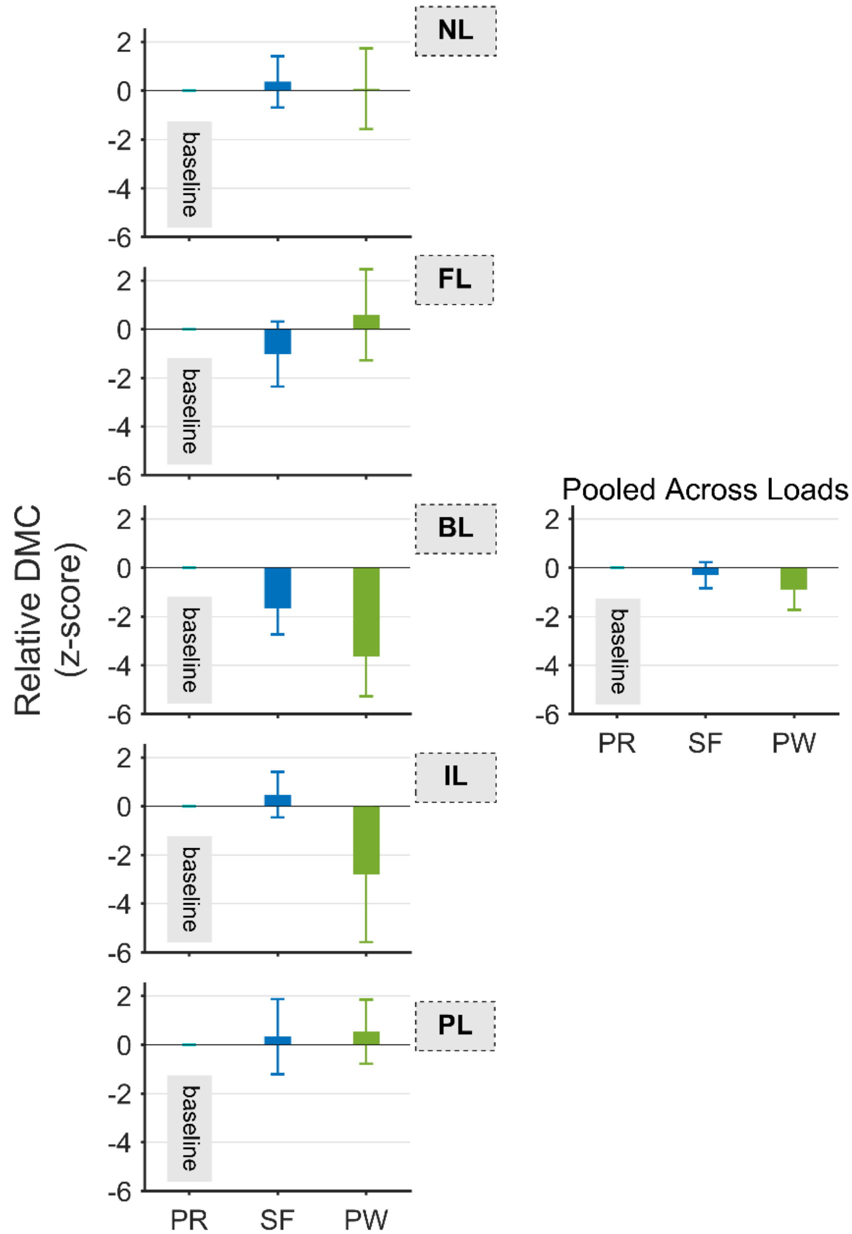

Fig 5.6 Average relative DMC_1 (z-score) (± SE) as a function of foot types in each load condition (left) and pooled across load conditions (right). If present, an asterisk (*) denotes pairwise significant differences between feet ($p < 0.05$).

5.4.3 Module Composition

Across all load conditions, similarity of the module weight vectors (W) was relatively conserved between feet. On average, the cosine similarity for module 1 ranged from 0.83 - 0.90 for PR-SF, 0.69 - 0.84 for PR-PW, and 0.74 - 0.87 for SF-PW similarities (Fig. 5.7). Slightly lower values were observed for module 4.

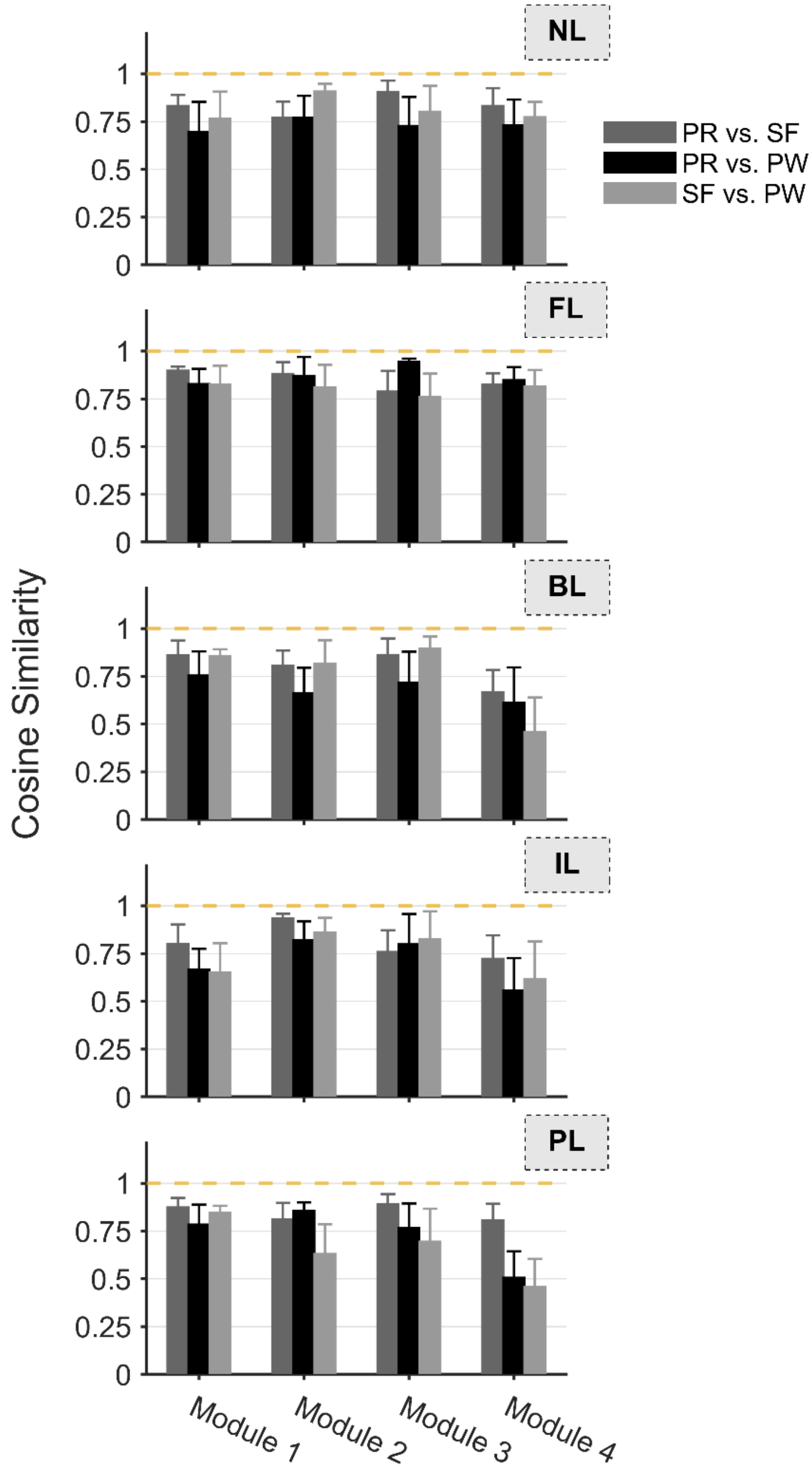

Fig 5.7 Average cosine similarities (± SE) as a function of n-modules across load conditions.

A few trends were observed to slightly vary in module activations (C) between feet across load conditions, but no statistically significant differences were detected for all modules n = 1-4 (SPM pairwise analyses detected zero clusters across all load conditions) (see Additional file A5.1-A5.5 for trends).

5.5 DISCUSSION

This study investigated how changing prosthetic foot prescription influenced muscle activation and motor module structure (i.e., complexity, composition, and timing) in individuals with TTA walking with load carriage. We hypothesized that a stiffer foot (SF) or a powered foot (PW) would modify muscle activation and module composition relative to the non-powered prescribed foot (PR). Overall, we found insufficient evidence to support our hypotheses. Although foot type influenced specific muscle activation patterns, module complexity, composition, and timing were largely conserved between feet across load conditions.

5.5.1 Muscle activation and co-contraction were influenced by foot type

Foot prescription affected intact-limb muscle activation with considerable variability across load conditions. For example, in the NL and IL conditions, PW use increased ankle muscle activity (MGAS), and partially in loaded conditions, SF increased RF or VASM activity. These empirical findings were consistent with prior simulation results showing GAS contributions to forward propulsion for some of the loaded conditions (e.g., BL and PL) (Lefranc et al., 2024). The higher intact plantarflexor activity observed in this study may reflect greater reliance on the intact limb to accelerate forward propulsion when walking with the heavier, higher-inertia PW foot. A trend of higher BFLH activity with non-prescribed feet relative to PR was also observed in this study, and this trend is consistent with increased contributions to forward propulsion in the FL condition compared to other load conditions (Lefranc et al., 2024).

Differences in muscle co-contraction were also observed predominantly in the NL condition, where PW increased TA/MGAS co-contraction in early stance and increased BFLH/RF co-contraction in late swing. These patterns are consistent with a previous study suggesting that increased intact thigh muscle co-contraction during late stance provides compensatory limb-stiffening strategy in response to walking with the PW foot with higher inertia (Kim et al., 2021a). However, across most loaded conditions, co-contraction differences were non-significant, suggesting that foot-specific effects on antagonist muscle coordination are minimal with increased loading demands, and the absence of such biomechanical responses may explain the variable compensatory mechanisms to overcome plantarflexor loss in individuals with TTA.

Although metabolic cost estimates were not measured in this study, our findings provide important context when compared with prior work in the literature. Changes in the intact limb TA/MGAS co-contraction are moderately correlated with changes in cost of transport in early stance when walking with PW (Kim et al., 2021a). Compared to other feet, PW produces the highest metabolic power across load conditions, and this change may be due to increased contributions from the intact plantarflexors and hip extensors, while SF also elevated metabolic power in most muscles in all load conditions except the FL condition (Lefranc et al., 2025). Our results align with these reported patterns where PW increased intact-limb MGAS activity in NL and IL conditions, TA activity in the PL condition, and PERL activity in the BL and PL conditions. Additionally, both PW and SF elevated RF or VASM activity in specific load conditions. The persistence of these increases, even when mechanical demand changed with load carriage, suggests that the non-prescribed feet did not offload the neuromuscular system but instead required greater active control from the intact limb. Collectively, this evidence supports the interpretation that SF or PW may introduce additional energetic demands rather than reducing them during loaded gait.

Despite increases in the intact-limb muscle activities and co-contractions, our results imply that when walking with load carriage, the amputee neuromuscular system may prioritize stability over foot-specific compensations and meet the increased energetic requirements without reorganizing its underlying control structure. These observations support the theory that modules are not necessarily a reflection of gait pattern or biomechanical constraints (Kutch and Valero-Cuevas, 2012).

5.5.2 Module complexity remained highly conserved between foot types across load conditions

Across all load conditions, three modules were most frequently required to exceed the N90 threshold, with two-module solutions occurring in a minority of cases and four-module solutions rarely used. This pattern is consistent with prior work in individuals with lower-limb amputation (Mehryar et al., 2020), and with module analyses in other clinical populations (Hoveizavi et al., 2025) demonstrating that motor module complexity is relatively stable despite substantial biomechanical perturbations. Importantly, no systematic differences in N90 were observed between PR, SF, and PW, indicating that different prosthetic foot mechanical properties did not meaningfully alter the complexity of motor control during loaded walking.

Small foot effects were detected in $tVAF_1$ for two load conditions (PW < PR in BL, and PW < SF in IL), but these differences were modest (~2–3% difference) and did not reflect consistent shifts in either direction. Group-level analyses of relative DMC_1 revealed some differing points between feet with small average deviations (SF: −0.3; PW: −0.89 points relative to PR), reinforcing that module complexity did not systematically increase or decrease with foot stiffness or powered assistance.

5.5.3 Module composition and timing were not adaptive to foot type

Despite muscle-specific activation differences, the structure of module weight vectors (W) remained conserved between feet, with cosine similarity values typically ≥ 0.75 for modules 1–3 (i.e., for PR-SF and SF-PW similarities) and only slightly lower for module 4. No pairwise comparisons of activation coefficients (C) yielded significant clusters, confirming that the temporal profiles of module activations were statistically indistinguishable between PR, SF, and PW. These results demonstrate that the motor control underlying ambulation during load carriage is relatively non-adaptive to changes in prosthetic foot mechanics.

The module structures extracted in this study were consistent with previously reported module complexities in adult individuals with somewhat similar sets of muscles (e.g., (Magrath et al., 2022; Neptune et al., 2009)). The observed trends were relatively similar across all load conditions and are reported in Additional file A5.1 for the NL condition, A5.2 for the FL condition, A5.3 for the BL condition, A5.4 for the IL condition, and A5.5 for the PL condition. Overall, previous work (Allen and Neptune, 2012; Neptune et al., 2009) has shown in the first module, GMED, GMAX, RF, VASM, and TA are activated to provide body support during weight acceptance and stabilization during early stance. In the second module, MGAS and PERL are activated to provide propulsion during late stance. In the third module, RF and TA are activated to initiate leg swing and transfer trunk energy. In the fourth module, BFLH is activated for deceleration in late swing and energy absorption in early stance. Additionally, muscles such as GMAX, active for body support in early stance, and BFLH, which have been shown to contribute energy to the leg in early stance and swing, contributed to module structures and were consistent with their known biomechanical roles reported in the literature. These functional interpretations align with the module functions described in prior studies and further highlight the stability of module composition even when prosthetic foot mechanics change.

Our findings on module complexity complement and extend previous work examining the influence of load carriage and prosthetic foot prescription on neuromuscular demands in individuals with TTA (Lefranc et al., 2025, 2024). Load carriage has been shown to increase the mechanical demands relative to body support and propulsion from the intact-limb muscles and often elevate metabolic cost, with high variability for the optimal prosthetic foot. In this study, we observed PW tended to increase intact plantarflexor and knee extensor activations in specific phases, but this did not translate into systematic changes in module complexity as hypothesized. Instead, motor module complexity appeared highly resistant to perturbation from prosthetic foot mechanics, reinforcing the concept that the neuromuscular system relies on deeply ingrained module strategies during gait, even in the presence of additional mechanical demands from load carriage.

5.5.4 Limitations

Several limitations should be considered when interpreting the findings of this study. First, the sample was small, predominantly male, and mostly traumatic in etiology. Because sex-specific differences in lower-limb motor control and load carriage-related injury risks have been reported to exist (Cammarata and Dhaher, 2010; Orr et al., 2020), future studies should strive to recruit balanced cohorts and evaluate sex-specific responses. Second, only seven of the subjects were able to use the PW due to residual-limb length constraints, resulting in unbalanced group sizes across foot conditions. This reduced statistical power may limit generalizability. A larger, more balanced sample may have confirmed some of the observed trends as significant. Third, this retrospective study was limited by experimental protocols. Subjects walked at their comfortable speed, and trials were restricted to ±10% of their preferred speed. However, varying speeds have been reported to influence module activation patterns in individuals with transfemoral amputation during unloaded walking (Mehryar et al., 2024) and could therefore influence our results. Next, the weight of the load carried in this study (13.6 kg) was selected to exceed the typically recommended 10-kg stiffness-classification range by most prosthetic manufacturers and to ensure feasibility for all subjects. A heavier load, typically used for military activity purposes, may have elicited more pronounced neuromuscular differences.

Methodological limitations should also be noted. EMG data were collected from eight major intact-lower limb muscles, excluding other equally important muscles such as soleus. Because the structure and dimensionality of modules is dependent upon the number and choice of muscles included in the analysis, module composition and VAF metrics should be interpreted within the context of the sampled muscle set. Module similarity increases with larger muscle sets included (i.e., 0.8 for > 10 muscles) (Steele et al., 2013), and thus absolute VAF values may differ if additional muscles were included. EMG from the residual limb did not include a complete set of ankle muscles, precluding its inclusion in NNMF-based analyses that require a consistent muscle matrix across conditions. Accordingly, our results characterize motor control using the available intact-limb muscle set and should be interpreted as such. Nonetheless, future work should analyze residual-limb muscle activation and co-contraction to further characterize bilateral neuromuscular strategies.

5.5.5 Conclusion

This study shows that although prosthetic foot selection alters specific intact-limb muscle activation patterns, most notably with non-prescribed SF and PW feet, the underlying structure, including composition, complexity, and timing of motor modules, remain highly conserved between these feet relative to PR across load conditions. Increased activity of plantarflexors and knee extensors with PW and SF, consistent with prior simulations predicting changes in support and propulsion contributions and metabolic demands, did not translate into changes in module organization. These findings suggest that individuals with TTA accommodate differences in foot mechanics and added load primarily through adjustments in the magnitude of muscle activation rather than through neuromuscular reorganization strategies. Overall, motor control during loaded walking appears non-adaptive to perturbations introduced by non-prescribed prosthetic feet.

Acknowledgments

Krista Cyr collected the experimental data, Christina Carranza (CPO) fit and aligned the study prostheses for all subjects, and Jane Shofer provided statistical consulting.

CHAPTER 6

MEDIAL KNEE LOADING RESPONSES TO PROSTHETIC FOOT STIFFNESS DURING VARIOUS AMBULATORY ACTIVITIES

Under Review in *Journal of Biomechanics*

Satria Ardianuari

Eric H. Hu

Nicholas P. Fey

Richard R. Neptune

Glenn K. Klute

6.1 ABSTRACT

Individuals with unilateral transtibial amputation are at elevated risk of knee osteoarthritis, often associated with increased medial compartment loading on the intact limb. Prosthetic foot stiffness has been shown to influence this loading, yet it remains unclear whether such effects persist across various ambulatory activities. This study investigated the influence of prosthetic stiffness on estimates of medial knee contact force (MCF). We hypothesized that the effect would be activity dependent. Fifteen subjects completed a randomized crossover protocol using three passive-elastic feet of identical design differing by ± two categories. Motion capture and ground reaction force data were collected during walking conditions relative to surface (level, incline, decline), speed (faster, slower), load (on the residual side), and direction (turns with the prosthesis outside and inside). Peak MCF was estimated from external knee adduction and flexion moments using a linear regression approach. Prosthetic stiffness influenced MCF during several activities, although the direction and magnitude of effects varied by activity. On the intact limb, stiffer feet were generally associated with lower first peak MCF during level, faster, and loaded walking. In contrast, during decline walking, the stiffest foot resulted in a higher first peak MCF while the more compliant foot resulted in a lower second peak MCF. During turning with the prosthesis outside, the more compliant foot was associated with lower first peak MCF. On the residual limb, prosthetic stiffness effects were less consistent. Overall, across both limbs, the observed changes were below the minimal detectable change threshold, suggesting that prosthetic foot stiffness alone may only provide modest, activity-dependent contributions to medial knee loading.

6.2 INTRODUCTION

Following unilateral transtibial amputation (TTA), the risk of intact-limb knee osteoarthritis (OA) is elevated, leading to additive disability (Morgenroth et al., 2012; Norvell et al., 2005; Struyf et al., 2009). The prevalence of knee OA in this population is approximately twice that of non-amputees (Farrokhi et al., 2016), with imaging studies documenting increased degenerative changes in the knee joint (Melzer et al., 2001). These findings are often attributable, at least in part, to increased mechanical loading on the intact limb (Gailey et al., 2008). Musculoskeletal simulation studies have reported greater axial joint contact forces at the intact-limb knee in individuals with TTA than in non-amputees (Silverman and Neptune, 2014), and greater knee pain has been reported in the intact limb relative to the residual limb (Norvell et al., 2005), highlighting the substantial contribution of biomechanical factors to the presence of OA. However, among asymptomatic or relatively new amputees, intact-limb knee loading may not exceed that of non-amputees, suggesting that elevated loading may develop over time with prolonged prosthesis use or joint degeneration (Fey and Neptune, 2012).

Knee OA is often isolated to the medial compartment, and the incidence rate of medial knee OA is approximately 5-10 times higher than lateral knee OA (Jones et al., 2013). Thus, medial knee OA has been associated with elevated compressive medial loading (Andriacchi et al., 2004). Despite its clinical significance, knee loading severity and progression are difficult to quantify in vivo without invasive force-measuring implants. Alternatively, kinetic measures such as external knee adduction moment (KAM) may serve as a reliable surrogate of compressive medial knee contact force (MCF) and OA progression (Andrag et al., 2024; Miyazaki et al., 2002; Morgenroth et al., 2014). Prior studies also suggest that combining KAM with knee flexion moment (KFM) further improves MCF estimation accuracy (Manal et al., 2015; Miller et al., 2017; Uhlrich et al., 2018; Walter et al., 2010).

Activities beyond level-ground walking, such as sloped walking, significantly increase knee tibiofemoral compressive forces (Alexander and Schwameder, 2016; Haggerty et al., 2014). This increased biomechanical demand may be modified by adaptable prosthetic foot stiffness to varying walking conditions to help mitigate elevated MCF and knee OA risk. Yet most individuals with TTA use passive-elastic prosthetic feet with a fixed stiffness. Standard-of-care feet are typically prescribed according to manufacturer-defined stiffness categories (e.g., 1-9) based on user body mass and anticipated activity level, although this categorization is not standardized across models or manufacturers. Limited attempts exist to provide objective values, including a linear regression approach to estimate axial and torsional mechanical foot stiffness (Tacca et al., 2024).

Although prosthetic mechanical properties like stiffness play an integral role in gait biomechanics for individuals with TTA (Rogers-Bradley et al., 2024), their relative contributions to intact-limb knee loading are somewhat inconsistent. Some studies report that increased forefoot stiffness is associated with decreased internal tibiofemoral contact forces (Fey et al., 2012) and that a one-category higher stiffness is associated with decreased KAM (Slater et al., 2024). In contrast, others found no significant stiffness effect on KAM (Tacca et al., 2026) or associated increased hindfoot stiffness with increased indirect loading measures, such as peak ground reaction forces (Fey et al., 2011) and loading rates (Adamczyk et al., 2017).

Despite enhancing our understanding of prosthetic foot mechanics, most prior studies focused on level-ground walking, leaving an open question regarding the effects of prosthetic foot stiffness on intact-limb knee loading during more complex activities, such as walking on slopes, walking while turning, and walking with load carriage. Additionally, much of the existing evidence is based on experimental or tunable prostheses, limiting its applicability to standard clinical prescriptions. Therefore, the objective of this study was to investigate the influence of commercial prosthetic foot stiffness on intact-limb MCF across a range of ambulatory activities. As an exploratory objective, we also investigated this effect on the residual-limb knee. Although loading-induced OA occurs more frequently in the intact-limb knee, evaluating the residual-limb knee may provide insight into device-user loading mechanics at the limb most directly affected by the stiffness intervention. Based on the previously observed experimental findings in the literature, we hypothesized that higher prosthetic stiffness would decrease MCF, and this association would be more significant during downhill walking (relative to surface), faster walking (relative to speed), loaded walking (relative to load), and turning (relative to direction).

6.3 METHODS

This study was a subset of a randomized, subject-blinded crossover experimental protocol (NCT06711588) approved by the governing institutional review boards.

6.3.1 Human Subjects

Subjects were recruited from the VA Puget Sound Health Care System. Eligible subjects were adults with unilateral TTA (aged 18-80 years) for a minimum of one year who had used a well-fitting prosthesis daily for at least six months and were able to walk on a treadmill. All subjects provided informed consent.

6.3.2 Instrumentation

Three passive-elastic carbon-fiber feet of the same design, differing by ± two consecutive stiffness categories, were fit to each subject's prescribed socket/suspension system (Fig. 6.1A). A manufacturer-recommended "prescribed" stiffness category (PF) was determined for each subject based on their body mass and activity level. A low-profile version (build height 0.068 m) was selected to accommodate a simulated powered ankle mass (i.e., 1.74 kg) (Azocar et al., 2020). As increased prosthetic mass has shown negligible influence on gait biomechanics (Selles et al., 1999), we did not expect significant effects on the study outcomes.

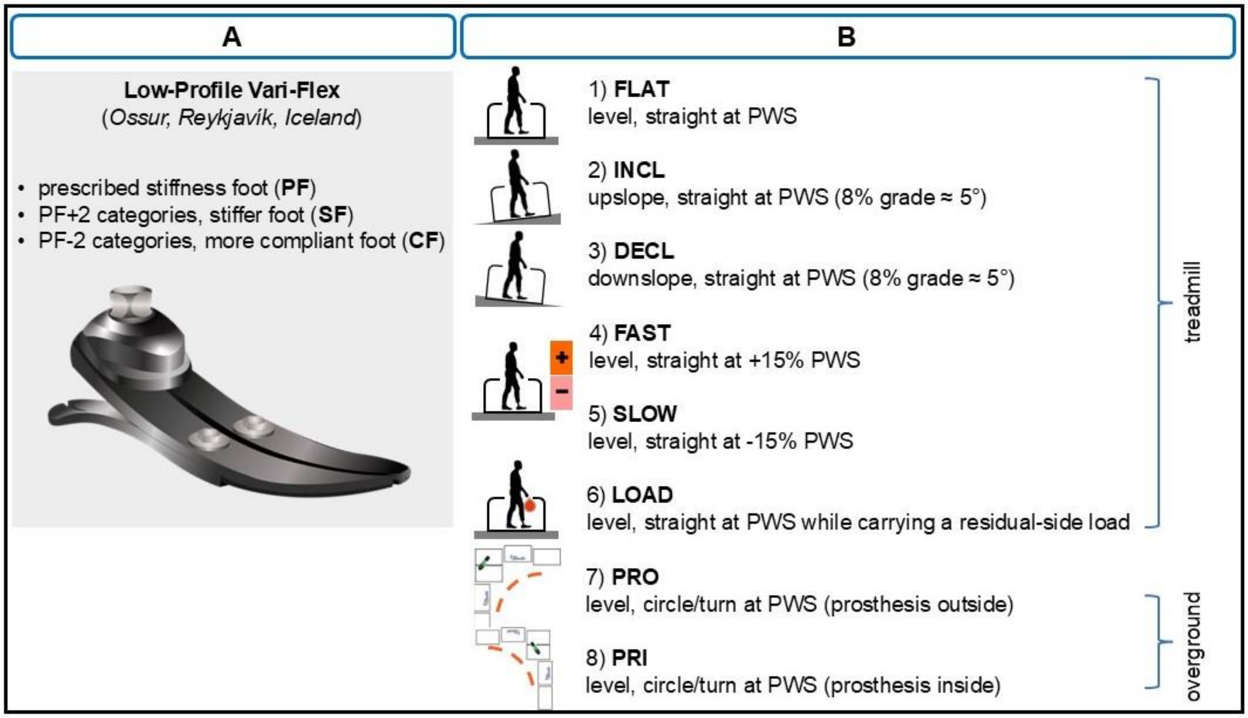

Fig 6.1 Illustrations of A) study prostheses; B) in-laboratory ambulatory activities. Abbreviations: PWS, preferred walking speed.

A full-view 16-camera motion capture system (Vicon Motion Systems, Oxford, UK), with an instrumented split-belt treadmill and eight embedded overground force plates (AMTI, Watertown, MA), recorded marker trajectories at 120 Hz and force plate data at 1200 Hz. Reflective tracking markers were placed on each subject using Vicon's standard Plug-in-Gait marker set. Additional anatomical and cluster markers were placed bilaterally to define segment kinematics, and prosthetic-side markers mirrored the intact limb (see (Ardianuari et al., (2024) (Chapter 2) for details). For load carriage trials, three additional markers were added to define and track the load segment.

6.3.3 Experimental Protocol

At the first visit, all three study feet were fit in random order. Subjects performed in-laboratory ambulatory activities on the treadmill (Fig. 6.1B: 1-6) and overground on a 2-m-diameter circle (Fig. 6.1B: 7-8). For treadmill activities, preferred walking speeds (PWS) were determined by asking them to select their comfortable speeds that change from slow to fast or fast to slow speeds (Dal et al., 2010; Malatesta et al., 2017). Subjects were allowed at least 10-15 min of walking to acclimate to each study foot stiffness. Subjects were blinded using identical foot shells across conditions.

After at least one overnight rest, each subject came back for a second visit for motion capture procedures. Stiffness conditions and activity order were randomized within subjects (Fig. 6.1A and 6.1B). For activity 6, subjects carried a 5-kg load to simulate a typical grocery bag (Sutton et al., 2010). Activities 1-6 were collected for one minute, while activities 7-8 were performed in four to five bouts in each direction, ensuring sufficient strides to obtain knee loading estimates in individuals with TTA (Syrett et al., 2025). Prosthetic alignment was optimized by the prosthetist for each stiffness condition using standard clinical procedures. While alignment can be experimentally constrained to control variability within the same foot model (Slater et al., 2024), this approach is not reflective of clinical practice and was therefore not imposed. Rest breaks were provided as needed. Once the protocol was completed, subjects switched back to their prescribed prostheses.

6.3.4 Data Analysis

Marker trajectories were pre-filtered in Vicon Nexus using a Woltring quintic spline-interpolating algorithm (mean-square-error 10 mm^2) (Woltring, 1986). A 15-segment whole-body model (head, torso, and bilateral upper arms, forearms, hands, Visual 3D Composite pelvis, thighs, shanks, and feet, and a load segment when applicable) was created from each standing static trial using Visual 3D software (v.2025.05.2, HAS-Motion, Kingston, Ontario, Canada). Segment masses were estimated as percentages of whole-body mass (Dempster, 1995), and inertial properties and center-of-mass (CoM) locations were calculated using geometric approximations in Visual 3D. To represent a TTA model, prosthetic-side shank mass was reduced to 35% of the intact-side shank mass, and the prosthetic-side CoM location was shifted 35% proximally toward the knee joint (Smith et al., 2014). Kinematic and ground reaction force data were low-pass filtered using a fourth-order, zero-lag Butterworth filter with cutoff frequencies of 6 Hz and 20 Hz, respectively. Heel-strike and toe-off events were identified using a force threshold of 20 N as well as kinematic pattern recognition. All events were inspected visually and corrected when necessary.

6.3.5 Outcomes

Using the standard inverse-dynamics approach, MCF was calculated in MATLAB (Mathworks, Natick, MA) via a validated linear regression model that combines peak KAM and KFM (Manal et al., 2015; Trepczynski et al., 2014):

$$MCF \approx c_1 \times KAM + c_2 \times |KFM| + c3 \qquad \text{eq (1)}$$

Peak KAM and absolute KFM were identified as local maxima during early (0–50%) and late stance (51–100%). Coefficients reported from an instrumented knee implant were c1=0.38, c2=0.13, c3=0.50 (Walter et al., 2010), while coefficients from a study estimating EMG-driven MCF following ACL reconstruction were c1=0.34, c2=0.13, c3=0.83 (Manal et al., 2015). The averages of these coefficients were used in this study (c1=0.36, c2=0.13, c3=0.67), consistent with prior work examining gait modifications to reduce peak KAM (Uhlrich et al., 2018). Peak KAM and KFM were normalized by body weight (BW) × height (Ht) (see Appendix) and the resulting peak MCF estimates were expressed in BW.

6.3.6 Statistical Analysis

Linear mixed-effects regression was performed separately for each activity and outcome, with stiffness as a fixed effect, centered speed as a covariate, and subject as a random effect. Several candidate random-effects structures were compared with the best model chosen based on likelihood ratio tests. This model assumes a common variance in outcomes; thus, standard errors for the means are similar across stiffness and activity. Hypothesis testing for the overall association between outcome and stiffness was carried out using conditional F-tests for each activity. Additionally, the Benjamini-Hochberg (BH) adjustment was applied to the F-tests for each model to maintain a false discovery rate of 5% (Benjamini and Hochberg, 1995). Hypothesis testing for pairwise differences across stiffness conditions was carried out using Tukey's method to account for the inflation of the Type 1 error due to assessment of three pairwise differences for each activity. Significance was set a priori at $\alpha = 0.05$. Analyses were performed in R (R Foundation for Statistical Computing, Vienna, Austria) using packages *lme4*, *lmerTest*, and *emmeans*. To contextualize the magnitude of changes in MCF, pairwise differences between stiffness conditions were compared against a reported minimal detectable change (MDC) threshold of ~0.25 BW (9%) in peak MCF (Barrios and Willson, 2017).

6.4 RESULTS

6.4.1 Human subjects

Fifteen male veterans (n=15) completed the protocol (Table 6.1). The demographics information includes axial stiffness corresponding to each study prosthesis category, estimated using linear regression equations characterizing LP Vari-flex mechanical stiffness (Tacca et al., 2024).

6.4.2 Stiffness effects on speed

Stiffness did not significantly affect PWS in any activity except PRO (Table 6.2), where subjects walked faster with SF than with PF ($p = 0.04$) or CF ($p = 0.01$). Overall, subjects tended to walk slower during treadmill vs. overground activities.

Table 6.1 Subject demographics

Sub ID	Age (yrs)	Body mass (kg)	Height (m)	Amp. etiology	Time since amp. (yrs)	MFCL K-level (0-4)	Stiffness			Estimated axial stiffness (kN/m)†						Prescribed prosthesis		
										PF		SF		CF				
							PF	SF	CF	Forefoot	Heel	Forefoot	Heel	Forefoot	Heel	Socket	Suspension	Foot (manufacturer)
S01	45	130	1.84	trauma	8	K4	7	9	5	49.9	46.7	57.6	56.0	42.2	37.5	hybrid PTB	seal-in	LP Vari-Flex (Ossur)
S02	45	104	1.83	trauma	18	K4	7	9	5	45.0	41.7	52.7	51.0	37.3	32.4	hybrid PTB	sleeve	All Pro (Fillauer)
S03	59	145	1.94	trauma	17	K3	9	N/A	7	56.0	54.3	N/A	N/A	48.3	45.1	hybrid PTB	anatomic	BladeXT (Blatchford)
S04	60	96	1.76	dysvascular	15	K3	6	8	4	46.1	42.1	53.8	51.4	38.4	32.8	hybrid PTB	sleeve	ElanIC (Blatchford)
S05	62	106	1.73	infection	4	K2	5	7	3	45.5	40.8	53.2	50.1	37.8	31.5	hybrid PTB	pin lock	Vari-Flex (Ossur)
S06	74	79	1.78	dysvascular	4	K3	4	6	N/A	40.0	34.5	47.7	43.8	N/A	N/A	hybrid PTB	pin lock	Trustep (College Park)
S07	68	90	1.73	trauma	6	K3	6	8	4	47.7	43.8	55.4	53.0	40.0	34.5	hybrid PTB	pin lock	Proflex XC (Ossur)
S08	40	104	1.63	trauma	18	K4	7	9	5	45.0	41.7	52.7	51.0	37.3	32.4	hybrid PTB	suction	All Pro (Fillauer)
S09	79	85	1.79	trauma	57	K3	5	7	3	40.6	35.8	48.3	45.1	32.9	26.5	TSB	pin lock	Re-flex Rotate (Ossur)
S10	67	84	1.69	dysvascular	6	K3	4	6	N/A	38.4	32.8	46.1	42.1	N/A	N/A	hybrid PTB	sleeve	Elan Hydraulic (Blatchford)
S11	72	96	1.81	trauma	43	K3	5	7	3	42.2	37.5	49.9	46.7	34.6	28.2	TSB	sleeve	LP Vari-Flex (Ossur)
S12	42	98	1.62	trauma	1	K4	6	8	4	46.1	42.1	53.8	51.4	38.4	32.8	TSB	pin lock	Terra Dual Keel (Ossur)
S13	64	87	1.86	trauma	46	K4	5	7	3	40.6	35.8	48.3	45.1	32.9	26.5	PTB	sleeve	Proflex ST (Ossur)
S14	31	69	1.77	trauma	2	K4	5	7	3	42.2	37.5	49.9	46.7	34.6	28.2	PTB	pin lock	Rush (Proteor)
S15	64	84	1.82	trauma	8	K4	6	8	4	44.4	40.4	52.1	49.7	36.8	31.1	hybrid PTB	pin lock	BladeXT (Blatchford)
Mean ± SD	**58 ± 14**	**97 ± 19**	**1.77 ± 0.08**		**17 ± 18**					**44.7 ± 4.4**	**40.5 ± 5.4**	**51.5 ± 3.3**	**48.8 ± 3.9**	**37.8 ± 4.1**	**32.3 ± 5.0**			

Abbreviations: MFCL, Medicare Functional Classification Level (by self-report and prosthetist assessment); PF, prescribed stiffness foot; SF, +2 categories (stiffer foot); CF, -2 categories (more compliant foot); PTB, patellar tendon bearing; TSB, total surface bearing; SD, standard deviation. Notes: N/A in the stiffness category denotes conditions in which the corresponding category exceeded the available range (1-9) or was not manufactured for the foot size at the specified body mass. †Calculated via a linear regression form as intercept + B1 × stiffness category + B2 × foot size + B3 × shoe/no shoe, with the corresponding intercepts and B coefficients for forefoot and heel axial stiffness reported by (Tacca et al., 2024).

Table 6.2 Average in-laboratory PWS (m/s)

Activity	**Mean ± SE**			**p-value**
	PF	**SF**	**CF**	
1. FLAT	0.77 ± 0.08	0.78 ± 0.08	0.78 ± 0.08	0.34
2. INCL	0.70 ± 0.06	0.70 ± 0.06	0.69 ± 0.06	0.48
3. DECL	0.68 ± 0.07	0.68 ± 0.07	0.68 ± 0.07	0.75
4. FAST	0.89 ± 0.09	0.90 ± 0.09	0.90 ± 0.09	0.39
5. SLOW	0.66 ± 0.07	0.66 ± 0.07	0.67 ± 0.07	0.25
6. LOAD	0.74 ± 0.07	0.75 ± 0.07	0.75 ± 0.07	0.22
7. PRO	0.92 ± 0.05	0.95 ± 0.05	0.90 ± 0.05	**0.01***
8. PRI	0.92 ± 0.05	0.94 ± 0.05	0.92 ± 0.05	0.40

Abbreviations: PWS, preferred walking speed; SD, standard deviation; PF, prescribed stiffness foot; SF, +2 categories (stiffer foot); CF, -2 categories (more compliant foot). Notes: Mean is estimated marginal mean from the linear mixed-effects regression model. When **significant*** ($p < 0.05$), adjusted pairwise comparisons were performed.

6.4.3 Outcomes

Intact Limb

For activities relative to surface, stiffness influenced peak MCF during walking on FLAT, INCL, and DECL (Fig. 6.2A; Table 6.3). On FLAT, both the PF and SF resulted in a lower first peak MCF than CF. During INCL, CF had the lowest first peak MCF. On DECL, PF and CF resulted in a lower first peak MCF than SF. Stiffness effects were observed for CF with the lowest second peak MCF during FLAT. On DECL, PF and SF had a lower second peak MCF than CF.

For activities relative to speed, stiffness influenced first peak MCF during FAST but not during SLOW (Fig. 6.2B; Table 6.3). During FAST, PF resulted in the lowest first peak MCF, while SF and CF had a lower second peak MCF than PF. On SLOW, SF and CF also had a lower second peak MCF than PF.

For activities relative to load, stiffness influenced first peak MCF but not second peak MCF during LOAD (Fig. 6.3A; Table 6.3). During LOAD, PF and SF resulted in a lower first peak MCF than CF. For activities relative to direction, stiffness only influenced first peak MCF during PRO but not in PRI (Fig. 6.3B; Table 6.3). During PRO, CF resulted in a lower first peak MCF than SF.

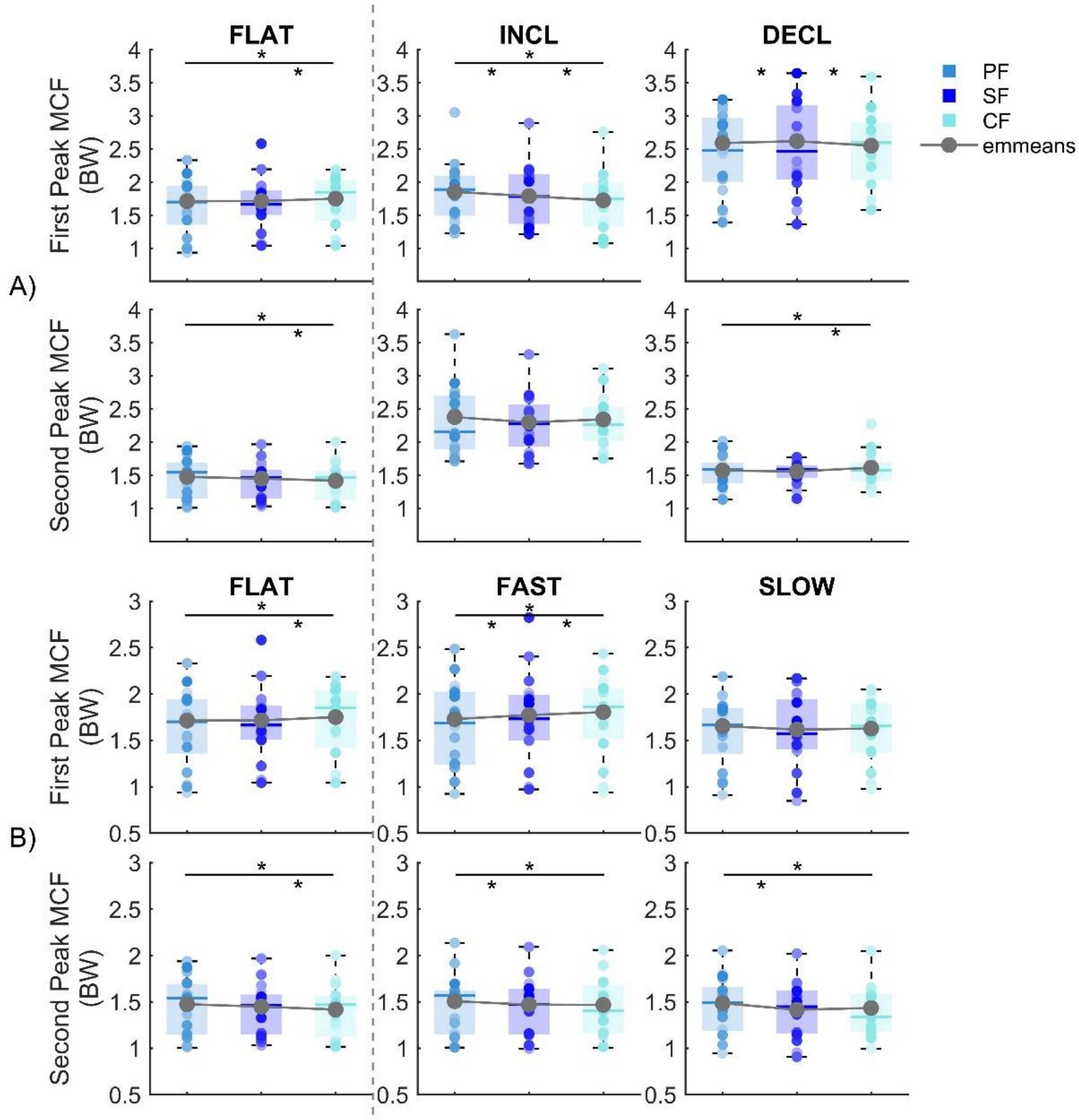

Fig 6.2 A) Average intact-limb first peak (first row) and second peak MCF (second row) comparing prosthetic foot stiffness conditions across ambulatory activities relative to surface; B) Average intact-limb first peak (first row) and second peak MCF (second row) comparing prosthetic foot stiffness conditions across ambulatory activities relative to speed. Scatters represent individual subject means. Asterisks represent significant pairwise comparisons. Abbreviations: MCF, medial knee contact force; BW, body weight; PF, prescribed stiffness foot; SF, +2 categories (stiffer foot); CF, -2 categories (more compliant foot); emmeans, estimated marginal means (from the linear mixed-effects regression models).

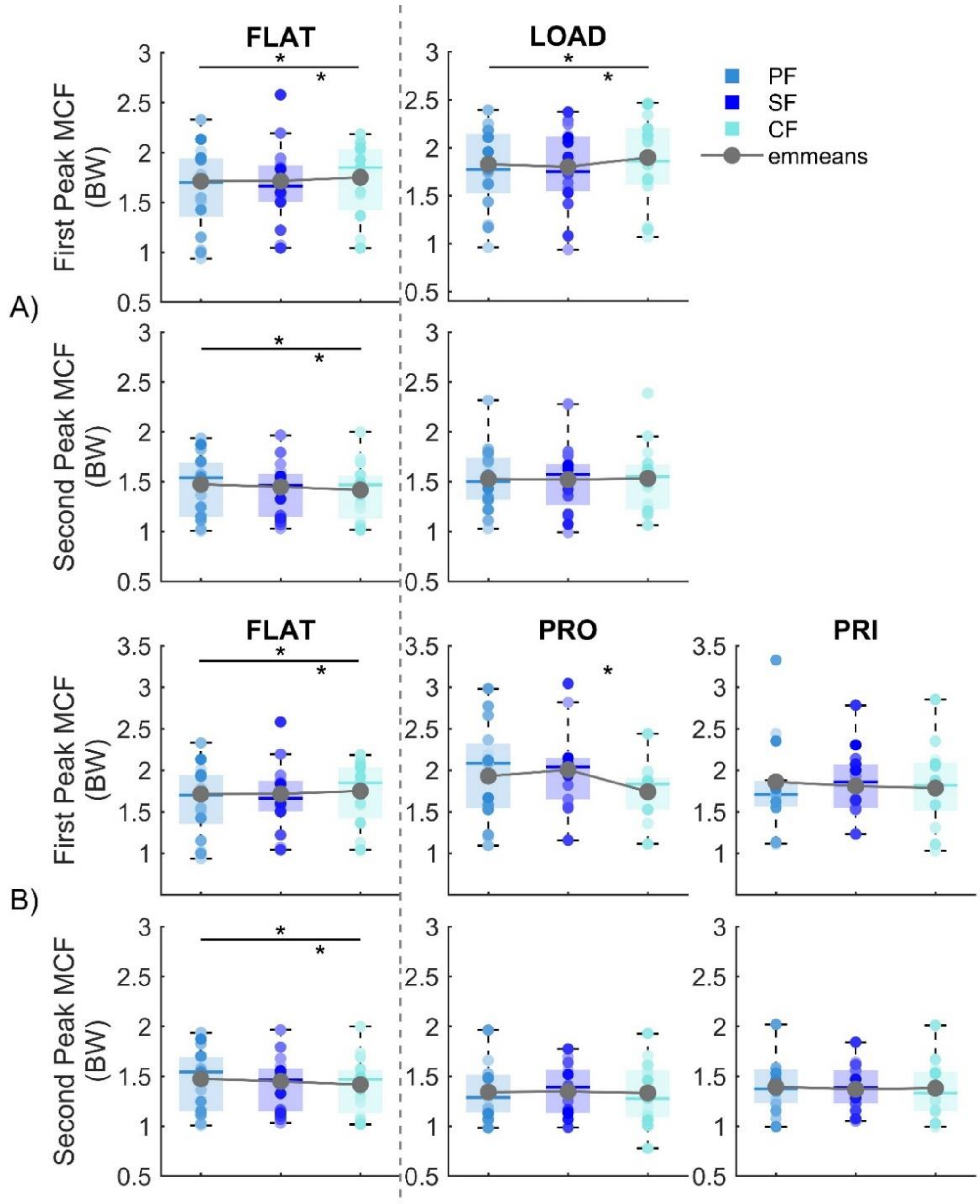

Table 6.3 A) Average intact-limb first peak (first row) and second peak MCF (second row) comparing prosthetic foot stiffness conditions across ambulatory activities relative to load; B) Average intact-limb first peak (first row) and second peak MCF (second row) comparing prosthetic foot stiffness conditions across ambulatory activities relative to direction. Scatters represent individual subject means. Asterisks represent significant pairwise comparisons. Abbreviations: MCF, medial knee contact force; BW, body weight; PF, prescribed stiffness foot; SF, +2 categories (stiffer foot); CF, -2 categories (more compliant foot); emmeans, estimated marginal means (from the linear mixed-effects regression models).

Table 6.4 Averages and pairwise differences of the intact-limb first and second peak MCF between stiffness conditions across ambulatory activities.

Outcome (BW)	Activity	Mean (± SE)			p-value	Pairwise Difference					
		PF	SF	CF		PF vs SF	BH-p [95% CI]	PF vs CF	BH-p [95% CI]	CF vs SF	BH-p [95% CI]
First Peak	FLAT	1.73 (0.11)	1.73 (0.11)	1.79 (0.11)	**<0.01***	0	0.92 [-0.03, 0.02]	-0.06	**<0.01* [-0.09, -0.03]**	0.06	**<0.01* [0.03, 0.09]**
Second Peak		1.44 (0.07)	1.42 (0.07)	1.39 (0.07)	**<0.01***	0.01	0.19 [-0.01, 0.03]	0.05	**<0.01* [0.03, 0.07]**	-0.04	**<0.01* [-0.06, -0.02]**
First Peak	INCL	1.85 (0.11)	1.81 (0.11)	1.75 (0.11)	**<0.01***	0.04	**<0.01* [0.02, 0.07]**	0.10	**<0.01* [0.07, 0.13]**	-0.06	**<0.01* [-0.09, -0.03]**
Second Peak		2.19 (0.14)	2.16 (0.14)	2.18 (0.14)	0.02	0.03	0.06 [0.00, 0.06]	0	0.98 [-0.03, 0.03]	0.03	0.11 [0.00, 0.06]
First Peak	DECL	2.44 (0.14)	2.49 (0.14)	2.43 (0.14)	**<0.01***	-0.05	**<0.01* [-0.09, -0.02]**	0	0.98 [-0.04, 0.04]	-0.06	**<0.01* [-0.09, -0.02]**
Second Peak		1.40 (0.11)	1.39 (0.11)	1.47 (0.11)	**<0.01***	0.01	0.88 [-0.03, 0.04]	-0.07	**<0.01* [-0.11, -0.04]**	0.08	**<0.01* [0.05, 0.11]**
First Peak	FAST	1.67 (0.23)	1.73 (0.23)	1.78 (0.23)	**<0.01***	-0.05	**<0.01* [-0.08, -0.02]**	-0.11	**<0.01* [-0.14, -0.08]**	0.06	**<0.01* [0.03, 0.09]**
Second Peak		1.45 (0.09)	1.40 (0.09)	1.39 (0.09)	**<0.01***	0.05	**<0.01* [0.03, 0.07]**	0.06	**<0.01* [0.04, 0.08]**	-0.01	0.23 [-0.03, 0.01]
First Peak	SLOW	1.69 (0.10)	1.67 (0.10)	1.68 (0.10)	0.09	0.02	0.22 [0.00, 0.04]	0.01	0.61 [-0.01, 0.03]	0.01	0.61 [-0.01, 0.04]
Second Peak		1.50 (0.08)	1.44 (0.08)	1.42 (0.08)	**<0.01***	0.06	**<0.01* [0.04, 0.08]**	0.07	**<0.01* [0.05, 0.09]**	-0.01	0.19 [-0.03, 0.01]
First Peak	LOAD	1.80 (0.10)	1.78 (0.10)	1.88 (0.10)	**<0.01***	0.02	0.26 [-0.01, 0.04]	-0.08	**<0.01* [-0.10, -0.05]**	0.09	**<0.01* [0.07, 0.12]**
Second Peak		1.53 (0.06)	1.52 (0.06)	1.54 (0.06)	0.18	0	0.87 [-0.01, 0.02]	-0.01	0.62 [-0.03, 0.01]	0.01	0.52 [0.00, 0.03]
First Peak	PRO	1.93 (0.12)	2.01 (0.12)	1.74 (0.13)	**0.01***	-0.08	0.59 [-0.26, 0.11]	0.19	0.11 [-0.01, 0.39]	-0.26†	**0.02* [-0.47, -0.06]**
Second Peak		1.34 (0.07)	1.35 (0.07)	1.33 (0.07)	0.93	-0.01	0.99 [-0.09, 0.08]	0.01	0.99 [-0.08, 0.10]	-0.01	0.99 [-0.11, 0.08]
First Peak	PRI	1.86 (0.12)	1.81 (0.12)	1.79 (0.13)	0.51	0.05	0.94 [-0.09, 0.19]	0.07	0.94 [-0.09, 0.23]	-0.02	0.94 [-0.18, 0.14]
Second Peak		1.39 (0.06)	1.37 (0.06)	1.38 (0.07)	0.76	0.02	0.96 [-0.05, 0.10]	0.01	0.96 [-0.07, 0.10]	0.01	0.96 [-0.07, 0.09]

Abbreviations: SE, standard error; BH-p, Benjamini-Hochberg adjusted p-value; CI, confidence interval; PF, prescribed stiffness foot; SF, +2 categories (stiffer foot); CF, -2 categories (more compliant foot). Notes: Mean is estimated marginal mean from the linear mixed-effects regression models. Bold **p-values*** with indicate statistical significance. †Indicates pairwise difference exceeding MDC threshold.

Residual Limb

For activities relative to surface, CF and SF resulted in a lower first peak MCF than PF, while CF had the lowest second peak MCF during FLAT. On INCL, PF and CF resulted in a lower first peak MCF compared with SF. For DECL, SF had the lowest first and second peak MCF (Fig.6.4A; Table 6.4). For activities relative to speed, PF resulted in the lowest first peak MCF during FAST. During SLOW, PF and CF had a lower first peak MCF. PF and CF resulted in a lower second peak MCF than SF on FAST and CF resulted in the lowest second peak MCF on SLOW (Fig. 6.4B; Table 6.4).

For activities relative to load, stiffness influenced both peaks during LOAD (Fig. 6.5A; Table 6.4), with CF having the lowest first peak MCF, as well as PF and CF having a lower second peak MCF than SF. For activities relative to direction, no significant pairwise comparisons were observed in PRO or PRI (Fig. 6.5B; Table 6.4).

Pairwise differences between stiffness conditions did not exceed the MDC across both limbs, except for the comparison between CF and SF during PRO in the intact limb (i.e., 0.26 BW $\approx$ 9.4%; Fig. 6.4B; Table 6.3).

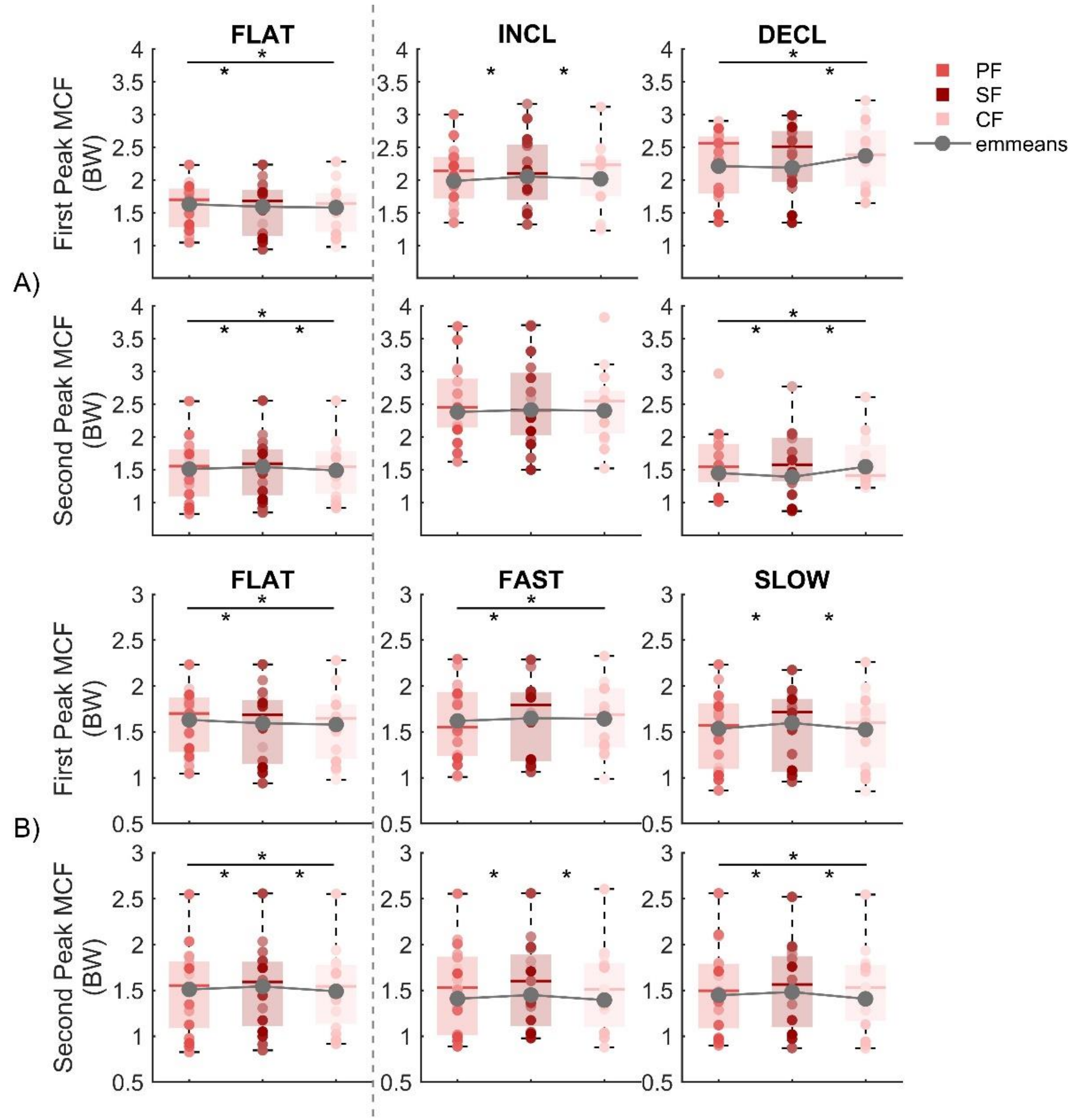

Fig 6.3 A) Average residual-limb first peak (first row) and second peak MCF (second row) comparing prosthetic foot stiffness conditions across ambulatory activities relative to surface; B) Average residual-limb first peak (first row) and second peak MCF (second row) comparing prosthetic foot stiffness conditions across ambulatory activities relative to speed. Scatters represent individual subject means. Asterisks represent significant pairwise comparisons. Abbreviations: MCF, medial knee contact force; BW, body weight; PF, prescribed stiffness foot; SF, +2 categories (stiffer foot); CF, -2 categories (more compliant foot); emmeans, estimated marginal means (from the linear mixed-effects regression models).

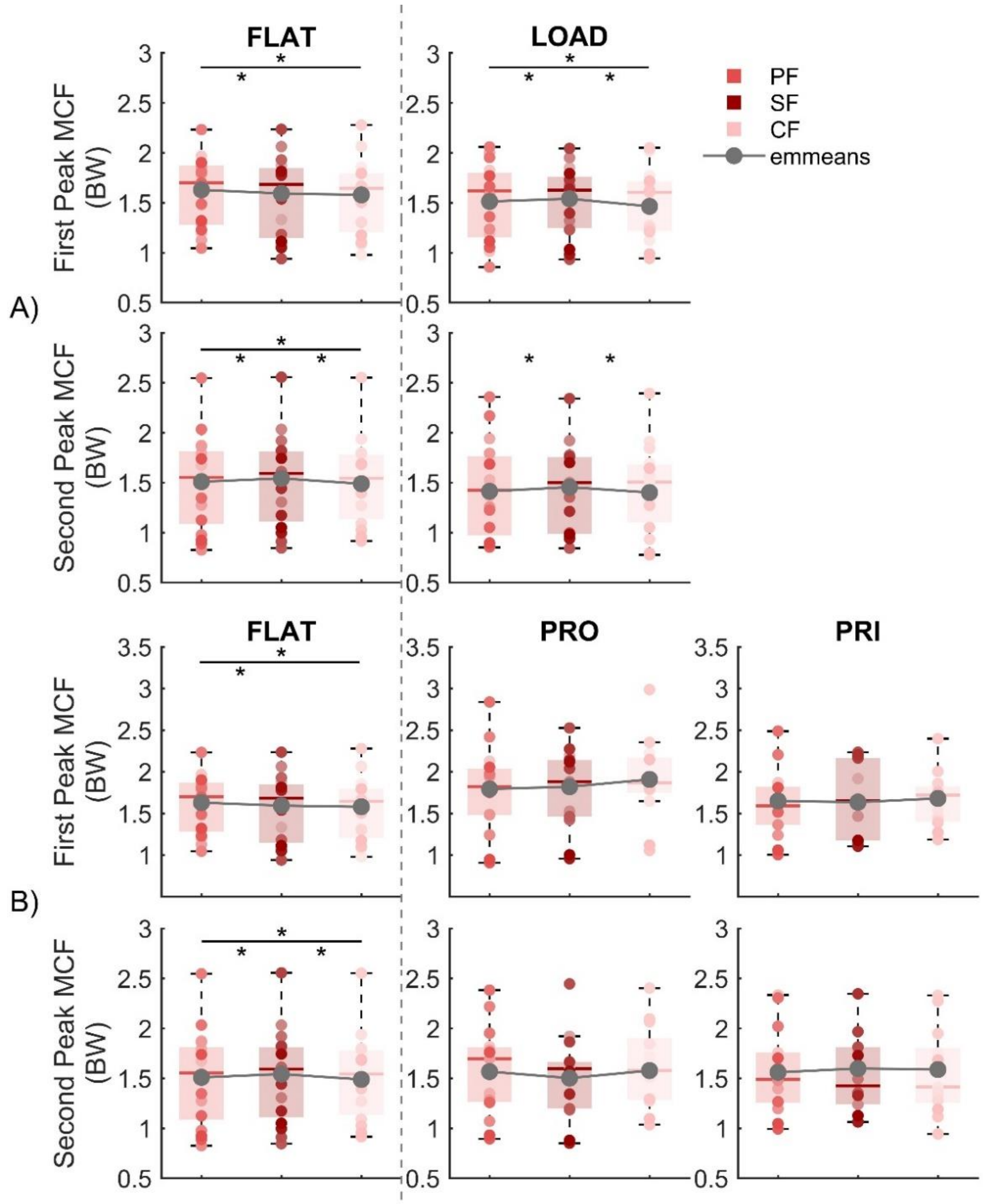

Fig 6.4 A) Average residual-limb first peak (first row) and second peak MCF (second row) comparing prosthetic foot stiffness conditions across ambulatory activities relative to load; B) Average residual-limb first peak (first row) and second peak MCF (second row) comparing prosthetic foot stiffness conditions across ambulatory activities relative to direction. Scatters represent individual subject means. Asterisks represent significant pairwise comparisons. Abbreviations: MCF, medial knee contact force; BW, body weight; PF, prescribed stiffness foot; SF, +2 categories (stiffer foot); CF, -2 categories (more compliant foot); emmeans, estimated marginal means (from the linear mixed-effects regression models).

Table 6.5 Averages and pairwise differences of the residual-limb first and second peak MCF between stiffness conditions across ambulatory activities.

Outcome (BW)	**Activity**	**Mean (± SE)**			**p-value**	**Pairwise Difference**					
		PF	**SF**	**CF**		**PF vs SF**	**BH-p [95% CI]**	**PF vs CF**	**BH-p [95% CI]**	**CF vs SF**	**BH-p [95% CI]**
First Peak	FLAT	1.63 (0.09)	1.59 (0.09)	1.58 (0.09)	**<0.01***	0.04	**<0.01* [0.02, 0.06]**	0.05	**<0.01* [0.03, 0.07]**	-0.01	0.24 [-0.03, 0.01]
Second Peak		1.51 (0.12)	1.54 (0.12)	1.49 (0.12)	**<0.01***	-0.03	**<0.01* [-0.05, -0.01]**	0.02	**0.04* [0.00, 0.04]**	-0.05	**<0.01* [-0.07, -0.03]**
First Peak	INCL	1.99 (0.16)	2.05 (0.16)	2.02 (0.16)	**<0.01***	-0.07	**<0.01* [-0.10, -0.04]**	-0.03	0.05 [-0.06, 0.00]	-0.04	**0.04* [-0.07, 0.00]**
Second Peak		2.38 (0.15)	2.41 (0.15)	2.40 (0.15)	0.08	-0.03	0.20 [-0.06, 0.00]	-0.02	0.64 [-0.05, 0.02]	-0.01	0.73 [-0.05, 0.02]
First Peak	DECL	2.21 (0.16)	2.19 (0.16)	2.37 (0.16)	**<0.01***	0.02	0.12 [0.00, 0.05]	-0.16	**<0.01* [-0.19, -0.13]**	0.18	**<0.01* [0.15, 0.21]**
Second Peak		1.45 (0.10)	1.39 (0.10)	1.55 (0.10)	**<0.01***	0.06	**<0.01* [0.02, 0.10]**	-0.10	**<0.01* [-0.14, -0.05]**	0.15	**<0.01* [0.12, 0.19]**
First Peak	FAST	1.62 (0.13)	1.65 (0.13)	1.64 (0.13)	**<0.01***	-0.03	**<0.01* [-0.05, -0.01]**	-0.02	**0.02* [-0.04, 0.00]**	-0.01	0.77 [-0.03, 0.01]
Second Peak		1.41 (0.14)	1.45 (0.14)	1.39 (0.14)	**<0.01***	-0.04	**<0.01* [-0.06, -0.02]**	0.02	0.10 [0.00, 0.03]	-0.05	**<0.01* [-0.07, -0.04]**
First Peak	SLOW	1.53 (0.10)	1.60 (0.10)	1.52 (0.10)	**<0.01***	-0.06	**<0.01* [-0.08, -0.05]**	0.01	0.44 [-0.01, 0.03]	-0.07	**<0.01* [-0.09, -0.05]**
Second Peak		1.45 (0.11)	1.48 (0.11)	1.41 (0.11)	**<0.01***	-0.04	**<0.01* [-0.05, -0.02]**	0.04	**<0.01* [0.02, 0.06]**	-0.07	**<0.01* [-0.09, -0.06]**
First Peak	LOAD	1.51 (0.09)	1.54 (0.09)	1.47 (0.09)	**<0.01***	-0.03	**<0.01* [-0.04, -0.01]**	0.05	**<0.01* [0.03, 0.07]**	-0.08	**<0.01* [-0.09, -0.06]**
Second Peak		1.41 (0.09)	1.46 (0.09)	1.40 (0.09)	**<0.01***	-0.04	**<0.01* [-0.06, -0.02]**	0.01	0.30 [-0.01, 0.03]	-0.05	**<0.01* [-0.07, -0.03]**
First Peak	PRO	1.79 (0.16)	1.82 (0.16)	1.91 (0.16)	**0.02***	-0.03	0.82 [-0.13, 0.08]	-0.12	0.06 [-0.22, -0.01]	0.09	0.25 [-0.03, 0.20]
Second Peak		1.57 (0.11)	1.50 (0.11)	1.58 (0.11)	0.11	0.06	0.28 [-0.02, 0.15]	-0.01	0.96 [-0.10, 0.08]	0.08	0.28 [-0.02, 0.17]
First Peak	PRI	1.65 (0.10)	1.64 (0.10)	1.68 (0.10)	0.62	0.02	0.94 [-0.10, 0.13]	-0.03	0.94 [-0.14, 0.08]	0.05	0.94 [-0.07, 0.16]
Second Peak		1.56 (0.12)	1.59 (0.12)	1.60 (0.12)	0.81	-0.04	0.99 [-0.19, 0.11]	-0.03	0.99 [-0.17, 0.12]	-0.01	0.99 [-0.16, 0.14]

Abbreviations: SE, standard error; BH-p, Benjamini-Hochberg adjusted p-value; CI, confidence interval; PF, prescribed stiffness foot; SF, +2 categories (stiffer foot); CF, -2 categories (more compliant foot). Notes: Mean is estimated marginal mean from the linear mixed-effects regression models. Bold **p-values*** indicate statistical significance. †Indicates pairwise difference exceeding MDC threshold.

6.5 DISCUSSION

We investigated the influence of commercial prosthetic stiffness on intact-limb knee loading measures across ambulatory activities and explored whether similar effects existed in the residual limb. Overall, stiffness influenced MCF, but the observed effects varied by activity. In the intact limb, stiffer conditions were associated with lower peak MCF in several activities, partially supporting our hypotheses that the effect of foot stiffness on MCF would be activity dependent. In the residual limb, the effects were less consistent.

In the intact limb, we observed reductions in first peak MCF and KAM with stiffer feet, particularly PF, compared with CF on FLAT (Fig.6.2A, Table 6.3, and Appendix Fig. A6.1). This finding is consistent with a previous study reporting reduced first peak KAM with a one-category increase in stiffness at overground PWS (Slater et al., 2024). However, another study found no significant stiffness effects across a +1 to -2 category range during treadmill walking at increasing speeds (Tacca et al., 2026). Interestingly, we also observed lower first peak MCF and KAM with PF compared with CF for FAST at treadmill PWS (Fig.6.2B, Table 6.3, and Appendix Fig. A6.1), which may be advantageous, as faster walking has been shown to exacerbate KAM (Robbins and Maly, 2009). Contrasts with the Tacca et al. (2026) work may reflect slightly different accommodation to each stiffness condition in the present study. While the difference may be modest (± 10 min), it may have allowed somewhat longer adaptation to the altered prosthetic mechanics.

During LOAD, reduced intact-limb first peak MCF was observed with stiffer feet compared with CF (Fig.6.4A, Table 6.3), while trend in first peak KAM was relatively comparable (Appendix Fig. A6.1). Our prior work did not detect significant effects of prosthetic foot type or stiffness on KAM metrics (Ardianuari et al., 2025) (Chapter 3). However, we demonstrated that load carriage on the residual-limb side increased intact-limb first peak KAM and impulse the most (by 20-35%). Additionally, this load condition reduced peak propulsive force in the intact limb (Ardianuari et al., 2024) (Chapter 2). Altogether, these findings suggest that a stiffer prosthetic foot may offer a biomechanical advantage during residual-side load carriage by reducing intact-limb knee loading. The reduced propulsive demand on the intact limb may also be advantageous for those with plantarflexor weakness following TTA (Ardianuari et al., 2024; Lefranc et al., 2024) (Chapter 2).

With activities relative to surface, reductions in intact-limb MCF with stiffer feet during DECL were observed only at second peak MCF (Fig.6.2A, Table 6.3), while the stiffest foot (SF) had the highest first peak MCF. This divergence between peaks may reflect the distinct biomechanical mechanisms governing joint loading across stance. First peak MCF occurs in early stance and is largely associated with KAM, a reasonable surrogate for medial knee loading at this phase. In contrast, second peak MCF occurs in late stance, where medial knee loading is influenced by a combination of high co-contraction between the rectus femoris and plantar flexors and the moment arm of the rectus femoris, resulting in a weaker relationship between KAM, KFM, and the internal MCF (Richards et al., 2018). During DECL, increased braking demands and altered forward progression may elevate medial knee loading during early stance regardless of prosthetic stiffness, potentially explaining the higher first peak MCF observed with SF. However, a stiffer foot may alter energy return in late stance, which could reduce collision on the intact limb through late stance (Childers and Takahashi, 2018), contributing to the observed reduction in second peak MCF. Consistent with this pattern, we observed a general tendency toward higher first peak but a lower second peak MCF across stiffness conditions on DECL.

Another notable finding was observed with first peak MCF during PRO. Subjects walked faster with the stiffest foot (SF), which in turn increased first peak MCF (Table 6.2, Fig. 6.3B, Table 6.3).

In contrast, the CF had a lower first peak MCF (Fig. 6.3B, Table 6.3). During turning with the prosthesis on the outside, the residual limb must generate greater lateral forces to maintain the curved trajectory (Orendurff et al., 2006). Faster speeds with a stiffer foot may, therefore, increase centripetal demands, contributing to higher first peak MCF. With the magnitude exceeding the MDC, a less stiff foot may be more effective in reducing MCF during PRO.

In the residual limb, we observed a similar pattern for DECL in which stiffer feet (PF and SF) reduced both first and second peak MCF (Fig.6.4A, Table 6.4). Consistent with earlier discussion on DECL condition, a stiffer foot may provide better support and limit excessive deflection in early stance, thus reducing residual-limb medial knee loading. In contrast to the intact limb, the influence of prosthetic stiffness on residual-limb MCF was less consistent across activities (Figs. 6.4-5, Table 6.4). This variability suggests the complex mechanics of the limb, whose medial knee loading may be subject to socket reaction forces and prosthetic alignment (Kobayashi et al., 2014), as well as the absence of active ankle control. This may reflect a causal effect of greater reliance on the intact limb, leading to asymmetrical loading.

The magnitude of the related changes observed in this study may partly reflect the relatively small mechanical differences between the prosthetic feet tested. The average estimated forefoot stiffness difference between the SF and CF in this study is 13.7 kN/m (see Table 6.1), similar to a range used by the study with no significant stiffness effects on first peak KAM during level walking (Tacca et al., 2026, 2024). Despite this relatively modest stiffness range, significant differences in MCF were detected across several activities beyond level-ground walking. However, the majority of the observed differences remained below the MDC, suggesting that acute changes in MCF in response to prosthetic stiffness may be small relative to measurement variability and may not represent meaningful reductions in medial knee loading. The nature of knee loading during gait is multifactorial (Heijink et al., 2011), where prosthetic stiffness represents only one of several potential modifiers. It may also be that individuals with TTA quickly adapt to varying prosthetic stiffness conditions, thereby attenuating changes in MCF. As a result, stiffness alone may be insufficient to substantially reduce medial knee loading during walking. Instead, stiffness in combination with other mechanical properties, such as additional push-off (e.g., +10% power above the biological ankle), may reduce medial knee loading and thus the risk of knee pain and OA (Tacca et al., 2026).

6.5.1. Limitations

Potential limitations should be considered when interpreting the results. First, study recruitment was conducted at a VA medical facility where all subjects were male veteran patients with primarily traumatic etiology. This is consistent with the sex distribution of veteran population in Washington State, which is predominantly male (U.S. NCVAS, 2024). This homogeneous sample may limit the generalizability of the findings to the broader population, including female and dysvascular individuals with TTA. Second, the MCF measure used here is largely driven by KAM contributions. The changes observed in this study likely reflect alterations in external joint moments rather than estimates of joint contact forces. Although musculoskeletal simulations, which account for the compressive forces from muscles, can provide estimates of internal joint contact forces, external joint moments remain widely used measures of knee loading. Reductions in joint moments have been associated with reductions in joint contact forces (Hu et al., 2025), supporting the validity of this approach for estimating relative changes in medial knee loading. Finally, subjective ratings of perceived stiffness were not collected, which may have helped contextualize the MCF responses observed across stiffness conditions. Future studies should recruit a larger and more diverse sample, examine walking across varied terrains, and assess long-term musculoskeletal outcomes to better inform clinical recommendations.

6.5.2. Conclusion

Prosthetic foot stiffness influenced MCF estimates during several ambulatory activities in individuals with TTA, although the magnitude and direction of these effects varied. On the intact limb, stiffer feet were generally associated with reduced MCF during level, faster, and loaded walking, partially supporting our hypotheses, whereas specific patterns were observed during downhill and turning. On the residual limb, effects were inconsistent, suggesting that stiffness may primarily influence contralateral-limb knee loading that compensates for the altered distal ankle mechanics. Although statistically significant, differences between stiffness conditions in both limbs were below the reported minimal detectable change threshold, indicating limited immediate, important effects. Altogether, these findings suggest that prosthetic stiffness alone contributes only moderately to changes in medial knee joint loading across ambulatory activities and should be considered alongside other mechanical properties, such as additional powered push-off, when aiming to mitigate knee OA risk. Finally, activity-appropriate or activity-adaptive foot stiffness may be important for consistently offloading intact-limb knee loading in individuals with TTA.

Acknowledgements

This study was supported in part by the Eunice Kennedy Shriver National Institute of Child Health and Human Development (NICHD) (R01HD111514) and the U.S. Department of Veterans Affairs (IK6 RX002974 and I50 RX002357). The authors thank Christina Carranza, L/CPO, for fitting and aligning the study prostheses for all subjects, Jocelyn Berge for assistance with data collection, and Jane Shofer for providing statistical consulting.

CHAPTER 7

ON THE ASSOCIATION BETWEEN PROSTHETIC ANKLE-FOOT BIOMECHANICAL METRICS AND MEDIAL KNEE LOADING OF THE INTACT LIMB DURING AMBULATION

In preparation for submission to *IEEE Transactions on Neural Systems and Rehabilitation Engineering*

Satria Ardianuari

Nicholas P. Fey

Richard R. Neptune

Glenn K. Klute

7.1 ABSTRACT

The objective of this study was to compare multiple widely-used biomechanical metrics, parameters local to a prosthesis, and their associations with medial loading of the contralateral knee. These relationships are expected to better translate how prosthetic ankle-feet are prescribed with the objective to mitigate osteoarthritis risk in individuals with unilateral transtibial amputation (TTA). Fifteen subjects with TTA completed walking trials on treadmill and overground using three prosthetic ankle-foot stiffness categories (prescribed ± 2). Linear mixed-effects models were used to evaluate stiffness effects and stiffness-specific associations. We hypothesized prosthetic ankle-foot peak push-off power and work, dynamic mean ankle moment arm (DMAMA), and roll-over radius (ROR) would be influenced by stiffness across common ambulatory activities. We also hypothesized whether the associations between these prosthetic ankle-foot biomechanical metrics and intact-limb medial knee contact force (MCF) varied with stiffness within each activity. Results partially supported our hypothesis, demonstrating that stiffness effects were evident and most consistent for ROR, whereas push-off metrics and DMAMA were more variable across activities. Contrary to our hypothesis, greater prosthetic ankle-foot push-off was not consistently associated with reduced intact-limb first peak MCF. Instead, ROR demonstrated the most consistent inverse associations with first peak MCF, particularly during upslope walking, faster walking, and load carriage. These findings suggest that the relationships between prosthetic ankle-foot stiffness, relevant biomechanical metrics, and intact-limb MCF are complex and activity-dependent. Optimizing prosthetic ankle-foot intervention to offload the contralateral knee may require prioritizing effective forefoot lever arm characteristics over energy return. Further, this process would benefit from an activity-adaptive perspective.

7.2 INTRODUCTION

Individuals with unilateral transtibial amputation (TTA) have elevated risk of intact-limb knee osteoarthritis (OA) (Morgenroth et al., 2012; Norvell et al., 2005; Struyf et al., 2009), with the prevalence approximately twice that of those without amputation (Farrokhi et al., 2016). This higher prevalence is likely, at least partially, attributable to asymmetrical mechanical loading (Gailey et al., 2008). Imaging and simulation studies have documented increased degenerative changes (Melzer et al., 2001) and increased joint contact forces in the intact-limb knee in this population than in non-amputees (Silverman and Neptune, 2014). Further, these individuals report more knee pain in their intact limb than in their residual limb (Norvell et al., 2005), highlighting a substantial contribution from biomechanical factors to the progression of knee OA. Despite this clinical significance, intact-limb knee loading among asymptomatic or relatively new amputees may not necessarily exceed that of non-amputees, suggesting that elevated loading may develop over time with prolonged prosthesis use or joint degeneration (Fey and Neptune, 2012).

Knee OA is often isolated to the medial compartment and is much more prevalent than lateral knee OA (Jones et al., 2013). A non-invasive, easier-to-estimate reliable measure of medial knee loading, associated with medial knee OA (Andriacchi et al., 2004), is external knee adduction moment (KAM) (Andrag et al., 2024; Miyazaki et al., 2002; Morgenroth et al., 2014). Combined with knee flexion moment (KFM), KAM provides a more accurate measure of medial knee contact force (MCF) (Manal et al., 2015; Miller et al., 2017; Uhlrich et al., 2018; Walter et al., 2010).

More complex activities beyond level-ground walking significantly increase knee compressive forces in non-amputee population (Alexander and Schwameder, 2016; Haggerty et al., 2014). For individuals with TTA, this increased demand may be reduced by a prosthetic device that actively adjusts ankle-foot stiffness to adapt to varying walking conditions to help mitigate elevated MCF and thus OA risk. However, individuals with TTA are typically prescribed prosthetic feet with a fixed stiffness. Our prior study found that stiffness effects were significant on intact-limb peak MCF during several activities (Ardianuari et al., 2026a) (Chapter 6). For example, increased stiffness was generally associated with decreased first peak MCF during level, faster, and loaded walking but resulted in increased first peak MCF during downslope walking. During turning with the prosthesis outside, decreased stiffness was associated with decreased first peak MCF. Overall, these results suggest that stiffness effects were largely activity-dependent, and the underlying biomechanical mechanisms to explain these associations are an open question.

Dynamic walking models and experimental studies of non-amputees suggest that the ability to push off the trailing limb can reduce the collisional loading on the leading limb (Adamczyk and Kuo, 2009; Donelan et al., 2002a, 2002b; Kuo, 2007; Kuo et al., 2005). During the transition from one stance limb to the next during the gait cycle, the trailing prosthetic limb must produce a sufficient push-off, otherwise the leading intact limb will perform a greater share of the body center of mass velocity redirection, thus increasing the ground reaction and joint loading impulse on the leading limb (Morgenroth et al., 2011). Therefore, a prosthetic foot that improves push-off could potentially reduce intact-limb MCF, specifically during early stance.

Despite existing knowledge of the effects of prosthetic ankle-foot stiffness on intact-limb medial knee loading measures, how relevant biomechanical metrics, including push-off, are associated with intact-limb MCF across a range of ambulatory activities, remains unclear. During level-ground walking, increased prosthetic forefoot stiffness is associated with decreased prosthetic push-off power and decreased intact-limb tibiofemoral contact forces (Fey et al., 2012). By contrast, increased prosthetic push-off work is linked to decreased intact-limb KAM (Grabowski and D'Andrea, 2013; Morgenroth et al., 2011). Prior studies have also demonstrated that increased prosthetic ankle-foot stiffness decreases intact-limb KAM while also decreasing prosthetic push-off peak power and work, suggesting that competing mechanisms may exist (i.e., tradeoff between stiffness and push-off) in altering intact-limb medial knee loading measures (Halsne et al., 2020; Slater et al., 2024).

Other relevant biomechanical metrics that may explain the associations between prosthetic ankle-foot stiffness and intact-limb MCF warrant further exploration. For example, prosthetic roll over radius (ROR) also increases with foot stiffness (Halsne et al., 2020; Slater et al., 2024), potentially decreasing intact-limb MCF. Another functional biomechanical metric like dynamic mean ankle moment arm (DMAMA) measures the cumulative ankle-foot loading dynamics and is related to ankle angle and stiffness interaction (Adamczyk, 2020; Leestma et al., 2021), which could potentially play a significant role in modulating intact-limb MCF.

The objective of this study was to examine how these prosthetic ankle-foot biomechanical metrics (i.e., peak push-off power and work, DMAMA, and ROR) vary with stiffness and how these metrics are associated with intact-limb MCF across a range of ambulatory activities. Based on previous findings in the literature and our prior study, we hypothesized that prosthetic ankle-foot stiffness would influence the relevant biomechanical metrics, with increased stiffness generally associated with decreased peak push-off power and work but increased DMAMA and ROR, and that these effects would be activity-dependent (i.e., significant associations during more demanding activities, such as walking downhill, walking at a faster speed, walking with load carriage, and turning). We further hypothesized that these biomechanical metrics would be associated with decreased intact-limb MCF, but these associations would also depend on activity and stiffness condition.

7.3 METHODS

This study was a subset of a larger investigation based on a shared dataset. The randomized, subject-blinded crossover experimental protocol (NCT06711588) was approved by the governing institutional review boards.

7.3.1 Human Subjects

Eligible subjects were recruited from the VA Puget Sound Health Care System and included: 1) individuals with unilateral TTA (aged 18-80 years); 2) post TTA for at least one year; 3) daily use of a well-fitting prosthesis for at least six months; 4) absence of coexisting musculoskeletal disorders and pain (including knee pain) that interfere with gait; 5) ability to walk on a treadmill. All subjects provided informed consent.

Fifteen male subjects participated in the study (average ± SD: age (58 ± 14 yrs); body mass (97 ± 19 kg); height (1.77 ± 0.08 m); and traumatic etiology (n = 10)). Refer to (Ardianuari et al., 2026a) (Chapter 6) for detailed demographic and clinical information including prosthetic stiffness category levels.

7.3.2 Instrumentation

Three passive-elastic carbon-fiber feet of the same design (Vari-Flex; Össur, Reykjavík, Iceland) were fit to each subject's prescribed socket/suspension system, including a clinically prescribed stiffness category (PF), a stiffer foot (SF) and a more compliant foot (CF) that is ±2 category levels from PF. The PF was determined by the manufacturer's recommendations based on their body mass and activity level. A low-profile version (build height: 0.068 m) was mounted on a simulated powered ankle (mass = 1.74 kg) (Azocar et al., 2020) that was used in passive mode to emulate a typical passive prosthetic ankle-foot.

A 16-camera motion capture system (Vicon Motion Systems, Oxford, UK), an instrumented split-belt treadmill, and eight embedded overground force plates (AMTI, Watertown, MA), recorded marker trajectories (120 Hz) and force plate data (1200 Hz). Reflective tracking markers were placed on each subject using Vicon's standard Plug-in-Gait marker set with additional bilateral markers and cluster markers to define segment kinematics (Ardianuari et al., 2024) (Chapter 2). Three additional markers were added to define and track the load segment during load-carrying ambulatory activities.

7.3.3 Experimental Protocol

At the first visit, subjects acclimated for approximately 10-15 minutes to each of the three stiffness conditions (CF, PF, SF) in random order while performing the ambulatory activities (Table 7.1) after alignment by a certified prosthetist. For each stiffness condition, treadmill preferred walking speeds (PWS) were determined by asking subjects to select their comfortable speeds while changing from slow to fast speeds (Dal et al., 2010; Malatesta et al., 2017). Additionally, overground PWS were collected for turning activities. After at least an overnight rest, subjects came back for the second visit to undergo motion capture procedures. Stiffness condition and activity order were block-randomized within each subject.

Table 7.1 In-laboratory ambulatory activities

1)	FLAT: level walking at preferred walking speed (PWS)	Treadmill
2)	INCL: uphill walking at PWS on a 8%-grade (5°) slope	
3)	DECL: downhill walking at PWS on a 8%-grade (5°) slope	
4)	FAST: level walking at +15% PWS (faster)	
5)	SLOW: level walking at -15% PWS (slower)	
6)	LOAD: level walking while carrying a prosthetic-side load at PWS	
7)	PRO: level turning with the prosthesis outside at PWS	Overground
8)	PRI: level turning with the prosthesis inside at PWS	

Activities 1-6 were collected for one minute, while activities 7-8 were performed in four to five turns in each direction (Ardianuari et al., 2026a) (Chapter 6). Rest breaks were provided as needed during both visits. Subjects were blinded to the stiffness conditions, and blinding was maintained using identical foot shells across stiffness conditions and activities.

7.3.4 Data Analysis

Marker trajectories were pre-filtered in Vicon Nexus using a Woltring quintic spline-interpolating algorithm (MSE: 10 mm^2). A 15-segment body model (head, torso, Visual 3D Composite pelvis, and bilateral upper arms, forearms, hands, thighs, shanks, and feet, and a load segment when applicable) was created from each standing static trial in Visual 3D software (HAS-Motion, Kingston, Ontario, Canada). A Visual 3D virtual foot model was created by modifying the heel-to-toe method to better represent prosthetic ankle-foot deformation when estimating ankle kinematics (HAS-Motion, 2026). Specifically, a virtual forefoot landmark was defined midway between the first and fifth metatarsal markers and used with the heel and fifth metatarsal markers to define the foot segment. This modified marker-based coordinate system was intended to provide a more clinically meaningful representation of prosthetic ankle angle and moment than a simple rigid single-segment foot model.

Segment masses were estimated as percentages of whole-body mass (Dempster, 1995), and inertial properties and center-of-mass locations were calculated using geometric approximations in Visual 3D. Prosthetic-side shank mass was reduced to 35% of the intact-side shank mass, and the prosthetic-side center-of-mass location was shifted 35% proximally toward the knee joint (Smith et al., 2014). Kinematic and ground reaction force data were low-pass filtered using a fourth-order, zero-lag Butterworth filter with cutoff frequencies of 6 Hz and 20 Hz, respectively. Heel-strike and toe-off events were identified using a vertical ground reaction force (GRF) threshold of 20 N as well as kinematic pattern recognition. All events were inspected visually and corrected when necessary. All further analyses were performed using custom scripts in MATLAB (Mathworks, Natick, MA).

Prosthetic Ankle-Foot Biomechanical Metrics

Ankle push-off power was computed via the unified deformable segment method, accounting for the below-knee total power for direct comparison with biological ankle function (Takahashi et al., 2012). Push-off work was calculated by time integrating the push-off power (positive for all activities, except DECL), corresponding to energy return during late stance (see Appendix Fig.A7.1. A). The specified push-off work was calculated during late stance, from midstance (defined as the instant when the anterior-posterior GRF crossed zero) to toe-off (identified using the vertical GRF threshold described earlier).

ROR represents the effective rocker shape and prosthetic ankle-foot mechanics during walking (Adamczyk et al., 2006; Curtze et al., 2009; Hansen et al., 2004a; Hansen and Childress, 2010). ROR was calculated using an ankle marker on the lateral malleolus and a knee marker on the lateral femoral condyle. Center of pressure data were transformed from laboratory coordinates into a shank (tibia)-based coordinate, with the origin at the ankle marker and the shank orientation defined by the ankle-knee segment. The transformed center-of-pressure trajectory was projected onto the sagittal-plane roll-over shape, and ROR was estimated by fitting a best-fit circular arc using least-squares regression (Curtze et al., 2009; Hansen et al., 2004a, 2004b). Steps yielding nonphysiological ROR estimates (e.g., negative values or values exceeding subject height), indicative of irregular roll-over shapes, were excluded from analysis.

Prosthetic DMAMA, defined as a single-value functional metric summarizing ankle biomechanics across stance, was computed as the ratio of the sagittal ankle moment impulse ($\bar{M}$) to the vertical ground reaction force impulse ($\bar{F}$) during the period of stance from heel-strike (HS) to toe-off (TO) (Adamczyk, 2020) (see Appendix Fig.A7.B and Fig.A7.C). DMAMA was normalized to percent prosthetic foot size (length) to enable comparison with prior literature.

$$\text{DMAMA: } \frac{\int_{TO}^{HS} M\,dt}{\left\| \int_{TO}^{HS} F\,dt \right\|} = \frac{\bar{M}}{\bar{F}} \qquad \text{(eq.1)}$$

Intact-Limb Medial Knee Loading Measures

Intact-limb MCF was calculated using a validated linear regression model combining external knee moments, KAM and KFM (Manal et al., 2015; Trepczynski et al., 2014).

$$\text{MCF} \approx c_1 \times \text{KAM} + c_2 \times |\text{KFM}| + c3 \qquad \text{(eq.2)}$$

First peak MCF was identified as local maxima during early stance (i.e., during 0-50% gait cycle). We excluded second peak MCF in late stance because we were interested in first peak MCF which occurs during the step-to-step transition, roughly corresponding to double support (i.e., simultaneously in early and late stance for the leading and trailing limbs, respectively). As we alluded to earlier in the Introduction, prior dynamic human walking models have shown that in this instance, push-off from the trailing prosthetic limb reduces the collisional loads on the leading intact limb (Adamczyk and Kuo, 2015, 2009). Coefficients used in this study (c1=0.36, c2=0.13, c3=0.67) were the averages of the coefficients reported from studies on an instrumented knee implant (Walter et al., 2010), and EMG-driven MCF estimation following ACL reconstruction (Manal et al., 2015), and were consistent with those used in a study on KAM reduction regimes using gait modifications (Uhlrich et al., 2018).

7.3.5 Statistical Analysis

Linear mixed-effects regression was performed separately for each activity. To evaluate the effect of stiffness on prosthetic ankle-foot biomechanical metrics, models were fit with stiffness as a fixed effect, activity-specific mean-centered walking speed as a covariate, and subject as a random effect. Candidate random-effects structures were compared using Bayesian information criterion (BIC) and likelihood ratio tests, and hypothesis testing for stiffness effects was conducted using conditional F-tests with Benjamini-Hochberg adjustment applied within each metric to control the false discovery rate at 5%. Pairwise differences between stiffness conditions were assessed using Tukey-adjusted comparisons. To evaluate associations between biomechanical metrics (predictors) and intact-limb first peak MCF (response), separate activity-specific models were fit with fixed effects for stiffness, each predictor, their interaction, and centered PWS, with subject included as a random intercept. Stiffness-specific slopes (β), 95% confidence intervals, and p-values were extracted to quantify predictor-response associations. To provide descriptive statistics for associations, subject-level Pearson correlations (r) were reported. Statistical significance was set a priori at $\alpha = 0.05$, and analyses were performed in R (R Foundation for Statistical Computing, Vienna, Austria) using packages *lme4*, *lmerTest*, and *emmeans*, and in MATLAB using *Statistical Toolbox*.

7.4 RESULTS

7.4.1 Prosthetic Ankle/Foot Biomechanical Properties

Ankle peak push-off power differed by stiffness in most activities and generally decreased with increasing foot stiffness (Fig.7.1A and Table 7.2). During FLAT, FAST, and LOAD, peak power in CF and PF were greater than that in SF, with a stepwise decrease observed during LOAD (CF > PF > SF). During SLOW, CF was greater than PF and SF. During DECL, peak power became more negative with increasing stiffness (CF > PF > SF). During PRI, peak power in PF was greater than those in both CF and SF. No stiffness differences in peak push-off power were observed during INCL or PRO.

Ankle push-off work showed similar trends (Fig.7.1B and Table 7.2), with increased work in CF and decreased work in SF across FLAT, FAST, SLOW, and LOAD. However, activity-dependent deviations were observed, including greater work in SF during DECL and greater work in PF during PRI. No stiffness differences in push-off work were observed during INCL.

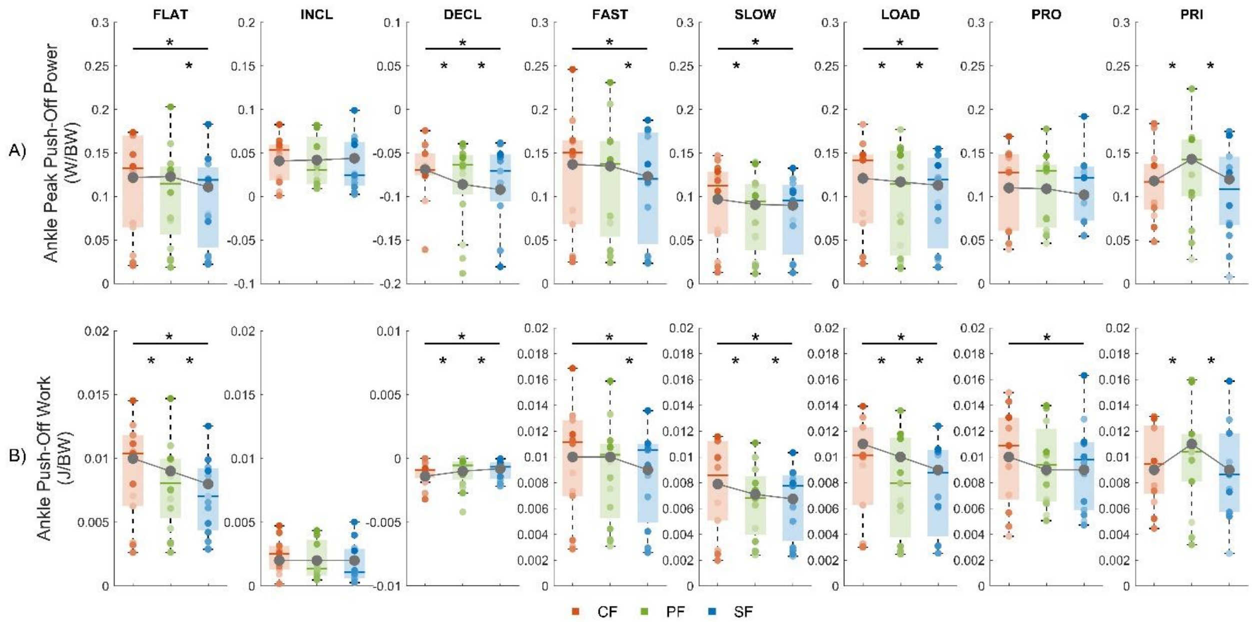

Fig 7.1 A) Average prosthetic ankle-foot peak push-off power, and B) Average prosthetic ankle-foot push-off work comparing stiffness conditions across ambulatory activities. Gray filled circles represent estimated marginal means from the linear mixed-effects regression models. Scatters represent individual subject means. Asterisks and asterisks with horizontal bars represent significant pairwise comparisons. Abbreviations: W/BW, Watt/Body Weight; J/BW, Joule/Body Weight; CF, -2 categories (more compliant foot); PF, prescribed stiffness category; SF, +2 categories (stiffer foot).

DMAMA showed activity-specific and non-monotonic stiffness effects (Fig.7.2A and Table 7.2). DMAMA in SF was greater than that in CF during FLAT and LOAD, but this pattern reversed or became mixed in other activities (e.g., CF > SF > PF during INCL, and SF > CF > PF during DECL). No stiffness differences in DMAMA were observed during FAST, SLOW, or PRI. ROR showed the most consistent stiffness effects (Fig.7.2B and Table 7.2), generally increasing with stiffness (CF < PF < SF) across FLAT, INCL, DECL, FAST, SLOW, and LOAD. In contrast, this pattern reversed during PRO, while ROR during PRI was greater in CF than in SF.

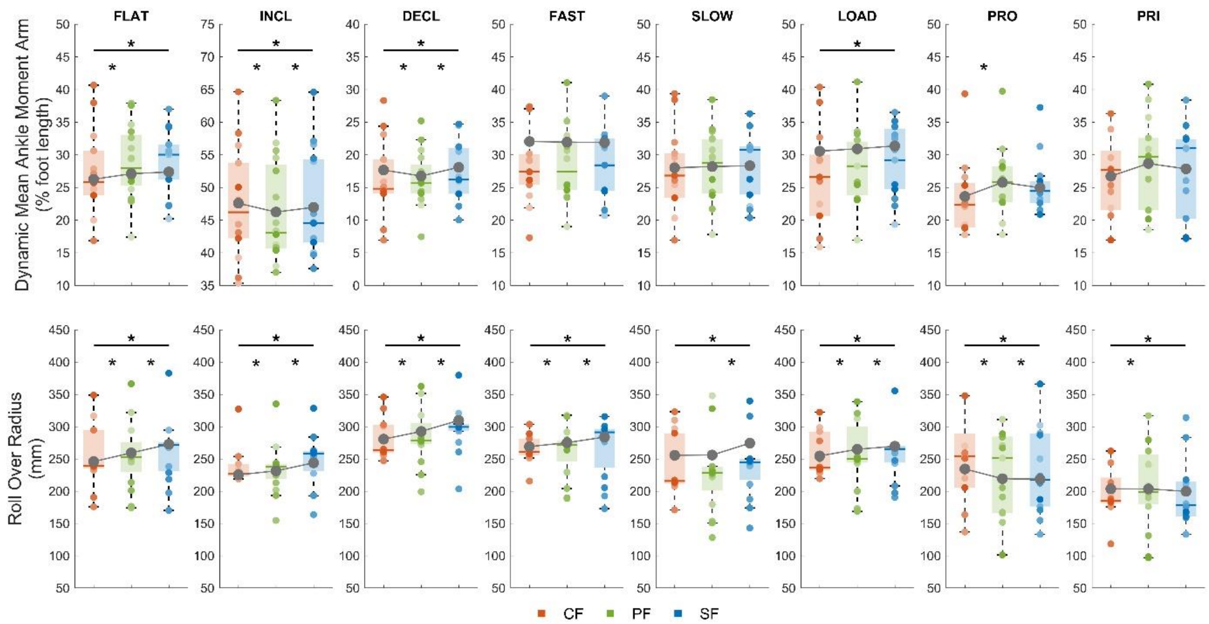

Fig 7.2 A) Average prosthetic ankle-foot DMAMA, and B) Average prosthetic ankle-foot ROR comparing stiffness conditions across ambulatory activities. Gray filled circles represent estimated marginal means from the linear mixed-effects regression models. Scatters represent individual subject means. Asterisks and asterisks with horizontal bars represent significant pairwise comparisons. Abbreviations: W/BW, Watt/Body Weight; J/BW, Joule/Body Weight; CF, -2 categories (more compliant foot); PF, prescribed stiffness category; SF, +2 categories (stiffer foot).

Table 7.2 Pairwise differences between stiffness conditions. Asterisks represent significant differences. Abbreviations: p, p-value; BH-p, Benjamini-Hochberg p-value (correction for multiple comparisons); CI, confidence intervals; CF, -2 categories (more compliant foot); PF, prescribed stiffness category; SF, +2 categories (stiffer foot); W/BW, Watt/Body Weight; J/BW, Joule/Body Weight.

Prosthetic Ankle-Foot Biomechanical Metrics	**Activity**	**p**	**Pairwise difference**					
			PF - CF	**BH-p [95% CI]**	**PF - SF**	**BH-p [95% CI]**	**PF - CF**	**BH-p [95% CI]**
Ankle Peak Push-Off Power (W/BW)	FLAT	**<0.01***	0	0.9 [-0.002, 0.003]	0.01	**<0.01* [0.01, 0.01]**	0.01	**<0.01* [0.01, 0.01]**
	INCL	0.07	0	0.9 [-0.002, 0.003]	0	0.23 [-0.01, 0.001]	0	0.23 [-0.01, 0]
	DECL	**<0.01***	-0.02	**<0.01* [-0.02, -0.01]**	0.01	**0.04* [0, 0.01]**	0.02	**<0.01* [0.02, 0.03]**
	FAST	**<0.01***	0	0.09 [-0.01, 0]	0.01	**<0.01* [0.01, 0.01]**	0.01	**<0.01* [0.01, 0.02]**
	SLOW	**<0.01***	-0.01	**<0.01* [-0.01, -0.004]**	0	0.2 [-0.001, 0.004]	0.01	**<0.01* [0.01, 0.01]**
	LOAD	**<0.01***	-0.01	**<0.01* [-0.01, -0.002]**	0.01	**<0.01* [0.001, 0.01]**	0.01	**<0.01* [0.01, 0.01]**
	PRO	0.26	0	0.99 [-0.01, 0.01]	0.01	0.48 [-0.004, 0.02]	0.01	0.48 [-0.01, 0.02]
	PRI	**<0.01***	0.03	**<0.01* [0.01, 0.04]**	0.02	**0.01* [0.01, 0.04]**	0	0.94 [-0.02, 0.01]
Ankle Push-Off Work (J/BW)	FLAT	**<0.01***	-0.001	**<0.01* [-0.001, 0]**	0.001	**<0.01* [0.001, 0.001]**	0.002	**<0.01* [0.002, 0.002]**
	INCL	0.42	0	0.79 [0, 0]	0	0.79 [0, 0]	0	0.79 [0, 0]
	DECL	**<0.01***	-0.0004	**<0.01* [0, 0.001]**	-0.0006	**<0.01* [0, 0]**	-0.001	**<0.01* [-0.001, 0]**
	FAST	**<0.01***	0	0.07 [0, 0]	0.001	**<0.01* [0.001, 0.001]**	0.001	**<0.01* [0.001, 0.001]**
	SLOW	**<0.01***	-0.001	**<0.01* [-0.001, -0.001]**	0.001	**<0.01* [0, 0.001]**	0.001	**<0.01* [0.001, 0.001]**
	LOAD	**<0.01***	-0.001	**<0.01* [-0.001, -0.001]**	0.001	**0.02* [0, 0]**	0.001	**<0.01* [0.001, 0.001]**
	PRO	**0.02***	0.001	0.48 [-0.001, 0]	0.001	0.17 [0, 0.002]	0.001	**0.04* [0, 0.002]**
	PRI	**0.01***	0.002	**0.03* [0, 0.003]**	0.001	**0.04* [0, 0.003]**	0	0.95 [-0.001, 0.001]
Dynamic Mean Ankle Moment Arm (% foot length)	FLAT	**<0.01***	0.84	**<0.01* [0.45, 1.24]**	-0.27	0.25 [-0.67, 0.13]	-1.11	**<0.01* [-1.52, -0.71]**
	INCL	**<0.01***	-1.34	**<0.01* [-1.87, -0.82]**	-0.72	**<0.01* [-1.20, -0.25]**	0.62	**0.02* [0.08, 1.16]**
	DECL	**<0.01***	-0.92	**<0.01* [-1.32, -0.51]**	-1.33	**<0.01* [-1.71, -0.94]**	-0.41	**0.03* [-0.79, -0.03]**
	FAST	0.56	-0.1	0.89 [-0.45, 0.26]	0.07	0.89 [-0.29, 0.44]	0.17	0.89 [-0.20, 0.54]
	SLOW	0.24	0.19	0.76 [-0.23, 0.62]	-0.13	0.76 [-0.54, 0.29]	-0.32	0.63 [-0.75, 0.12]

	LOAD	**<0.01***	0.37	0.12 [-0.07, 0.81]	-0.43	0.09 [-0.87, 0.01]	-0.8	**<0.01*** **[-1.23, -0.36]**
	PRO	**0.01***	2.15	**0.02*** **[0.47, 3.82]**	0.82	0.47 [-0.82, 2.45]	-1.33	0.25 [-3.07, 0.4]
	PRI	0.12	1.94	0.29 [-0.27, 4.15]	0.82	0.66 [-1.41, 3.05]	-1.12	0.66 [-3.34, 1.10]
Roll Over Radius (mm)	FLAT	**<0.01***	12.96	**<0.01*** **[11.18, 14.74]**	-13.50	**<0.01*** **[-15.32, -11.69]**	-26.46	**<0.01*** **[-28.3, -24.62]**
	INCL	**<0.01***	8.09	**<0.01*** **[6.17, 10.02]**	-10.75	**<0.01*** **[-12.51, -8.98]**	-18.84	**<0.01*** **[-20.82, -16.86]**
	DECL	**<0.01***	8.50	**<0.01*** **[6.35, 10.66]**	-16.81	**<0.01*** **[-18.82, -14.8]**	-25.31	**<0.01*** **[-27.38, -23.24]**
	FAST	**<0.01***	9.31	**<0.01*** **[6.76, 11.86]**	-7.71	**<0.01*** **[-10.35, -5.06]**	-17.02	**<0.01*** **[-19.71, -14.32]**
	SLOW	**<0.01***	-2.19	0.22 [-5.27, 0.9]	-23.77	**<0.01*** **[-26.83, -20.71]**	-21.58	**<0.01*** **[-24.66, -18.51]**
	LOAD	**<0.01***	10.3	**<0.01*** **[7.99, 12.62]**	-4.71	**<0.01*** **[-7.01, -2.41]**	-15.01	**<0.01*** **[-17.30, -12.72]**
	PRO	**<0.01***	-24.93	**<0.01*** **[-29.75, -20.11]**	-18.01	**<0.01*** **[-23.26, -12.75]**	6.93	**0.01*** **[1.62, 12.23]**
	PRI	**<0.01***	-21.56	**<0.01*** **[-29.38, -13.73]**	0.28	0.99 [-5.56, 6.12]	21.83	**<0.01*** **[14.96, 28.71]**

7.4.2 Association Between Prosthetic Ankle/Foot Biomechanical Properties (Predictors) and Intact-Limb Knee Loading (Responses)

Associations between ankle peak push-off power and first peak MCF were activity- and stiffness-dependent but were generally positive during activities (Fig.7.3A and Fig.7.5). Positive associations were observed during FLAT (CF, PF), INCL (PF, SF), DECL (all stiffness conditions), FAST (all stiffness conditions), and SLOW (all stiffness conditions). Negative associations were found for SF during FLAT and for PF during LOAD. No significant associations were observed during PRO or PRI.

There were more variable associations between ankle push-off work and first peak MCF, with both positive and negative effects depending on activity and stiffness (Fig.7.3B and Fig.7.5). Positive associations were observed during FLAT (CF, PF), INCL (PF, SF), FAST (PF, SF), SLOW (all stiffness conditions), LOAD (CF), and PRI (SF). Negative associations were observed during FLAT (SF), DECL (PF, SF), LOAD (PF, SF), and PRO (PF).

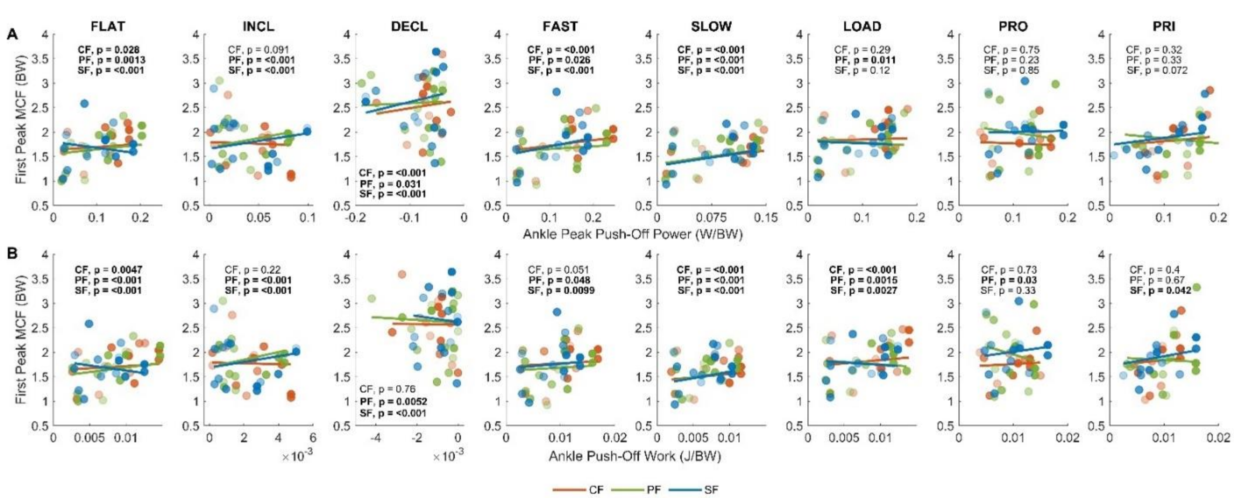

Fig 7.3 A) Prosthetic ankle-foot peak push-off power and B) push-off work as predictors for changes in intact-limb first peak MCF (response). Scatters represent individual subject means. Bold p-values indicate statistical significance. Abbreviations: MCF, medial contact force; W/BW, Watt/Body Weight; J/BW, Joule/Body Weight. CF, -2 categories (more compliant foot); PF, prescribed stiffness category; SF, +2 categories (stiffer foot).

Associations between DMAMA and first peak MCF were also activity- and stiffness-dependent (Fig.7.4A and Fig.7.5). Negative associations were observed during FLAT (CF, PF), DECL (all stiffness conditions), FAST (CF, PF), LOAD (CF) and PRO (SF), whereas positive associations were observed for SF during FLAT, FAST, and SLOW, and for PF and SF during LOAD. No significant associations were found during PRI.

Several associations between ROR and first peak MCF were observed with predominantly negative effects during INCL, FAST, and LOAD (Fig.7.4B and Fig.7.5). Specifically, negative associations were observed during INCL (CF, PF), DECL (SF), FAST (all stiffness conditions), and LOAD (all stiffness conditions). Positive associations were observed during FLAT (PF), SLOW (SF), and PRI (PF). No significant associations were found during PRO.

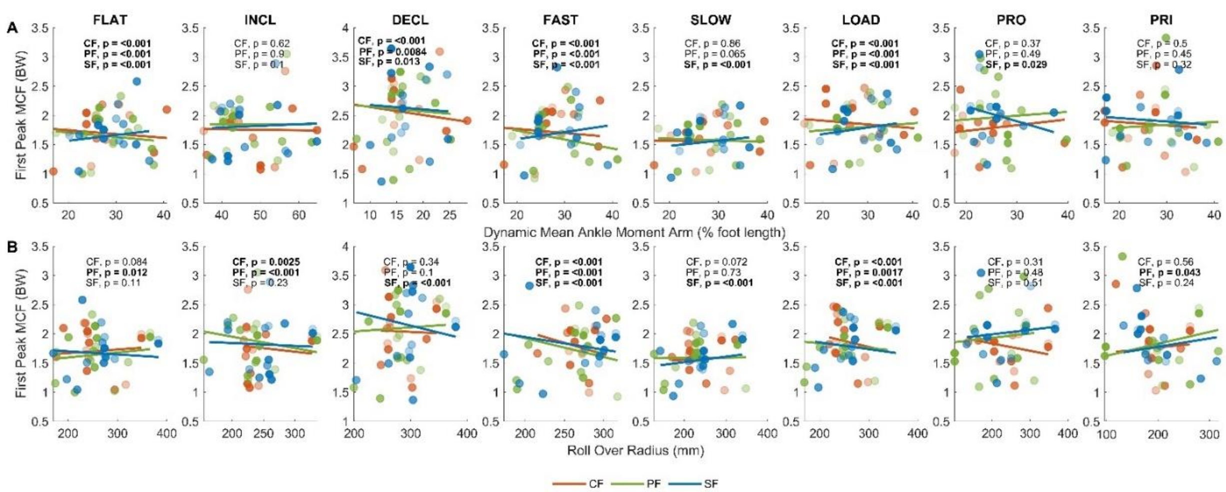

Fig 7.4 A) Prosthetic ankle-foot DMAMA and B) ROR as predictors for changes in intact-limb first peak MCF (response). Scatters represent individual subject means. Bold p-values indicate statistical significance. Abbreviations: MCF, medial contact force; BW, body weight. CF, -2 categories (more compliant foot); PF, prescribed stiffness category; SF, +2 categories (stiffer foot).

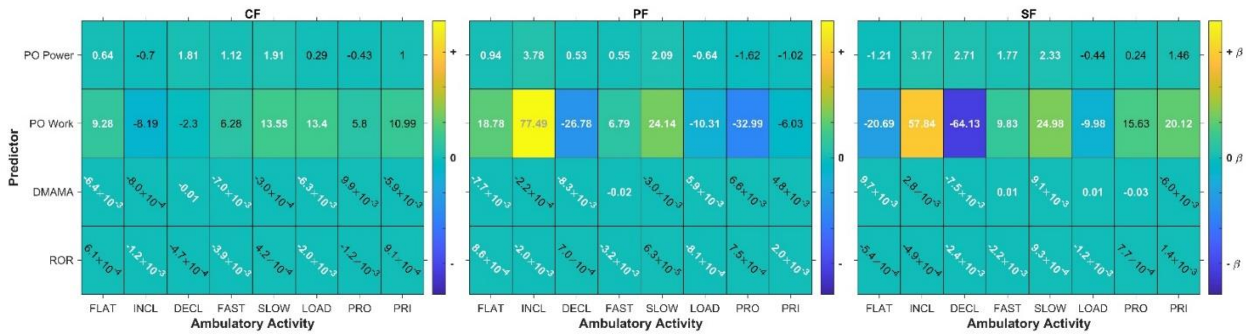

Fig 7.5 Slope estimates (β) representing the magnitude and direction of the associations between prosthetic ankle-foot biomechanical metrics (predictors) and intact-limb first peak MCF (response). Bold white β values represent statistically significant associations ($p < 0.05$, see Figs. 3 and 4 for p-values). Abbreviations: PO, push-off; DMAMA, dynamic mean ankle moment arm; ROR, roll-over radius.

Precision (standard error), ranges of plausible true slopes (95% CI) of the slope estimates, and descriptive subject-level Pearson correlations (r) are reported in Appendix Table A7 and Fig.A7.2 for reference.

7.5 DISCUSSION

This study investigated how prosthetic ankle-foot biomechanical metrics varied with stiffness and how these metrics were associated with intact-limb first peak MCF across ambulatory activities. We hypothesized that increased stiffness category would decrease push-off metrics but increase DMAMA and ROR with activity-dependent effects. Our results partially supported our hypothesis, showing that stiffness effects were evident and most consistent for ROR, whereas push-off metrics and DMAMA were more variable across activities. In contrast, the expected inverse (negative) relationships between the metrics and first peak MCF were not consistently observed. For example, peak push-off power was often positively associated with first peak MCF, push-off work and DMAMA showed mixed effects, and only ROR demonstrated more consistent negative associations in select activities.

In agreement with prior work on overground walking (Halsne et al., 2020; Slater et al., 2024), increased stiffness category was associated with decreased peak push-off power and work during level-ground ambulation including walking at varying speeds and during load carriage. However, stiffness effects on these metrics varied while walking on slopes and turning with the prosthesis inside, with the less stiff foot (CF) producing less push-off work. These findings suggest that during non-level-ground ambulation, particularly during downslope walking (DECL), a stiffer foot may reflect altered energy return in late stance, and thus increasing propulsion (Childers and Takahashi, 2018).

A potential tradeoff may exist between the effects of prosthetic ankle-foot stiffness and push-off on intact-limb knee loading (Slater et al., 2024). For example, our prior study suggested that increased prosthetic ankle-foot stiffness category generally decreases intact-limb first peak MCF, but this effect was activity-dependent (Ardianuari et al., 2026a) (Chapter 6). Previous studies show that increased prosthetic ankle-foot push-off is associated with decreased intact-limb KAM (for example, (Grabowski and D'Andrea, 2013; Morgenroth et al., 2011)). The current study demonstrated a contrasting pattern, with prosthetic push-off predominantly positively associated with intact-limb first peak MCF across activities, with notable exceptions in stiffer feet during FLAT (SF) and LOAD (PF). This suggests that increased push-off may not necessarily reduce intact-limb loading in all activities and may instead reflect increased intact-limb knee loading demands during more demanding tasks. Thus, when prosthetic push-off differences are relatively small or inconsistent, other biomechanical factors may play a more dominant role in influencing intact-limb knee loading (Slater et al., 2024). Our study results indicate that despite less push-off compared to more compliant feet, a stiffer foot may still reduce intact-limb knee loading during level-ground walking, highlighting another tradeoff between propulsion and joint loading.

Increased stiffness category was generally associated with increased DMAMA and ROR, particularly during level-ground walking with and without load carriage. While both metrics were also largely activity-dependent, stiffness effects were more consistent on ROR. Our results for

DMAMA were somewhat consistent with previous studies that suggest DMAMA decreases with an increasing walking speed but then increases upon the transition to running and is positively associated with increasing stiffness during level-ground walking (Adamczyk, 2020; Leestma et al., 2021). Increased prosthetic ankle-foot ROR (i.e., longer effective forefoot lever arm) has been demonstrated to strongly associate with increasing stiffness category (Halsne et al., 2020; Slater et al., 2024; Turner et al., 2022), and this association was also observed in this study for most activities except turning.

Stiffness effects on DMAMA and ROR were also consistent with the associations between these metrics and intact-limb first MCF. Overall, DMAMA showed non-monotonic associations across stiffness, with negative relationships more common in more compliant feet and positive relationships more common in a stiffer foot for several activities. This inconsistency may reflect considerable variability with DMAMA during ambulatory activities relative to speed or terrain (Fehr et al., 2024; Leestma et al., 2021), and greater sensitivity to ambulation at a much faster speed like running (Adamczyk, 2020). On the other hand, ROR was mostly negatively associated with intact-limb MCF with stronger effects observed for the stiffer foot in activities such as DECL, FAST, and LOAD. Previous studies have suggested that a significant decrease in ROR may be associated with an adverse "drop-off" effect, potentially leading to increased intact limb loading due to the abrupt impact at the intact leading-limb heel strike after "dropping off" from the forefoot of the trailing prosthetic limb (Hansen et al., 2006; Klodd et al., 2010). Our results support the evidence that a stiffer foot with increased ROR may provide potential for reducing intact-limb knee loading in more complex ambulatory activities than level-ground walking.

7.5.1 Limitations

Some limitations to the current study should be acknowledged when interpreting the results (for further discussion of the limitations related to sample and intact-limb knee loading estimate, please refer to (Ardianuari et al., 2026a) (Chapter 6)). Briefly, only male subjects with predominantly traumatic etiology participated in this study. Therefore, our results may not be generalizable to individuals with TTA who are female and with amputation of other causes, such as dysvascular diseases. Second, the MCF measures were derived from external joint moments, excluding muscle force contributions to joint compressive forces. Third, subjective perception of foot stiffness was not collected, which could have captured user's preference and experience as a key part of a successful prosthesis prescription (Ruxin et al., 2024). Methodologically, the current study compared feet that vary in stiffness with minimal differences in other metrics whereas some of the previous studies included comparisons of prosthetic feet with substantially different mechanical metrics (e.g., powered push-off). Additionally, the magnitude of prosthetic push-off power across stiffness conditions in prior work (for example, (Halsne et al., 2020; Slater et al., 2024)) was nearly two times greater than the push-off power observed in the present study. This phenomenon likely reflects altered gait mechanics inherent to treadmill compared to overground locomotion which resulted in slower PWS, and thus reduced propulsion demands. Future studies should consider subject-specific characteristics, such as residual limb length and prescribed prosthesis as potential confounders that may have influenced the results. Additionally, future research should recruit a larger and more diverse sample, examine ambulatory activities across varied terrains and walking-running transitions, and assess long-term joint musculoskeletal outcomes to further inform clinical recommendations.

7.5.2 Conclusion

Prosthetic ankle-foot stiffness has been demonstrated to influence relevant biomechanical metrics, with the most consistent effects observed for ROR, while push-off and DMAMA were more variable and activity-dependent. Contrary to our hypothesis, greater prosthetic push-off was not consistently associated with reduced intact-limb first peak MCF across ambulatory activities. Instead, prosthetic ankle-foot ROR demonstrated the most consistent inverse (negative) associations with intact-limb first peak MCF, particularly during more demanding tasks such as upslope walking, faster walking, and walking with load carriage. These findings highlight a complex and activity-dependent relationship between prosthetic ankle-foot biomechanics and intact-limb knee loading, suggesting that optimizing prosthetic ankle-foot intervention for reducing joint loading may require prioritizing effective forefoot lever arm characteristics over push-off alone. Finally, activity-appropriate or activity-adaptive prosthetic ankle-foot stiffness may therefore be critical for consistently offloading intact-limb knee for individuals with TTA as they perform a range of typical ambulatory activities.

Acknowledgements

This study was supported in part by the Eunice Kennedy Shriver National Institute of Child Health and Human Development (NIH, NICHD: R01HD111514) and the U.S. Department of Veterans Affairs (IK6 RX002974 and I50 RX002357). The authors thank Christina Carranza, L/CPO, for fitting and aligning the study prostheses for all subjects, Jocelyn Berge for assistance with data collection, and Eric Hu for assistance with processing some of the experimental data.

CHAPTER 8

CONCLUSION

8.1 Summary

This dissertation describes multiple studies with an overall objective to investigate how prosthetic ankle-foot mechanical metrics influence lower-limb biomechanical demand during functional tasks, with particular emphasis on intact-limb medial knee loading during load carriage and other ambulatory activities. Across Chapters 2–7, this work examined load carriage strategy, prosthetic ankle-foot type, prosthetic ankle-foot stiffness, lower-limb joint work, muscle activation, motor module organization, and prosthetic ankle-foot biomechanical metrics to provide insights into changes in intact-limb medial knee loading. Together, these studies demonstrate that intact-limb medial knee loading is influenced by both task demands and prosthetic ankle-foot mechanics, but that these influences are not uniform across outcomes or activities.

Chapter 2 examined whether individuals with unilateral TTA should carry a side load on the intact or prosthetic side. Carrying a load on the prosthetic side reduced intact-limb propulsive force, whereas carrying a load on the intact side was associated with smaller intact-limb hip flexor and knee flexor moments. Hip and knee abductor moments increased on the limb opposite to the load, and hip extensor power increased on the same limb carrying the load. These findings indicate that the preferred side for carrying a load depends on the desired biomechanical effect, particularly on the intact limb, with clinical implications for gait rehabilitation.

Chapter 3 extended this work by examining how load carriage position and prosthetic ankle-foot type influence intact-limb medial knee loading estimates associated with osteoarthritis risk. Intact-side load carriage produced the smallest first peak KAM and KAM impulse, whereas prosthetic-side load carriage produced the largest first peak KAM and KAM impulse. Prosthetic ankle-foot type did not significantly affect KAM-related outcomes, and only a weak trend was observed between prosthetic push-off work and first peak KAM. These findings suggest that load carriage strategy may be more important than prosthetic ankle-foot selection for modulating intact-limb knee loading during moderate load carriage.

Chapter 4 evaluated how prosthetic ankle-foot selection influences lower-limb mechanical work during load carriage. Most differences across feet occurred in the prosthetic limb at the ankle. The powered ankle-foot produced the greatest positive ankle work in late stance, enhancing forward propulsion, whereas the prescribed and heel-wedge feet produced greater negative ankle work in early stance, supporting absorption and stability. However, knee and hip joint work did not differ substantially across feet. These results suggest that prosthetic ankle-foot type primarily modifies distal prosthetic ankle mechanics rather than substantially altering proximal joint work during moderate load carriage.

Chapter 5 investigated whether changes in prosthetic ankle-foot mechanics translate to changes in muscle activation and motor control during load carriage. Prosthetic ankle-foot type influenced activation of several intact-limb muscles, with powered and stiffer feet often associated with greater plantarflexor and knee extensor activity. However, differences in co-contraction were limited, and motor module complexity, composition, and activation timing remained largely conserved across feet and load conditions. These findings indicate that individuals with TTA accommodate altered prosthetic mechanics and added load primarily through muscle-level activation adjustments rather than broad reorganization of motor control strategies.

Chapter 6 examined the influence of prosthetic ankle-foot stiffness on MCF across various ambulatory activities. Prosthetic stiffness influenced MCF estimates during several activities, but the direction and magnitude of these effects varied by activity. On the intact limb, stiffer feet were generally associated with reduced MCF during level, faster, and loaded walking. However, different patterns were observed during downhill walking and turning, and residual-limb effects were inconsistent. Although some differences were statistically significant, they were below the minimal detectable change threshold, suggesting that prosthetic stiffness alone provides only modest, activity-dependent changes in medial knee loading.

Chapter 7 evaluated whether prosthetic ankle-foot peak push-off power, push-off work, DMAMA, and ROR were associated with intact-limb MCF across ambulatory activities. Contrary to the initial hypothesis, greater prosthetic push-off was not consistently associated with reduced intact-limb first peak MCF. Instead, ROR demonstrated the most consistent inverse associations with intact-limb first peak MCF, particularly during upslope walking, faster walking, and load carriage. These findings suggest that effective forefoot lever-arm behavior may be more important than push-off magnitude alone for reducing intact-limb medial knee loading during functional activities.

Load carriage position consistently influenced intact-limb KAM-related measures, whereas prosthetic ankle-foot type primarily affected prosthetic ankle mechanics and muscle activation. Prosthetic ankle-foot stiffness and relevant metrics influenced intact-limb medial knee loading in an activity-dependent manner. These findings support the need for activity-specific prosthetic prescription guidance for individuals with TTA and motivate future prosthetic ankle-foot designs with activity-adaptive stiffness behavior.

8.2 Limitations

Several limitations should be considered when interpreting the findings of this dissertation. First, the studies included relatively small samples of individuals with TTA (n = 12 and n = 15), with cohorts that were predominantly male veterans and of mostly traumatic etiology. Although these sample sizes are common in laboratory-based, experimental prosthetics research and reflect the predominantly male veteran population in Washington State (U.S. NCVAS, 2024), the results may not be fully generalizable to the broader population with TTA, including patients who are female, younger, have dysvascular etiology, or lower activity levels.

Second, we did not control for certain subject-specific characteristics that may have influenced gait biomechanics. For example, residual limb lengths varied across participants, with several individuals having relatively longer lengths based on TTA ratios (Cognetti et al., 2025). This variability also contributed to only 7/12 participants being able to use the powered ankle-foot due to build-height constraints (Chapters 3-5). Difference in residual limb lengths may alter knee kinematics, socket rotational/reaction forces, and effective limb lever arm to control for the prosthesis during ground contact and forward momentum during gait. However, the within-subject study design likely reduced the potential influence of these factors on the biomechanical outcomes. Next, some participants in the first cohort had relatively high BMIs (Chapters 2-5 and see Table 3.1), which could have influenced changes in medial knee loading. However, our analyses in Chapter 3 (Ardianuari et al., 2025) showed comparable findings for body mass and non-body mass normalized outcomes (Appendix Fig.A3.1 and Table A3.1). Additionally, prosthetic ankle-foot alignment was optimized by the research prosthetist for each condition. While reflective of clinical practice, methodological control to maintain alignment consistency across tasks and prosthetic conditions might have reduced potential variability in gait biomechanical outcomes.

Third, the load carriage studies used a relatively moderate load to simulate common daily load carriage objects and it exceeded the typical 10-kg body mass range for which a prosthetic ankle-foot stiffness category change would be recommended by the manufacturers if the added mass was permanent (see Chapter 2 (Ardianuari et al., 2024) (Chapter 2) for detailed justification).

While not reflective of daily load carriage, heavier loads typically carried during military activities may produce different or more significant biomechanical effects. In addition, load carriage exposure was acute, so the studies did not determine whether the observed biomechanical differences would persist, diminish, or increase over longer periods.

Fourth, the experiments were conducted in a controlled laboratory setting. Although the walking activities were designed to simulate functional tasks, in-laboratory walking may not fully capture real-world conditions such as variable terrain, fatigue, turning in constrained environments, obstacle negotiation, or long-duration community ambulation. Treadmill and overground tasks may also elicit different gait strategies, including speeds, which should be considered when interpreting cross-activity comparisons.

Fifth, the prosthetic ankle-foot comparisons were limited to selected commercially available types and stiffness categories. Therefore, the findings only reflect the mechanical behavior inherent to the tested types and may not generalize to other designs, including research-grade active prosthetic ankle-foot devices. In the powered ankle-foot studies, only a subset of participants (from the first cohort) could be fit and completed the protocol because of residual-limb length and build-height constraints, reducing statistical power and limiting direct comparisons across prosthetic ankle-foot types.

Sixth, several outcomes were indirect estimates of medial knee joint loading. KAM and KAM impulse are widely used surrogates of medial knee loading, but they do not directly measure internal joint contact forces. MCF was estimated using regression-based approaches from external joint moments rather than subject-specific musculoskeletal simulations. Although these approaches are appropriate for estimating relative changes across conditions, they may not capture all subject-specific muscle force contributions to internal joint contact mechanics.

Seventh, EMG analyses were limited to recorded intact-limb muscles and surface EMG measurements. While residual-limb EMG was also recorded, this data did not include a complete set of ankle muscles required for the NNMF-based analyses. Our results characterize motor control using the available intact-limb muscle set and should therefore be interpreted as such. Surface EMG is sensitive to electrode placement, soft tissue artifact, and cross-talk. While the motor module analysis provides insight into low-dimensional neuromuscular organization, it does not directly establish causal mechanisms between prosthetic ankle-foot mechanics and neuromotor coordination.

Finally, several studies evaluated immediate biomechanical responses rather than long-term adaptation. Participants were provided 10-30 minutes of acclimation, depending on the study protocol; however the studies did not assess whether this allocated acclimation was sufficient or whether individuals would adopt different strategies following weeks or months of prosthetic use, gait training, or repeated load carriage exposure. Subjective outcomes, such as comfort, perceived stability, perceived stiffness, fatigue, confidence, and user preference, were also not measured, limiting interpretation of clinical acceptability.

8.3 Future Work

Future research should recruit larger and more diverse cohorts of individuals with TTA, including greater representation of women, individuals with dysvascular amputation, younger adults, and users with varied functional mobility levels. Larger samples would also allow more detailed examination of subject-specific responses, including whether certain users benefit more from specific load carriage strategies, stiffness categories, or prosthetic ankle-foot types.

Future studies should evaluate longer-term adaptation to prosthetic ankle-foot mechanics and load carriage. Repeated exposure studies could determine whether the immediate biomechanical responses and trends observed in this dissertation persist after accommodation, whether gait training enhances beneficial adaptations, and whether changes in intact-limb medial knee loading meaningfully affect knee pain, function, or OA progression over time.

Additional work should test a broader range of task demands. Heavier loads, asymmetric real-world carried objects, variable terrain, stairs, ramps, obstacle negotiation, and prolonged walking may better represent community and occupational ambulation. These studies should include both biomechanical and user-centered outcomes, such as comfort, fatigue, perceived stability, confidence, and preference.

Future work should also use alternative tools in biomechanics (e.g., subject-specific musculoskeletal modeling and simulation via joint reaction analysis) to estimate and decompose medial knee contact forces, accounting for contributions from relevant muscle forces, as well as motors and actuators. Combining motion capture, force data, EMG-validated and -informed modeling, and imaging-based alignment or joint geometry could improve estimates of and changes in medial knee compartment loading and clarify the mechanisms linking prosthetic ankle-foot mechanics to intact-limb knee demand.

The findings from Chapters 6 and 7 may inform mechanical engineering to improve prosthetic ankle-foot systems. Prosthetic ankle-foot selection should consider function beyond push-off (i.e., positive power and energy return during late stance) alone. Further studies should determine whether ROR and DMAMA can serve as biomechanical variables for optimizing prosthetic ankle-foot systems to reduce intact-limb medial knee loading across diverse ambulatory activities.

Finally, future work should explore activity-adaptive prosthetic ankle-foot systems. Because no single stiffness condition appeared optimal across all tasks, future devices may benefit from actively or semi-actively modulating mechanical characteristics such as effective stiffness, roll-over and forefoot lever-arm behavior, and late-stance positive power or energy return in response to changing task demands. Importantly, these biomechanical metrics can be achieved through multiple design approaches, including passive ankle-feet with different stiffness categories, standalone prosthetic ankle-feet, semi-active or powered ankle-foot prostheses. Such devices should be evaluated not only for forward propulsion and metabolic performance, but also for their effects on intact-limb medial knee loading, device-user mechanical interactions, neuromuscular adaptation, and long-term musculoskeletal health.

8.4 Impact

The primary contribution of this dissertation is to demonstrate that changes in intact-limb medial knee loading are not modulated by prosthetic mechanics alone, but by the interaction with the activities users perform in daily life. The translational impact of this dissertation spans two interconnected fields: 1) rehabilitation biomechanics and 2) mechanical engineering.

Within rehabilitation biomechanics, this dissertation demonstrates that **task demands strongly influence intact-limb medial knee loading.** Load carriage is a practical, modifiable factor influencing intact-limb medial knee loading. The finding that intact-side load carriage reduced KAM-related measures relative to prosthetic-side load carriage may represent a simple behavioral strategy to help reduce measures of medial knee loading associated with secondary joint loading risk. Additionally, this dissertation demonstrates a potential tradeoff in the use of powered ankle-foot systems. While improving prosthetic-side propulsion, they may also increase positive work and plantarflexor muscle activity at the intact ankle. Understanding this effect may help inform and provide **further guidance for prosthetic ankle-foot selection in clinical practice**.

Within mechanical engineering, particularly biomechanical engineering for prosthetic applications, this work contributes in several ways. It clarifies that **prosthetic ankle-foot type and stiffness have activity-dependent effects**, and that no single stiffness category appears optimal across all walking activities. This finding supports the need for **activity-specific prosthetic ankle-foot prescription and motivates future activity-adaptive prosthetic ankle-foot stiffness**.

This work also reframes how prosthetic ankle-foot performance may be evaluated. While prosthetic push-off (i.e., late-stance positive power and energy return) is often emphasized as a key performance metric, these studies suggest that **effective rocker shape, as well as forefoot lever-arm behavior**, particularly roll-over radius and dynamic mean ankle moment arm, **may be more strongly associated with reduced intact-limb medial knee loading**, particularly during demanding walking activities. This finding shifts attention toward mechanical design characteristics that govern how forces are transmitted through the user-device interaction and identifies potential new targets for prosthetic ankle-foot optimization. These mechanical metrics can be rendered by a spectrum of prosthetic ankle-foot systems, including passive, standalone, semi-active, and active/powered.

Additionally, this dissertation contributes to the **understanding of human-prosthesis interaction**. Specifically, it establishes quantitative relationships between controllable prosthetic ankle-foot mechanical characteristics, task demands, whole-body biomechanical responses, and medial knee loading. These findings provide a foundation for future human-in-the-loop optimization and design for prosthetic ankle-foot systems targeted at mitigating elevated intact-limb knee loading in individuals with TTA.

Finally, this dissertation contributes to a broader clinical goal: **reducing measures of medial knee loading associated with long-term joint health while improving mobility.** By linking prosthetic ankle-foot mechanics, task demands, and surrogate measures of intact-limb medial knee loading, this work provides additional evidence to inform prosthetic rehabilitation strategies and next-generation prosthetic ankle-foot development aimed at mitigating increases in medial knee loading in individuals with TTA while informing the engineering design of prosthetic ankle-foot systems that better adapt to the diverse mechanical demands of daily life.

APPENDICES

Chapter 2

The following is the supplementary material related to this article. Consistent with the kinetic results, the intact and prosthetic hip and knee kinematics during no load and loaded conditions suggest less variability in the sagittal plane than the frontal plane.

Note that due to the unclear central axis around the ankle/foot complex of the prosthetic foot, we did not include an estimate of the corresponding ankle angle in our analysis. Please refer to (Zelik and Honert, 2018) for how treating the entire foot as a rigid body (such as using standard marker placement and marker-based motion capture system) can lead to substantial misunderstandings of ankle and muscle-tendon dynamics (i.e., an overestimated ankle angle and/or moment).

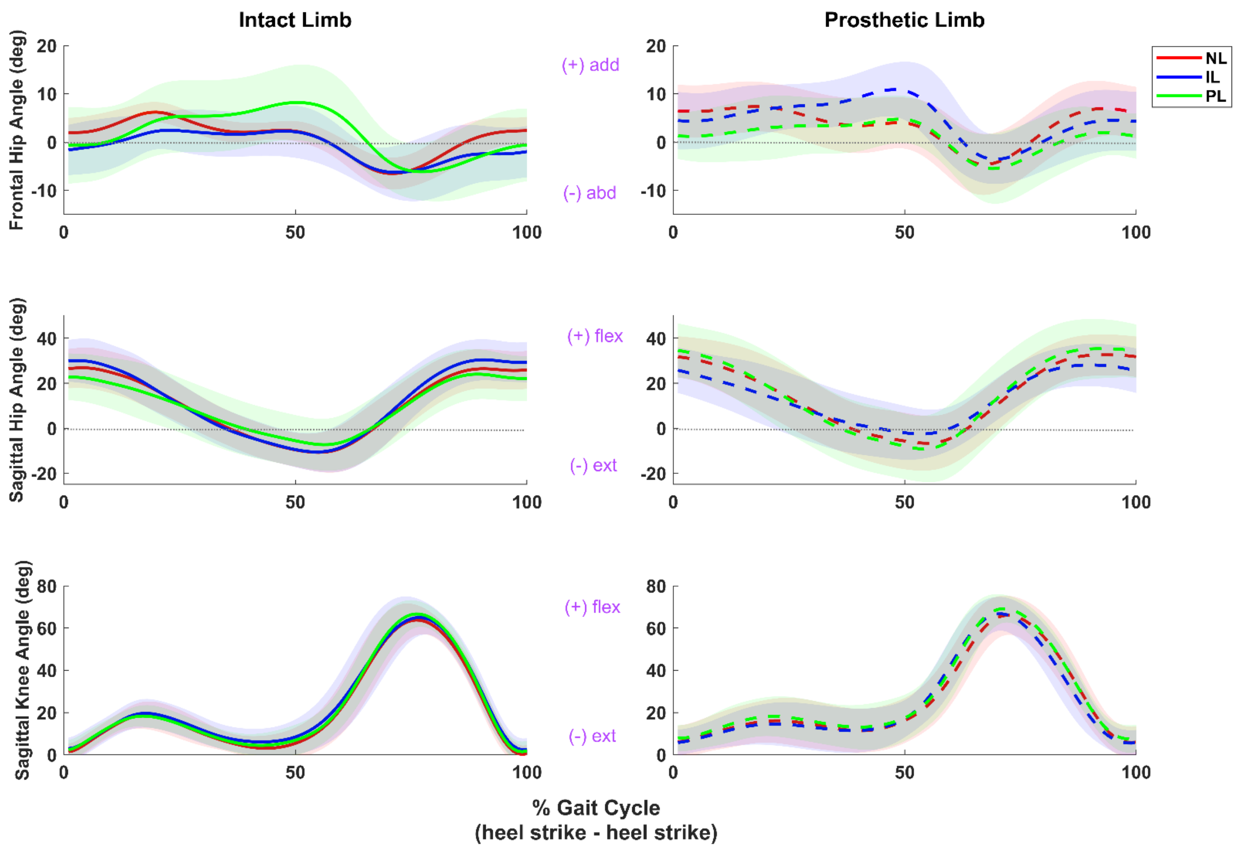

Fig A2.1 Mean frontal hip, sagittal hip, and sagittal knee kinematics for the intact (solid lines) and prosthetic (dashed lines) limbs in NL: no load condition, IL: intact-side load condition, PL: prosthetic-side load condition.

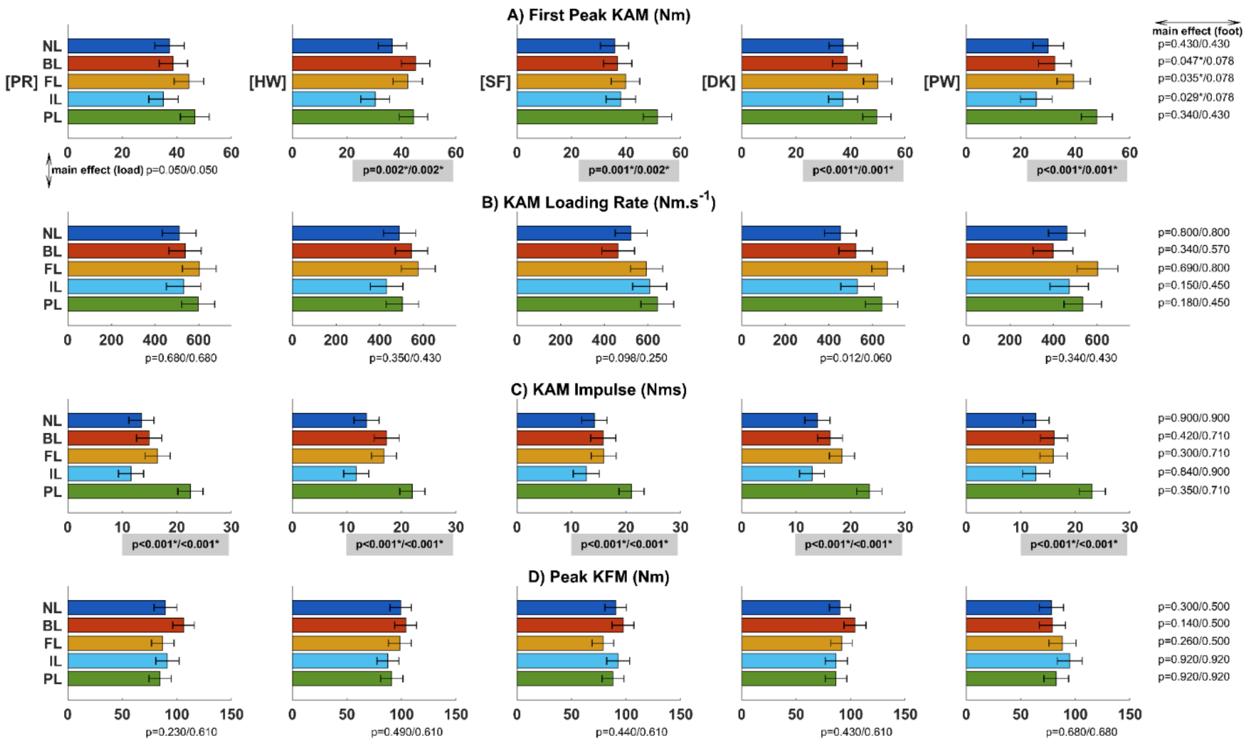

Fig A3.1 Mean (standard error) outcome metrics: intact first peak external knee adduction moment (KAM), KAM loading rate, KAM impulse and peak knee flexion moment (KFM) by load and foot from the fitted linear mixed-effect models. Bars and error bars represent means and standard errors, respectively. Vertical lines represent significant within-foot pairwise differences between loads. Values are NOT normalized to body mass. Statistical significance is annotated by **bold** P-value with an asterisk (*). ↨ P-values below plots = main effect of load, and ↔ P-values right of plots = main effect of foot. P-values: unadjusted/adjusted. Abbreviations: load conditions (NL: no load, BL: back load, FL: front load, IL: intact load, PL: prosthetic load) and prosthetic foot types (PR: prescribed, HW: heel wedge, SF: one category stiffer, SK: dual-keel, PW: powered). Refer to Fig.3.1 for details.

Table A3.1 Within-load pairwise comparisons between feet. Values are normalized to body mass for NL and body mass + 13.6 kg for loaded conditions. Statistical significance is annotated by **bold** P-value with an asterisk (*) (shaded for clarity). Abbreviations: load conditions (NL: no load, BL: back load, FL: front load, IL: intact load, PL: prosthetic load) and prosthetic foot types (PR: prescribed, HW: heel wedge, SF: one category stiffer, SK: dual-keel, PW: powered). Refer to Fig.3.1 for details.

Mean difference [95% confidence interval] | Pairwise *P*-value										
Prosthetic (+) Peak Ankle Power (W.kg^{-1})										
	NL		**BL**		**FL**		**IL**		**PL**	
PR vs **HW**	-0.04 [-0.38, 0.29]	0.997	-0.26 [-0.56, 0.04]	0.118	-0.10 [-0.40, 0.21]	0.910	0.01 [-0.30, 0.33]	1.000	-0.10 [-0.45, 0.24]	0.918
PR vs **SF**	**0.38 [0.04, 0.72]**	**0.020***	0.07 [-0.23, 0.36]	0.969	0.23 [-0.07, 0.53]	0.214	**0.32 [0.00, 0.64]**	**0.045***	0.25 [-0.08, 0.57]	0.229
PR vs **DK**	**0.46 [0.12, 0.80]**	**0.002***	0.06 [-0.25, 0.37]	0.982	**0.47 [0.17, 0.76]**	**0.000***	**0.37 [0.06, 0.69]**	**0.010***	**0.50 [0.18, 0.82]**	**0.000***
PR vs **PW**	-0.36 [-0.74, 0.02]	0.077	**-1.03 [-1.40, -0.65]**	**<.001***	**-0.52 [-0.85, -0.18]**	**0.000***	**-0.63 [-1.01, -0.25]**	**0.000***	**-0.71 [-1.07, -0.35]**	**<.001***
HW vs **SF**	**0.42 [0.10, 0.74]**	**0.003***	**0.33 [0.03, 0.62]**	**0.020***	**0.33 [0.02, 0.63]**	**0.030***	**0.31 [0.01, 0.61]**	**0.038***	**0.35 [0.02, 0.68]**	**0.032***
HW vs **DK**	**0.50 [0.19, 0.82]**	**0.000***	**0.32 [0.01, 0.63]**	**0.039***	**0.56 [0.26, 0.86]**	**<.001***	**0.36 [0.06, 0.65]**	**0.008***	**0.60 [0.27, 0.93]**	**<.001***
HW vs **PW**	-0.32 [-0.69, 0.05]	0.131	**-0.77 [-1.14, -0.39]**	**<.001***	**-0.42 [-0.76, -0.08]**	**0.007***	**-0.64 [-1.01, -0.27]**	**<.001***	**-0.61 [-0.97, -0.24]**	**0.000***
SF vs **DK**	0.08 [-0.24, 0.40]	0.960	-0.01 [-0.32, 0.30]	1.000	0.23 [-0.06, 0.53]	0.191	0.05 [-0.25, 0.35]	0.990	0.25 [-0.06, 0.56]	0.173
SF vs **PW**	**-0.74 [-1.11, -0.37]**	**<.001***	**-1.10 [-1.46, -0.73]**	**<.001***	**-0.75 [-1.08, -0.41]**	**<.001***	**-0.95 [-1.32, -0.58]**	**<.001***	**-0.96 [-1.31, -0.61]**	**<.001***
DK vs **PW**	**-0.82 [-1.19, -0.45]**	**<.001***	**-1.09 [-1.47, -0.71]**	**<.001***	**-0.98 [-1.31, -0.65]**	**<.001***	**-1.00 [-1.37, -0.63]**	**<.001***	**-1.21 [-1.55, -0.86]**	**<.001***
Prosthetic (+) Ankle Work (J.kg^{-1})										
PR vs **HW**	0.00 [-0.03, 0.02]	0.997	0.00 [-0.03, 0.02]	0.997	-0.01 [-0.03, 0.01]	0.856	0.01 [-0.02, 0.03]	0.960	0.00 [-0.03, 0.03]	1.000
PR vs **SF**	0.03 [0.00, 0.05]	0.060	0.01 [-0.01, 0.04]	0.521	0.01 [-0.01, 0.04]	0.528	0.02 [0.00, 0.04]	0.127	0.02 [-0.01, 0.04]	0.235
PR vs **DK**	**0.03 [0.00, 0.05]**	**0.028***	0.02 [0.00, 0.04]	0.157	**0.03 [0.00, 0.05]**	**0.009***	0.02 [0.00, 0.05]	0.093	**0.03 [0.01, 0.06]**	**0.001***
PR vs **PW**	**-0.06 [-0.09, -0.03]**	**<.001***	**-0.09 [-0.12, -0.06]**	**<.001***	**-0.07 [-0.10, -0.05]**	**<.001***	**-0.07 [-0.10, -0.04]**	**<.001***	**-0.08 [-0.11, -0.06]**	**<.001***
HW vs **SF**	**0.03 [0.00, 0.05]**	**0.013***	0.02 [-0.01, 0.04]	0.310	0.02 [0.00, 0.04]	0.094	0.01 [-0.01, 0.04]	0.375	0.02 [-0.01, 0.04]	0.269
HW vs **DK**	**0.03 [0.01, 0.05]**	**0.004***	0.02 [0.00, 0.05]	0.073	**0.04 [0.01, 0.06]**	**0.000***	0.02 [-0.01, 0.04]	0.309	**0.03 [0.01, 0.06]**	**0.002***
HW vs **PW**	**-0.06 [-0.08, -0.03]**	**<.001***	**-0.09 [-0.12, -0.06]**	**<.001***	**-0.06 [-0.09, -0.04]**	**<.001***	**-0.07 [-0.10, -0.05]**	**<.001***	**-0.08 [-0.11, -0.06]**	**<.001***
SF vs **DK**	0.00 [-0.02, 0.03]	0.999	0.01 [-0.02, 0.03]	0.932	0.01 [-0.01, 0.04]	0.436	0.00 [-0.02, 0.02]	1.000	0.02 [-0.01, 0.04]	0.392
SF vs **PW**	**-0.08 [-0.11, -0.06]**	**<.001***	**-0.11 [-0.13, -0.08]**	**<.001***	**-0.08 [-0.11, -0.06]**	**<.001***	**-0.09 [-0.12, -0.06]**	**<.001***	**-0.10 [-0.13, -0.07]**	**<.001***
DK vs **PW**	**-0.09 [-0.11, -0.06]**	**<.001***	**-0.11 [-0.14, -0.08]**	**<.001***	**-0.10 [-0.12, -0.07]**	**<.001***	**-0.09 [-0.12, -0.06]**	**<.001***	**-0.12 [-0.14, -0.09]**	**<.001***

Chapter 4

Table A4.1 Mean differences ± SE, (Pairwise 95% confidence intervals), and p-values for net positive and negative ankle work over the intact limb gait cycle (heel strike to heel strike) within each load condition. If present, pairwise significant differences are denoted in bold with asterisk (*). Abbreviations: clinically prescribed prosthetic foot (CP), same foot with a heel-stiffening wedge (HW), same foot but one category stiffer (SF), dual-keel foot (DK), powered ankle-foot (PW).

Ankle Work

Positive (J/kg)

	CP - HW	CP - SF	CP - DK	CP - PW	HW - SF	HW - DK	HW - PW	SF - DK	SF - PW	DK - PW
No Load	0.008 ± 0.011, [-0.021, 0.038], 0.945	-0.003 ± 0.011, [-0.033, 0.027], 0.999	0.002 ± 0.011, [-0.027, 0.032], 0.999	0.002 ± 0.013, [-0.033, 0.037], 1.000	-0.011 ± 0.011, [-0.040, 0.018], 0.830	-0.006 ± 0.010, [-0.034, 0.023], 0.983	-0.006 ± 0.013, [-0.041, 0.028], 0.988	0.006 ± 0.011, [-0.023, 0.034], 0.985	0.005 ± 0.013, [-0.030, 0.040], 0.995	-0.001 ± 0.013, [-0.035, 0.034], 1.000
Anterior Load	-0.005 ± 0.012, [-0.037, 0.028], 0.995	0.001 ± 0.011, [-0.029, 0.031], 1.000	-0.014 ± 0.011, [-0.044, 0.016], 0.708	-0.040 ± 0.014, [-0.079, -0.002], 0.035 *	0.006 ± 0.012, [-0.027, 0.038], 0.990	-0.010 ± 0.012, [-0.042, 0.023], 0.927	-0.036 ± 0.014, [-0.075, 0.004], 0.103	-0.015 ± 0.011, [-0.045, 0.015], 0.651	-0.041 ± 0.014, [-0.080, -0.003], 0.028 *	-0.026 ± 0.014, [-0.064, 0.012], 0.336
Posterior Load	-0.006 ± 0.011, [-0.037, 0.025], 0.986	0.008 ± 0.011, [-0.022, 0.037], 0.958	0.005 ± 0.011, [-0.025, 0.035], 0.991	0.004 ± 0.013, [-0.032, 0.041], 0.998	0.013 ± 0.011, [-0.017, 0.044], 0.753	0.011 ± 0.011, [-0.020, 0.042], 0.874	0.010 ± 0.014, [-0.027, 0.047], 0.948	-0.002 ± 0.011, [-0.032, 0.027], 0.999	-0.003 ± 0.013, [-0.040, 0.033], 0.999	-0.001 ± 0.013, [-0.037, 0.036], 1.000
Intact-side Load	-0.009 ± 0.011, [-0.041, 0.022], 0.927	-0.019 ± 0.011, [-0.050, 0.012], 0.428	-0.016 ± 0.011, [-0.047, 0.014], 0.588	-0.031 ± 0.015, [-0.072, 0.010], 0.228	-0.010 ± 0.011, [-0.041, 0.021], 0.901	-0.007 ± 0.011, [-0.037, 0.023], 0.971	-0.022 ± 0.015, [-0.063, 0.019], 0.588	0.003 ± 0.011, [-0.027, 0.033], 0.999	-0.012 ± 0.015, [-0.052, 0.029], 0.929	-0.015 ± 0.015, [-0.055, 0.025], 0.846
Prosthetic-side Load	-0.000 ± 0.012, [-0.032, 0.032], 1.000	0.006 ± 0.011, [-0.025, 0.037], 0.984	0.020 ± 0.011, [-0.010, 0.051], 0.369	-0.004 ± 0.013, [-0.039, 0.030], 0.997	0.006 ± 0.012, [-0.025, 0.038], 0.981	0.021 ± 0.011, [-0.011, 0.052], 0.369	-0.004 ± 0.013, [-0.039, 0.031], 0.998	0.014 ± 0.011, [-0.016, 0.044], 0.693	-0.010 ± 0.012, [-0.044, 0.024], 0.926	-0.024 ± 0.012, [-0.058, 0.010], 0.282

Negative (J/kg)

	CP - HW	CP - SF	CP - DK	CP - PW	HW - SF	HW - DK	HW - PW	SF - DK	SF - PW	DK - PW
No Load	-0.004 ± 0.010, [-0.030, 0.023], 0.996	-0.006 ± 0.010, [-0.033, 0.021], 0.971	-0.005 ± 0.010, [-0.032, 0.021], 0.982	-0.000 ± 0.012, [-0.032, 0.032], 1.000	-0.003 ± 0.010, [-0.029, 0.024], 0.999	-0.002 ± 0.009, [-0.028, 0.024], 1.000	0.003 ± 0.011, [-0.028, 0.035], 0.998	0.001 ± 0.010, [-0.026, 0.027], 1.000	0.006 ± 0.012, [-0.026, 0.038], 0.986	0.005 ± 0.011, [-0.026, 0.037], 0.991
Anterior Load	0.001 ± 0.011, [-0.029, 0.030], 1.000	-0.001 ± 0.010, [-0.029, 0.026], 1.000	0.013 ± 0.010, [-0.015, 0.041], 0.702	0.016 ± 0.013, [-0.019, 0.051], 0.725	-0.002 ± 0.011, [-0.031, 0.027], 1.000	0.012 ± 0.011, [-0.017, 0.042], 0.787	0.015 ± 0.013, [-0.021, 0.051], 0.783	0.014 ± 0.010, [-0.013, 0.042], 0.619	0.017 ± 0.013, [-0.018, 0.052], 0.658	0.003 ± 0.013, [-0.032, 0.038], 0.999
Posterior Load	-0.001 ± 0.010, [-0.029, 0.028], 1.000	-0.009 ± 0.010, [-0.036, 0.019], 0.905	-0.001 ± 0.010, [-0.029, 0.026], 1.000	0.014 ± 0.012, [-0.020, 0.047], 0.783	-0.008 ± 0.010, [-0.036, 0.020], 0.929	-0.001 ± 0.010, [-0.029, 0.027], 1.000	0.015 ± 0.012, [-0.019, 0.049], 0.766	0.007 ± 0.010, [-0.020, 0.035], 0.949	0.023 ± 0.012, [-0.011, 0.056], 0.334	0.015 ± 0.012, [-0.018, 0.049], 0.712
Intact-side Load	0.016 ± 0.010, [-0.013, 0.045], 0.546	0.013 ± 0.010, [-0.015, 0.041], 0.706	0.018 ± 0.010, [-0.010, 0.046], 0.399	0.020 ± 0.014, [-0.017, 0.058], 0.559	-0.003 ± 0.010, [-0.031, 0.025], 0.999	0.002 ± 0.010, [-0.026, 0.030], 1.000	0.005 ± 0.014, [-0.033, 0.042], 0.997	0.005 ± 0.010, [-0.023, 0.032], 0.990	0.007 ± 0.013, [-0.030, 0.044], 0.982	0.003 ± 0.013, [-0.034, 0.039], 1.000
Prosthetic-side Load	-0.000 ± 0.011, [-0.029, 0.029], 1.000	-0.008 ± 0.010, [-0.036, 0.020], 0.931	-0.000 ± 0.010, [-0.028, 0.027], 1.000	0.009 ± 0.011, [-0.022, 0.041], 0.927	-0.008 ± 0.010, [-0.037, 0.021], 0.939	-0.000 ± 0.010, [-0.029, 0.028], 1.000	0.009 ± 0.012, [-0.023, 0.041], 0.928	0.008 ± 0.010, [-0.019, 0.035], 0.935	0.018 ± 0.011, [-0.014, 0.049], 0.539	0.010 ± 0.011, [-0.021, 0.041], 0.910

Table A4.2 Mean differences ± SE, (Pairwise 95% confidence intervals), and p-values for net positive and negative knee work over the intact limb gait cycle (heel strike to heel strike) within each load condition. If present, pairwise significant differences are denoted in bold with asterisk (*). Abbreviations: clinically prescribed prosthetic foot (CP), same foot with a heel-stiffening wedge (HW), same foot but one category stiffer (SF), dual-keel foot (DK), powered ankle-foot (PW).

Knee Work

Positive (J/kg)

	CP - HW	CP - SF	CP - DK	CP - PW	HW - SF	HW - DK	HW - PW	SF - DK	SF - PW	DK - PW
No Load	0.002 ± 0.010, [-0.025, 0.029], 1.000	0.005 ± 0.010, [-0.022, 0.032], 0.988	0.002 ± 0.010, [-0.025, 0.029], 1.000	0.019 ± 0.012, [-0.013, 0.051], 0.459	0.003 ± 0.010, [-0.023, 0.029], 0.998	0.000 ± 0.009, [-0.026, 0.026], 1.000	0.017 ± 0.011, [-0.014, 0.049], 0.547	-0.003 ± 0.010, [-0.029, 0.023], 0.998	0.014 ± 0.011, [-0.017, 0.046], 0.718	0.017 ± 0.011, [-0.014, 0.049], 0.555
Anterior Load	-0.004 ± 0.011, [-0.033, 0.026], 0.997	-0.000 ± 0.010, [-0.028, 0.027], 1.000	-0.016 ± 0.010, [-0.043, 0.012], 0.506	-0.001 ± 0.013, [-0.036, 0.034], 1.000	0.003 ± 0.011, [-0.026, 0.032], 0.998	-0.012 ± 0.011, [-0.042, 0.017], 0.770	0.002 ± 0.013, [-0.034, 0.038], 1.000	-0.016 ± 0.010, [-0.043, 0.012], 0.529	-0.001 ± 0.013, [-0.036, 0.034], 1.000	0.015 ± 0.013, [-0.020, 0.049], 0.774
Posterior Load	-0.021 ± 0.010, [-0.049, 0.007], 0.252	0.001 ± 0.010, [-0.026, 0.028], 1.000	-0.012 ± 0.010, [-0.040, 0.015], 0.744	0.029 ± 0.012, [-0.005, 0.062], 0.129	0.022 ± 0.010, [-0.005, 0.050], 0.183	0.009 ± 0.010, [-0.019, 0.037], 0.919	0.049 ± 0.012, [0.016, 0.083], 7.2e-04 *	-0.014 ± 0.010, [-0.041, 0.014], 0.650	0.027 ± 0.012, [-0.006, 0.060], 0.157	0.041 ± 0.012, [0.008, 0.074], 0.007 *
Intact-side Load	-0.012 ± 0.010, [-0.040, 0.016], 0.775	-0.011 ± 0.010, [-0.039, 0.017], 0.813	-0.005 ± 0.010, [-0.033, 0.023], 0.988	0.001 ± 0.014, [-0.037, 0.038], 1.000	0.001 ± 0.010, [-0.027, 0.029], 1.000	0.007 ± 0.010, [-0.021, 0.035], 0.956	0.013 ± 0.014, [-0.025, 0.050], 0.885	0.006 ± 0.010, [-0.021, 0.033], 0.971	0.012 ± 0.013, [-0.025, 0.048], 0.906	0.006 ± 0.013, [-0.031, 0.042], 0.993
Prosthetic-side Load	-0.005 ± 0.011, [-0.034, 0.024], 0.992	-0.002 ± 0.010, [-0.030, 0.026], 0.999	0.009 ± 0.010, [-0.019, 0.036], 0.911	0.003 ± 0.011, [-0.028, 0.034], 0.999	0.002 ± 0.010, [-0.026, 0.031], 0.999	0.013 ± 0.010, [-0.015, 0.042], 0.692	0.008 ± 0.012, [-0.024, 0.040], 0.961	0.011 ± 0.010, [-0.016, 0.038], 0.803	0.005 ± 0.011, [-0.026, 0.037], 0.989	-0.006 ± 0.011, [-0.036, 0.025], 0.988

Negative (J/kg)

	CP - HW	CP - SF	CP - DK	CP - PW	HW - SF	HW - DK	HW - PW	SF - DK	SF - PW	DK - PW
No Load	0.006 ± 0.016, [-0.038, 0.049], 0.997	0.003 ± 0.016, [-0.041, 0.048], 1.000	0.010 ± 0.016, [-0.034, 0.053], 0.976	0.008 ± 0.019, [-0.045, 0.060], 0.994	-0.002 ± 0.016, [-0.045, 0.041], 1.000	0.004 ± 0.015, [-0.039, 0.046], 0.999	0.002 ± 0.019, [-0.049, 0.053], 1.000	0.006 ± 0.016, [-0.037, 0.049], 0.995	0.004 ± 0.019, [-0.047, 0.056], 0.999	-0.002 ± 0.019, [-0.053, 0.050], 1.000
Anterior Load	-0.004 ± 0.017, [-0.052, 0.044], 0.999	-0.002 ± 0.017, [-0.047, 0.044], 1.000	0.016 ± 0.016, [-0.029, 0.061], 0.865	0.010 ± 0.021, [-0.047, 0.067], 0.990	0.002 ± 0.017, [-0.046, 0.050], 1.000	0.020 ± 0.017, [-0.028, 0.068], 0.786	0.014 ± 0.022, [-0.045, 0.073], 0.969	0.018 ± 0.016, [-0.028, 0.063], 0.821	0.011 ± 0.021, [-0.046, 0.069], 0.982	-0.006 ± 0.021, [-0.063, 0.051], 0.998
Posterior Load	0.004 ± 0.017, [-0.042, 0.050], 0.999	-0.010 ± 0.016, [-0.055, 0.034], 0.971	0.017 ± 0.016, [-0.028, 0.063], 0.826	0.002 ± 0.020, [-0.052, 0.057], 1.000	-0.014 ± 0.016, [-0.059, 0.031], 0.915	0.014 ± 0.017, [-0.032, 0.060], 0.927	-0.002 ± 0.020, [-0.057, 0.054], 1.000	0.028 ± 0.016, [-0.017, 0.072], 0.436	0.012 ± 0.020, [-0.042, 0.067], 0.971	-0.015 ± 0.020, [-0.070, 0.039], 0.940
Intact-side Load	0.004 ± 0.017, [-0.043, 0.051], 0.999	0.037 ± 0.017, [-0.009, 0.083], 0.175	0.034 ± 0.017, [-0.012, 0.079], 0.250	0.032 ± 0.022, [-0.029, 0.093], 0.600	0.033 ± 0.017, [-0.013, 0.079], 0.276	0.030 ± 0.017, [-0.016, 0.075], 0.375	0.028 ± 0.022, [-0.033, 0.089], 0.714	-0.003 ± 0.016, [-0.048, 0.041], 1.000	-0.005 ± 0.022, [-0.065, 0.055], 0.999	-0.002 ± 0.022, [-0.061, 0.058], 1.000
Prosthetic-side Load	0.009 ± 0.017, [-0.038, 0.057], 0.982	0.003 ± 0.017, [-0.043, 0.049], 1.000	0.003 ± 0.017, [-0.042, 0.049], 1.000	0.011 ± 0.019, [-0.040, 0.062], 0.978	-0.006 ± 0.017, [-0.053, 0.041], 0.996	-0.006 ± 0.017, [-0.052, 0.040], 0.996	0.001 ± 0.019, [-0.051, 0.054], 1.000	0.000 ± 0.016, [-0.044, 0.045], 1.000	0.008 ± 0.019, [-0.043, 0.059], 0.994	0.008 ± 0.018, [-0.043, 0.058], 0.994

Table A4.3 Mean differences ± SE, (Pairwise 95% confidence intervals), and *p*-values for net positive and negative hip work over the intact limb gait cycle (heel strike to heel strike) within each load condition. If present, pairwise significant differences are denoted in bold with asterisk (*). Abbreviations: clinically prescribed prosthetic foot (CP), same foot with a heel-stiffening wedge (HW), same foot but one category stiffer (SF), dual-keel foot (DK), powered ankle-foot (PW).

Hip Work

Positive (J/kg)

	CP - HW	CP - SF	CP - DK	CP - PW	HW - SF	HW - DK	HW - PW	SF - DK	SF - PW	DK - PW
No Load	-0.011 ± 0.015, [-0.050, 0.029], 0.951	-0.007 ± 0.015, [-0.048, 0.033], 0.988	-0.011 ± 0.014, [-0.051, 0.029], 0.944	0.002 ± 0.017, [-0.045, 0.050], 1.000	0.003 ± 0.014, [-0.036, 0.042], 0.999	-0.000 ± 0.014, [-0.039, 0.038], 1.000	0.013 ± 0.017, [-0.034, 0.059], 0.942	-0.004 ± 0.014, [-0.043, 0.035], 0.999	0.010 ± 0.017, [-0.037, 0.057], 0.981	0.013 ± 0.017, [-0.033, 0.060], 0.937
Anterior Load	0.000 ± 0.016, [-0.043, 0.044], 1.000	0.003 ± 0.015, [-0.039, 0.044], 1.000	-0.005 ± 0.015, [-0.046, 0.036], 0.996	0.029 ± 0.019, [-0.022, 0.081], 0.523	0.002 ± 0.016, [-0.041, 0.046], 1.000	-0.006 ± 0.016, [-0.049, 0.038], 0.997	0.029 ± 0.020, [-0.024, 0.083], 0.565	-0.008 ± 0.015, [-0.049, 0.033], 0.984	0.027 ± 0.019, [-0.025, 0.079], 0.609	0.035 ± 0.019, [-0.017, 0.087], 0.347
Posterior Load	-0.014 ± 0.015, [-0.056, 0.028], 0.885	-0.002 ± 0.015, [-0.043, 0.038], 1.000	-0.010 ± 0.015, [-0.051, 0.031], 0.968	0.007 ± 0.018, [-0.043, 0.056], 0.996	0.012 ± 0.015, [-0.029, 0.053], 0.933	0.004 ± 0.015, [-0.037, 0.046], 0.998	0.021 ± 0.018, [-0.030, 0.071], 0.791	-0.007 ± 0.015, [-0.048, 0.033], 0.987	0.009 ± 0.018, [-0.040, 0.058], 0.988	0.016 ± 0.018, [-0.033, 0.066], 0.897
Intact-side Load	-0.011 ± 0.015, [-0.053, 0.031], 0.955	-0.022 ± 0.015, [-0.064, 0.020], 0.599	-0.033 ± 0.015, [-0.074, 0.008], 0.181	-0.024 ± 0.020, [-0.079, 0.031], 0.751	-0.011 ± 0.015, [-0.053, 0.031], 0.950	-0.022 ± 0.015, [-0.063, 0.019], 0.580	-0.013 ± 0.020, [-0.069, 0.042], 0.965	-0.011 ± 0.015, [-0.051, 0.029], 0.944	-0.002 ± 0.020, [-0.057, 0.052], 1.000	0.009 ± 0.020, [-0.045, 0.063], 0.992
Prosthetic-side Load	-0.001 ± 0.016, [-0.045, 0.042], 1.000	-0.001 ± 0.015, [-0.043, 0.041], 1.000	-0.008 ± 0.015, [-0.049, 0.033], 0.985	-0.000 ± 0.017, [-0.047, 0.046], 1.000	0.000 ± 0.016, [-0.042, 0.043], 1.000	-0.006 ± 0.015, [-0.048, 0.036], 0.993	0.001 ± 0.017, [-0.046, 0.048], 1.000	-0.007 ± 0.015, [-0.047, 0.034], 0.990	0.001 ± 0.017, [-0.046, 0.047], 1.000	0.008 ± 0.017, [-0.038, 0.053], 0.991

Negative (J/kg)

	CP - HW	CP - SF	CP - DK	CP - PW	HW - SF	HW - DK	HW - PW	SF - DK	SF - PW	DK - PW
No Load	0.001 ± 0.017, [-0.047, 0.048], 1.000	0.000 ± 0.018, [-0.048, 0.049], 1.000	-0.006 ± 0.017, [-0.053, 0.042], 0.997	0.023 ± 0.021, [-0.033, 0.080], 0.788	-0.000 ± 0.017, [-0.047, 0.047], 1.000	-0.006 ± 0.017, [-0.052, 0.040], 0.995	0.023 ± 0.020, [-0.033, 0.078], 0.792	-0.006 ± 0.017, [-0.053, 0.040], 0.996	0.023 ± 0.020, [-0.033, 0.079], 0.793	0.029 ± 0.020, [-0.026, 0.085], 0.601
Anterior Load	-0.009 ± 0.019, [-0.061, 0.043], 0.989	0.013 ± 0.018, [-0.036, 0.062], 0.948	-0.010 ± 0.018, [-0.059, 0.039], 0.980	0.002 ± 0.023, [-0.060, 0.064], 1.000	0.022 ± 0.019, [-0.030, 0.074], 0.767	-0.001 ± 0.019, [-0.053, 0.051], 1.000	0.011 ± 0.023, [-0.053, 0.075], 0.990	-0.023 ± 0.018, [-0.072, 0.026], 0.691	-0.011 ± 0.022, [-0.073, 0.051], 0.988	0.012 ± 0.022, [-0.050, 0.074], 0.984
Posterior Load	0.009 ± 0.018, [-0.041, 0.059], 0.988	0.011 ± 0.018, [-0.037, 0.059], 0.967	0.004 ± 0.018, [-0.045, 0.053], 0.999	0.005 ± 0.022, [-0.055, 0.064], 1.000	0.002 ± 0.018, [-0.047, 0.051], 1.000	-0.005 ± 0.018, [-0.055, 0.045], 0.999	-0.004 ± 0.022, [-0.064, 0.056], 1.000	-0.007 ± 0.018, [-0.055, 0.041], 0.994	-0.007 ± 0.021, [-0.065, 0.052], 0.998	0.000 ± 0.021, [-0.059, 0.059], 1.000
Intact-side Load	-0.005 ± 0.018, [-0.056, 0.045], 0.999	-0.005 ± 0.018, [-0.054, 0.045], 0.999	-0.004 ± 0.018, [-0.053, 0.045], 0.999	0.019 ± 0.024, [-0.047, 0.085], 0.937	0.001 ± 0.018, [-0.049, 0.050], 1.000	0.001 ± 0.018, [-0.048, 0.050], 1.000	0.024 ± 0.024, [-0.042, 0.090], 0.861	0.001 ± 0.018, [-0.048, 0.049], 1.000	0.023 ± 0.024, [-0.042, 0.088], 0.867	0.023 ± 0.024, [-0.042, 0.087], 0.872
Prosthetic-side Load	0.009 ± 0.019, [-0.042, 0.061], 0.988	0.024 ± 0.018, [-0.026, 0.074], 0.690	0.023 ± 0.018, [-0.026, 0.072], 0.714	0.007 ± 0.020, [-0.049, 0.062], 0.998	0.014 ± 0.019, [-0.036, 0.065], 0.936	0.013 ± 0.018, [-0.037, 0.063], 0.949	-0.003 ± 0.021, [-0.059, 0.054], 1.000	-0.001 ± 0.018, [-0.049, 0.047], 1.000	-0.017 ± 0.020, [-0.072, 0.038], 0.914	-0.016 ± 0.020, [-0.071, 0.038], 0.928

Table A4.4 Mean differences ± SE, (Pairwise 95% confidence intervals), and p-values for net positive and negative knee work over the prosthetic limb gait cycle (heel strike to heel strike) within each load condition. If present, pairwise significant differences are denoted in bold with asterisk (*). Abbreviations: clinically prescribed prosthetic foot (CP), same foot with a heel-stiffening wedge (HW), same foot but one category stiffer (SF), dual-keel foot (DK), powered ankle-foot (PW).

Knee Work

Positive (J/kg)

	CP - HW	CP - SF	CP - DK	CP - PW	HW - SF	HW - DK	HW - PW	SF - DK	SF - PW	DK - PW
No Load	0.000 ± 0.005, (-0.014, 0.014), 1	-0.001 ± 0.005, (-0.017, 0.014), 1	0.002 ± 0.005, (-0.012, 0.017), 0.98	0.002 ± 0.008, (-0.025, 0.028), 1	-0.002 ± 0.005, (-0.016, 0.013), 1	0.002 ± 0.004, (-0.012, 0.016), 0.98	0.002 ± 0.008, (-0.025, 0.028), 1	0.004 ± 0.005, (-0.011, 0.019), 0.92	0.003 ± 0.008, (-0.023, 0.03), 1	-0.001 ± 0.008, (-0.027, 0.025), 1
Anterior Load	0.001 ± 0.004, (-0.012, 0.014), 1	-0.004 ± 0.004, (-0.017, 0.009), 0.89	-0.002 ± 0.004, (-0.014, 0.011), 0.99	0.006 ± 0.007, (-0.016, 0.028), 0.91	-0.005 ± 0.004, (-0.019, 0.009), 0.77	-0.003 ± 0.004, (-0.015, 0.01), 0.95	0.005 ± 0.007, (-0.017, 0.027), 0.96	0.002 ± 0.004, (-0.011, 0.015), 0.98	0.01 ± 0.007, (-0.013, 0.032), 0.66	0.007 ± 0.007, (-0.014, 0.029), 0.82
Posterior Load	-0.008 ± 0.005, (-0.023, 0.006), 0.4	-0.012 ± 0.005, (-0.028, 0.003), 0.15	-0.011 ± 0.005, (-0.026, 0.004), 0.19	0.001 ± 0.009, (-0.025, 0.028), 1	-0.004 ± 0.005, (-0.02, 0.012), 0.92	-0.003 ± 0.005, (-0.018, 0.012), 0.97	0.010 ± 0.009, (-0.017, 0.037), 0.79	0.001 ± 0.005, (-0.015, 0.017), 1	0.014 ± 0.009, (-0.014, 0.042), 0.54	0.013 ± 0.009, (-0.015, 0.04), 0.62
Intact-side Load	-0.006 ± 0.004, (-0.018, 0.006), 0.6	-0.010 ± 0.005, (-0.024, 0.004), 0.22	-0.005 ± 0.004, (-0.017, 0.007), 0.68	-0.002 ± 0.007, (-0.024, 0.021), 1	-0.005 ± 0.005, (-0.019, 0.01), 0.86	0.001 ± 0.004, (-0.012, 0.013), 1	0.004 ± 0.007, (-0.019, 0.027), 0.98	0.005 ± 0.005, (-0.009, 0.02), 0.78	0.009 ± 0.008, (-0.015, 0.032), 0.79	0.003 ± 0.007, (-0.019, 0.026), 0.99
Prosthetic-side Load	0.001 ± 0.004, (-0.011, 0.014), 1	-0.005 ± 0.005, (-0.019, 0.009), 0.79	-0.001 ± 0.004, (-0.013, 0.012), 1	0.001 ± 0.008, (-0.023, 0.026), 1	-0.007 ± 0.004, (-0.021, 0.008), 0.6	-0.002 ± 0.004, (-0.015, 0.011), 0.98	0.000 ± 0.008, (-0.025, 0.024), 1	0.004 ± 0.005, (-0.01, 0.019), 0.85	0.006 ± 0.008, (-0.019, 0.031), 0.93	0.002 ± 0.008, (-0.023, 0.026), 1

Negative (J/kg)

	CP - HW	CP - SF	CP - DK	CP - PW	HW - SF	HW - DK	HW - PW	SF - DK	SF - PW	DK - PW
No Load	-0.014 ± 0.014, (-0.053, 0.025), 0.86	-0.020 ± 0.014, (-0.059, 0.02), 0.65	-0.029 ± 0.014, (-0.069, 0.011), 0.26	-0.028 ± 0.017, (-0.074, 0.018), 0.44	-0.005 ± 0.014, (-0.043, 0.033), 1	-0.015 ± 0.014, (-0.053, 0.024), 0.83	-0.014 ± 0.016, (-0.059, 0.031), 0.91	-0.01 ± 0.014, (-0.048, 0.029), 0.96	-0.009 ± 0.016, (-0.054, 0.036), 0.98	0.001 ± 0.017, (-0.045, 0.046), 1
Anterior Load	0.008 ± 0.014, (-0.032, 0.047), 0.98	-0.01 ± 0.014, (-0.048, 0.028), 0.95	-0.01 ± 0.014, (-0.048, 0.028), 0.96	-0.013 ± 0.017, (-0.059, 0.032), 0.93	-0.018 ± 0.014, (-0.057, 0.021), 0.71	-0.017 ± 0.014, (-0.056, 0.022), 0.74	-0.021 ± 0.017, (-0.067, 0.025), 0.73	0.001 ± 0.013, (-0.036, 0.037), 1	-0.003 ± 0.016, (-0.047, 0.041), 1	-0.004 ± 0.016, (-0.048, 0.041), 1
Posterior Load	0.018 ± 0.014, (-0.021, 0.056), 0.72	-0.015 ± 0.014, (-0.053, 0.023), 0.81	-0.002 ± 0.014, (-0.041, 0.037), 1	-0.019 ± 0.018, (-0.068, 0.03), 0.83	-0.033 ± 0.014, (-0.07, 0.005), 0.11	-0.019 ± 0.014, (-0.058, 0.019), 0.64	-0.036 ± 0.018, (-0.085, 0.012), 0.25	0.013 ± 0.014, (-0.024, 0.051), 0.87	-0.004 ± 0.018, (-0.052, 0.045), 1	-0.017 ± 0.018, (-0.067, 0.032), 0.87
Intact-side Load	-0.017 ± 0.014, (-0.055, 0.021), 0.74	-0.009 ± 0.014, (-0.049, 0.03), 0.97	-0.012 ± 0.014, (-0.049, 0.026), 0.92	-0.016 ± 0.016, (-0.059, 0.027), 0.85	0.007 ± 0.015, (-0.033, 0.048), 0.99	0.005 ± 0.014, (-0.033, 0.044), 1	0.001 ± 0.016, (-0.043, 0.045), 1	-0.002 ± 0.015, (-0.042, 0.038), 1	-0.007 ± 0.017, (-0.052, 0.039), 0.99	-0.005 ± 0.016, (-0.048, 0.039), 1
Prosthetic-side Load	-0.004 ± 0.014, (-0.043, 0.035), 1	-0.012 ± 0.014, (-0.051, 0.028), 0.93	-0.019 ± 0.014, (-0.058, 0.02), 0.66	-0.045 ± 0.018, (-0.094, 0.005), 0.10	-0.008 ± 0.014, (-0.047, 0.032), 0.98	-0.015 ± 0.014, (-0.054, 0.024), 0.82	-0.041 ± 0.018, (-0.09, 0.009), 0.16	-0.008 ± 0.014, (-0.047, 0.032), 0.98	-0.033 ± 0.018, (-0.082, 0.016), 0.36	-0.025 ± 0.018, (-0.075, 0.024), 0.63

Table A4.5 Mean differences ± SE, (Pairwise 95% confidence intervals), and p-values for net positive and negative hip work over the prosthetic limb gait cycle (heel strike to heel strike) within each load condition. If present, pairwise significant differences are denoted in bold with asterisk (*). Abbreviations: clinically prescribed prosthetic foot (CP), same foot with a heel-stiffening wedge (HW), same foot but one category stiffer (SF), dual-keel foot (DK), powered ankle-foot (PW).

Hip Work

Positive (J/kg)

	CP - HW	CP - SF	CP - DK	CP - PW	HW - SF	HW - DK	HW - PW	SF - DK	SF - PW	DK - PW
No Load	0.009 ± 0.019, (-0.042, 0.06), 0.99	0.002 ± 0.019, (-0.049, 0.053), 1	0.019 ± 0.019, (-0.032, 0.071), 0.84	0.034 ± 0.022, (-0.026, 0.094), 0.53	-0.007 ± 0.018, (-0.056, 0.042), 0.99	0.011 ± 0.018, (-0.039, 0.061), 0.98	0.025 ± 0.021, (-0.033, 0.083), 0.76	0.018 ± 0.018, (-0.032, 0.068), 0.87	0.032 ± 0.021, (-0.026, 0.09), 0.55	0.014 ± 0.022, (-0.045, 0.073), 0.96
Anterior Load	-0.001 ± 0.019, (-0.053, 0.051), 1	0.009 ± 0.018, (-0.04, 0.059), 0.98	0.002 ± 0.018, (-0.047, 0.051), 1	0.037 ± 0.022, (-0.022, 0.096), 0.42	0.010 ± 0.018, (-0.04, 0.061), 0.98	0.003 ± 0.018, (-0.047, 0.053), 1	0.038 ± 0.022, (-0.022, 0.098), 0.41	-0.007 ± 0.017, (-0.055, 0.04), 0.99	0.028 ± 0.021, (-0.03, 0.086), 0.68	0.035 ± 0.021, (-0.022, 0.093), 0.45
Posterior Load	-0.006 ± 0.018, (-0.056, 0.044), 1	0.007 ± 0.018, (-0.043, 0.056), 1	-0.011 ± 0.018, (-0.062, 0.04), 0.97	0.035 ± 0.023, (-0.029, 0.099), 0.56	0.012 ± 0.018, (-0.036, 0.061), 0.96	-0.006 ± 0.018, (-0.056, 0.044), 1	0.041 ± 0.023, (-0.023, 0.104), 0.4	-0.018 ± 0.018, (-0.067, 0.031), 0.86	0.028 ± 0.023, (-0.035, 0.091), 0.73	0.046 ± 0.023, (-0.018, 0.11), 0.28
Intact-side Load	-0.016 ± 0.018, (-0.065, 0.033), 0.9	0.019 ± 0.019, (-0.033, 0.07), 0.86	-0.011 ± 0.018, (-0.06, 0.037), 0.97	0.023 ± 0.02, (-0.033, 0.079), 0.78	0.035 ± 0.019, (-0.018, 0.087), 0.38	0.005 ± 0.018, (-0.045, 0.055), 1	0.039 ± 0.021, (-0.018, 0.097), 0.33	-0.030 ± 0.019, (-0.082, 0.022), 0.52	0.005 ± 0.022, (-0.054, 0.064), 1	0.034 ± 0.021, (-0.022, 0.091), 0.45
Prosthetic-side Load	-0.01 ± 0.019, (-0.061, 0.04), 0.98	-0.004 ± 0.019, (-0.055, 0.047), 1	-0.01 ± 0.019, (-0.061, 0.041), 0.98	0.026 ± 0.023, (-0.039, 0.09), 0.81	0.006 ± 0.019, (-0.045, 0.057), 1	0.000 ± 0.019, (-0.05, 0.051), 1	0.036 ± 0.023, (-0.028, 0.1), 0.54	-0.006 ± 0.019, (-0.057, 0.045), 1	0.030 ± 0.023, (-0.034, 0.094), 0.7	0.036 ± 0.023, (-0.029, 0.1), 0.55

Negative (J/kg)

	CP - HW	CP - SF	CP - DK	CP - PW	HW - SF	HW - DK	HW - PW	SF - DK	SF - PW	DK - PW
No Load	-0.004 ± 0.012, (-0.036, 0.028), 1	0.001 ± 0.012, (-0.031, 0.033), 1	-0.001 ± 0.012, (-0.033, 0.032), 1	0.002 ± 0.014, (-0.036, 0.04), 1	0.004 ± 0.011, (-0.026, 0.035), 0.99	0.003 ± 0.011, (-0.028, 0.035), 1	0.006 ± 0.013, (-0.031, 0.043), 0.99	-0.001 ± 0.011, (-0.033, 0.03), 1	0.002 ± 0.013, (-0.035, 0.038), 1	0.003 ± 0.014, (-0.034, 0.04), 1
Anterior Load	0.003 ± 0.012, (-0.03, 0.035), 1	0.003 ± 0.011, (-0.028, 0.034), 1	0.007 ± 0.011, (-0.025, 0.038), 0.98	0.002 ± 0.014, (-0.035, 0.039), 1	0.000 ± 0.012, (-0.031, 0.032), 1	0.004 ± 0.012, (-0.028, 0.036), 1	-0.001 ± 0.014, (-0.039, 0.037), 1	0.003 ± 0.011, (-0.027, 0.033), 1	-0.001 ± 0.013, (-0.038, 0.035), 1	-0.005 ± 0.013, (-0.041, 0.032), 1
Posterior Load	-0.003 ± 0.011, (-0.034, 0.029), 1	-0.008 ± 0.011, (-0.039, 0.023), 0.95	0.008 ± 0.012, (-0.024, 0.04), 0.97	0.022 ± 0.015, (-0.018, 0.062), 0.57	-0.005 ± 0.011, (-0.036, 0.025), 0.99	0.010 ± 0.011, (-0.021, 0.042), 0.9	0.025 ± 0.015, (-0.015, 0.065), 0.44	0.016 ± 0.011, (-0.015, 0.047), 0.64	0.030 ± 0.014, (-0.01, 0.07), 0.23	0.014 ± 0.015, (-0.026, 0.055), 0.86
Intact-side Load	-0.013 ± 0.011, (-0.044, 0.018), 0.77	0.000 ± 0.012, (-0.032, 0.032), 1	0.011 ± 0.011, (-0.019, 0.042), 0.86	0.021 ± 0.013, (-0.015, 0.056), 0.5	0.013 ± 0.012, (-0.02, 0.047), 0.81	0.024 ± 0.011, (-0.007, 0.056), 0.21	0.034 ± 0.013, (-0.002, 0.07), 0.079	0.011 ± 0.012, (-0.022, 0.044), 0.88	0.021 ± 0.014, (-0.017, 0.058), 0.55	0.009 ± 0.013, (-0.026, 0.045), 0.95
Prosthetic-side Load	0.006 ± 0.012, (-0.026, 0.038), 0.98	-0.003 ± 0.012, (-0.035, 0.029), 1	-0.002 ± 0.012, (-0.034, 0.03), 1	0.008 ± 0.015, (-0.033, 0.048), 0.99	-0.010 ± 0.012, (-0.042, 0.022), 0.92	-0.008 ± 0.012, (-0.04, 0.024), 0.95	0.001 ± 0.015, (-0.039, 0.042), 1	0.001 ± 0.012, (-0.031, 0.033), 1	0.011 ± 0.015, (-0.029, 0.051), 0.95	0.01 ± 0.015, (-0.031, 0.05), 0.97

Across feet in the NL condition, the first module (GMED, GMAX, RF, VASM) primarily support body weight and stabilize the limb during early stance; the second module (MGAS, PERL) generate propulsion in late stance; the third module (RF, TA) facilitate leg swing initiation and trunk energy transfer; and the fourth module (BFLH) contribute to late-swing deceleration and early-stance energy absorption. The involvement of muscles such as GMAX, associated with early-stance body support, and BFLH, known to contribute energy during early stance and swing, is consistent with their established biomechanical roles.

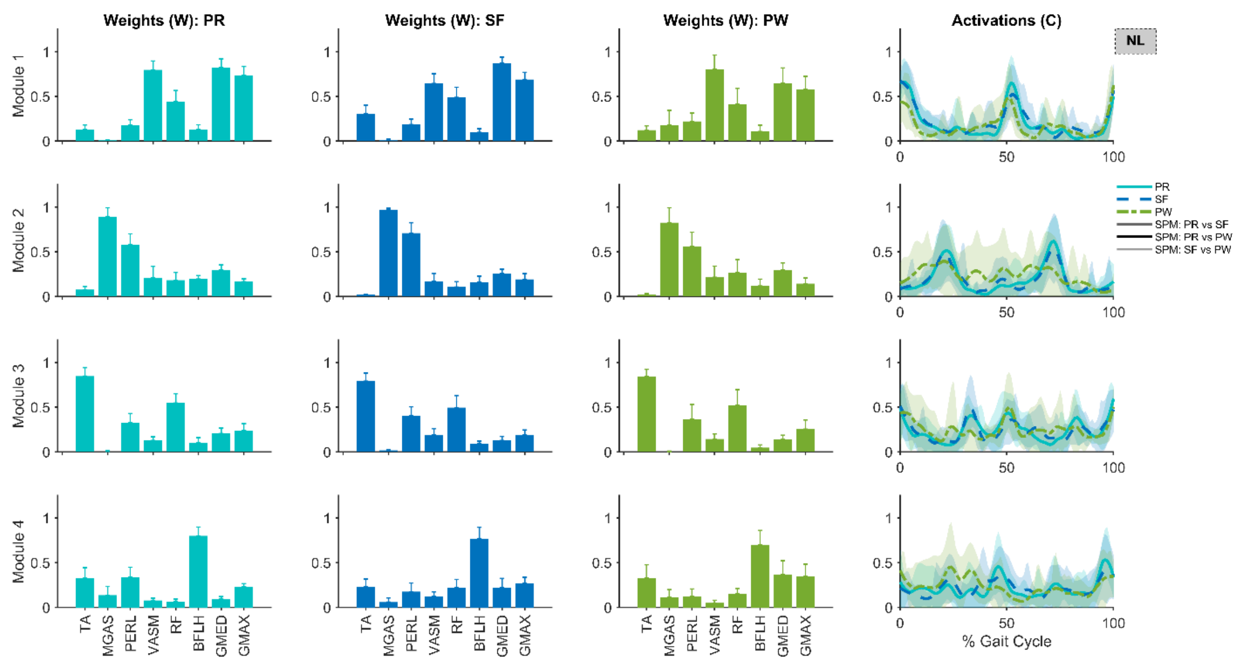

Fig A5.1 Average module weights (± SE) and activations (± SD shading) for a four-module solution in the NL condition. Module weights (W) are shown as a function of the muscles and module activations (C) are shown as a function of the gait cycle. If present, horizontal lines in the C plots represent pairwise differences from SPM analyses.

Across feet in the FL condition, the first module (GMED, GMAX, RF, VASM) primarily support body weight and stabilize the limb during early stance; the second module (MGAS, PERL) generate propulsion in late stance; the third module (TA) facilitate leg swing initiation and trunk energy transfer; and the fourth module (BFLH) contribute to late-swing deceleration and early-stance energy absorption. The involvement of muscles such as GMAX, associated with early-stance body support, and BFLH, known to contribute energy during early stance and swing, is consistent with their established biomechanical roles.

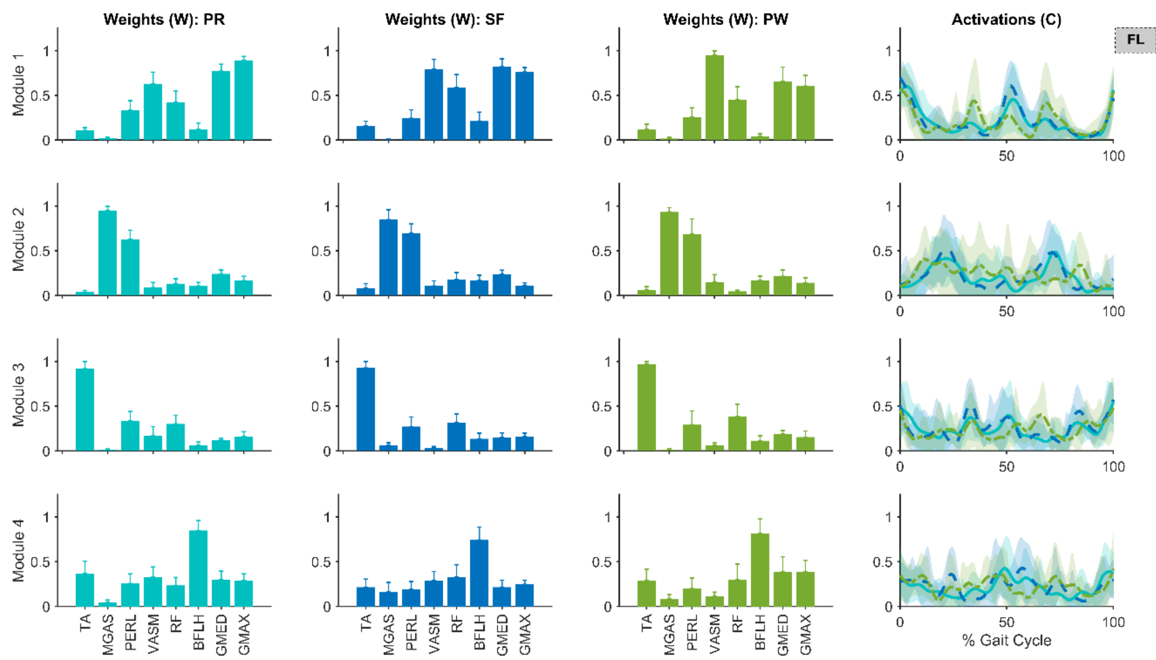

Fig A5.2 Average module weights (± SE) and activations (± SD shading) for a four-module solution in the FL condition. Module weights (W) are shown as a function of the muscles and module activations (C) are shown as a function of the gait cycle. If present, horizontal lines in the C plots represent pairwise differences from SPM analyses.

Across feet in the BL condition, the first module (GMED, GMAX, RF, VASM) primarily support body weight and stabilize the limb during early stance; the second module (MGAS, PERL) generate propulsion in late stance; the third module (TA) facilitate leg swing initiation and trunk energy transfer; and the fourth module (BFLH) contribute to late-swing deceleration and early-stance energy absorption. The involvement of muscles such as GMAX, associated with early-stance body support, and BFLH, known to contribute energy during early stance and swing, is consistent with their established biomechanical roles.

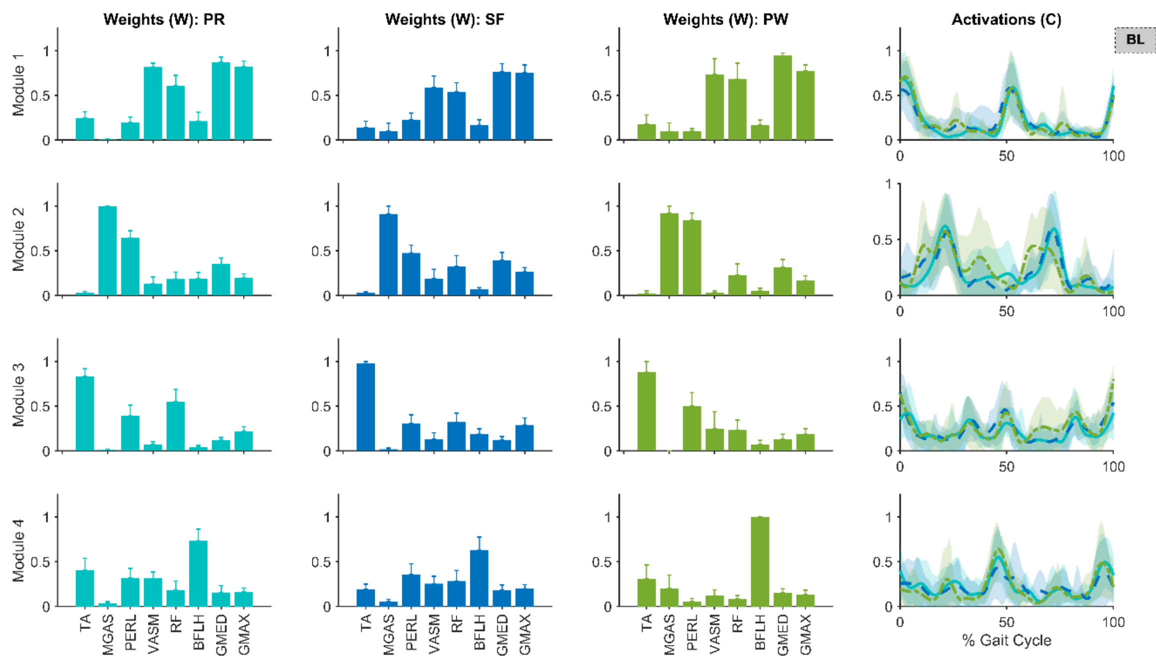

Fig A5.3 Average module weights (± SE) and activations (± SD shading) for a four-module solution in the BL condition. Module weights (W) are shown as a function of the muscles and module activations (C) are shown as a function of the gait cycle. If present, horizontal lines in the C plots represent pairwise differences from SPM analyses.

Across feet in the IL condition, the first module (GMED, GMAX, RF, VASM) primarily support body weight and stabilize the limb during early stance; the second module (MGAS, PERL) generate propulsion in late stance; the third module (primarily TA) facilitate leg swing initiation and trunk energy transfer; and the fourth module (BFLH) contribute to late-swing deceleration and early-stance energy absorption. The involvement of muscles such as GMAX, associated with early-stance body support, and BFLH, known to contribute energy during early stance and swing, is consistent with their established biomechanical roles.

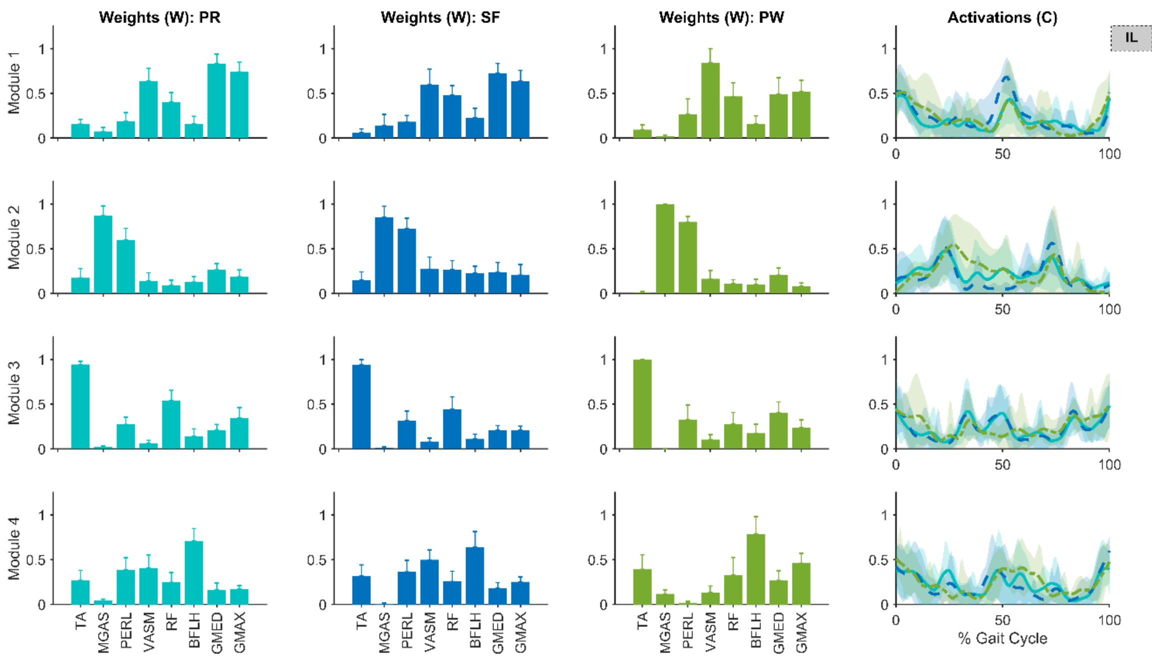

Fig A5.4 Average module weights (± SE) and activations (± SD shading) for a four-module solution in the IL condition. Module weights (W) are shown as a function of the muscles and module activations (C) are shown as a function of the gait cycle. If present, horizontal lines in the C plots represent pairwise differences from SPM analyses.

Across feet in the PL condition, the first module (GMED, GMAX, RF, VASM) primarily support body weight and stabilize the limb during early stance; the second module (MGAS, PERL) generate propulsion in late stance; the third module (primarily RF, TA) facilitate leg swing initiation and trunk energy transfer; and the fourth module (BFLH) contribute to late-swing deceleration and early-stance energy absorption. The involvement of muscles such as GMAX, associated with early-stance body support, and BFLH, known to contribute energy during early stance and swing, is consistent with their established biomechanical roles.

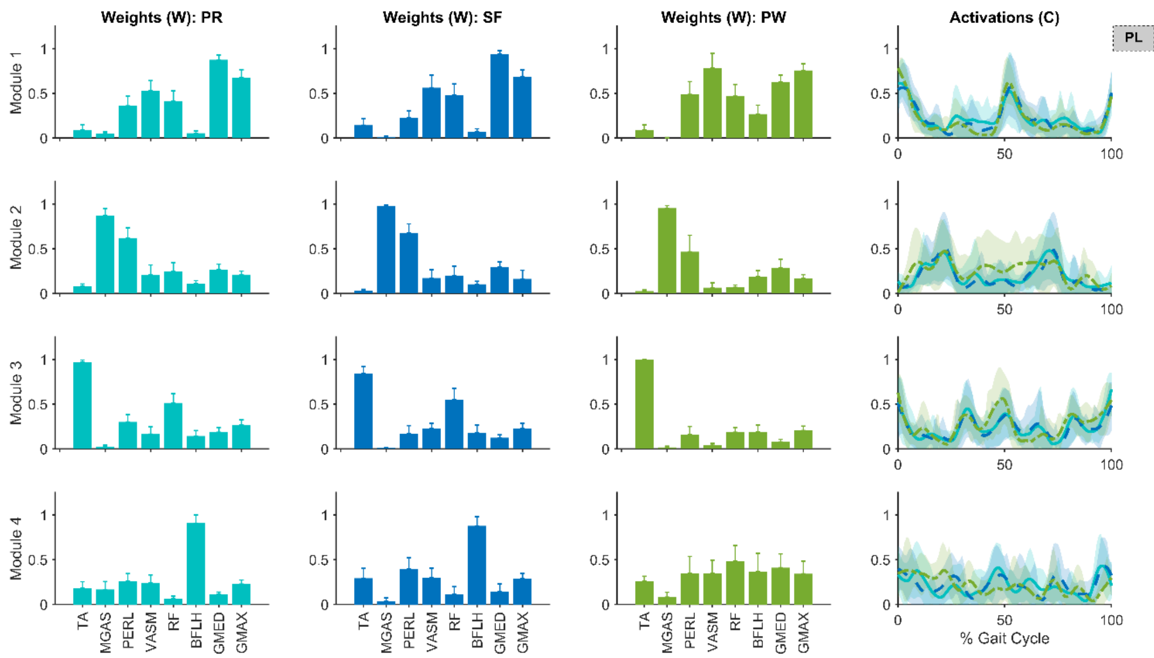

Fig A5.5 Average module weights (± SE) and activations (± SD shading) for a four-module solution in the PL condition. Module weights (W) are shown as a function of the muscles and module activations (C) are shown as a function of the gait cycle. If present, horizontal lines in the C plots represent pairwise differences from SPM analyses.

Chapter 6

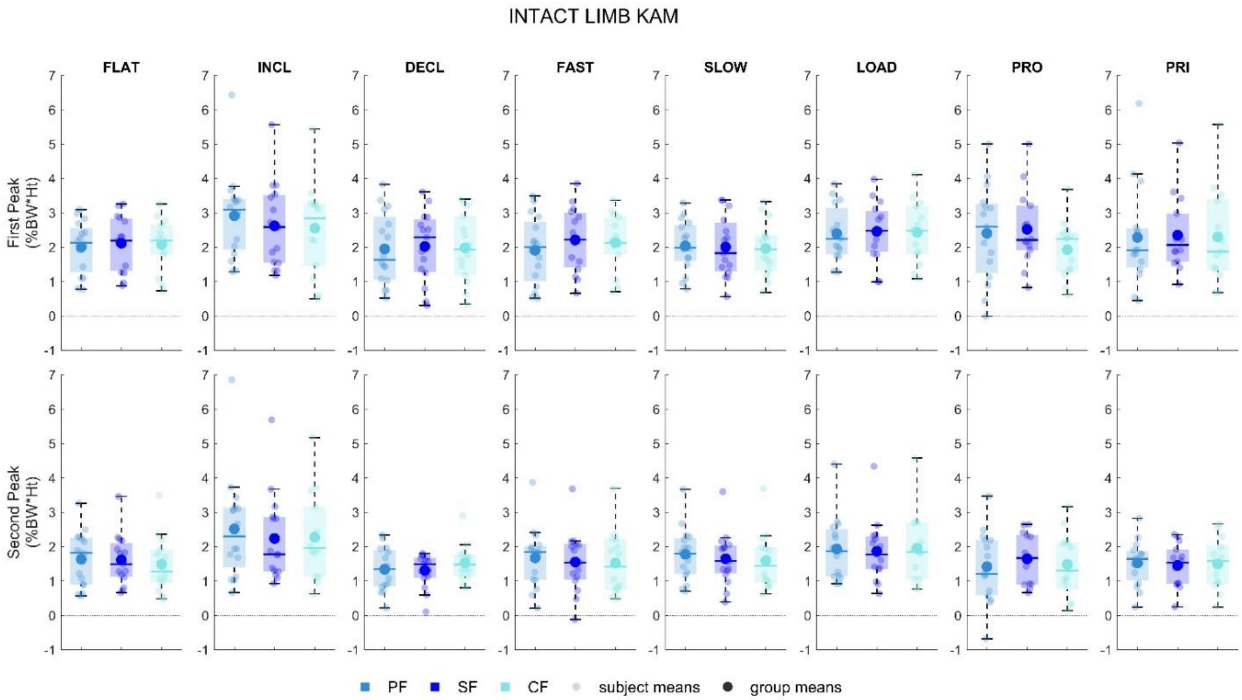

Fig A6.1 Average first peak (first row) and second peak KAM (second row) comparing prosthetic foot stiffness conditions across ambulatory activities. Abbreviations: PF, prescribed stiffness foot; SF, +2 categories (stiffer foot); CF, -2 categories (more compliant foot).

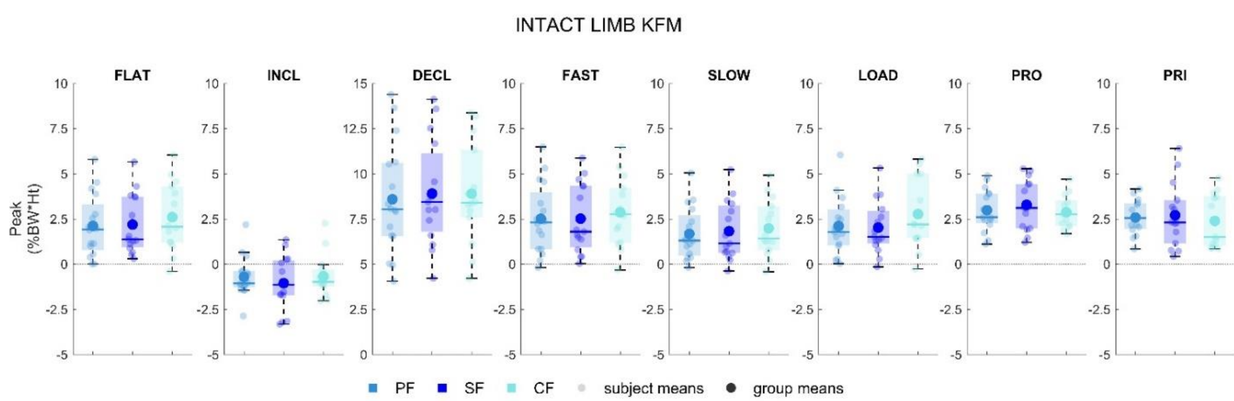

Fig A6.2 Average peak KFM comparing prosthetic foot stiffness conditions across ambulatory activities. Abbreviations: PF, prescribed stiffness foot; SF, +2 categories (stiffer foot); CF, -2 categories (more compliant foot).

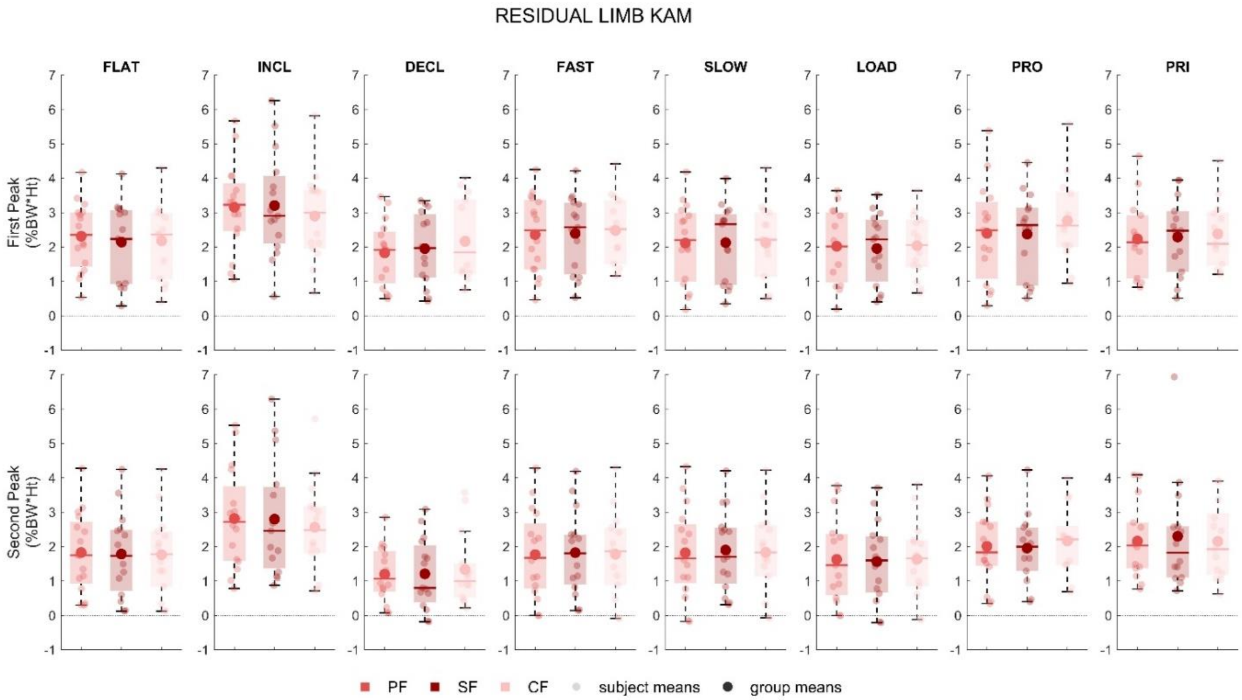

Fig A6.3 Average first peak (first row) and second peak KAM (second row) comparing prosthetic foot stiffness conditions across ambulatory activities. Abbreviations: PF, prescribed stiffness foot; SF, +2 categories (stiffer foot); CF, -2 categories (more compliant foot).

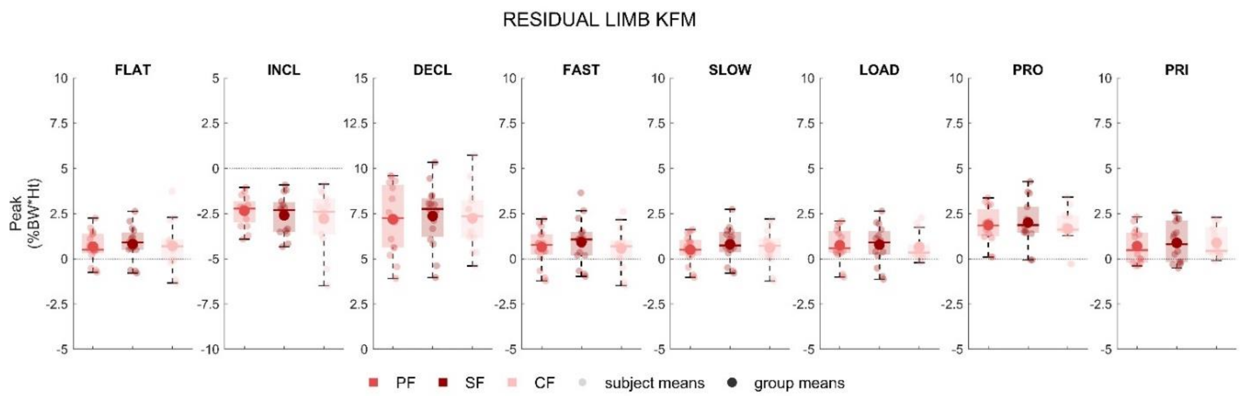

Fig A6.4 Average peak KFM comparing prosthetic foot stiffness conditions across ambulatory activities. Abbreviations: PF, prescribed stiffness foot; SF, +2 categories (stiffer foot); CF, -2 categories (more compliant foot).

Chapter 7

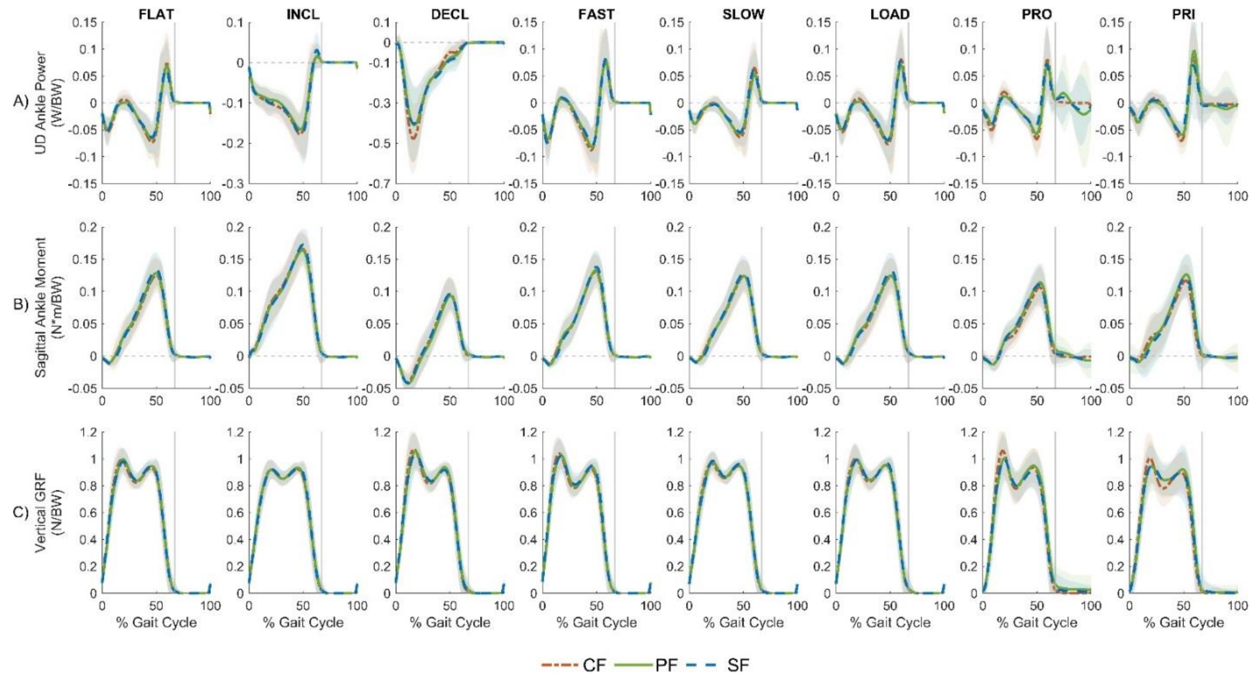

Fig A7.1 A) average prosthetic UD ankle power curves, B) average prosthetic sagittal ankle moment curves, C) average prosthetic vertical GRF curves comparing stiffness conditions across ambulatory activities. Vertical lines represent average transitions from stance to swing. Abbreviations: UD, unified deformable; GRF, ground reaction force; CF, -2 categories (more compliant foot); PF, prescribed stiffness category; SF, +2 categories (stiffer foot).

Table A7.1 Standard error and 95% CI of the slope estimates from linear mixed-effects regression models between prosthetic ankle-foot biomechanical metrics (predictors) and intact-limb MCF (responses) in each stiffness condition. Abbreviations: CI, confidence interval; CF, -2 categories (more compliant foot); PF, prescribed stiffness category; SF, +2 categories (stiffer foot); MCF, medial contact force; DMAMA, dynamic mean ankle moment arm; ROR, roll over radius.

Prosthetic Ankle/Foot Properties (Predictors)	Activity	SE			[95% CI]		
		CF	PF	SF	CF	PF	SF
Ankle Peak Push-Off Power (W/BW)	FLAT	0.29	0.29	0.31	[0.07, 1.21]	[0.37, 1.51]	[-1.82, -0.59]
	INCL	0.41	0.37	0.32	[-1.50, 0.11]	[3.05, 4.51]	[2.54, 3.79]
	DECL	0.34	0.24	0.23	[1.15, 2.47]	[0.05, 1.00]	[2.27, 3.16]
	FAST	0.25	0.25	0.29	[0.64, 1.60]	[0.07, 1.04]	[1.20, 2.34]
	SLOW	0.30	0.30	0.35	[1.32, 2.49]	[1.50, 2.68]	[1.64, 3.03]
	LOAD	0.27	0.25	0.29	[-0.24, 0.82]	[-1.13, -0.15]	[-1.00, 0.12]
	PRO	1.31	1.34	1.28	[-3.01, 2.16]	[-4.27, 1.03]	[-2.29, 2.77]
	PRI	1.00	1.05	0.81	[-0.98, 2.98]	[-3.10, 1.06]	[-0.13, 3.05]
Ankle Push-Off Work (J/BW)	FLAT	3.28	3.47	3.94	[2.85, 15.71]	[2.85, 15.71]	[2.85, 15.71]
	INCL	6.62	6.57	5.63	[-21.18, 4.80]	[64.59, 90.38]	[46.79, 68.89]
	DECL	7.68	9.56	12.39	[-17.36, 12.77]	[-45.52, -8.03]	[-88.43, -39.82]
	FAST	3.22	3.43	3.81	[-0.03, 12.60]	[0.06, 13.52]	[2.36, 17.30]
	SLOW	3.57	3.63	4.28	[6.54, 20.56]	[17.02, 31.25]	[16.58, 33.38]
	LOAD	3.15	3.23	3.32	[7.23, 19.58]	[-16.65, -3.97]	[-16.50, -3.46]
	PRO	16.87	15.11	15.95	[-27.45, 39.05]	[-62.76, -3.21]	[-15.81, 47.08]
	PRI	13.15	13.92	9.81	[-14.96, 36.94]	[-33.48, 21.43]	[0.77, 39.47]
Dynamic Mean Ankle Moment Arm (% foot length)	FLAT	0.0018	0.0019	0.0022	[-0.01, 0.00]	[-0.01, 0.00]	[0.01, 0.01]
	INCL	0.0016	0.0017	0.0017	[0.00, 0.00]	[0.00, 0.00]	[0.00, 0.01]
	DECL	0.0027	0.0031	0.0030	[-0.02, -0.01]	[-0.01, 0.00]	[-0.01, 0.00]
	FAST	0.0020	0.0020	0.0020	[-0.01, 0.00]	[-0.02, -0.01]	[0.01, 0.02]

	SLOW	0.0017	0.0016	0.0018	[0.00, 0.00]	[-0.01, 0.00]	[0.01, 0.01]
	LOAD	0.0015	0.0017	0.0018	[-0.01, 0.00]	[0.00, 0.01]	[0.01, 0.01]
	PRO	0.0109	0.0097	0.0117	[-0.01, 0.03]	[-0.01, 0.03]	[-0.05, 0.00]
	PRI	0.0087	0.0063	0.0061	[-0.02, 0.01]	[-0.01, 0.02]	[-0.02, 0.01]
Roll Over Radius (mm)	FLAT	0.0004	0.0003	0.0003	[0.000, 0.001]	[0.000, 0.002]	[-0.001, 0.000]
	INCL	0.0004	0.0004	0.0004	[-0.002, 0.000]	[-0.003, -0.001]	[-0.001, 0.000]
	DECL	0.0005	0.0004	0.0005	[-0.001, 0.000]	[0.000, 0.002]	[-0.003, -0.001]
	FAST	0.0005	0.0003	0.0002	[-0.005, -0.003]	[-0.004, -0.003]	[-0.003, -0.002]
	SLOW	0.0002	0.0002	0.0002	[0.000, 0.001]	[0.000, 0.000]	[0.001, 0.001]
	LOAD	0.0003	0.0003	0.0003	[-0.003, -0.001]	[-0.001, 0.000]	[-0.002, -0.001]
	PRO	0.0012	0.0011	0.0012	[-0.004, 0.001]	[-0.001, 0.003]	[-0.002, 0.003]
	PRI	0.0016	0.0010	0.0012	[-0.002, 0.004]	[0.000, 0.004]	[-0.001, 0.004]

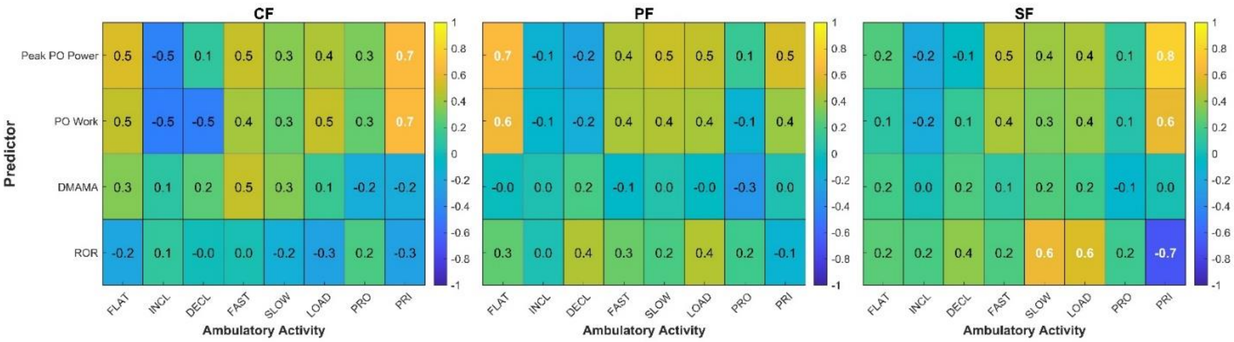

Fig A7.2 Subject-level Pearson correlations (r) between prosthetic ankle-foot biomechanical metrics (predictors) and intact-limb MCF (responses) in each stiffness condition. Bold white r values indicate a stronger linear relationship where |r| ≥ 0.6, while |r| < 0.2 is considered weak. Abbreviations: CF, -2 categories (more compliant foot); PF, prescribed stiffness category; SF, +2 categories (stiffer foot); PO, push-off; DMAMA, dynamic mean ankle moment arm; ROR, roll over radius.

BIBLIOGRAPHY

Adamczyk, P.G., 2020. Ankle control in walking and running: Speed- And gait-related changes in dynamic mean ankle moment arm. J. Biomech. Eng. 142. https://doi.org/10.1115/1.4045817

Adamczyk, P.G., Collins, S.H., Kuo, A.D., 2006. The advantages of a rolling foot in human walking. Journal of Experimental Biology 209, 3953–3963. https://doi.org/10.1242/JEB.02455

Adamczyk, P.G., Kuo, A.D., 2015. Mechanisms of gait asymmetry due to push-off deficiency in unilateral amputees. IEEE Transactions on Neural Systems and Rehabilitation Engineering 23, 776–785. https://doi.org/10.1109/TNSRE.2014.2356722

Adamczyk, P.G., Kuo, A.D., 2009. Redirection of center-of-mass velocity during the step-to-step transition of human walking. Journal of Experimental Biology 212, 2668–2678. https://doi.org/10.1242/jeb.027581

Adamczyk, P.G., Roland, M., Hahn, M.E., 2017. Sensitivity of biomechanical outcomes to independent variations of hindfoot and forefoot stiffness in foot prostheses. Hum. Mov. Sci. 54, 154–171. https://doi.org/10.1016/J.HUMOV.2017.04.005

Alexander, N., Schwameder, H., 2016. Lower limb joint forces during walking on the level and slopes at different inclinations. Gait Posture 45, 137–142. https://doi.org/10.1016/J.GAITPOST.2016.01.022

Allen, J.L., Neptune, R.R., 2012. Three-dimensional modular control of human walking. J. Biomech. 45, 2157–2163. https://doi.org/10.1016/J.JBIOMECH.2012.05.037

Anderson, F.C., Pandy, M.G., 2003. Individual muscle contributions to support in normal walking. Gait Posture 17, 159–169.

Andrag, L., Kunorozva, L., Derman, W., Runciman, P., 2024. Knee contact forces of individuals with osteoarthritis and those with lower limb amputation: A systematic review. Am. J. Phys. Med. Rehabil. https://doi.org/10.1097/PHM.0000000000002567

Andriacchi, T.P., Mündermann, A., Smith, R.L., Alexander, E.J., Dyrby, C.O., Koo, S., 2004. A framework for the in vivo pathomechanics of osteoarthritis at the knee. Ann. Biomed. Eng. 32, 447–457. https://doi.org/10.1023/B:ABME.0000017541.82498.37

Ardianuari, S., Cyr, K.M., Neptune, R.R., Klute, G.K., 2024. Should individuals with unilateral transtibial amputation carry a load on their intact or prosthetic side? J. Biomech. 112385. https://doi.org/10.1016/J.JBIOMECH.2024.112385

Ardianuari, S., Hu, E., Fey, N., Neptune, R., Klute, G., 2026a. Medial Knee Loading Responses to Prosthetic Foot Stiffness During Various Ambulatory Activities. In Review Journal of Biomechanics.

Ardianuari, S., Morgenroth, D.C., Neptune, R.R., Klute, G.K., 2025. Load carriage influences intact limb knee loading estimate associated with osteoarthritis in individuals with transtibial amputation. Clinical Biomechanics 124. https://doi.org/10.1016/j.clinbiomech.2025.106486

Ardianuari, S., Neptune, R., Klute, G., 2026b. Amputee Motor Control During Loaded Walking with Stiffer and Powered Feet. In Review Journal of NeuroEngineering and Rehabilitation.

Attwells, R.L., Birrell, S.A., Hooper, R.H., Mansfield, N.J., 2006. Influence of carrying heavy loads on soldiers' posture, movements and gait. Ergonomics 49, 1527–1537. https://doi.org/10.1080/00140130600757237

Azocar, A.F., Mooney, L.M., Duval, J.F., Simon, A.M., Hargrove, L.J., Rouse, E.J., 2020. Design and clinical implementation of an open-source bionic leg. Nature Biomedical Engineering 2020 4:10 4, 941–953. https://doi.org/10.1038/s41551-020-00619-3

Barrios, J., Willson, J., 2017. Minimum detectable change in medial tibiofemoral contact force parameters: Derivation and application to a load-altering intervention. J. Appl. Biomech. 33, 171–175. https://doi.org/10.1123/jab.2016-0163

Bateni, H., Olney, S.J., 2002. Kinematic and kinetic variations of below-knee amputee gait. Journal of Prosthetics and Orthotics 14.

Benjamini, Y., Hochberg, Y., 1995. Controlling the False Discovery Rate: A Practical and Powerful Approach to Multiple Testing, Source: Journal of the Royal Statistical Society. Series B (Methodological).

Birrell, S.A., Haslam, R.A., 2009. The effect of military load carriage on 3-D lower limb kinematics and spatiotemporal parameters. Ergonomics 52, 1298–1304. https://doi.org/10.1080/00140130903003115

Boutwell, E., Stine, R., Gard, S., 2017. Shock absorption during transtibial amputee gait: Does longitudinal prosthetic stiffness play a role? Prosthet. Orthot. Int. 41, 178–185. https://doi.org/10.1177/0309364616640945

Brandt, A., Wen, Y., Liu, M., Stallings, J., Huang, H.H., 2017. Interactions Between Transfemoral Amputees and a Powered Knee Prosthesis During Load Carriage. Scientific Reports 2017 7:1 7, 1–12. https://doi.org/10.1038/s41598-017-14834-7

Burke, M.J., Roman, V., Wright, V., 1978. Bone and joint changes in lower limb amputees, Annals of the Rheumatic Diseases.

Butowicz, C.M., Golyski, P.R., Acasio, J.C., Hendershot, B.D., 2024. Comparing spinal loads in individuals with unilateral transtibial amputation with and without chronic low back pain: An EMG-informed approach. J. Biomech. 166, 111966. https://doi.org/10.1016/J.JBIOMECH.2024.111966

Byrnes, S.K., Holder, J., Stief, F., Wearing, S., Böhm, H., Dussa, C.U., Horstmann, T., 2022. Frontal plane knee moment in clinical gait analysis: A systematic review on the effect of kinematic gait changes. Gait Posture 98, 39–48. https://doi.org/10.1016/J.GAITPOST.2022.07.258

Cammarata, M.L., Dhaher, Y.Y., 2010. Evidence of gender-specific motor templates to resist valgus loading at the knee. Muscle Nerve 41, 614–623. https://doi.org/10.1002/MUS.21509;REQUESTEDJOURNAL:JOURNAL:10974598;WGROUP:STRING:PUBLICATION

Childers, W.L., Takahashi, K.Z., 2018. Increasing prosthetic foot energy return affects whole-body mechanics during walking on level ground and slopes. Scientific Reports 2018 8:1 8, 5354-. https://doi.org/10.1038/s41598-018-23705-8

Cognetti, D.J., DeFoor, M.T., Arave, M., Alderete, J.F., Mills, G., 2025. Optimizing below knee amputation osteotomy length: a ratio-based approach. OTA International 8. https://doi.org/10.1097/OI9.0000000000000449

Crowell, H.P., Milnert, C.E., Hamill, J., Davis, I.S., 2010. Reducing impact loading during running with the use of real-time visual feedback. Journal of Orthopaedic and Sports Physical Therapy 40, 206–213. https://doi.org/10.2519/jospt.2010.3166

Curtze, C., Hof, A.L., van Keeken, H.G., Halbertsma, J.P.K., Postema, K., Otten, B., 2009. Comparative roll-over analysis of prosthetic feet. J. Biomech. 42, 1746–1753. https://doi.org/10.1016/J.JBIOMECH.2009.04.009

Cutti, A.G., Verni, G., Migliore, G.L., Amoresano, A., Raggi, M., 2018. Reference values for gait temporal and loading symmetry of lower-limb amputees can help in refocusing rehabilitation targets. J. Neuroeng. Rehabil. 15. https://doi.org/10.1186/s12984-018-0403-x

Cyr, K.M., Neptune, R.R., Klute, G.K., 2025. Influence of prosthetic foot selection on walking performance during various load carriage conditions. Clinical Biomechanics 122. https://doi.org/10.1016/j.clinbiomech.2025.106440

Dal, U., Erdogan, T., Resitoglu, B., Beydagi, H., 2010. Determination of preferred walking speed on treadmill may lead to high oxygen cost on treadmill walking. Gait Posture 31, 366–369. https://doi.org/10.1016/j.gaitpost.2010.01.006

D'Andrea, S., Wilhelm, N., Silverman, A.K., Grabowski, A.M., 2014. Does Use of a Powered Ankle-foot Prosthesis Restore Whole-body Angular Momentum During Walking at Different Speeds? Clin. Orthop. Relat. Res. 472, 3044–3054. https://doi.org/10.1007/S11999-014-3647-1

Davidson, A.M., Childers, W.L., Chang, Y.H., 2021. Altering the tuning parameter settings of a commercial powered prosthetic foot to increase power during push-off may not reduce collisional work in the intact limb during gait. Prosthet. Orthot. Int. 45, 410–416. https://doi.org/10.1097/PXR.0000000000000036

Dean, J.C., Alexander, N.B., Kuo, A.D., 2007. The effect of lateral stabilization on walking in young and old adults. IEEE Trans. Biomed. Eng. 54, 1919–1926. https://doi.org/10.1109/TBME.2007.901031

Dempster, W.T., 1995. Space requirements of the seated operator : geometrical, kinematic, and mechanical aspects of the body, with special reference to the limbs. WADC Technical Report 55–159.

Donelan, J.M., Kram, R., Kuo, A.D., 2002a. Mechanical work for step-to-step transitions is a major determinant of the metabolic cost of human walking. Journal of Experimental Biology 205, 3717–3727. https://doi.org/10.1242/JEB.205.23.3717

Donelan, J.M., Kram, R., Kuo, A.D., 2002b. Simultaneous positive and negative external mechanical work in human walking. J. Biomech. 35, 117–124. https://doi.org/10.1016/S0021-9290(01)00169-5

Doyle, S.S., Lemaire, E.D., Besemann, M., Dudek, N.L., 2015. Changes to transtibial amputee gait with a weighted backpack on multiple surfaces. Clinical Biomechanics 30, 1119–1124. https://doi.org/10.1016/j.clinbiomech.2015.08.015

Doyle, S.S., Lemaire, E.D., Besemann, M., Dudek, N.L., 2014. Changes to level ground transtibial amputee gait with a weighted backpack. Clinical Biomechanics 29, 149–154. https://doi.org/10.1016/j.clinbiomech.2013.11.019

Drew, M.D., Krammer, S.M., Brown, T.N., 2021. Effects of prolonged walking with body borne load on knee adduction biomechanics. Gait Posture 84, 192–197. https://doi.org/10.1016/J.GAITPOST.2020.12.004

Farrokhi, S., Mazzone, B., Yoder, A., Grant, K., Wyatt, M., 2016. A Narrative Review of the Prevalence and Risk Factors Associated With Development of Knee Osteoarthritis After Traumatic Unilateral Lower Limb Amputation. Mil. Med. 181, 38–44. https://doi.org/10.7205/MILMED-D-15-00510

Fehr, K.H., Kent, J.A., Major, M.J., Adamczyk, P.G., 2024. Changes in Dynamic Mean Ankle Moment Arm in Unimpaired Walking Across Speeds, Ramps, and Stairs. J. Biomech. Eng. 146. https://doi.org/10.1115/1.4065269/1199178

Ferris, A.E., Aldridge, J.M., Rábago, C.A., Wilken, J.M., 2012. Evaluation of a powered ankle-foot prosthetic system during walking. Arch. Phys. Med. Rehabil. 93, 1911–1918. https://doi.org/10.1016/j.apmr.2012.06.009

Fey, N.P., Klute, G.K., Neptune, R.R., 2012. Optimization of prosthetic foot stiffness to reduce metabolic cost and intact knee loading during below-knee amputee walking: A theoretical study. J. Biomech. Eng. 134. https://doi.org/10.1115/1.4007824

Fey, N.P., Klute, G.K., Neptune, R.R., 2011. The influence of energy storage and return foot stiffness on walking mechanics and muscle activity in below-knee amputees. Clinical Biomechanics 26, 1025–1032. https://doi.org/10.1016/J.CLINBIOMECH.2011.06.007

Fey, N.P., Neptune, R.R., 2012. 3D intersegmental knee loading in below-knee amputees across steady-state walking speeds. Clinical Biomechanics 27, 409–414. https://doi.org/10.1016/J.CLINBIOMECH.2011.10.017

Foroughi, N., Smith, R., Vanwanseele, B., 2009. The association of external knee adduction moment with biomechanical variables in osteoarthritis: A systematic review. Knee 16, 303–309. https://doi.org/10.1016/J.KNEE.2008.12.007

Fryar, C.D., Carroll, M.D., Gu, Q., Afful, J., Ogden, C.L., 2021. Anthropometric Reference Data for Children and Adults: United States, 2015-2018. Vital Health Stat. 3 1–44.

Gaffney, B.M.M., Davis-Wilson, H.C., Christiansen, C.L., Awad, M.E., Lev, G., Tracy, J., Stoneback, J.W., 2023. Osseointegrated prostheses improve balance and balance confidence in individuals with unilateral transfemoral limb loss. Gait Posture 100, 132–138. https://doi.org/10.1016/J.GAITPOST.2022.12.011

Gailey, R., Allen, K., Castles, J., Kucharik, J., Roeder, M., 2008. Review of secondary physical conditions associated with lower-limb amputation and long-term prosthesis use. J. Rehabil. Res. Dev. 45, 15–30. https://doi.org/10.1682/JRRD.2006.11.0147

Ghori, G.M.U., Luckwill, R.G., 1985. Responses of the lower limb to load carrying in walking man. Eur. J. Appl. Physiol. Occup. Physiol. 54, 145–150.

Gitter, A., Czerniecki, J., DeGroot, D.M., 1991. Biomechanical analysis of the influence of prosthetic feet on below-knee amputee walking. Am. J. Phys. Med. Rehabil. 70, 142–148.

Gittleman, M., Monaco, K., Nestoriak, N., 2016. The Requirements of Jobs: Evidence from a Nationally Representative Survey. Cambridge, MA. https://doi.org/10.3386/w22218

Golyski, P.R., Hendershot, B.D., Chomack, J.M., Gladish, J.R., Herlihy, D. V., Maikos, J.T., 2026. Powered prosthetic feet do not decrease contralateral knee loads relative to energy storing and returning feet during walking in a functionally diverse cohort of individuals with unilateral transtibial limb loss. J. Biomech. 194, 113031. https://doi.org/10.1016/J.JBIOMECH.2025.113031

Grabowski, A.M., 2010. Metabolic and Biomechanical Effects of Velocity and Weight Support Using a Lower-Body Positive Pressure Device During Walking. Arch. Phys. Med. Rehabil. 91, 951–957. https://doi.org/10.1016/j.apmr.2010.02.007

Grabowski, A.M., D'Andrea, S., 2013. Effects of a powered ankle-foot prosthesis on kinetic loading of the unaffected leg during level-ground walking. J. Neuroeng. Rehabil. 10, 1–12. https://doi.org/10.1186/1743-0003-10-49/FIGURES/3

Grumillier, C., Martinet, N., Paysant, J., André, J.M., Beyaert, C., 2008. Compensatory mechanism involving the hip joint of the intact limb during gait in unilateral trans-tibial amputees. J. Biomech. 41, 2926–2931. https://doi.org/10.1016/j.jbiomech.2008.07.018

Haggerty, M., Dickin, D.C., Popp, J., Wang, H., 2014. The influence of incline walking on joint mechanics. Gait Posture 39, 1017–1021. https://doi.org/10.1016/J.GAITPOST.2013.12.027

Halsne, E.G., Czerniecki, J.M., Shofer, J.B., Morgenroth, D.C., 2020. The effect of prosthetic foot stiffness on foot-ankle biomechanics and relative foot stiffness perception in people with transtibial amputation. Clinical Biomechanics 80, 105141. https://doi.org/10.1016/J.CLINBIOMECH.2020.105141

Hansen, A.H., Childress, D.S., 2010. Investigations of roll-over shape: implications for design, alignment, and evaluation of ankle-foot prostheses and orthoses. Disabil. Rehabil. 32, 2201–2209. https://doi.org/10.3109/09638288.2010.502586

Hansen, A.H., Childress, D.S., Knox, E.H., 2004a. Roll-over shapes of human locomotor systems: effects of walking speed. Clinical Biomechanics 19, 407–414. https://doi.org/10.1016/J.CLINBIOMECH.2003.12.001

Hansen, A.H., Childress, D.S., Miff, S.C., Gard, S.A., Mesplay, K.P., 2004b. The human ankle during walking: implications for design of biomimetic ankle prostheses. J. Biomech. 37, 1467–1474. https://doi.org/10.1016/J.JBIOMECH.2004.01.017

Hansen, A.H., Meier, M.R., Sessoms, P.H., Childress, D.S., 2006. The effects of prosthetic foot roll-over shape arc length on the gait of trans-tibial prosthesis users. Prosthet. Orthot. Int. 30, 286–299. https://doi.org/10.1080/03093640600816982

Harman, E., Han, H.-H., Frykman, P., Johnson, M., Russell, F., Rosenstein, M., 1992. The Effects on Gait Timing, Kinetics, and Muscle Activity of Various Loads Carried on The Back. Med. Sci. Sports Exerc.

HAS-Motion, V., 2026. Foot and Ankle Angles [HAS-Motion Software Documentation] [WWW Document]. URL https://wiki.has-motion.com/doku.php?id=visual3d:tutorials:kinematics_and_kinetics:foot_and_ankle_angles#virtual_foot_method_1_-_heel_to_toe (accessed 4.26.26).

Heijink, A., Gomoll, A.H., Madry, H., Drobnič, M., Filardo, G., Espregueira-Mendes, J., van Dijk, C.N., 2011. Biomechanical considerations in the pathogenesis of osteoarthritis of the knee. Knee Surgery, Sports Traumatology, Arthroscopy 2011 20:3 20, 423–435. https://doi.org/10.1007/s00167-011-1818-0

Hermens, H.J., Freriks, B., Disselhorst-Klug, C., Rau, G., 2000. Development of recommendations for SEMG sensors and sensor placement procedures. Journal of Electromyography and Kinesiology 10, 361–374. https://doi.org/10.1016/S1050-6411(00)00027-4

Herr, H.M., Grabowski, A.M., 2012. Bionic ankle–foot prosthesis normalizes walking gait for persons with leg amputation. Proceedings of the Royal Society B: Biological Sciences 279, 457. https://doi.org/10.1098/RSPB.2011.1194

Highsmith, M.J., Goff, L.M., Lewandowski, A.L., Farrokhi, S., Hendershot, B.D., Hill, O.T., Rábago, C.A., Russell-Esposito, E., Orriola, J.J., Mayer, J.M., 2019. Low back pain in persons with lower extremity amputation: a systematic review of the literature. Spine Journal 19, 552–563. https://doi.org/10.1016/j.spinee.2018.08.011

Hoveizavi, R., Fisher, S.J., Shuman, B.R., Joiner, J.C., Gao, F., 2025. Muscle synergies are largely unaffected in individuals with diabetes who do not have diabetic neuropathy. Clinical Biomechanics 125, 106520. https://doi.org/10.1016/j.clinbiomech.2025.106520

Hu, J., Ding, Z., Anthony, ·, Bull, M.J., 2025. Alterations in Muscle Coordination to Reduce Knee Joint Loading for People with Limb Loss. Annals of Biomedical Engineering 2025 1–11. https://doi.org/10.1007/S10439-025-03682-6

Jiang, Z., He, A., Zheng, N., Mao, Y., Lin, W., Zhang, X., Guo, H., Liu, Y., Tsai, T.Y., Liu, W., 2025. Medial Compartment Knee Osteoarthritis Altered Tibiofemoral Joint Kinematics and Contact Pattern During Daily

Weight-Bearing Extension. Orthop. Surg. 17, 1478–1485. https://doi.org/10.1111/OS.70023;SUBPAGE:STRING:FULL

Jones, R.K., Chapman, G.J., Findlow, A.H., Forsythe, L., Parkes, M.J., Sultan, J., Felson, D.T., 2013. A New Approach to Prevention of Knee Osteoarthritis: Reducing Medial Load in the Contralateral Knee. J. Rheumatol. 40, 309–315. https://doi.org/10.3899/jrheum.120589

Kannenberg, A., Morris, A.R., Hibler, K.D., 2022. Free-Living User Perspectives on Musculoskeletal Pain and Patient-Reported Mobility With Passive and Powered Prosthetic Ankle-Foot Components: A Pragmatic, Exploratory Cross-Sectional Study. Frontiers in Rehabilitation Sciences 2. https://doi.org/10.3389/fresc.2021.805151

Kellis, E., Arabatzi, F., Papadopoulos, C., 2003. Muscle co-activation around the knee in drop jumping using the co-contraction index. Journal of Electromyography and Kinesiology 13, 229–238. https://doi.org/10.1016/S1050-6411(03)00020-8

Kern, A.M., Papachatzis, N., Patterson, J.M., Bruening, D.A., Takahashi, K.Z., 2019. Ankle and midtarsal joint quasi-stiffness during walking with added mass. PeerJ 2019, e7487. https://doi.org/10.7717/PEERJ.7487/SUPP-1

Kim, J., Gardinier, E.S., Vempala, V., Gates, D.H., 2021a. The effect of powered ankle prostheses on muscle activity during walking. J. Biomech. 124. https://doi.org/10.1016/j.jbiomech.2021.110573

Kim, J., Wensman, J., Colabianchi, N., Gates, D.H., 2021b. The influence of powered prostheses on user perspectives, metabolics, and activity: a randomized crossover trial. J. Neuroeng. Rehabil. 18. https://doi.org/10.1186/s12984-021-00842-2

Klodd, E., Hansen, A., Fatone, S., Edwards, M., 2010. Effects of prosthetic foot forefoot flexibility on gait of unilateral transtibial prosthesis users. J. Rehabil. Res. Dev. 47, 899–910. https://doi.org/10.1682/JRRD.2009.10.0166

Kobayashi, T., Orendurff, M.S., Arabian, A.K., Rosenbaum-Chou, T.G., Boone, D.A., 2014. Effect of prosthetic alignment changes on socket reaction moment impulse during walking in transtibial amputees. J. Biomech. 47, 1315–1323. https://doi.org/10.1016/j.jbiomech.2014.02.012

Koehler-McNicholas, S.R., Nickel, E.A., Barrons, K., Blaharski, K.E., Dellamano, C.A., Ray, S.F., Schnall, B.L., Hendershot, B.D., Hansen, A.H., 2018. Mechanical and dynamic characterization of prosthetic feet for high activity users during weighted and unweighted walking. PLoS One 13, e0202884. https://doi.org/10.1371/JOURNAL.PONE.0202884

Kuhn, H.W., 1955. The Hungarian method for the assignment problem. Naval Research Logistics Quarterly 2, 83–97. https://doi.org/10.1002/NAV.3800020109

Kuo, A.D., 2007. The six determinants of gait and the inverted pendulum analogy: A dynamic walking perspective. Hum. Mov. Sci. 26, 617–656. https://doi.org/10.1016/j.humov.2007.04.003

Kuo, A.D., Maxwell Donelan, J., Ruina, Andy, Donelan, J., Ruina, A, 2005. Energetic Consequences of Walking Like an Inverted Pendulum: Step-to-Step Transitions, Exerc. Sport Sci. Rev.

Kutch, J.J., Valero-Cuevas, F.J., 2012. Challenges and New Approaches to Proving the Existence of Muscle Synergies of Neural Origin. PLoS Comput. Biol. 8, e1002434. https://doi.org/10.1371/JOURNAL.PCBI.1002434

Latash, M.L., 2021. One more time about motor (and non-motor) synergies. Exp. Brain Res. 239, 2951–2967. https://doi.org/10.1007/s00221-021-06188-4

Leestma, J.K., Fehr, K.H., Adamczyk, P.G., 2021. Adapting semi-active prostheses to real-world movements: Sensing and controlling the dynamic mean ankle moment arm with a variable-stiffness foot on ramps and stairs. Sensors 21. https://doi.org/10.3390/s21186009

Lefranc, A.S., Klute, G.K., Neptune, R.R., 2025. The influence of load carriage and prosthetic foot type on measures of biomechanical demand. J. Biomech. 193, 112992. https://doi.org/10.1016/J.JBIOMECH.2025.112992

Lefranc, A.S., Klute, G.K., Neptune, R.R., 2024. The influence of load carriage and prosthetic foot type on individual muscle and prosthetic foot contributions to body support and propulsion. J. Biomech. 112379. https://doi.org/10.1016/J.JBIOMECH.2024.112379

Li, Y., Ngom, A., 2013. The non-negative matrix factorization toolbox for biological data mining. Source Code for Biology and Medicine 2013 8:1 8, 10-. https://doi.org/10.1186/1751-0473-8-10

Liu, M.Q., Anderson, F.C., Pandy, M.G., Delp, S.L., 2006. Muscles that support the body also modulate forward progression during walking. J. Biomech. 39, 2623–2630. https://doi.org/10.1016/j.jbiomech.2005.08.017

MacKinnon, C.D., Winter, D.A., 1993. Control of whole body balance in the frontal plane during human walking. J. Biomech. 26, 633–644. https://doi.org/10.1016/0021-9290(93)90027-C

Madou, E.J., Haber, C., Moudy, S.C., Strike, S.C., 2022. Altered mechanics and increased loading on intact limbs of individuals with a unilateral transtibial amputation in comparison with non-amputees during a start-stop task. J. Biomech. 137, 111088. https://doi.org/10.1016/J.JBIOMECH.2022.111088

Magrath, W.J., Qiu, C.S., Hanwright, P.J., Tuffaha, S.H., Khavanin, N., 2022. A Systematic Review of Muscle Synergies during a Walking Gait to Define Optimal Donor-Recipient Pairings for Lower Extremity Functional Reconstruction. Plast. Reconstr. Surg. Glob. Open 10, E4438. https://doi.org/10.1097/GOX.0000000000004438

Mahaffey, R., Morrison, S.C., Bassett, P., Drechsler, W.I., Cramp, M.C., 2018. Biomechanical characteristics of lower limb gait waveforms: Associations with body fat in children. Gait Posture 61, 220–225. https://doi.org/10.1016/J.GAITPOST.2018.01.019

Malatesta, D., Canepa, M., Menendez Fernandez, A., 2017. The effect of treadmill and overground walking on preferred walking speed and gait kinematics in healthy, physically active older adults. European Journal of Applied Physiology 2017 117:9 117, 1833–1843. https://doi.org/10.1007/s00421-017-3672-3

Malcolm, P., Quesada, R.E., Caputo, J.M., Collins, S.H., 2015. The influence of push-off timing in a robotic ankle-foot prosthesis on the energetics and mechanics of walking. J. Neuroeng. Rehabil. 12, 1–15. https://doi.org/10.1186/S12984-015-0014-8/FIGURES/9

Manal, K., Gardinier, E., Buchanan, T.S., Snyder-Mackler, L., 2015. A more informed evaluation of medial compartment loading: the combined use of the knee adduction and flexor moments. Osteoarthritis Cartilage 23, 1107–1111. https://doi.org/10.1016/j.joca.2015.03.032

McAndrew, P.M., Wilken, J.M., Dingwell, J.B., 2011. Dynamic stability of human walking in visually and mechanically destabilizing environments. J. Biomech. 44, 644–649. https://doi.org/10.1016/j.jbiomech.2010.11.007

McGowan, C.P., Neptune, R.R., Clark, D.J., Kautz, S.A., 2010. Modular control of human walking: Adaptations to altered mechanical demands. J. Biomech. 43, 412–419. https://doi.org/10.1016/J.JBIOMECH.2009.10.009

Mehryar, P., Shourijeh, M., Rezaeian, T., Khandan, A., Messenger, N., O'Connor, R., Farahmand, F., Dehghani-Sanij, A., 2024. The Impact of Different Self-Selected Walking Speeds on Muscle Synergies in Transfemoral Amputees during Transient-State Gait. Biomechanics (Switzerland) 4, 14–33. https://doi.org/10.3390/BIOMECHANICS4010002/S1

Mehryar, P., Shourijeh, M.S., Maqbool, H.F., Torabi, M., Dehghani-Sanij, A.A., 2016. Muscle Synergy Analysis in Transtibial Amputee during Ramp Ascending Activity, in: IEEE EMBC (Ed.), 38th Annual International Conference of the IEEE Engineering in Medicine and Biology Society. IEEE.

Mehryar, P., Shourijeh, M.S., Rezaeian, T., Iqbal, N., Messenger, N., Dehghani-Sanij, A.A., 2017. Changes in synergy of transtibial amputee during gait: A pilot study, in: IEEE BHI (Ed.), IEEE EMBS International Conference on Biomedical & Health Informatics (BHI). IEEE.

Mehryar, P., Shourijeh, M.S., Rezaeian, T., Khandan, A.R., Messenger, N., O'Connor, R., Farahmand, F., Dehghani-Sanij, A., 2020. Differences in muscle synergies between healthy subjects and transfemoral amputees during normal transient-state walking speed. Gait Posture 76, 98–103. https://doi.org/10.1016/J.GAITPOST.2019.10.034

Melzer, I., Yekutiel, M., Sukenik, S., 2001. Comparative study of osteoarthritis of the contralateral knee joint of male amputees who do and do not play volleyball. J. Rheumatol. 28.

Miller, R.H., Krupenevich, R.L., Pruziner, A.L., Wolf, E.J., Schnall, B.L., 2017. Medial knee joint contact force in the intact limb during walking in recently ambulatory service members with unilateral limb loss: A cross-sectional study. PeerJ 2017, e2960. https://doi.org/10.7717/PEERJ.2960/SUPP-1

Miyazaki, T., Wada, M., Kawahara, H., Sato, M., Baba, H., Shimada, S., 2002. Dynamic load at baseline can predict radiographic disease progression in medial compartment knee osteoarthritis. Ann. Rheum. Dis. 61, 617–622. https://doi.org/10.1136/ARD.61.7.617

Molitor, S.L., Cyr, K.M., Klute, G.K., Neptune, R.R., 2026. Lower-limb joint work symmetry responses to load carriage and prosthetic foot type during transtibial amputee walking. J. Biomech. 194, 113047. https://doi.org/10.1016/J.JBIOMECH.2025.113047

Montgomery, J.R., Grabowski, A.M., 2018. Use of a powered ankle–foot prosthesis reduces the metabolic cost of uphill walking and improves leg work symmetry in people with transtibial amputations. J. R. Soc. Interface 15. https://doi.org/10.1098/rsif.2018.0442

Morgenroth, D.C., Gellhorn, A.C., Suri, P., 2012. Osteoarthritis in the Disabled Population: A Mechanical Perspective, in: PM and R. https://doi.org/10.1016/j.pmrj.2012.01.003

Morgenroth, D.C., Medverd, J.R., Seyedali, M., Czerniecki, J.M., 2014. The relationship between knee joint loading rate during walking and degenerative changes on magnetic resonance imaging. Clinical Biomechanics 29, 664–670. https://doi.org/10.1016/J.CLINBIOMECH.2014.04.008

Morgenroth, D.C., Segal, A.D., Zelik, K.E., Czerniecki, J.M., Klute, G.K., Adamczyk, P.G., Orendurff, M.S., Hahn, M.E., Collins, S.H., Kuo, A.D., 2011. The effect of prosthetic foot push-off on mechanical loading associated with knee osteoarthritis in lower extremity amputees. Gait Posture 34, 502–507. https://doi.org/10.1016/J.GAITPOST.2011.07.001

National Bureau of Economic Research, 2016. The Requirements of Jobs: Evidence from a Nationally Representative Survey. Cambridge, MA.

National Center for Health Statistics, 2021. Anthropometric Reference Data for Children and Adults: United States, 2015-2018.

Neptune, R.R., Clark, D.J., Kautz, S.A., 2009. Modular control of human walking: A simulation study. J. Biomech. 42, 1282–1287. https://doi.org/10.1016/J.JBIOMECH.2009.03.009

Neptune, R.R., Kautz, S.A., Zajac, F.E., 2001. Contributions of the individual ankle plantar flexors to support, forward progression and swing initiation during walking, Journal of Biomechanics.

Neptune, R.R., McGowan, C.P., 2016. Muscle contributions to frontal plane angular momentum during walking. J. Biomech. 49, 2975–2981. https://doi.org/10.1016/j.jbiomech.2016.07.016

Neptune, R.R., McGowan, C.P., 2011. Muscle contributions to whole-body sagittal plane angular momentum during walking. J. Biomech. 44, 6–12. https://doi.org/10.1016/j.jbiomech.2010.08.015

Neptune, R.R., Zajac, F.E., Kautz, S.A., 2004. Muscle force redistributes segmental power for body progression during walking. Gait Posture 19, 194–205. https://doi.org/10.1016/S0966-6362(03)00062-6

Neumann, D.A., Cook, T.M., Sholty, R.L., Sobush, D.C., 1992. An Electromyographic Analysis of Hip Abductor Muscle Activity When Subjects Are Carrying Loads in One or Both Hands. Phys. Ther. 72, 207–217. https://doi.org/10.1093/PTJ/72.3.207

Neumann, D.A., Hase, A.D., 1994. An Electromyographic Analysis of the Hip Abductors During Load Carriage: Implications for Hip Joint Protection. https://doi.org/10.2519/jospt.1994.19.5.296 19, 296–304. https://doi.org/10.2519/JOSPT.1994.19.5.296

Nolan, L., Wit, A., Dudziñ, K., Lees, A., Lake, M., Wychowañ, M., 2003. Adjustments in gait symmetry with walking speed in trans-femoral and trans-tibial amputees. Gait Posture 17, 142–151.

Norvell, D.C., Czerniecki, J.M., Reiber, G.E., Maynard, C., Pecoraro, J.A., Weiss, N.S., 2005. The prevalence of knee pain and symptomatic knee osteoarthritis among veteran traumatic amputees and nonamputees. Arch. Phys. Med. Rehabil. 86, 487–493. https://doi.org/10.1016/j.apmr.2004.04.034

Orendurff, M.S., Segal, A.D., Berge, J.S., Flick, K.C., Spanier, D., Klute, G.K., 2006. The kinematics and kinetics of turning: limb asymmetries associated with walking a circular path. Gait Posture 23, 106–111. https://doi.org/10.1016/j.gaitpost.2004.12.008

Orr, R., Pope, R., Lopes, T.J.A., Leyk, D., Blacker, S., Bustillo-Aguirre, B.S., Knapik, J.J., 2021. Soldier Load Carriage, Injuries, Rehabilitation and Physical Conditioning: An International Approach. International Journal of Environmental Research and Public Health 2021, Vol. 18, Page 4010 18, 4010. https://doi.org/10.3390/IJERPH18084010

Orr, R.M., Pope, R.P., O'Shea, S., Knapik, J.J., 2020. Load Carriage for Female Military Personnel. Strength Cond. J. 42, 50–58. https://doi.org/10.1519/SSC.0000000000000514

Parr, T.E., Farrokhi, S., Hendershot, B.D., Butowicz, C.M., 2024. Peak tibial axial acceleration during walking is related to intact-side lower limb pain in persons with unilateral transtibial amputation. Gait Posture 109, 165–169. https://doi.org/10.1016/J.GAITPOST.2024.01.033

Pataky, T.C., 2012. One-dimensional statistical parametric mapping in Python. Comput. Methods Biomech. Biomed. Engin. 15, 295–301. https://doi.org/10.1080/10255842.2010.527837

Prinsen, E.C., Nederhand, M.J., Rietman, J.S., 2011. Adaptation Strategies of the Lower Extremities of Patients With a Transtibial or Transfemoral Amputation During Level Walking: A Systematic Review. Arch. Phys. Med. Rehabil. 92, 1311–1325. https://doi.org/10.1016/J.APMR.2011.01.017

Richards, R.E., Andersen, M.S., Harlaar, J., van den Noort, J.C., 2018. Relationship between knee joint contact forces and external knee joint moments in patients with medial knee osteoarthritis: effects of gait modifications. Osteoarthritis Cartilage 26, 1203–1214. https://doi.org/10.1016/j.joca.2018.04.011

Robbins, S.M.K., Birmingham, T.B., Jones, G.R., Callaghan, J.P., Maly, M.R., 2009. Developing an estimate of daily cumulative loading for the knee: Examining test–retest reliability. Gait Posture 30, 497–501. https://doi.org/10.1016/J.GAITPOST.2009.07.118

Robbins, S.M.K., Maly, M.R., 2009. The effect of gait speed on the knee adduction moment depends on waveform summary measures. Gait Posture 30, 543–546. https://doi.org/10.1016/j.gaitpost.2009.08.236

Rogers-Bradley, E., Yeon, S.H., Landis, C., Lee, D.R.C., Herr, H.M., 2024. Variable-stiffness prosthesis improves biomechanics of walking across speeds compared to a passive device. Sci. Rep. 14, 16521. https://doi.org/10.1038/s41598-024-67230-3

Routson, R.L., Clark, D.J., Bowden, M.G., Kautz, S.A., Neptune, R.R., 2013. The influence of locomotor rehabilitation on module quality and post-stroke hemiparetic walking performance. Gait Posture 38, 511–517. https://doi.org/10.1016/J.GAITPOST.2013.01.020

Routson, R.L., Kautz, S.A., Neptune, R.R., 2014. Modular organization across changing task demands in healthy and poststroke gait. Physiol. Rep. 2, e12055. https://doi.org/10.14814/PHY2.12055;WGROUP:STRING:PUBLICATION

Russell Esposito, E., Wilken, J.M., 2014. Biomechanical risk factors for knee osteoarthritis when using passive and powered ankle-foot prostheses. Clinical Biomechanics 29, 1186–1192. https://doi.org/10.1016/j.clinbiomech.2014.09.005

Ruxin, T.R., Halsne, E.G., Hafner, B.J., Shofer, J., Hansen, A.H., Childers, W.L., Caputo, J.M., Morgenroth, D.C., 2024. The development of rating scales to evaluate experiential prosthetic foot preference for people with lower limb amputation. PM&R 16, 150–159. https://doi.org/10.1002/PMRJ.13024

Sadeghi, H., Allard, P., Duhaime, M., Hospital, J., 2001. Muscle Power Compensatory Mechanisms in Below-Knee Amputee Gait. Am. J. Phys. Med. Rehabil. 80, 25–32.

Sasaki, K., Neptune, R.R., Kautz, S.A., 2009. The relationships between muscle, external, internal and joint mechanical work during normal walking. Journal of Experimental Biology 212, 738–744. https://doi.org/10.1242/JEB.023267

Schnall, B.L., Dearth, C.L., Elrod, J.M., Golyski, P.R., Koehler-McNicholas, S.R., Ray, S.F., Hansen, A.H., Hendershot, B.D., 2020. A more compliant prosthetic foot better accommodates added load while walking among Servicemembers with transtibial limb loss. J. Biomech. 98, 109395. https://doi.org/10.1016/J.JBIOMECH.2019.109395

Schnall, B.L., Hendershot, B.D., Bell, J.C., Wolf, E.J., 2014. Kinematic analysis of males with transtibial amputation carrying military loads. J. Rehabil. Res. Dev. 51, 1505–1514. https://doi.org/10.1682/JRRD.2014.01.0022

Schnall, B.L., Wolf, E.J., Bell, J.C., Gambel, J., Bensel, C.K., 2012. Metabolic analysis of male servicemembers with transtibial amputations carrying military loads. J. Rehabil. Res. Dev. 49, 535–544. https://doi.org/10.1682/JRRD.2011.04.0075

Schwartz, M.H., Rozumalski, A., Steele, K.M., 2016. Dynamic motor control is associated with treatment outcomes for children with cerebral palsy. Dev. Med. Child Neurol. 58, 1139–1145. https://doi.org/10.1111/DMCN.13126;WEBSITE:WEBSITE:PERICLES;JOURNAL:JOURNAL:14698749;WGROUP:STRING:PUBLICATION

Seamon, B.A., Neptune, R.R., Kautz, S.A., 2018. Using a Module-Based Analysis Framework for Investigating Muscle Coordination during Walking in Individuals Poststroke: A Literature Review and Synthesis. Appl. Bionics Biomech. 2018, 3795754. https://doi.org/10.1155/2018/3795754

Selles, R.W., Bussmann, J.B.J., Wagenaar, R.C., Stam, H.J., 1999. Effects of prosthetic mass and mass distribution on kinematics and energetics of prosthetic gait: A systematic review. Arch. Phys. Med. Rehabil. 80, 1593–1599. https://doi.org/10.1016/S0003-9993(99)90336-2

Seyedali, M., Czerniecki, J.M., Morgenroth, D.C., Hahn, M.E., 2012. Co-contraction patterns of trans-tibial amputee ankle and knee musculature during gait. J. Neuroeng. Rehabil. 9. https://doi.org/10.1186/1743-0003-9-29

Shell, C.E., Segal, A.D., Klute, G.K., Neptune, R.R., 2017. The effects of prosthetic foot stiffness on transtibial amputee walking mechanics and balance control during turning. Clinical Biomechanics 49, 56–63. https://doi.org/10.1016/j.clinbiomech.2017.08.003

Shuman, B.R., Goudriaan, M., Desloovere, K., Schwartz, M.H., Steele, K.M., 2019. Muscle synergies demonstrate only minimal changes after treatment in cerebral palsy. Journal of NeuroEngineering and Rehabilitation 2019 16:1 16, 1–10. https://doi.org/10.1186/S12984-019-0502-3

Shuman, B.R., Goudriaan, M., Desloovere, K., Schwartz, M.H., Steele, K.M., 2018. Associations Between Muscle Synergies and Treatment Outcomes in Cerebral Palsy Are Robust Across Clinical Centers. Arch. Phys. Med. Rehabil. 99, 2175–2182. https://doi.org/10.1016/J.APMR.2018.03.006

Shuman, B.R., Schwartz, M.H., Steele, K.M., 2017. Electromyography data processing impacts muscle synergies during gait for unimpaired children and children with cerebral palsy. Front. Comput. Neurosci. 11, 251526. https://doi.org/10.3389/FNCOM.2017.00050/BIBTEX

Silder, A., Delp, S.L., Besier, T., 2013. Men and women adopt similar walking mechanics and muscle activation patterns during load carriage. J. Biomech. 46, 2522–2528. https://doi.org/10.1016/j.jbiomech.2013.06.020

Silverman, A.K., Fey, N.P., Portillo, A., Walden, J.G., Bosker, G., Neptune, R.R., 2008. Compensatory mechanisms in below-knee amputee gait in response to increasing steady-state walking speeds. Gait Posture 28, 602–609. https://doi.org/10.1016/j.gaitpost.2008.04.005

Silverman, A.K., Neptune, R.R., 2014. Three-dimensional knee joint contact forces during walking in unilateral transtibial amputees. J. Biomech. 47, 2556–2562. https://doi.org/10.1016/J.JBIOMECH.2014.06.006

Sinitski, E.H., Herbert-Copley, A.G., Lemaire, E.D., Doyle, S.S., Besemann, M., Dudek, N.L., 2016. Center of pressure and total force analyses for amputees walking with a backpack load over four surfaces. Appl. Ergon. 52, 169–176. https://doi.org/10.1016/j.apergo.2015.07.014

Slater, C., Halsne, E.G., Czerniecki, J.M., Morgenroth, D.C., 2024. The effect of prosthetic foot stiffness category on intact limb knee loading associated with osteoarthritis in people with transtibial amputation. J. Biomech. 176, 112368. https://doi.org/10.1016/J.JBIOMECH.2024.112368

Smith, J.D., Ferris, A.E., Heise, G.D., Hinrichs, R.N., Martin, P.E., 2014. Oscillation and reaction board techniques for estimating inertial properties of a below-knee prosthesis. Journal of Visualized Experiments. https://doi.org/10.3791/50977

Snyder, R.D., Powers, C.M., Fontaine, C., Perry, J., 1995. The effect of five prosthetic feet on the gait and loading of the sound limb in dysvascular below-knee amputees. J. Rehabil. Res. Dev. 32, 309–315.

Soangra, R., Bhatt, H., Rashedi, E., 2018. Effects of load carriage and surface inclination on linear and non-linear postural variability. Saf. Sci. 110, 427–437. https://doi.org/10.1016/J.SSCI.2018.03.019

Steele, K.M., Tresch, M.C., Perreault, E.J., 2013. The number and choice of muscles impact the results of muscle synergy analyses. Front. Comput. Neurosci. 7, 55417. https://doi.org/10.3389/FNCOM.2013.00105/BIBTEX

Steeper, 2024. Sierra Prosthetic Feet Catalogue. www.steepergroup.com.

Struyf, P.A., van Heugten, C.M., Hitters, M.W., Smeets, R.J., 2009. The Prevalence of Osteoarthritis of the Intact Hip and Knee Among Traumatic Leg Amputees. Arch. Phys. Med. Rehabil. 90, 440–446. https://doi.org/10.1016/j.apmr.2008.08.220

Sutton, E., Bare, D., Taylor, M., Kinor, D., Schaeffer, J., Jules, A., Bigelow, K.E., 2010. Minimizing Postural Instability When Carrying Load: The Effects of Carrying Grocery Bags on The Elderly, in: American Society of Biomechanics Conference. American Society of Biomechanics.

Syrett, E.D., Peterson, C.L., Darter, B.J., Syrett, E.D., Peterson, C.L., Darter, B.J., 2025. The Number of Gait Cycles Necessary to Obtain a Representative Measure of Knee Joint Loads in Individuals With Lower Limb Amputation. J. Appl. Biomech. 41, 544–551. https://doi.org/10.1123/jab.2024-0282

Tacca, J.R., Colvin, Z.A., Grabowski, A.M., 2026. Effects of prosthetic ankle power and foot stiffness category on biomechanical asymmetry and knee moment during walking at different speeds. Sci. Rep. https://doi.org/10.1038/s41598-026-37225-3

Tacca, J.R., Colvin, Z.A., Grabowski, A.M., 2024. Low-profile prosthetic foot stiffness category and size, and shoes affect axial and torsional stiffness and hysteresis. Frontiers in Rehabilitation Sciences 5. https://doi.org/10.3389/fresc.2024.1290092

Takahashi, K.Z., Horne, J.R., Stanhope, S.J., 2015. Comparison of mechanical energy profiles of passive and active below-knee prostheses: A case study. Prosthet. Orthot. Int. 39, 150–156. https://doi.org/10.1177/0309364613513298

Takahashi, K.Z., Kepple, T.M., Stanhope, S.J., 2012. A unified deformable (UD) segment model for quantifying total power of anatomical and prosthetic below-knee structures during stance in gait. J. Biomech. 45, 2662–2667. https://doi.org/10.1016/j.jbiomech.2012.08.017

Teater, R.H., Wolf, D.N., McDonald, K.A., Zelik, K.E., 2023. Unilateral transtibial prosthesis users load their intact limb more than their prosthetic limb during sit-to-stand, squatting, and lifting. Clinical Biomechanics 108, 106041. https://doi.org/10.1016/J.CLINBIOMECH.2023.106041

Templin, T.N., Klute, G.K., Neptune, R.R., 2021. The influence of load carriage on knee joint loading and metabolic cost on walking with lower-limb amputation: a preliminary modeling study. Journal of Prosthetics and Orthotics 33.

Thomsen, P.B., Gaffney, B.M.M., Tracy, J.B., Vandenberg, N.W., Awad, M.E., Christiansen, C.L., Stoneback, J.W., 2024. Cumulative loading increases and loading asymmetries persist during walking for people with a transfemoral bone-anchored limb. Gait Posture 113, 46–52. https://doi.org/10.1016/J.GAITPOST.2024.05.019

Ting, L.H., Macpherson, J.M., 2005. A Limited Set of Muscle Synergies for Force Control During a Postural Task. https://doi.org/10.1152/jn.00681.2004 93, 609–613. https://doi.org/10.1152/JN.00681.2004

Toor, A.S., Limpisvasti, O., Ihn, H.E., McGarry, M.H., Banffy, M., Lee, T.Q., 2019. The significant effect of the medial hamstrings on dynamic knee stability. Knee Surgery, Sports Traumatology, Arthroscopy 27, 2608–2616. https://doi.org/10.1007/S00167-018-5283-X/FIGURES/5

Torres-Oviedo, G., Macpherson, J.M., Ting, L.H., 2006. Muscle Synergy Organization Is Robust Across a Variety of Postural Perturbations. https://doi.org/10.1152/jn.00810.2005 96, 1530–1546. https://doi.org/10.1152/JN.00810.2005

Torres-Oviedo, G., Ting, L.H., 2007. Muscle Synergies Characterizing Human Postural Responses. https://doi.org/10.1152/jn.01360.2006 98, 2144–2156. https://doi.org/10.1152/JN.01360.2006

Trepczynski, A., Kutzner, I., Bergmann, G., Taylor, W.R., Heller, M.O., 2014. Modulation of the Relationship Between External Knee Adduction Moments and Medial Joint Contact Forces Across Subjects and Activities. Arthritis & Rheumatology 66, 1218–1227. https://doi.org/10.1002/ART.38374

Turner, A.T., Halsne, E.G., Caputo, J.M., Curran, C.S., Hansen, A.H., Hafner, B.J., Morgenroth, D.C., 2022. Prosthetic forefoot and heel stiffness across consecutive foot stiffness categories and sizes. PLoS One 17, e0268136. https://doi.org/10.1371/JOURNAL.PONE.0268136

Ueda, T., Hobara, H., Kobayashi, Y., Heldoorn, T.A., Mochimaru, M., Mizoguchi, H., 2016. Comparison of 3 methods for computing loading rate during running. Int. J. Sports Med. 37, 1087–1090. https://doi.org/10.1055/s-0042-107248

Uhlrich, S.D., Silder, A., Beaupre, G.S., Shull, P.B., Delp, S.L., 2018. Subject-specific toe-in or toe-out gait modifications reduce the larger knee adduction moment peak more than a non-personalized approach. J. Biomech. 66, 103–110. https://doi.org/10.1016/J.JBIOMECH.2017.11.003

Umberger, B.R., Martin, P.E., 2007. Mechanical power and efficiency of level walking with different stride rates. Journal of Experimental Biology 210, 3255–3265. https://doi.org/10.1242/JEB.000950

U.S. NCVAS, 2024. NCVAS State Summary Washington FY2024 [WWW Document]. www.data.va.gov. URL https://www.data.va.gov/stories/s/NCVAS-State-Summary-Washington-FY2024/7nk8-2gmu/ (accessed 3.13.26).

Varrecchia, T., Serrao, M., Rinaldi, M., Ranavolo, A., Conforto, S., De Marchis, C., Simonetti, A., Poni, I., Castellano, S., Silvetti, A., Tatarelli, A., Fiori, L., Conte, C., Draicchio, F., 2019. Common and specific gait patterns in people with varying anatomical levels of lower limb amputation and different prosthetic components. Hum. Mov. Sci. 66, 9–21. https://doi.org/10.1016/J.HUMOV.2019.03.008

Voloshina, A.S., Collins, S.H., Seyfarth, A., 2025. Effects of prosthetic ankle stiffness on adaptation to uneven terrain in individuals with unilateral transtibial amputation. Hum. Mov. Sci. 102, 103371. https://doi.org/10.1016/J.HUMOV.2025.103371

Walter, J.P., D'Lima, D.D., Colwell, C.W., Fregly, B.J., 2010. Decreased knee adduction moment does not guarantee decreased medial contact force during gait. Journal of Orthopaedic Research 28, 1348–1354. https://doi.org/10.1002/JOR.21142

Wang, H., Frame, J., Ozimek, E., Leib, D., Dugan, E.L., 2012. Influence of fatigue and load carriage on mechanical loading during walking. Mil. Med. 177, 152.

Wilson, D.R., McWalter, E.J., Johnston, J.D., 2008. The Measurement of Joint Mechanics and their Role in Osteoarthritis Genesis and Progression. Rheumatic Disease Clinics of North America 34, 605–622. https://doi.org/10.1016/j.rdc.2008.05.002

Winter, D.A., 1991. Biomechanics and motor control of human gait: normal, elderly and pathological.

Winter, D.A., Sienko, S.E., 1988. Biomechanics of below-knee amputee gait. J. Biomech. 21, 361–367.

Woltring, H., 1986. A Fortran package for generalized, cross-validatory spline smoothing and differentiation. Advanced Engineering Software 8, 104–107.

Wong, C.K., Wong, R.J., 2017. Standard and Amputation-Adjusted Body Mass Index Measures: Comparison and Relevance to Functional Measures, Weight-Related Comorbidities, and Dieting. Am. J. Phys. Med. Rehabil. 96, 912–915. https://doi.org/10.1097/PHM.0000000000000796

Yang, Feng, Ban, R., Yang, Fei, 2022. Anterior load carriage increases the risk of falls in young adults following a slip in gait. Saf. Sci. 145. https://doi.org/10.1016/j.ssci.2021.105489

Zelik, K.E., Honert, E.C., 2018. Ankle and foot power in gait analysis: Implications for science, technology and clinical assessment. J. Biomech. 75, 1–12. https://doi.org/10.1016/j.jbiomech.2018.04.017